Curtin University

THE INSTITUTE FOR GEOSCIENCE RESEARCH (TIGeR)

TIGeR ANNUAL REPORT 2015

EXPLORING EARTH'S DYNAMIC EVOLUTION

Make tomorrow better.

scieng.curtin.edu.au

The Institute for Geoscience Research

About TIGeR – exploring Earth's dynamic evolution

The Institute for Geoscience Research (TIGeR) brings together active researchers across the spectrum of geosciences within Curtin University with the common goal of understanding the mechanisms and the timescales of the processes that control Earth's dynamic evolution.

TIGeR researchers study processes over a wide range of length scales, from the nanoscale to the macroscale – from reactions operating at grain boundaries in rocks to global tectonics and the origin of the Solar system.

Since the establishment of TIGeR, our researchers have been at the forefront of high-quality, world-leading research in the earth sciences. We produce geochronologic, geotectonic, geodetic and geochemical records, using the latest technology and field and laboratory data, to enhance our knowledge of the Earth's origin within the solar system, its evolution and its current configuration.

Our research forms the basis of understanding the element cycles operating on Earth and their application to the formation of natural resources such as mineral, oil, gas and coal deposits.

Widespread collaboration

TIGeR is a multidisciplinary group that brings together leading scientists in geology, inorganic and organic geochemistry, geodesy and geophysics with the common goal of advancing new and innovative geoscience research.

Our researchers are drawn from all the geoscience-related departments and centres across Curtin University, including the Department of Applied Geology, the John de Laeter Centre for Isotope Research, the Western Australian Centre for Geodesy, the Western Australian Organic and Isotope Geochemistry Group, the Department of Exploration Geophysics and the Department of Mining Engineering.

We work together with research teams across Australia and internationally and have an excellent track record of obtaining competitive national and international grants, publishing in leading international journals and producing highly-qualified postgraduates.

Contents

Mission statement

To obtain a fundamental understanding of the mechanisms behind complex processes in the Earth.

To establish and maintain a reputation as an international leader in this field.

To enhance our interdisciplinary research by establishing new collaborations and joint ventures.

To actively seek greater involvement with industrial applications of our research.

To find efficient ways of transmitting our basic research to industry, the education sector and the public.

Director's comments

The role of TIGeR is to represent and promote Geosciences research across the wide spectrum of activities at Curtin University. This 2015 Annual Report is the first of a regular series that summarises the peer-reviewed research publications for each year and serves as both a source of information as well as an archive.

The articles summarised in this report are a selection of the 238 publications, in ISI recognised journals, by TIGeR members in 2015. This level of productivity is also typical of previous years and is why Curtin University continues to be a leader in the "solid earth" disciplines of geology, geochemistry and geophysics. The Excellence in Research for Australia (ERA) 2015 results have acknowledged our international reputation with scores of 5 ("well above world standard") in geology and geochemistry and 4 ("above world standard") in geophysics.

Two TIGeR members (Simon Wilde and Zheng-Xiang Li), both from the Department of Applied Geology, have been featured on the Thomson Reuters Highly Cited Researchers list, with papers that have ranked among the top 1 per cent most cited in Geosciences in the world. We congratulate them on their continued research excellence. Our success is also reflected in the number of ARC and externally funded research projects. Notable among these is the award of an ARC Laureate Fellowship to Zheng-Xiang Li. This project, in global geodynamics and Earth evolution, has involved the construction of a new fully automated and magnetically shielded superconducting palaeomagnetic laboratory – the first of its kind in Australia.

Another major instrument acquisition installed in 2015 is the Geosciences Atom Probe that is part of a new Advanced Resource Characterisation Facility (ARCF) in partnership with Curtin, CSIRO and The University of Western Australia, and funded by a $12.4 million grant from the Science and Industry Endowment Fund (SIEF).

National and international collaboration is a characteristic of Geosciences research and TIGeR members continue to be active in multidisciplinary research projects, as evidenced from the publications and projects reported here. New initiatives with CSIRO, Centre for Exploration Targeting (CET), Minerals Research Institute of Western Australia (MRIWA) and Geological Survey of Western Australia (GSWA) establish TIGeR as a major player in Geosciences activities in Western Australia. National and international collaborations with ARC Centre of Excellence: Core to Crust Fluid Systems (CCFS) and Australia-China Joint Research Centre for Tectonics (ACTER) are just two of the formal collaborations currently active. TIGeR is also an Associate Partner in two current European Union Network Projects.



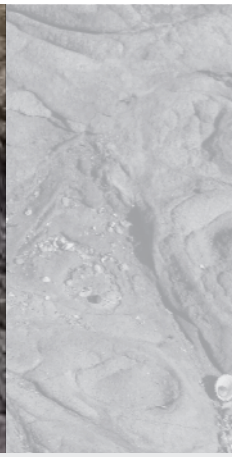

The National Geosequestration Laboratory (NGL), opened in July 2015, is a collaboration between CSIRO, The University of Western Australia (UWA) and Curtin University. TIGeR members from the Department of Exploration Geophysics are providing the seismic expertise to support this major initiative, funded through a $48.4 million grant from the Australian Government.

Fluid-rock and fluid-mineral interaction is a recurrent theme in TIGeR research, from the perspective of Earth processes as well as innovations in extracting metals from minerals. In the latter case, TIGeR members have patented a process to extract gold, silver and copper from a range of minerals using glycine solutions. This paves the way for a potentially much more environmentally-friendly extraction process than currently employed.

A new TIGeR initiative is the Annual TIGeR Conference. The 2015 Conference, on *Key issues on fluid-rock interaction: From the nano to the macroscale*, attracted international participation and promises to be a key event each year.

And just to top off the year, the Desert Fireball Team have recovered the first meteorite using their 32-camera array of observatories stationed across the Australian outback. The fall, on 27 November, was captured by the cameras and after some calculation, a 1.7 kg meteorite was located and recovered on New Year's Eve, buried in a 42 cm deep hole in a remote section of the lake bed of Kati Thanda-Lake Eyre.

All in all, a very good year!

Andrew Putnis
Director, The Institute for Geoscience Research (TIGeR)

2015 TIGeR Conference

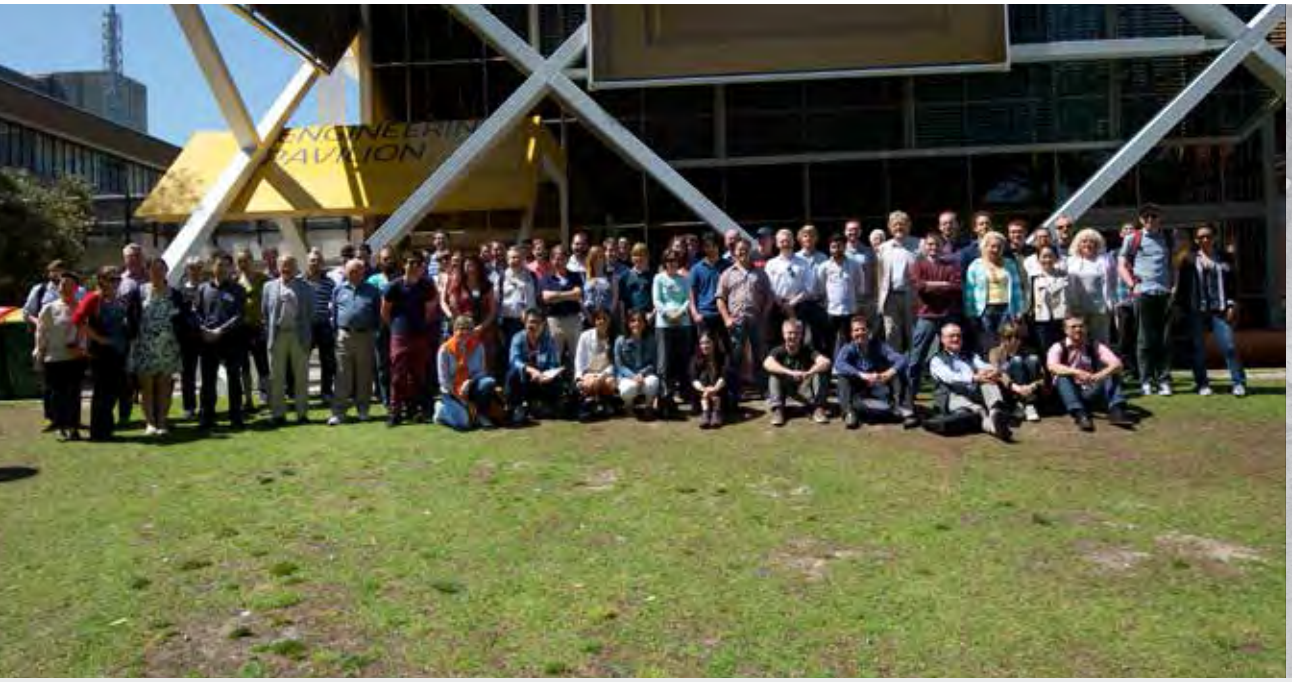

The first TIGeR Conference was held in September 2015, with 110 participants from universities and industry from 12 countries.

The details of the 2015 TIGeR Conference program as well as downloadable abstracts can be found at: **tiger.curtin.edu.au/conference-2015/**

Research reports

MINERAL SYSTEMS, FLUIDS AND ORE DEPOSITS

Coupled mass transfer and stress generation during volume-increasing hydration reactions.

Centrella et al. (2015) have studied the partial hydration of the Precambrian granulite facies rocks of Lindås Nappe, Bergen Arcs, Caledonides of W. Norway. The granulite (garnetite) displays sharp hydration fronts across which the granulite facies assemblage composed of garnet and clinopyroxene is replaced by an amphibolite facies mineralogy defined by chlorite, epidote and amphibole. The major element bulk composition does not change significantly across the hydration front, apart from the increase in the volatile components. However, the replacements of garnet and of clinopyroxene are pseudomorphic so that the grain shapes of the garnet and clinopyroxene are preserved even when they are completely replaced.

The textural evolution during the replacement of garnet by pargasite, epidote and chlorite and of pyroxene by hornblende and quartz in our rock sample conforms to that expected by a coupled dissolution–precipitation mechanism. The element losses and gains in replacing the garnet are approximately balanced by the opposite gains and losses associated with the replacement of clinopyroxene. The coupling between dissolution and precipitation on both the grain and whole rock spatial scale preserves the volume of the rock throughout the hydration process.

However, the hydration involves reduction of rock density and mass balance calculations, together with volume preservation (isovolumetric reaction) require a significant loss of the mass of the rock to the fluid phase. This suggests a mechanism for coupling between the local stress generated by hydration reactions and mass transfer, dependent on the spatial scale over which the system is open where the fluid infiltration is pervasive along grain boundaries.

Centrella S., Austrheim H., Putnis A. (2015) Coupled mass transfer through a fluid phase and volume preservation during hydration of granulite: An example from the Bergen Arcs, Norway. *Lithos*, 236,237, 245-255.

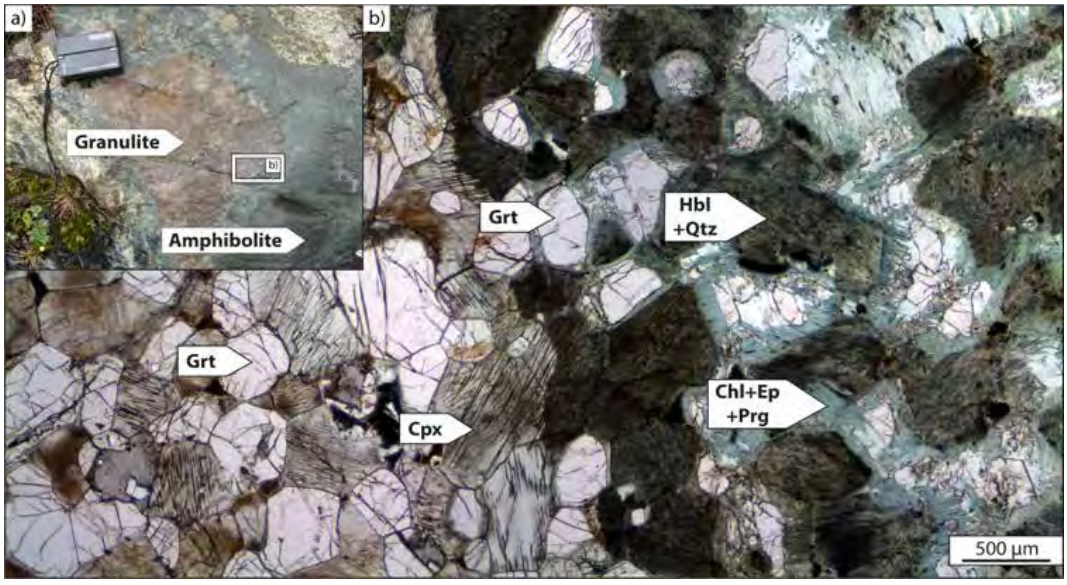

a) Outcrop photograph showing the relation between granulite and amphibolite.

b) Photograph of a thin section localised at the boundary between the granulite (left) and the amphibolite (right).

Metamorphic effects on the redox budget of subducted mantle lithosphere.

Subduction of hydrated lithospheric mantle introduces H_2O, ferric iron, oxidized carbon and sulphate to the subduction zone system. The fate of these components is poorly known, but is intimately linked to the global geochemical cycles of iron, carbon and sulphur, the genesis of arc-related ore deposits, the temporal evolution of mantle redox state and subduction-related earthquakes and magmatism.

Evans and Powell (2015) use newly-developed features and activity-composition models embedded in the thermodynamic modeling software THERMOCALC to explore the consequences of subduction for these oxidized elements hosted by ultramafic rocks in hydrated mantle lithosphere. The calculations replicated observed mineral assemblages very well, and indicated that metamorphism took place in open systems without, in most cases, significant fluid infiltration. Depths of fluid loss corresponded well with depths inferred for earthquakes centred in the subducting slab, but there was little correlation with the depths inferred for production of arc magmas. This latter point is important, because common existing models of subduction systems require water from deserpentinisation to fertilise sub-arc magma production, and the lack of a simple relationship between water loss and magma production suggests that the links are more complex than has been previously thought.

Carbon and sulfur are almost entirely retained within the subducting slab, so it is envisaged that the bulk of these elements are to the deep Earth and recycled over much longer timescales than elements recycled into arc magmas transported to >5 GPa.

The retention of oxidized carbon and sulfur in the subducting slab means that there is no fluid-induced mechanism for oxidation of sub arc mantle by transfer of redox budget from hydrated ultramafic lithologies. This result has important consequences for the current debate regarding the oxidation state of sub-arc mantle, which many workers contend is oxidized, somehow by transfer of redox budget from the slab to the wedge.

High P low T ultramafic rocks in outcrop in the Pouebo terrain, New Caledonia.

Evans K.A., Powell R. (2015). Metamorphic effects on the redox budget of subducted mantle lithosphere. *Journal of Metamorphic Geology*, 33: 649-670.

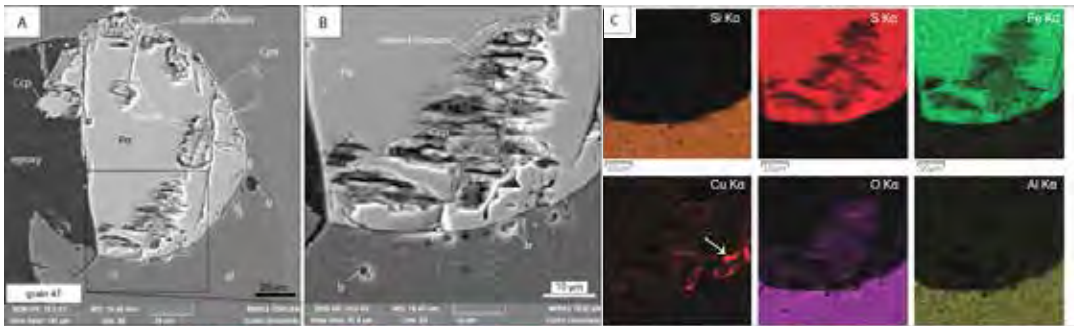

Sulfide globule co-trapped with melt in clinopyroxene (A and B, BSE images) and X-ray compositional maps (C). The globule is cracked and O- and Cu-enriched altered domains develop along cracks and along the globule margins (sample K2, Krakatau). Abbreviations: Po pyrrhotite, Ccp chalcopyrite.

Open-system behaviour of magmatic fluid phase and transport of copper in arc magmas at Krakatau and Batur volcanoes, Indonesia.

Magmatism associated with convergent margins is globally associated with important Cu-Au-Mo ore deposits. However, the mechanisms of ore formation are still not clear, so that the relative importance of source versus differentiation characteristics, and the complex interplay between processes at play from slab dehydration to mantle melting, magma fractionation and contamination are still unresolved. Processes of immiscibility are considered to be fundamental in scavenging metals from the magma and in their transport and deposition, and the relative timing of sulphide melt and aqueous fluid exsolution deeply affects melt concentration.

The Sunda-Banda volcanic arc of Indonesia is well endowed with Cu-Au-porphyry deposits. Agangi and Reddy (2015) studied samples of recent eruptions of Mt Krakatau (1963) and Mt Batur (2008) in order to clarify the distribution of metals (Cu, Ag, Sn, Zn, Mo) and S in these magmas and the interaction of these immiscible phases. Their observations suggest that most of the Cu of the magma was contained in fluid bubbles. This fluid was then trapped in various proportions with melt in different phenocrysts (plagioclase, pyroxene and olivine), resulting in precipitation of S-Fe-Cu-O globules, and causing variably Cu and S enriched compositions of melt inclusions. The alteration textures of sulphide globules exemplify how Cu and other chalcophile elements can be exchanged between aqueous fluid and sulphide phases during the last stages of magma evolution.

Agangi A., Reddy S. (2015) IAGR 2015 conference, Tsukuba, Japan, October 2015

Massive chalcopyrite mineralisation at Red Bore, WA. The deep roots of a sea floor hydrothermal system.

Agangi et al., (2015) have studied recently discovered mineralisation at Red Bore, in the Doolgunna region of central Western Australia which includes multiple pipe-like bodies composed of massive chalcopyrite surrounded by brecciated massive magnetite. Drill core indicated that the pipes are at least 100 m long and around 10–12 m in diameter, although the total extent is unknown. The ore replaced the mafic volcanic-subvolcanic host rocks of the Palaeoproterozoic Narracoota Formation. Accessory phases include pyrite, mixed sulfide-silicate phases (partially sulfidised silicates), pyrrhotite, and various Bi-Te-(Se)-Ag-(Au) phases. The mineralisation is enveloped by a narrow (<2 m) alteration halo composed of serpentine, amphibole, silica and talc. Laser ablation ICP-MS analyses of chalcopyrite and pyrite indicated high concentrations of Ag, Au (up to ~200 and 10 ppm, respectively), other than enrichments of Se and Pd. In situ sulfur isotope analyses of chalcopyrite and pyrite indicate narrow ranges of δ^{34}VCDT (0–3.3 ‰, but mostly 2–3.3 ‰) and no mass-independent fractionation, consistent with deposition from a homogeneous fluid derived from a magmatic source.

They interpret the mineralisation at Red Bore as the result of release of Cu-rich magmatic fluids in focussed channels, possibly along structural discontinuities. The fluids likely raised to the surface and contributed to the neighbouring VMS mineralisation known in the area. The deposit provides direct insight into deep portions of a magmatic-hydrothermal system developed in oceanic crust underneath VMS deposits.

pipes and co-genetic VMS deposits at DeGrussa. Copper Au, Ag, Bi and other metals were likely transported from a magmatic fluid phase and fed into VMS deposits at the surface, where they would have mixed with sea water-derived fluids. Other elements, such as Zn, are found in VMS deposits but are depleted at Red Bore and may have been derived from leaching of the volcano-sedimentary pile by sea water fluids.

sample TRCDD09 32.0m. B Massive magnetite breccia. Clasts are cross-cut by carbonate (cb) veinlets. C external contact of the ore body. Chalcopyrite (Ccp) truncates magnetite (Mag).

Agangi A., Vieru C., Reddy S., Plavsa D., Selvaraja V. (2015). Presented at SEG 2015 conference, Hobart, September 2015

Gold transport in aqueous vs organic ore fluids.

In several gold deposit types, gold is commonly associated with liquid petroleum (oil inclusions), bitumen and other organic material, which brings into question the role of organic liquids in the concentration of gold ore. In the Curtin Experimental Geochemistry Facility (John de Laeter Centre), a three-year experimental study is underway to assess the feasibility of gold transport in organic liquids (petroleum), via studies of gold solubility in organic liquids and the partitioning of gold between coexisting brine and liquid hydrocarbons.

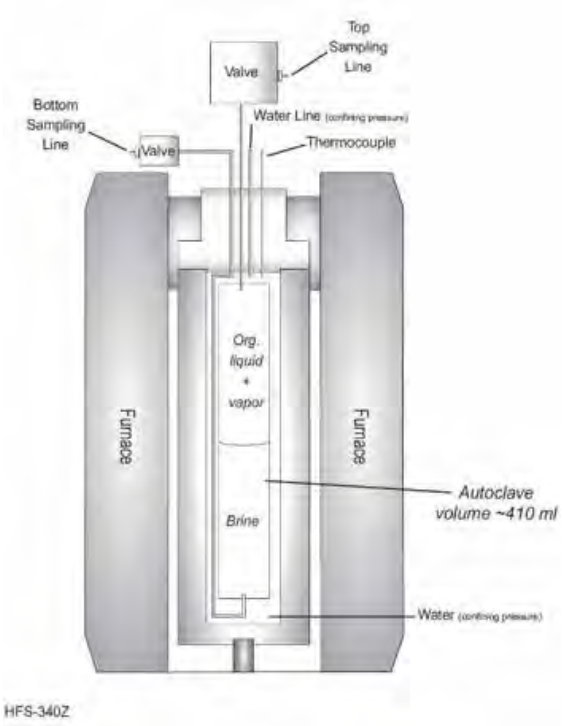

Schematic diagram of the Coretest in-situ sampling system used for partitioning experiments, purchased with a strategic equipment grant from Curtin's Office of Research and Development.

Dating hydrothermal mineralization and fluid flow from xenotime and monazite ages from the Capricorn Orogen.

Vital to the success of discovering new ore deposits is the understanding of their formation timing and genesis. Dating hydrothermal mineralisation has been challenging due to that zircon doesn't grow in such low-temperature processes. Zi et al., (2015) applied an innovative technique, by identifying minute phosphate mineral xenotime crystals intergrown (thus simultaneous) with ore minerals, and dating them in situ using SHRIMP ion microprobe. They precisely dated the mineralization of the largest known base-metal deposit in the expansive Capricorn Orogen of Western Australia, resolving a long-standing problem. The study showed that xnotime and monazite represent ideal chronometers for investigating the complex histories of hydrothermal mineralisation and fluid flow in major crustal structures.

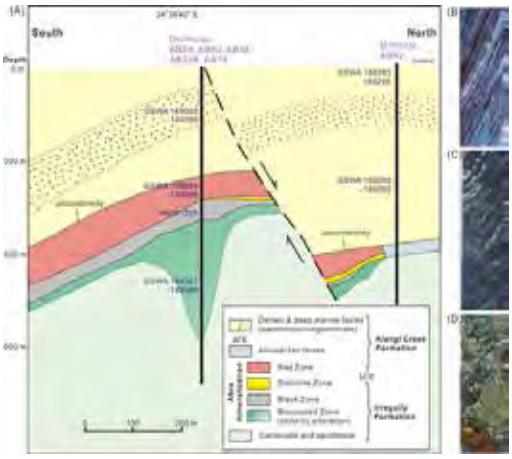

Simplified cross-section of the Abra poly-metallic deposit in the Capricorn Orogen. Pictures of drill core samples used for phosphate geochronology are also shown.

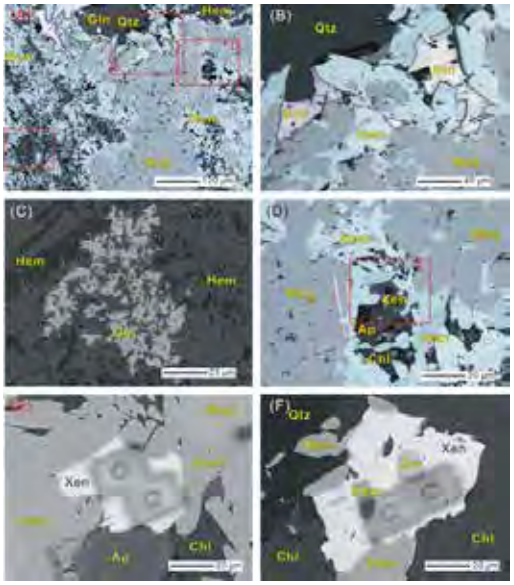

Photomicrograph showing the dated xenotime crystals intergrown with ore minerals galena and iron oxides.

Zi J.-W., Rasmussen B., Muhling J.R., Fletcher I.R., Thorne A.M., Johnson S.P., Cutten H.N., Dunkley D.J., Korhonen, F.J. (2015). In situ U–Pb geochronology of xenotime and monazite from the Abra polymetallic deposit in the Capricorn Orogen, Australia: Dating hydrothermal mineralization and fluid flow in a long-lived crustal structure. *Precambrian Research* 260, 91-112.

The composition of hydrothermally-derived apatite as a fluid probe for halogens.

Apatite ($Ca_5(PO_4)_3(OH, F, Cl)$) is one of the main host of halogens in magmatic and metamorphic rocks and plays a unique role during fluid–rock interaction as it incorporates halogens (i.e. F, Cl, Br, I) and OH from hydrothermal fluids to form a ternary solid solution of the endmembers F-apatite, Cl-apatite and OH-apatite. Kusebauch et al., (2015) present an experimental study to investigate the processes during interaction of Cl-apatite with different aqueous solutions (KOH, NaCl, NaF of different concentration also doped with NaBr, NaI) at crustal conditions (400–7000C and 0.2 GPa) leading to the formation of new apatite. They use the experimental results to calculate partition coefficients of halogens between apatite and fluid. Due to a coupled dissolution–reprecipitation mechanism new apatite is always formed as a pseudomorphic replacement of Cl-apatite. The composition of new apatite is mainly governed by complex characteristics of the fluid phase from which it is precipitating and depends on composition of the fluid, temperature and fluid to mineral ratio.

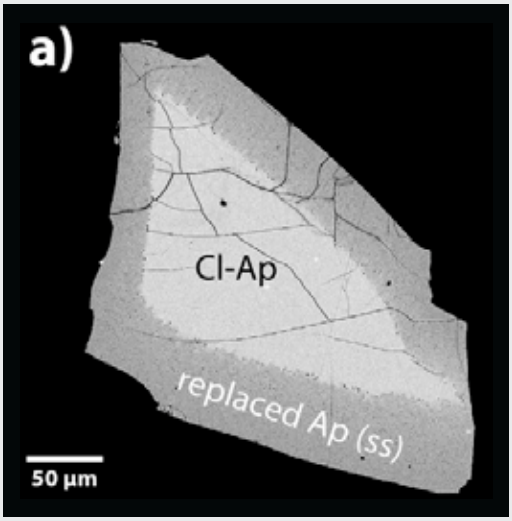

Back-scatter electron image of a Cl-apatite partially replaced by a F-rich apatite solid solution. The product phase is porous, allowing for fluid and mass transfer from the surrounding medium to the reaction front.

Kusebauch C., John T., Whitehouse M.J., Klemme S., Putnis A. (2015) Distribution of halogens between fluid and apatite during fluid-mediated replacement processes. *Geochimica et Cosmochimica Acta* 170, 225-246.

Fluid-mineral interaction, transient porosity and consequences to crystal growth in porous media.

The evolution of porosity during replacement reactions and the consequences to crystal growth in porous media has been reviewed by Putnis (2015).

Putnis A. (2015)Transient porosity resulting from fluid-mineral interaction and its consequences. *Reviews in Mineralogy & Geochemistry* 80, 1-23.

Experimental crystallization of barite – an example of nano-clustered growth.

How crystals grow is still a matter of considerable debate. Ruiz-Agudo et al report evidence for barite ($BaSO_4$) formation from aqueous solution via non-classical pathways. TEM and SEM observations of the nanostructure evolution of samples quenched at successive stages of crystallization indicate two levels of oriented aggregation of nanosized solid particles. The first is the aggregation of crystalline primary nanoparticles of ca. 2–10nm length to give larger but still nanometer-sized particles (ca.20–100 nm length). For the first time, clear evidence of crystallographically oriented aggregation of secondary, nanometer-sized particles to form a barite single crystal is reported. During the second aggregation step of these secondary nanoparticles, most of the porosity in the largest, micron-sized aggregates is annealed, resulting in perfect single crystals.

Ruiz-Agudo C., Ruiz-Agudo A., Putnis C.V., Putnis A. (2015) Mechanistic principles of barite formation: From nanoparticles to micron-sized crystals. *Crystal Growth and Design* 15, 3724-3733.

Ruiz-Agudo C., Putnis C.V., Ruiz-Agudo E., Putnis A. (2015) The influence of pH on barite nucleation and growth. *Chemical Geology* 391, 7-18.

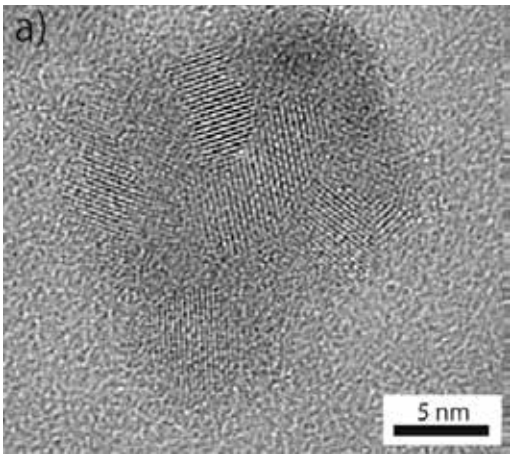

TEM photomicrograph of a barite nanoparticle composed of a random aggregate of primary particles (ca. 2–10 nm length) for barite formation.

How mineralogy and crystallographic preferred orientation (CPO) results in seismic anisotropy of evaporites.

Vargas-Meleza et al, (2015) calculated bulk elastic properties and seismic velocities for a suite of 20 evaporite samples. The rocks, made up from halite, anhydrite and gypsum all showed strong fabrics as a result of tectonic and diagenetic processes, and these were studied using EBSD (electron back scatter diffraction). Ultrasonic velocity measurements were also taken on cube shaped samples to assess the contribution of grain-scale shape preferred orientation (SPO) to the total seismic anisotropy. The sample results suggest that CPO is responsible for a significant fraction of the bulk seismic properties, in agreement with observations from previous studies. The proportions of the different phases in the evaporite controlled the seismic anisotropy.

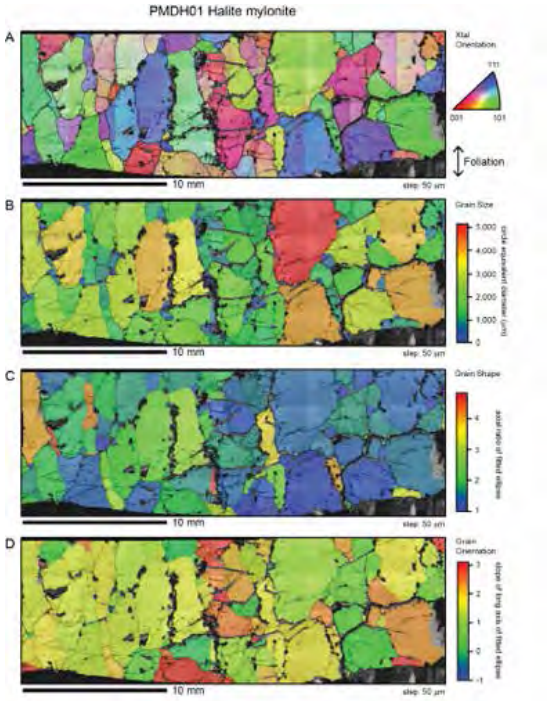

EBSD maps from evaporite samples.

Vargas-Meleza L., Healy D., Alsop I., Timms N. (2015). Exploring the relative contribution of mineralogy and CPO to the seismic velocity anisotropy of evaporites. *Journal of Structural Geology*, 70, 39-55.

Insights into changes in depositional environment in the Perth Basin.

Timms et al., (2015) have carried out a sedimentary facies analysis of a range of rocks from the central Perth Basin, obtained from drill cores to assess their potential as aquifers. Changes in the lithofacies, linked to local depositional environments, are probably associated with fluvial-alluvial to fluvio-deltaic systems that have complex 3D architecture, including braided and to probably meandering systems, and are affected by channel avulsion.

Individual lithofacies types show a trend of decreasing porosity with depth due to the increasing effects of compaction, quartz overgrowth cementation and authigenic clay mineral development. Lithofacies and depth are the main controls on permeability, and so lithofacies distribution exerts a key control on hydraulic behaviour.

Timms N.E., Olierook H.K.H., Willson M.E.J., Delle Piane C., Hamilton P.J., Cope P., Stütenbecker L. (2015). Sedimentary facies analysis, mineralogy and diagenesis of the Mesozoic aquifers of the central Perth Basin. *Marine and Petroleum Geology*, 60, 54-78.

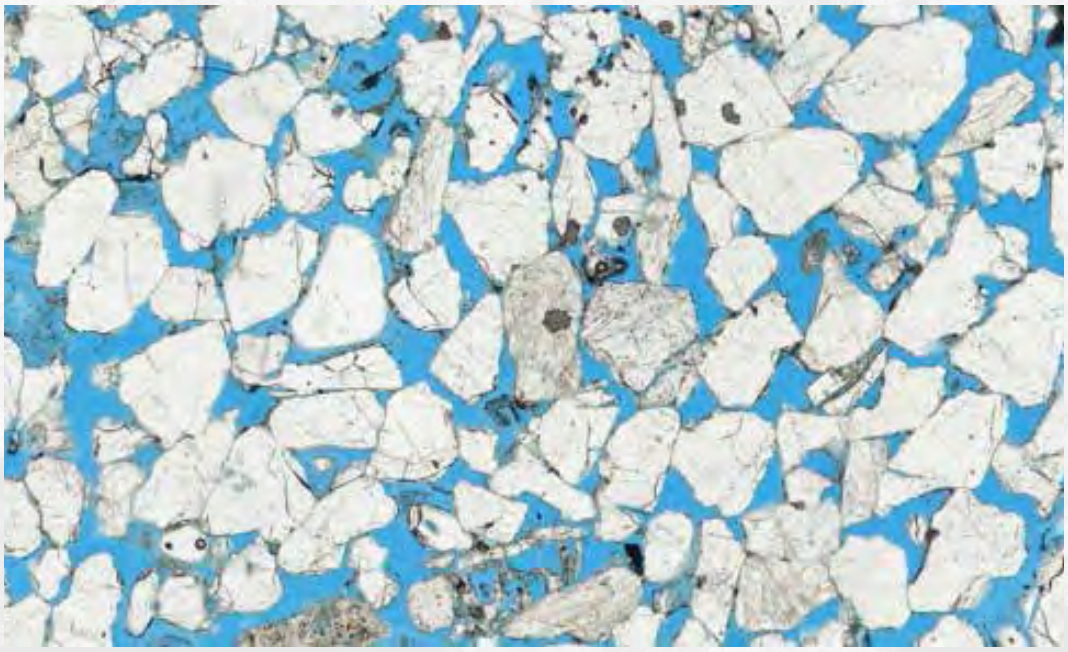

Porosity (blue) in a typical Perth Basin sediment.

Deriving thermal conductivity of geothermal reservoir rocks from P-wave velocity and porosity.

Esteban et al. (2015) have compared laboratory measurements of porosity, P-wave velocity and thermal conductivity from samples from two geothermal reservoirs in France and Australia to the predictions from different models. Thermal conductivity derived from models involving detailed mineralogy is in good agreement with laboratory-measured data. Possible explanations for minor discrepancies using SEM/XRD include the effects of secondary minerals (i.e. ± undetected carbonates and fine particles) and the hydration of clays.

Esteban L., Pimienta L., Sarout J., Delle Piane C., Haffen S., Geraud Y., Timms N.E. (2015). Study cases of thermal conductivity prediction from P-wave velocity and porosity. *Geothermics*, 53, 255-269.

Scott Rock. ? Caption

Deriving thermal conductivity of geothermal reservoir rocks from P-wave velocity and porosity.

Waddell et al (2015) have analysed the textures and ages of detrital zircons in the sediments in the Ragged Basin and ages of cross-cutting igneous rocks to determine a minimum age and environment for the deposition. Sediments were deposited within a shallow basin by a large fluvial system dominated by shifting, sandy braided channels, forming a quartz-rich succession defined as the Mount Ragged Formation. The gradual coarsening upwards sequence indicates a distal fluvial environment characterised by channel migration and abandonment, changing to a proximal fluvial environment characterised by rapid periods of sedimentation and coarser deposits. Ion microprobe (SHRIMP) U–Pb analysis of detrital zircons constrain a maximum depositional age of 1314 ± 19 Ma for the Mount Ragged Formation, so it is feasible that deposition started during the latter part of Stage I (c. 1330–1260 Ma) of the Albany–Fraser Orogeny. A minimum age for deposition, and structural emplacement, is provided by a crystallization age of 1175 ± 12 Ma for a cross-cutting monzogranite exposed at Scott Rock, part of the Esperance Supersuite.

Waddell, P.J., Timms, N.E., Kirkland, C.L., Wingate, M., & Spaggiari, C.V. (2015). Analysis of the Ragged Basin, Western Australia: insights into syn-orogenic basin evolution within the Albany-Fraser Orogen. *Precambrian Research*, 261, 166-187.

Dating deformation events in high-grade metamorphic rocks.

Erickson et al. (2015) have studied the relationship between deformation and age of deformed monazite in the polymetamorphic Sandmata granulite complex in India using a combination of EBSD (electron backscatter diffraction) and sensitive high-resolution ion microprobe (SHRIMP). Quantitative microstructural analyses document the development of deformation twins in {100}, {001}, and {122} orientations; low-angle (<10º) boundary development associated with dislocation creep; and the development of new grains due to dynamic recrystallization. These data represent the first quantitative evidence of crystal-plastic deformation of natural monazite. SHRIMP U-Th-Pb analysis shows that the host monazite preserves discordant ages as old as 1666 ± 28 Ma, along a trend from ca. 1720 Ma to ca. 1000 Ma, with increasingly discordant ages recorded in zones of higher lattice distortion. Domains of recrystallized new grains within the monazite record a tightly clustered concordia age of 970 ± 14 Ma. This age is interpreted to represent the timing of monazite dynamic recrystallization associated with deformation of the host protolith, and is consistent with partial resetting and Pb loss from domains deforming by dislocation creep. The complex, but systematic, relationship between microstructure and age data in monazite provide the first direct evidence of Pb isotope resetting during deformation. The approach illustrates a new methodology for the dating of deformation events in high-grade metamorphic rocks, which are typically difficult to constrain.

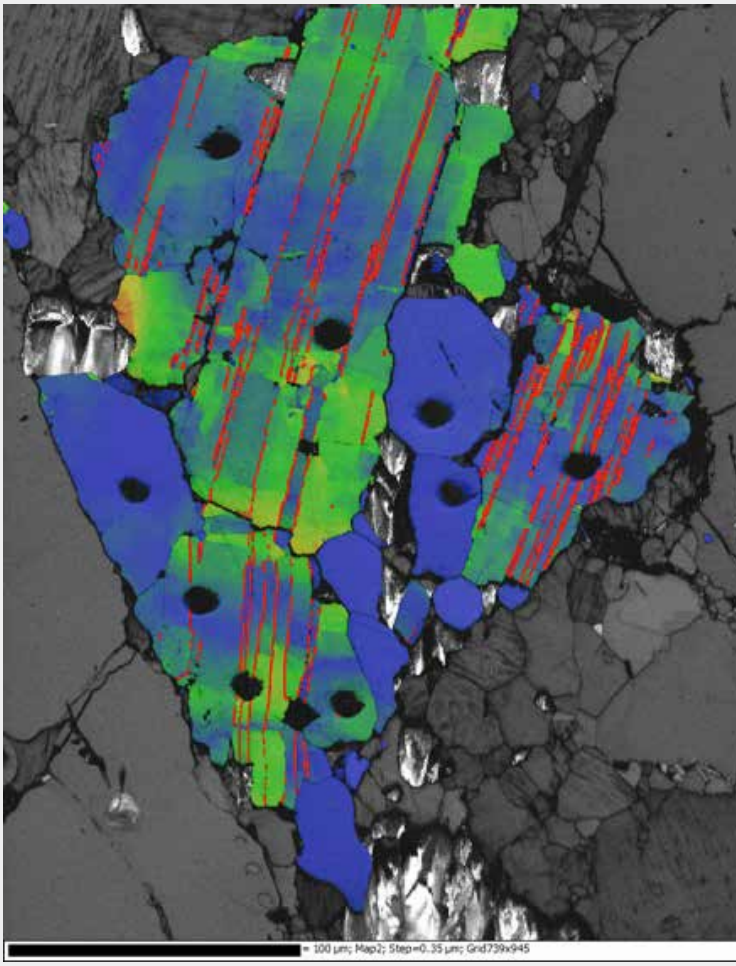

Erickson T.M., Pearce M.A., Taylor R.J., Timms N.E., Clark C., Reddy S.M., Buick I.S. (2015). Deformed monazite yields high temperature tectonic ages. *Geology*, 43, 383-386.

Erickson T.M., Pearce M.A., Taylor R.J., Timms N.E., Clark C., Reddy S.M., Buick I.S., (2016). Deformed monazite yields high temperature tectonic ages: Reply. *Geology*, 44, 378. .

History of rifting and breakup of Eastern Gondwana from the development and fill of the Perth Basin.

Olierook et al., (2015) integrate existing, publicly available geological, gravity, magnetic and digital elevation data to develop the first refined, regional structural and stratigraphic interpretation of the entire onshore and offshore Perth Basin, Western Australia. This new 3D model offers formation depth and thickness predictions in areas of sparse or no data. The model shows significant heterogeneity in the preserved formation thicknesses and depths at both local and regional scales. This new model of the entire Perth Basin provides a framework for numerical simulations of fluid and heat flow and large-scale tectonic analysis, such as stratigraphic forward modelling of the southwestern Australian margin.

Olierook H. K. H., Timms N. E., Wellmann J. F., Corbel S., Wilkes P., (2015). 3D structural and stratigraphic model of the Perth Basin, Western Australia: Implications for sub-basin evolution, *Australian Journal of Earth Sciences*. 62 (4), 447-467.

Olierook H.K.H., Timms N.E., (2015). Quantifying multiple Permian–Recent exhumation events during the breakup of eastern Gondwana: sonic transit time analysis of the central to southern Perth Basin. *Basin Research*, DOI: 10.1111/bre.12133.

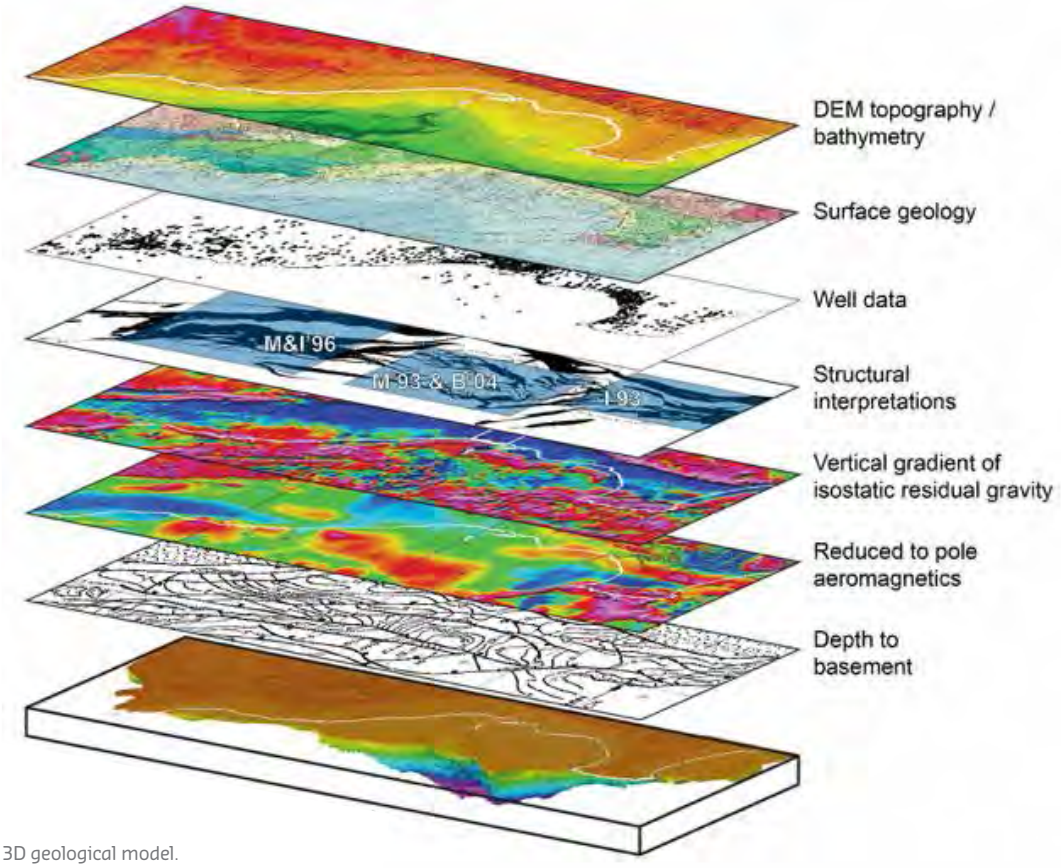

3D geological model.

The Bunbury basalt as a guide to the faults and palaeodrainage evolution of the Perth Basin.

The "Bunbury Basalt" lava flow is known to be to be synchronous with continental breakup. Olierook et al (2015) have used new aeromagnetic data, integrated with well intersections and outcrop constraints to establish the first 3D model of the Bunbury Basalt. This allows the orientation of flows and hence drainage patterns to be established and the offsets of the flows to be related to identify new northeast- and northwest-trending faults in the southern Perth Basin, and broad folding is interpreted as a consequence of drag into the Darling and Busselton faults. The source vents for the Bunbury Basalt were probably located at extensional jogs at intersections between the Darling Fault and subordinate oblique faults. These results challenge the views on longstanding quiescence of the post-breakup western Australian passive margin.

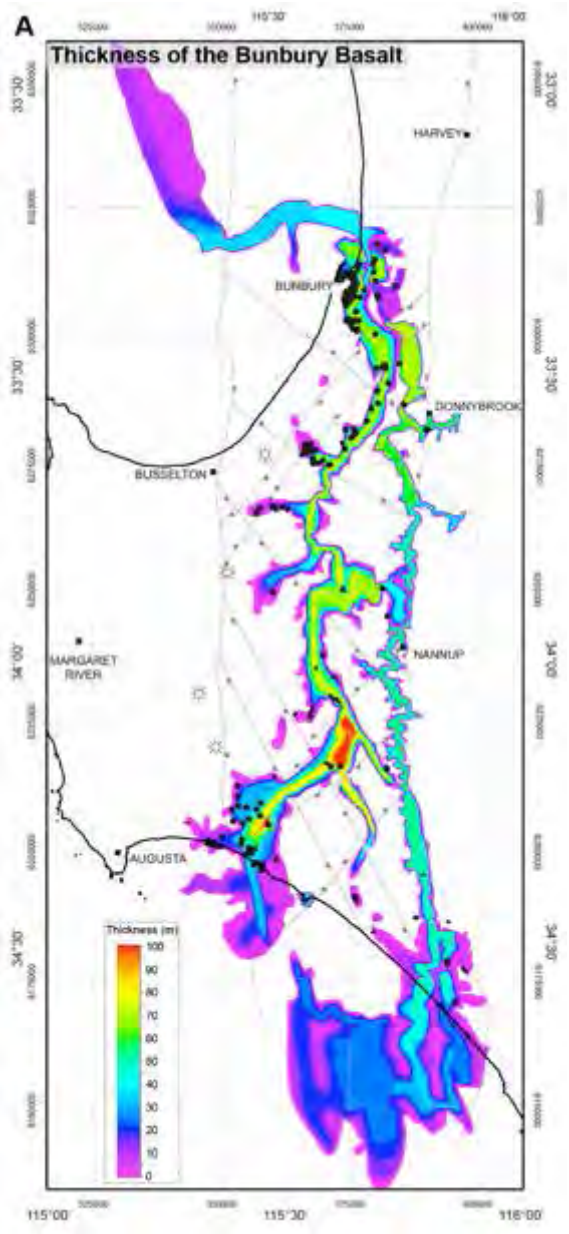

Timing of the Bunbury Basalt eruption: Gondwana breakup are an early product of the Kerguelen mantle plume?

Olierook et al. (2015) use high precision $^{40}Ar/^{39}Ar$ geochronology and whole-rock geochemistry to investigate the age and possible origin of the Bunbury basalt. Nine new plateau ages indicate that the Bunbury Basalt erupted in three distinct phases, at 136.96±0.43 Ma, 132.71±0.43 Ma and 130.45±0.82 Ma. All Bunbury Basalt samples are enriched tholeiitic basalts and may be related to other Kerguelen plume products. However, new age constraints of the oldest Bunbury Basalt are synchronous with the breakup of eastern Gondwana and the initial opening of the Indian Ocean at ca. 137–136 Ma, which may mean an alternative explanation is possible. The enriched geochemistry can equally be explained by a patch of shallow mantle beneath the southern Perth Basin. They conclude that although the proto-Kerguelen hotspot is certainly a possible explanation for the genesis of the Bunbury Basalt, decompression melting of an enriched patch of subcontinental lithospheric mantle is an alternative theory.

Olierook H.K.H., Jourdan F., Merle R.E., Timms N.E., Kusznir N., Muhling J.R. (2016). Bunbury Basalt: Gondwana breakup products or earliest vestiges of the Kerguelen mantle plume? *Earth and Planetary Science Letters*, 440, 20-32.

The Bunbury Basalt at Black Point.

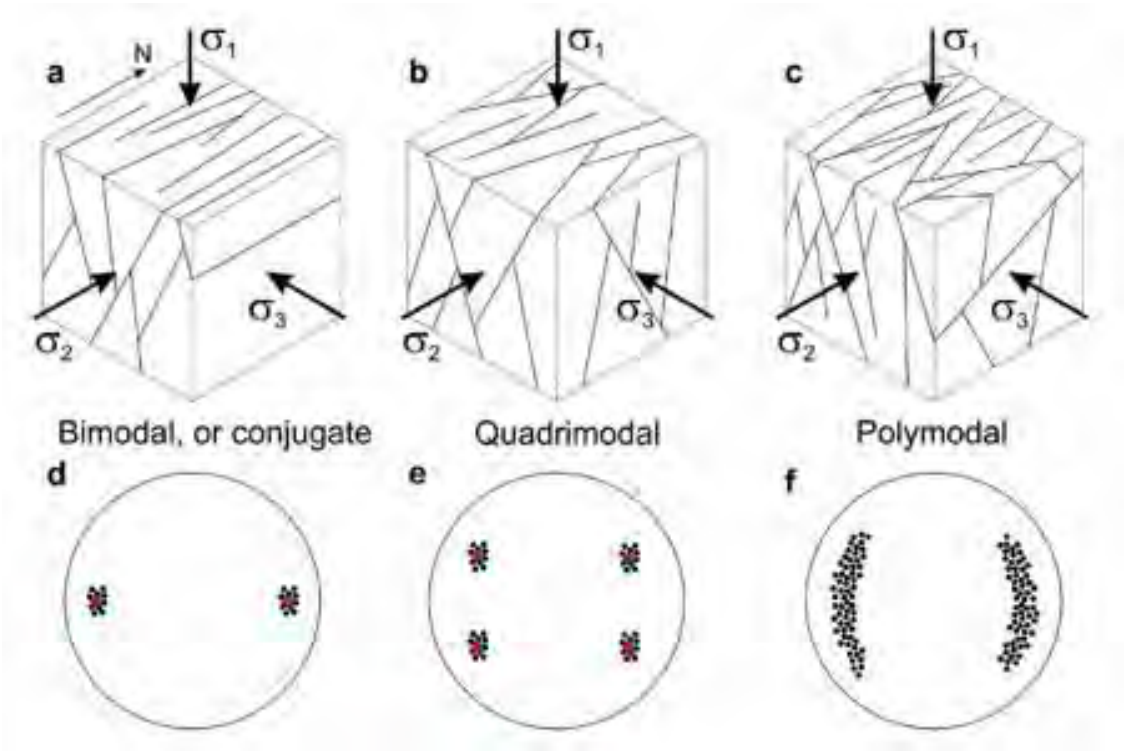

Time for a new angle on shear failure.

Healy et al., (2015) review the published evidence, theories and models for polymodal faulting and argue that to interpret three dimensional stresses and strains that characterise deformation in the Earth we need to go beyond the traditional application of the Mohr-Coulomb failure criterion as applied by Anderson (1905). Polymodal fault patterns in nature present a fundamental challenge to our understanding of shear failure in rocks, yet provide an opportunity to improve our understanding of seismic hazards and fluid flow in the subsurface. Healy et al. suggest ways to produce a truly general and valid failure criterion for triaxial failure.

Healy, D., Blenkinsop, T.G., Timms, N.E., Meredith, P.G., Mitchell, T.M., and Cooke, M.L., 2015. Polymodal faulting: Time for a new angle on shear failure. *Journal of Structural Geology*, 80, 57-71.

Conditions of deposition of Banded Iron Formations (BIFs).

Banded iron formations (BIFs) are important archives of the ancient oceans, atmosphere, and biosphere, but fundamental questions remain about their origin. It is widely assumed that BIFs were derived from layers of ferric oxyhydroxides and silica that precipitated directly from a water column that was enriched in dissolved iron and silica.

Rasmussen et al (2015a,2015b) report new sedimentological and petrographic results that show that laminated cherts in the 2.5 Ga Dales Gorge Member of the Brockman Iron Formation, Western Australia, preserve textures indicative of in situ brecciation immediately below the seafloor and the deposition of intraformational sandstones composed of chert clasts in a chert matrix. Chert intraclasts have two sedimentary components: silt-sized microgranules and submicron-sized particles, indicating that the original sediment comprised iron-rich silicate muds that were cemented on or just below the seafloor by pore-filling silica.

New high-resolution microscopy of BIFs and shales throughout the 2.63–2.45

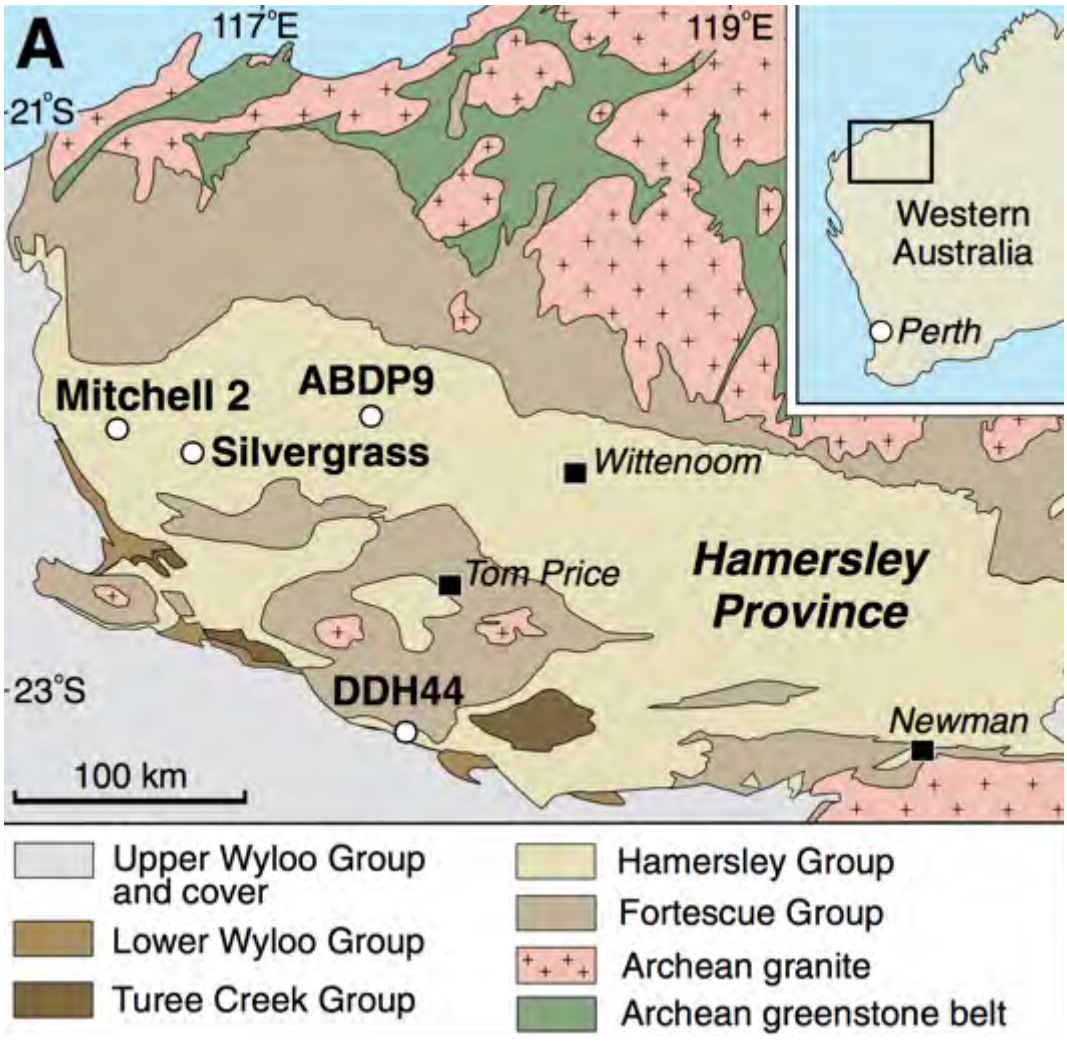

b.y. old Hamersley Group, Australia, reveals the presence of vast quantities of nanometer-sized iron-silicate particles in laminated chert. The nanoparticles are finely disseminated in early diagenetic chert and locally define sedimentary lamination, indicating that they represent relicts of the original sediments.

Their results support the hypothesis that high concentrations of silica in early Precambrian seawater favored episodic silica cementation of sediments on the seafloor. They further suggest that competition between sediment accumulation and seafloor silica cementation, with subsequent differential compaction, explains primary layering in BIFs between beds of relatively thickly laminated chert and beds of thinly laminated, iron-rich minerals.

Rasmussen B., Krapez B., Muhling J.R. and A. Suvorova A. (2015). Precipitation of iron silicate nanoparticles in early Precambrian oceans marks Earth's first iron age. *Geology* 43 (4): 303-306.

Rasmussen B., Krapez B. and Muhling J.R. (2015). Seafloor silicification and hardground development during deposition of 2.5 Ga banded iron formations. *Geology* 43 (3): 235-238.

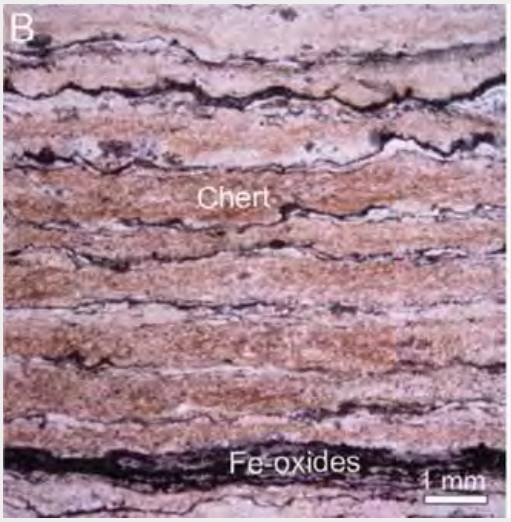

Transmitted light (TL) image of bedded chert with thin laminae of iron oxides (black).

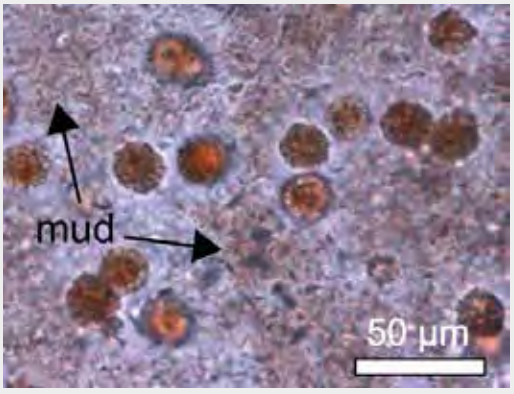

Spheroidal microgranules in mud-sized matrix of iron-silicate particles.

Raman characterisation of carbonaceous material in the Macraes orogenic gold deposit and metasedimentary host rocks, New Zealand.

The common association between carbonaceous material (CM) and gold in metasediment-hosted Au deposits has long been noted, but explanations for the association vary widely and there is little consensus. Hu et al., (2015) describe detailed analysis by SEM and Raman spectroscopy of mineralized and unmineralised samples of the Otago Schist, New Zealand to assess the potential role of CM in the formation of gold deposits.

Four types of CM were identified in samples from the lowest metamorphic grades (prehnite-pumpellyite) to the highest grades investigated (mineralized lower greenschist). In prehnite–pumpellyite and pumpellyite–actinolite grade rocks, low-maturity CM1 coexists with framboidal pyrite. This material is thought to have an in-situ, sedimentary origin, and trace element mapping currently in press indicates that the CM and framboidal pyrite are likely to be associated with the source of the gold. Low crystallinity CM 2 is also found in low grade samples, but textural indicators suggest that this CM was deposited from fluids unrelated to gold mobilization. CM 3 is the highest maturity CM recognized. CM 3 is found in samples from the highest metamorphic grades studied (lower greenschist facies), where bands of CM3 cross cut the foliation, CM3 is therefore thought to have been transported by fluids, though possibly only at short length scales. CM4 is less mature than CM3 and is also found in mineralized rocks in association with sulfide minerals and gold. CM 4 is likely to be in-situ and was therefore most likely present during gold deposition. However, thermodynamic modeling work (currently under review) suggests that its role in gold deposition is indirect and is limited to participation in sulfidation reactions.

Hu S.Y., Evans K., Craw D., Rempel K., Bourdet J., Dick J., Grice K., 2015. Raman characterization of carbonaceous material in the Macraes orogenic gold deposit and metasedimentary host rocks, New Zealand. *Ore Geology Reviews* 70, 80-95.

Shirley Hu crossing the river at Fiddler's Flat, New Zealand.

Shirley and Dave Craw collecting samples at the Golden Bar pit, New Zealand.

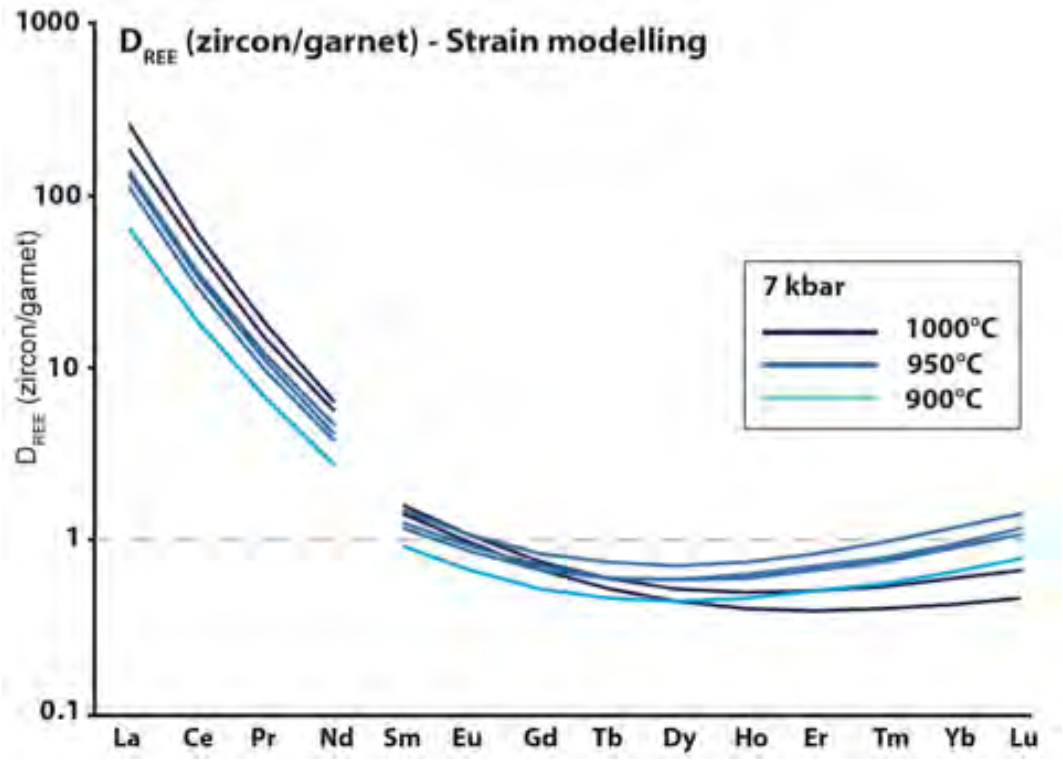

Zircon–garnet trace element partitioning.

Zircon is a key mineral for the U–Pb dating of major metamorphic events. Garnet is a metamorphic indicator mineral that can be used to identify pressure (*P*) and temperature (*T*) conditions. Taylor et al. (2015) present a set of rare earth element (REE) partitioning data between zircon and garnet at *P*–T conditions relevant to high grade crustal metamorphism. These data provide a key reference frame by which to identify zircon that has formed in the presence of stable garnet.

The ability to demonstrate the chemical equilibrium of these minerals during crustal metamorphism is a powerful tool, linking together pressure, temperature and time (*P–T–t*). This relationship is particularly important in complex rocks such as migmatites, where the migration of partial melts may artificially bring disparate mineral assemblages together, or in polymetamorphic terrains with multiple generations of zircon and garnet.

The modelled dataset (left) of REE partition coefficients (D values) shows a concave-up shape with light REE favouring zircon, middle REE slightly favouring garnet, and heavy REE D values close to 1.

Taylor R.J.M, Harley S.L., Hinton R., Elphick S., Clark C. (2015) Experimental determination of REE partition coefficients between zircon, garnet and melt: a key to understanding high-temperature crustal processes. *Journal of Metamorphic Geology*. 33, 231-248.

Dating impacts from shocked zircons.

Deformed lunar zircons yielding U-Pb ages from 4333 Ma to 1407 Ma have been interpreted as dating discrete impacts on the Moon. However, the cause of age resetting in lunar zircons is equivocal; as ex situ grains in breccias, they lack lithologic context and most do not contain microstructures diagnostic of shock that are found in terrestrial zircons. Detrital shocked zircons provide a terrestrial analog to ex situ lunar grains, for both identifying diagnostic shock evidence and also evaluating the feasibility of dating impacts with ex situ zircons. Using Electron backscatter diffraction and sensitive high-resolution ion microprobe U-Pb analysis of zircons eroded from the ca. 2020 Ma Vredefort impact structure (South Africa) Cavosie et al (2015) show that complete impact-age resetting did not occur in microstructural domains characterized by microtwins, planar fractures, and low-angle boundaries, which record ages from 2890 Ma to 2645 Ma. An impact age of 1975 ± 39 Ma was detected in neoblasts within a granular zircon that also contains shock microtwins, which link neoblast formation to the impact. However, they show that granular texture can form during regional metamorphism, and thus is not unique to impact environments.

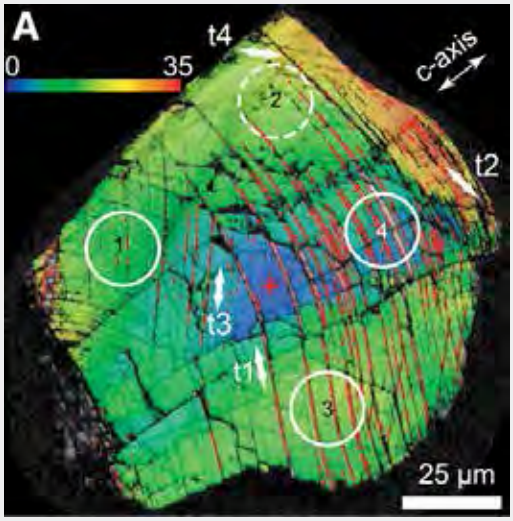

Planar deformation features in a shocked lunar zircon. Reidite lamellae (blue) within zircon (red).

These results demonstrate that dating an impact with ex situ shocked zircon requires identifying diagnostic shock evidence to establish impact provenance,and then targeting specific age-reset microstructures. With the recognition that zircon can deform plastically in both impact and magmatic environments, age-resetting in lunar zircons that lack diagnostic shock deformation may record magmatic processes rather than discrete impacts. Identifying shock microstructures that record complete age resetting for geochronological analysis is thus crucial for constructing accurate zircon-based impact chronologies for the Moon, Earth, or other planetary bodies.

Cavosie A.J., Erickson T.M., Timms N.E., Reddy S.M., Talavera C., Montalvo S.D., Pincus M.R., Gibbon R.J., Moser D. (2015) A terrestrial perspective on using ex situ shcked zircons to date lunar impacts. *Geology*, 43, 999-1002.

Precambrian high pressure phase reidite found in shocked zircon from Scotland.

The record of Precambrian impacts on Earth is poorly constrained due to the dynamic nature of plate tectonics, erosion and deposition of younger rocks that may destroy or cover the evidence. Reddy et al. (2015) report for the first time the occurrence of reidite ($ZrSiO_4$), the high pressure polymorph of zircon, forming planar lamellae in zircon. The reidite is unambiguous evidence of shock pressures in excess of ~30GPa. The reidite is itself locally deformed and shows breakdown to baddelyite and amorphous silica, the first natural example of this transformation. The findings confirm the impact origin of the rocks as well as demonstrate that the high-pressure phase can be preserved during diagenesis and low grade metamorphism. Reidite can be used as a means of recognising ancient terrestrial impact events.

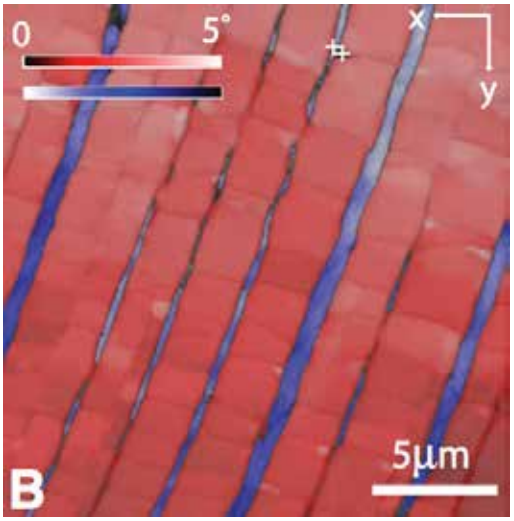

Reidite lamellae (blue) within zircon (red).

Reddy S. M., Johnson T.E., Fischer S., Rickard W.D. and R. J. Taylor R.J. (2015).Precambrian reidite discovered in shocked zircon from the Stac Fada impactite, Scotland. *Geology* 43, 899-902.

Are granites and granulites consanguineous?

Determining whether the production of granite magma in orogens is a closed-system process with respect to mass input from the mantle is an important question in petrology that is commonly addressed by inversion of geochemical data from upper crustal granites. A complementary approach is to assess the consanguinity of residual granulites and spatially associated granites in the exhumed deep crust of ultrahot orogens. Korhonen et al., (2015) report zircon and monazite geochronology, and elemental and isotope geochemical data for a suite of contemporaneous granulites and granites from the Eastern Ghats Province (EGP), part of a long-lived Grenville-age orogen. The prograde metamorphic evolution of the granulites involved increasing temperature (*T*) and pressure (*P*) to reach a metamorphic peak >1,000ºC at ~0.7 GPa followed by slow cooling.

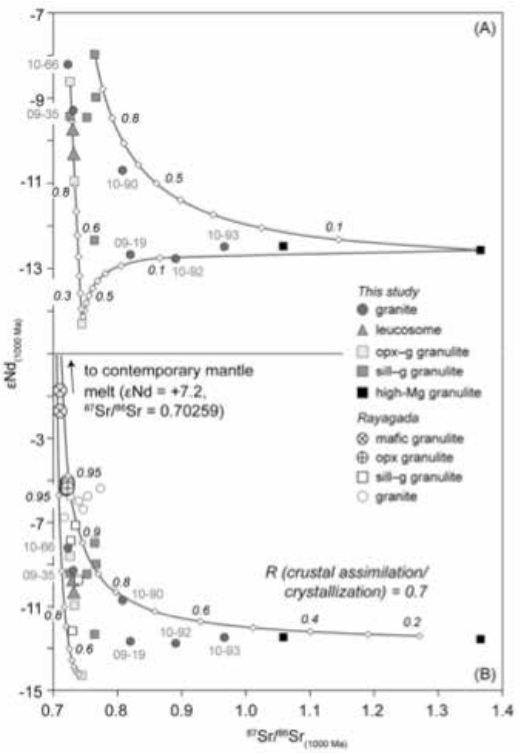

Variations in the elemental geochemistry of the granites are interpreted as due to local processes, including fractionation during melting or crystallization, and/or peritectic mineral entrainment. The Nd and Sr isotope compositions of the granites can be matched by mixing between the various granulites, suggesting that the granites may have been derived solely from these granulite-facies residues. However, by including published geochemical data from an adjacent area to the north, it becomes clear that an increasingly important mass input from the mantle was likely involved in granite genesis in traversing from southwest to northeast in the EGP, as confirmed by modeling assimilation–fractional crystallization between an exemplar mantle-derived melt at 1,000 Ma and the range of residual crustal lithologies. The extreme peak metamorphic temperature and *P–T* evolution require heat from the mantle, suggesting extended lithosphere that relaxed thermally to its former thickness during slow cooling. We postulate that the SW to NE spatial variation in mantle input to the granites is related to changing feedback between the rates of extension and mantle melt flux.

Korhonen F.J., Brow, M., Clark C., Foden J. (2015) Are granites and granulites consanguineous? *Geology*. 43, 991-994.

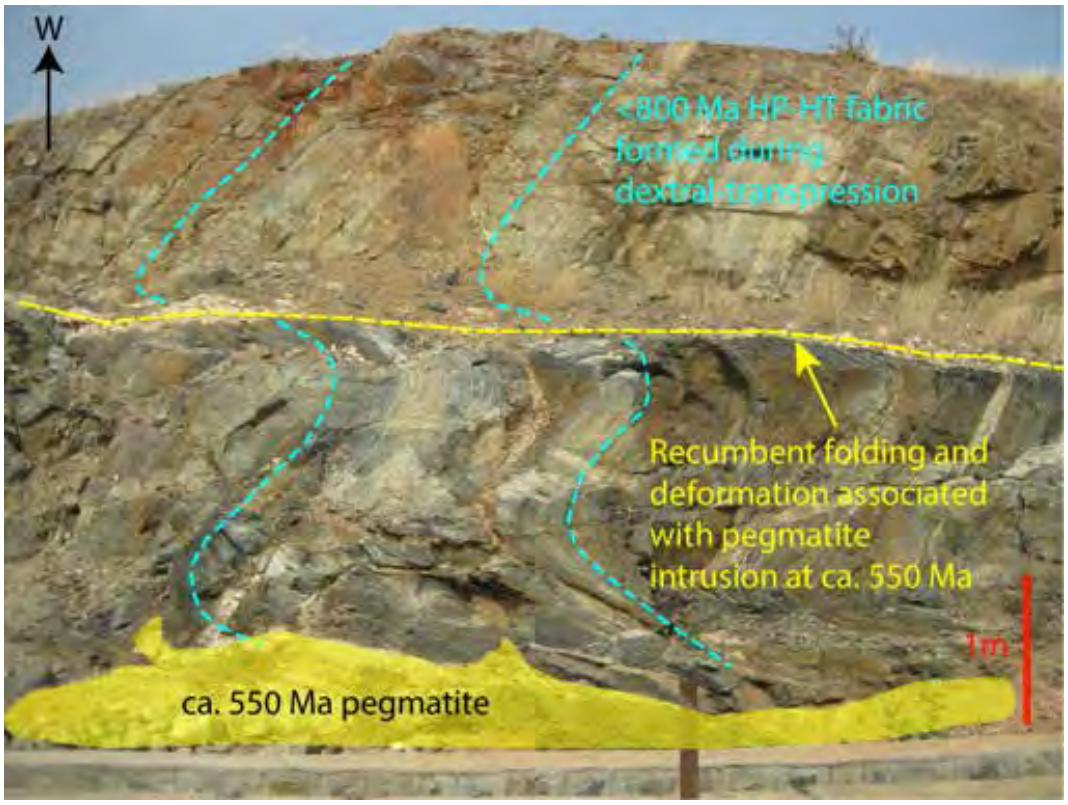

HP-HT mafic granulites (protolith age ca. 800 Ma) deformed during the late Neoproterozoic (age of pegmatites ca. 550 Ma) .

The evolution of a Gondwanan Collisional Orogen: A structural and geochronological appraisal from the Southern Granulite Terrane, South India.

The collision of the greater Archean Dharwar Craton (present-day India) with the Azania microcontinent (present-day Madagascar) took place along the Palghat-Cauvery Shear Zone (PCSS) during the amalgamation of Gondwana some 550 million years ago. Earlier studies believed the Neoproterozoic deformation took place along a ~50km wide belt forming a flower-type structure during dextral transpression. However, Plavsa et al. (2015) have made structural observations combined with U-Pb zircon dating of cross-cutting pegmatites, partial melts and basement rocks across the proposed suture and have revealed a two-stage deformational history, including an early Paleoproterozoic dextral strike-slip deformation in the northern part of the PCSS with a largely Neoproterozoic overprint during dextral-transpression to the south of the PCSS.

Plavsa D., Collins A.S., Foden J., Clark, C. (2015) The evolution of a Gondwanan collisional orogen: a structural and geochronological appraisal from the Southern Granulite Terrane, South India. *Tectonics*. 34, 820-857.

Hot orogens and supercontinent amalgamation: a Gondwanan example from southern India.

The Southern Granulite Terrane in southern India preserves evidence for regional-scale high to ultrahigh temperature metamorphism related to the amalgamation of the supercontinent Gondwana. Clark et al., (2015) present accessory mineral (zircon and monazite) geochronological and geochemical datasets linked to the petrological evolution of the rocks as determined by phase equilibria modelling. The results constrain the duration of high to ultrahigh temperature (>900ºC) metamorphism in the Madurai Block to be c. 40 Ma with peak conditions achieved c. 60 Ma after the formation of an orogenic plateau related to the collision of the microcontinent Azania with East Africa at c. 610 Ma. A 1D numerical model demonstrates that the attainment of temperatures >900ºC requires that the crust be moderately enriched in heat producing elements and that the duration of the orogenic event is sufficiently long to allow conductive heating through radioactive decay. Both of these conditions are met by the available data for the Madurai Block. Our results constrain the length of time it takes for the crust to evolve from collision to peak P–T (i.e. the prograde heating phase) then back to the solidus during retrogression. This evolution illustrates that not all metamorphic ages date sutures.

Clark C., Healy D., Johnson T.E., Collins A.S., Taylor R.J.M., Santosh M., Timms N.E. (2015) Hot orogens and supercontinent amalgamation: a Gondwanan example from southern India. *Gondwana Research*. 28, 1310-1328.

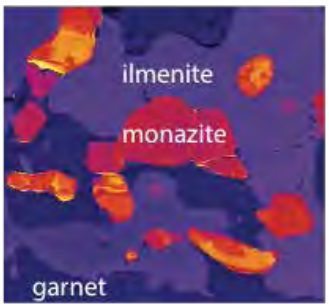

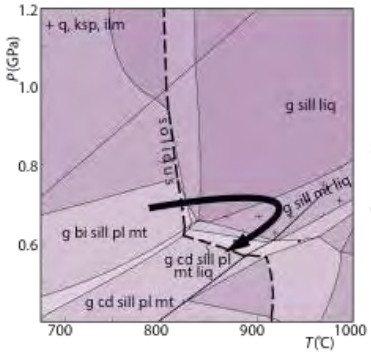

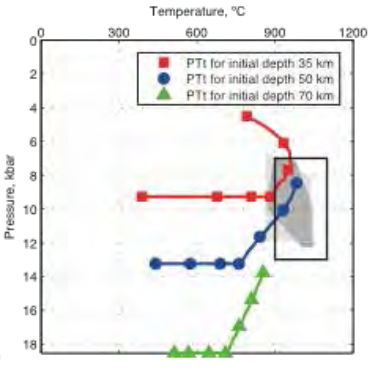

Unravelling a cryptic crustal suture.

Taylor et al. (2015) used a combination of analytical and modelling techniques to determine the nature of the Achankovil zone, an apparent crustal structure that separates the tip of India from the rest of the subcontinent.

U–Pb dating highlights the zone as being one of the last metamorphic events in the Pan-African assembly of Gondwana in this region. The metamorphism in the Achankovil zone also reached higher temperatures (up to 950ºC) than the rest of the region. The high temperatures and associated juvenile input identified from Hf isotopes suggest that the Achankovil zone does not form a separate suite of rocks in the region, but is the reworked southern margin of the craton to the north, the Madurai Block associated with the formation of a back arc basin.

This paper was the first to use the TCInvestigator software (right), calculating the expected modal abundances of key mineral phases in the samples to enable more accurate estimates of pressure-temperature conditions.

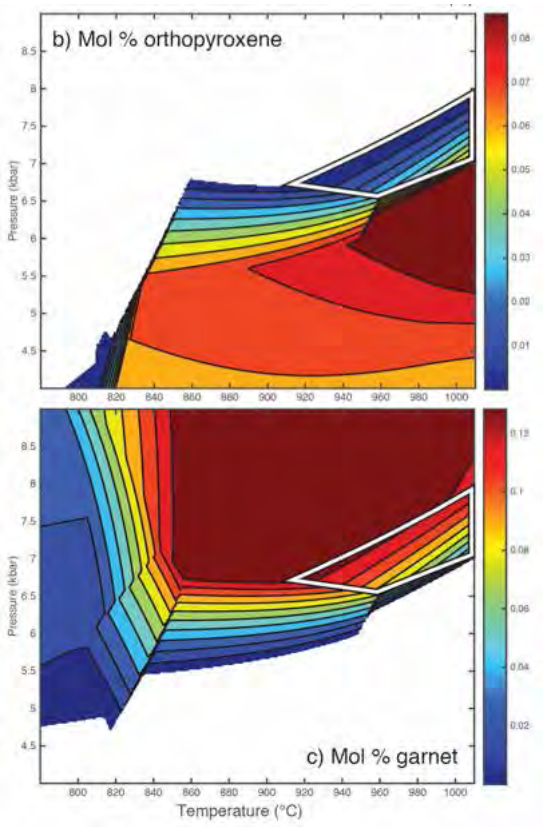

Taylor R.J.M., Clark C., Johnson T.E., Collins A.S., Santosh M. (2015) Unravelling the complexities in high-grade rocks using multiple techniques - the Achankovil Zone of southern India. *Contributions to Mineralogy and Petrology*. 169, 1-19.

Formation of the Kokchetav subduction-collision zone (northern Kazakhstan): Insights from zircon U-Pb and Lu-Hf isotope systematics.

The Kokchetav subduction-collision zone forms a part of the greater Central Asian Orogenic Belt (CAOB, ca. 1000 – 250 Ma) amalgam during which island-arc, ophiolites, accretionary wedges and Precambrian microcontinents came together to form present-day Asia. In Kazakhstan, the presence of an older Grenvillian-aged (ca. 1.2 – 1.1 Ga) basement was previously identified through U-Pb zircon dating suggesting the presence of older microcontinental blocks

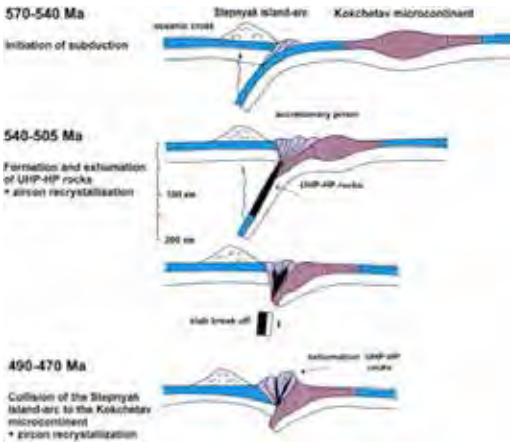

Tectonic model for the early Palaeozoic evolution of the Kokchetav subduction-collision zone (Glorie et al., 2015).

in the greater CAOB amalgam. Using U-Pb zircon dating along with Lu-Hf isotope study of the associated grains across the Kokchetav subduction-collision zone Glorie et al (2015) have shown that these Grenvillian-aged microcontinents, in fact, represent reworking of older Archean (ca. 2.5 Ga) crust believed to have been derived from Gondwana. The timing of the HP-UHP metamorphism and subsequent uplift during the collision of the Kokchetav microcontinent with the Stepnyak island-arc was established at ca. 540-520 Ma and ca. 490-480 Ma respectively.

Glorie S., Zhimulev F.I., Buslov M.M., Andersen T., Plavsa D., Izmer A., Vanhaecke F., De Grave J. (2015) Formation of the Kokchetav subduction-collision zone (northern Kazakhstan): Insights from zircon U-Pb and Lu-Hf isotope systematics. *Gondwana Research*, 27, 424-438.

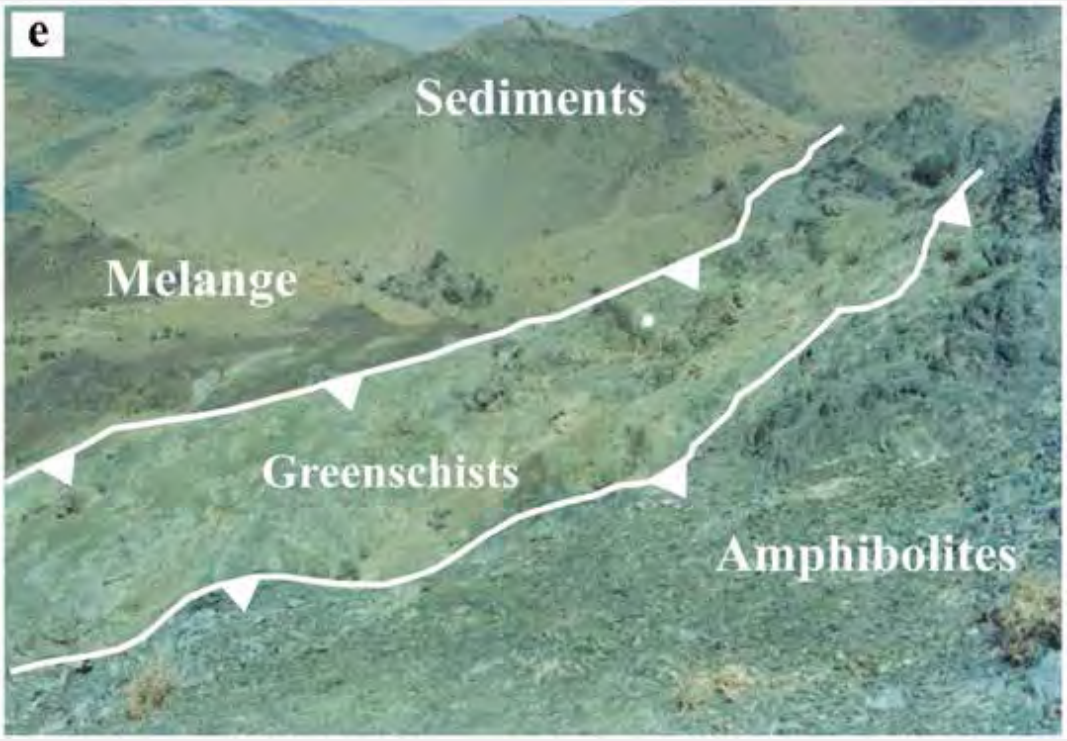

Photo showing the inverted sequence of amphibolites, greenschists and sediments of the metamorphic sole rocks underneath the Muslim Bagh Ophiolite (Pakistan).

Petrology and geochemistry of amphibolites and greenschists from the metamorphic sole of the Muslim Bagh ophiolite (Pakistan): implications for protolith and ophiolite emplacement.

Obduction of the Muslim Bagh ophiolite (Pakistan) onto the Indian continental margin occurred during the Late Cretaceous. Kakar et al (2015) have matched the geochemistry of the metamorphic sole rocks (inverted metamorphosed sequence at the base of the ophiolite) to the basalts found within the deep-ocean sediments deposited on the underlying Indian continental margin. The early basalts with OIB-type signatures found within sediments were matched to the high-grade garnet amphibolites in the metamorphic sole rocks, while the later MORB-type basalts within sediments were matched to amphibolite and greenschist-facies metamorphic sole rocks, thus providing, not only temporal, but spatial constraints on the obduction of Muslim Bagh ophiolite onto the Indian continental margin during the Late Cretaceous.

Kakar M.I., Mahmood K., Khan M., Plavsa D. (2015) Petrology and geochemistry of amphibolites and greenschists from the metamorphic sole of the Muslim Bagh ophiolite (Pakistan): implications for protolith and ophiolite emplacement. *Arabian Journal of Geosciences*, 8, 6105-6120.

Geological history of East Laurentian margin sequences: The Moine Supergroup, Scottish Caledonides.

Neoproterozoic to early Palaeozoic metasedimentary sequences of the British Caledonides provide an important record of the history of: (1) passive margin development and rifting of the supercontinent Rodinia; and (2) subsequent deformation and metamorphism associated with closure of the Iapetus Ocean and the Caledonian-Appalachian Orogeny. Cawood et al., (2015) focus on the Moine Supergroup of Scotland which occupies a central position among the now widely dispersed fragments of Neoproterozoic siliciclastic successions extending across the Atlantic Ocean from North America to East Greenland and Scandinavia. They present new U-Pb and Ar-Ar geochronological data on the provenance and timing of deformation/ metamorphism of the Moine Supergroup and consider these data in relation to previous data from the Moine and equivalent successions from other Rodinia marginal sequences. Summarised in a time-space plot our results highlight the older age of sedimentary accumulation of the Moine and correlated sequences with respect to those occurring along strike in eastern North America, and the differing record of pre-Caledonian orogeny. This is interpreted in terms of contrasting Laurentian paleaogeography during the breakup of Rodinia, i.e. the contrast between areas that were initially situated inboard and outboard of the evolving active margin.

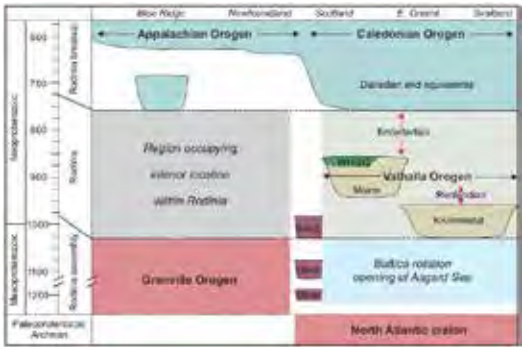

Schematic time-space plot of orogenic successions and events extending from the southeast US, through the Atlantic provinces of Canada, across Ireland and the UK to East Greenland and Svalbard. The Grenville orogen formed during Rodinia assembly, the Valhalla orogen developed along the margin of an assembled Rodinia, and the Appalachian-Caledonian orogen was initiated during Rodinia breakup.

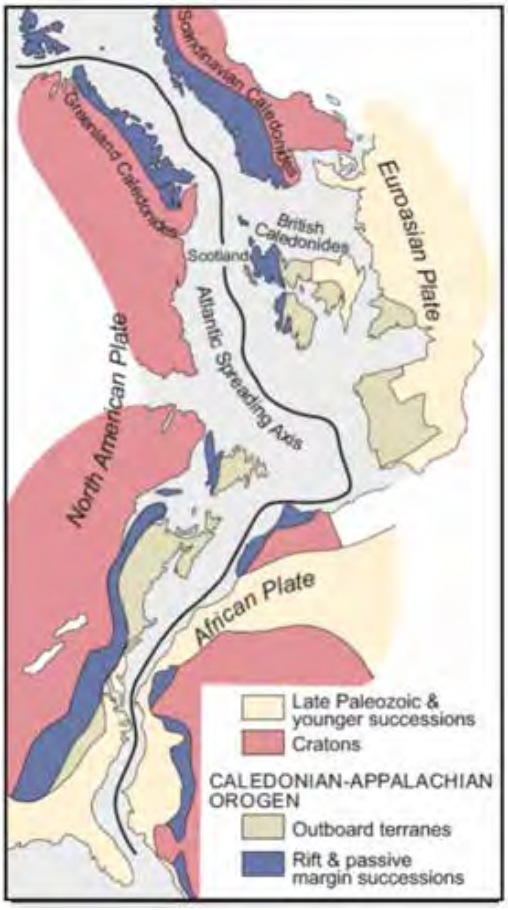

Pangean reconstruction of North America, Europe, and Africa prior to the opening of the Atlantic Ocean (after Williams 1984).

Cawood PA, Strachan RA, Merle RE, Millar IL, Loewy SL, Dalziel IWD, Kinny PD, Jourdan F, Nemchin AA & Connelly JN. (2015) *Geological Society of America Bulletin* 127, 349–371.

Growth of monazite in migmatites.

Johnson et al. (2015a) present data from a raft of metapelite enclosed within charnockite from the Nagercoil Block at the southernmost tip of peninsular India, to provide quantitative constraints on the pressure–temperature–time (*P–T–t)* evolution of the region. Phase equilibria modeling shows that the inferred peak metamorphic assemblage of garnet, K-feldspar, sillimanite, plagioclase, magnetite, ilmenite, spinel and melt is consistent with peak metamorphic pressures of 6–8 kbar and temperatures in excess of 900ºC. Subsequent growth of cordierite and biotite record high-temperature retrograde decompression to around 5 kbar and 800ºC.

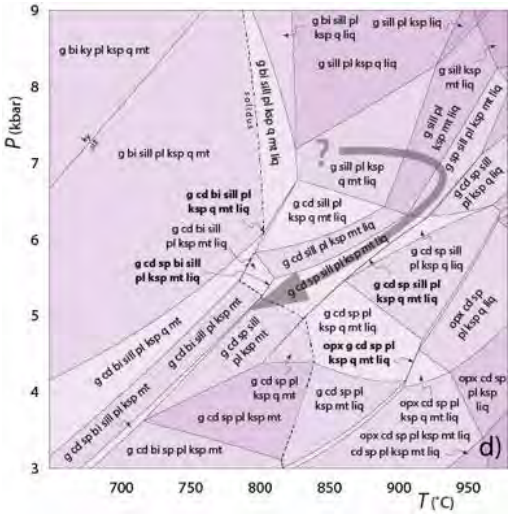

P–T pseudosection constructed for the composition of sample I12–005a, the aluminous metapelite raft at Nagercoil.

U–Pb dating of magmatic zircon cores suggests that the sedimentary protoliths were in part derived from felsic igneous rocks with Palaeoproterozoic crystallisation ages. New growth of metamorphic zircon on the rims of detrital grains constrains the onset of melt crystallisation, and the minimum age of the metamorphic peak, to around 560 Ma (Fig. 2b,c). The data suggest two stages of monazite growth. The first generation of REE-enriched monazite grew during partial melting along the prograde path at around 570 Ma via the incongruent breakdown of apatite. Relatively REE-depleted rims, which have a pronounced negative europium anomaly, grew during melt crystallisation along the retrograde path at around 535 Ma. The data suggest the rocks remained at suprasolidus temperatures for at least 35 million years and probably much longer, supporting a long-lived high-grade metamorphic history.

The combined results are similar to those previously established for other regions in peninsular India during the Ediacaran to Cambrian assembly of that part of the Gondwanan supercontinent.

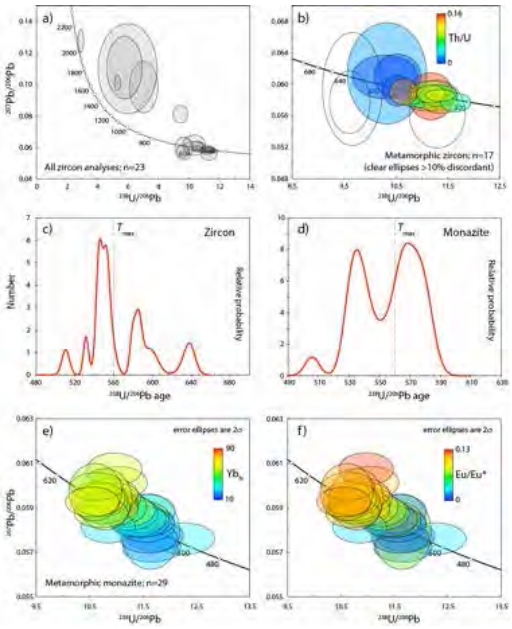

U–Pb and REE data from sample I12–005a. (a), (b) Tera-Wasserburg concordia plots showing (a) all zircon analyses and (b) metamorphic zircon colour coded for Th/U ratio. (c), (d) Probability-density plots for (c) metamorphic zirconand (d) monazite. (e), (f) Tera-Wasserburg concordia plots for monazite colour coded for (e) Yb and (f) Eu anomaly.

Johnson T.E., Clark C., Taylor R.J.M., Santosh M., Collins A.S. (2015a). Prograde and retrograde growth of monazite in migmatites: an example from the Nagercoil Block, southern India (Focus Paper). *Geoscience Frontiers*, 6, 373–387.

Grampian migmatites in Scotland.

Johnson et al., (2015b) investigated rocks exposed along the coast of NE Scotland between Fraserburgh and Inzie Head to gain insight into the evolution of the Buchan Block, the type locality for low–pressure, high–temperature regional metamorphism, and its relationship with the rest of the Grampian terrane, one of the major tectonostratigraphic components of the Scottish Caledonides. The ~8 km long section traverses a regional network of shear zones and, at the highest grades around Inzie Head, passes into the core of the Buchan Anticline, a large-scale open fold that is commonly regarded as a late structure, post-dating metamorphism. The metasedimentary rocks increase in grade from upper amphibolite to granulite facies and preserve unequivocal evidence for partial melting. The diatexite migmatites around Inzie Head, along with other gneissose units within the Buchan Block, have been regarded as allochthonous Precambrian basement rocks that were thrust into their current position during Grampian orogenesis.

However, field observations show that the onset of in situ partial melting in metapelitic rocks, associated with the formation of garnet-bearing aplites and associated pegmatites, occurred around Fraserburgh, where shear fabrics are absent. Thus, the rocks preserve a continuous metamorphic field gradient that straddles the shear zone network, suggesting that anatexis was the result of the mid-Ordovician (Grampian) metamorphism, rather than an older tectonothermal event, and that the Inzie Head gneisses are autochthonous.

Using an average mid-Dalradian pelite as a plausible representative protolith, phase equilibria modelling satisfactorily reproduces the observed appearance and disappearance of key minerals providing that peritectic garnet produced with the first formed

Contact between aplite and metapelite at Fraserburgh.

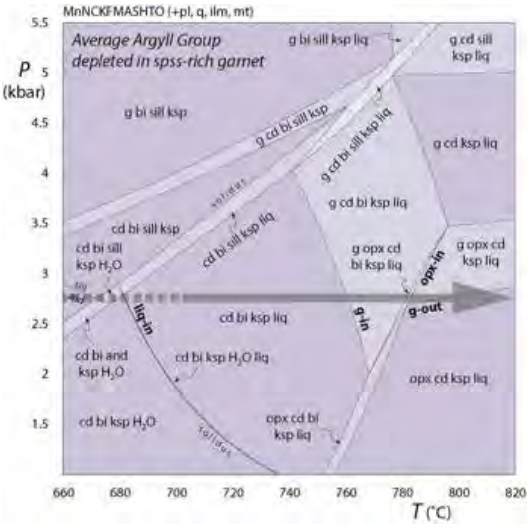

P–T pseudosection for an average Argyll Group metapelite with 0.5 mol.% spessartine-rich garnet removed The grey arrow shows an isobaric metamorphic field gradient consistent with field observations.

melts (represented by the garnet-bearing aplites) depleted the source rocks in Mn. The modelled metamorphic field gradient records a temperature increase of at least 150ºC (from around 650¬ºC near Fraserburgh to in excess of 800ºC at Inzie Head) but is isobaric at pressures of 2.7–2.8 kbar (Fig. 2), suggesting the Buchan Anticline developed synchronous with partial melting. The Buchan Anticline is likely an expression of crustal thinning and asthenospheric upwelling, which produced voluminous gabbroic intrusions that supplied the heat for Buchan metamorphism.

Johnson T.E., Kirkland C.L., Reddy S.M., Fische, S. (2015). Grampian migmatites in the Buchan Block, NE Scotland. *Journal of Metamorphic Geology*, 33, 695–709.

Timescales of mineral systems (Centre for Exploration Targeting – Curtin Node).

Mineral exploration models depend on having a reliable chronostratigraphic and tectonothermal framework, which can only be constructed with robust geochronological data. The absence of such a framework in many greenfield terrains including under regolith cover significantly increases the risk to exploration companies owing to the greater inherent uncertainty in exploration models. The recently established Curtin node of the Centre for Exploration Targeting seeks to address the broad area of Timescales of Mineral Systems, though application of innovative geochronology and isotope geology. The Timescales of Mineral Systems Theme integrates geochronology (which provides the temporal framework for mineralization) and isotope geology (which provides the crustal architecture and geodynamic setting), over a range of scales, to produce significant advancement for the understanding, predicting, and location (from proximal to ever more distal footprint) of metallogenesis.

The affinity of Archean crust on the Yilgarn-Albany-Fraser Orogen boundary: Implications for gold mineralisation in the Tropicana Zone.

Craton margins can be subject to a wide array of gold genesis and redistribution processes, although high-grade terrains on craton margins are frequently viewed as less prospective than lower-grade counterparts. In contrast to this, Kirkland et al., (2015) reported that the high-grade Tropicana Zone, a newly defined Archean crustal component on the eastern margin of the Yilgarn Craton within the Albany-Fraser Orogen, contains a significant Proterozoic gold deposit. Due to the intense granulite-facies overprinting of the Tropicana Zone rocks, determination of the magmatic protolith age is challenging. Nonetheless, the best age estimate for magmatism is 2692±16 Ma, based on the youngest zircons preserving textural evidence of growth within a viscous silicate melt. The Hf isotopic signature of the Tropicana Zone zircon shares strong similarity to that from the Eastern Goldfields Superterrane of the Yilgarn Craton. This implies that the Tropicana Zone reflects a deeper crustal level of the Yilgarn Craton, exhumed and thrust NW an unknown distance over the craton edge. Re-Os dating of pyrite coeval with one generation of gold in these rocks indicates model ages of c. 2100 Ma, supportive of a Palaeoproterozoic age of mineralisation. This mineralisation event is distinct from major Proterozoic tectonothermal events elsewhere in the AFO. Low-Si, LILE-enriched magmas are well-known for gold fertility and were likely the original source of gold in the Tropicana Zone, which was subsequently concentrated into brittle structures during several episodes. Gold mineralisation post-dated peak metamorphic conditions and is significantly younger than gold mineralisation within other parts of the adjoining Yilgarn Craton.

Kirkland C. L., Spaggiari C., Smithies R., Wingate M., Belousova E., Gréau Y., Sweetapple M., Watkins R., Tessalina S.G., Creaser R. (2015). The affinity of Archean crust on the Yilgarn-Albany-Fraser Orogen boundary: Implications for gold mineralisation in the Tropicana Zone. *Precambrian Research* 266: 260-281.

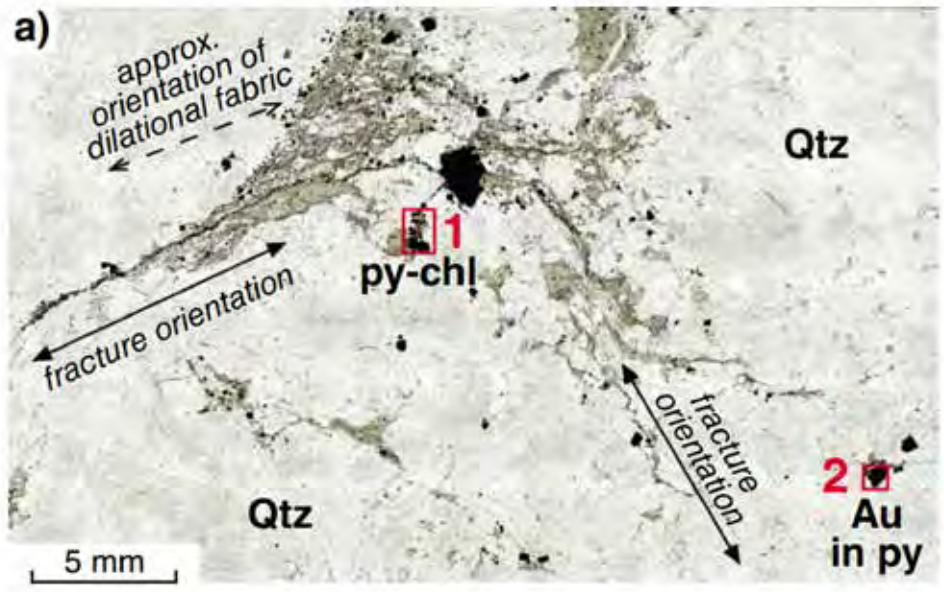

Transmitted-light image of chlorite–pyrite segregations and fracture fillings, and their structural relationships from the Tropicana Zone of the Albany-Fraser Orogen.

Superimposed giant rhyolite systems in the hot and thinned crust of Mesoproterozoic central Australia.

Smithies et al., (2015) discuss Mesoproterozoic bimodal volcanic sequences from the Talbot Sub-basin in central Australia which contain evidence of the world's most voluminous accumulation of ^{18}O-depleted rhyolite. This volcanic system differs from the better known, but geochemically similar, Miocene Snake River Plain – Yellowstone Plateau of North America. Both systems witnessed 'super' sized eruptions from shallow crustal chambers, and produced ^{18}O-depleted rhyolite. The Talbot system, however, accumulated over a much longer period (>30 Ma), at a single depositional centre, and from a magma with mantle-like isotopic compositions that contrast strongly with the isotopically evolved basement and country-rock compositions. Although giant low $\delta^{18}O$ volcanic systems are frequently viewed as being feed by voluminous melting of upper crust, this study indicates that felsic magmas generated at lower crustal depths can also contribute significantly to the thermal and material budget of these systems. In the case of the Talbot system, data reported in Smithies et al., (2015) suggests that an unusually hot pre-history might also be required to thermally prime the crust. Such unusually high thermal conditions have implications for the mineral systems developed in the Musgraves of central Australia.

Smithies R., Kirkland C.L., Cliff J., Howard H., Quentin de Gromard R. (2015). Syn-volcanic cannibalisation of juvenile felsic crust: Superimposed giant 18O-depleted rhyolite systems in the hot and thinned crust of Mesoproterozoic central Australia. *Earth and Planetary Science Letters* 424, 15-25.

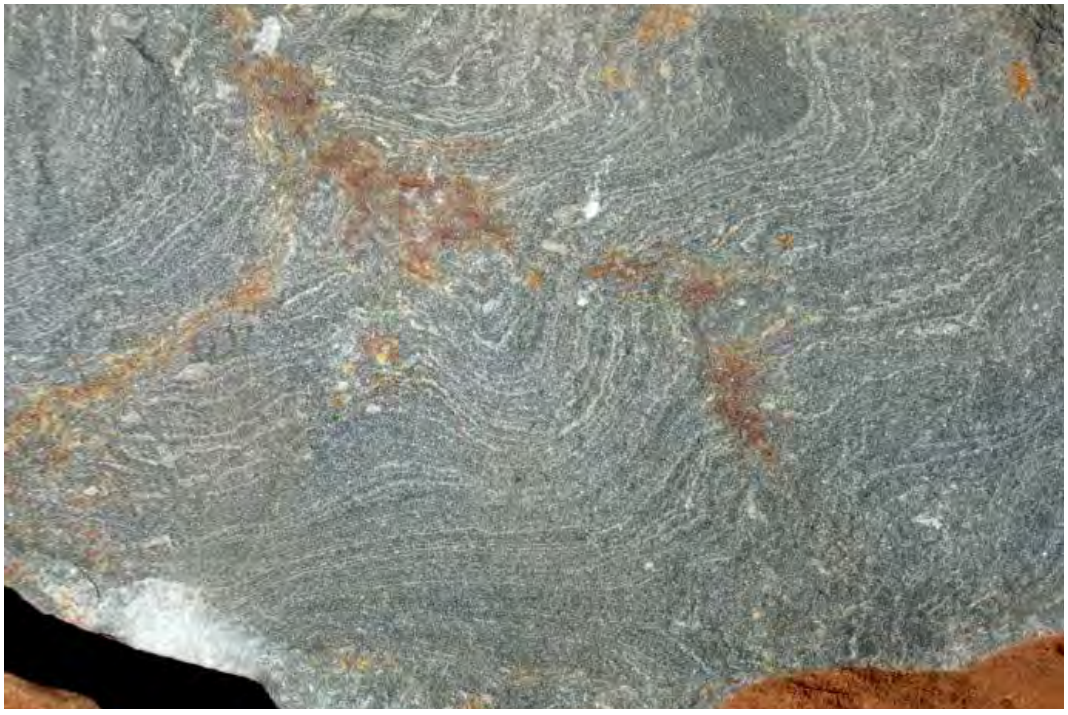

Welded ash-fall tuff from the Musgrave Province of central Australia reflecting one of the largest accumulations of ^{18}O-depleted rhyolite globally.

Oxygen isotopes in Pilbara Craton zircons support a global increase in crustal recycling at 3.2Ga.

Van Kranendonk et al., (2015) measured oxygen isotopes in zircon crystals from a suite of Paleo- to Mesoarchean igneous and sedimentary rocks from the Pilbara Craton in order to test prevailing models of early Earth tectonic evolution. Results from this work indicated that igneous zircon crystals older than 3.2Ga in the Pilbara Craton have mantle-like oxygen isotope signatures, whereas zircon grains younger than c. 3.2Ga show, on average, isotopically heavier $\delta^{18}O$ values.The data support a change in tectonic style in the Pilbara Craton at 3.2 Ga, from early crustal growth through magmatic accretion above upwelling, hot mantle, to crustal growth that involved significant amounts of crustal recycling arising from the onset of modern-style plate tectonics (steep subduction of old cold oceanic lithosphere). These results align with global datasets of oxygen isotopes, and point to a more general change in the geodynamics of Earth associated with the secular decrease in heat output of our planet.

Van Kranendonk M., Kirkland C.L., Cliff J. (2015). Oxygen isotopes in Pilbara Craton zircons support a global increase in crustal recycling at 3.2Ga. *Lithos* 228-229: 90-98.

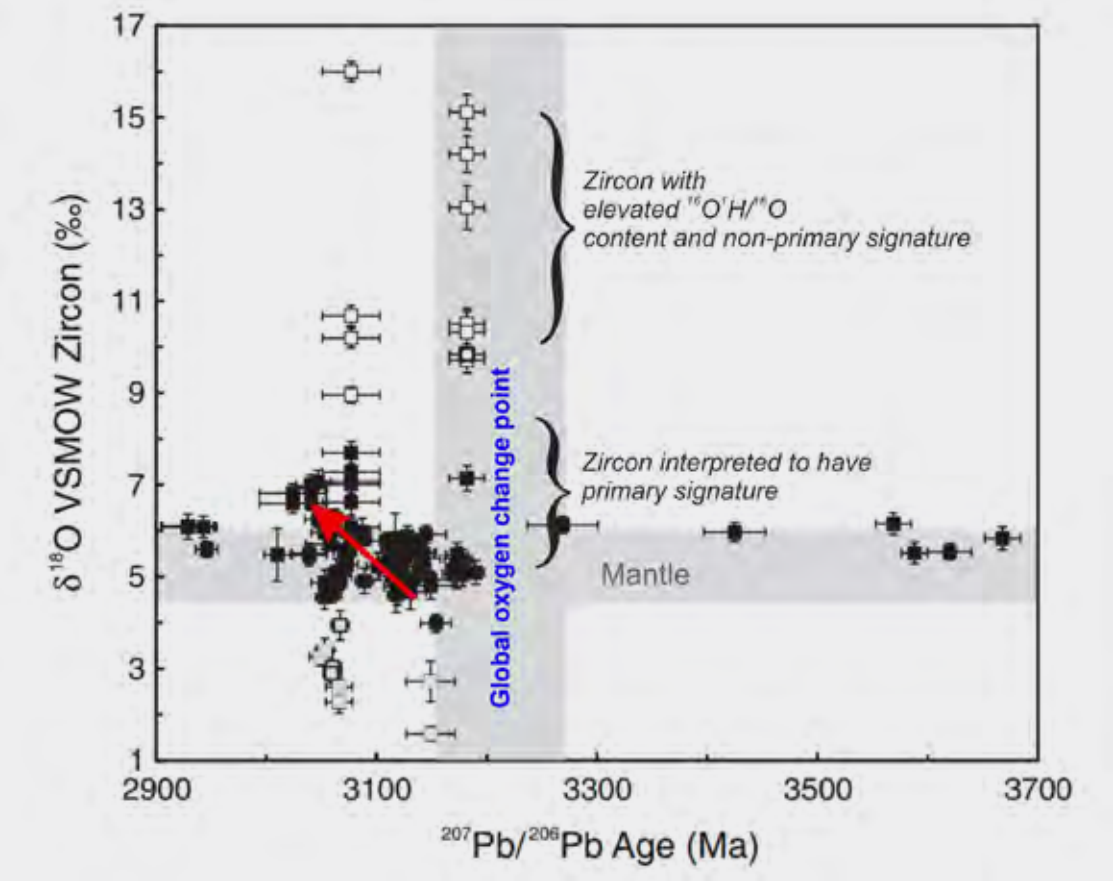

U-Pb and oxygen isotopic signatures from zircon grains in the Pilbara Craton used to characterize its geological evolution.

Constraining the age of suturing and basin formation in Northern Thailand and Myanmar.

There remains considerable uncertainty around the timing of major Mesozoic-Cenozoic tectonic events within Southeast Asia. The region has experienced a complex tectonic history related to the closing of Tethys, which within SE Asia is complicated by the ongoing clockwise rotation of accreted terranes around the Eastern Himalayan Syntaxis leading to major lateral faulting. Isotope geochemistry is one of the few ways of unpicking the geological history of this part of the Tethyan margin. Working with colleagues in Oxford, Keyworth and Chiang Mai, Gardiner et al., (2015) have focused on two major tectonic epochs affecting Northern Thailand and Eastern Myanmar (a) Mid-Mesozoic and the suturing of Palaeo-Tethys and (b) constraining the age of economically-important late Cenozoic basins.

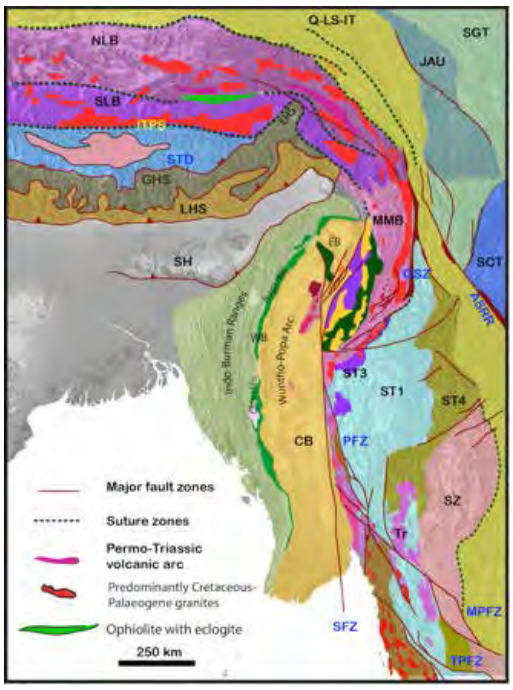

Terrane map of Southeast Asia.

The first ever zircon U-Pb and Lu-Hf data was reported from Eastern Myanmar. This, coupled with new data from northern Thailand, suggested that Palaeo-Tethyan suturing occurred ca. 220 Ma. Our data also proposed Palaeo-Proterozoic model ages for the basement beneath Eastern Myanmar (ca. 1750 Ma), which is a step towards understanding how this poorly-studied part of SE Asia may link through to Yunnan to the north, and the Malay Peninsula to the south. Through U-Pb geochronology in zircon and monazite they also proposed a new, younger, Miocene age of detachment faulting that unroofed the Doi Inthanon metamorphic core complex in Thailand, suggesting that this was part of a major extension event that led to the formation of the Chiang Mai basin.

Gardiner N.J., Searle M.P., Morley C.K., Whitehouse M.J., Spencer C.J., Robb L.J. (2015). The Closure of Palaeo-Tethys in Eastern Myanmar and Northern Thailand: New Insights from Zircon U-Pb and Hf Isotope Data. *Gondwana Research* doi:10.1016/j.gr.2015.03.001

Gardiner N.J., Roberts N.M.W., Morley C.K., Searle M.P., Whitehouse M.J. (2016). Did Oligocene crustal thickening precede basin development in Northern Thailand? A geochronological reassessment of Doi Inthanon and Doi Suthep. *Lithos* 240-243, 69-83.

Tin Mining in Myanmar.

A recent side-study of tin production in Myanmar focused on the sudden emergence of the country as the World's third biggest tin producer in 2014. Gardiner et al., (2015b) investigated the current state of the global tin mining industry and the role Myanmar may play in the medium-term. The tin price experienced a significant increase since 2000 due to the use of tin as a substitute for lead in solder. However, because of the tin price crash in the 1980s, the exploration pipeline has very few new tin projects at advanced stages. It appeared that Myanmar emerged from obscurity to plug this supply gap, a potential "black swan" event. However, this new production came from a mining region close to the Chinese border, and not from the traditional tin-producing areas in the south.

Gardiner N.J., Sykes J.P., Trench A., Robb L.J. (2015). Tin mining in Myanmar: Production and potential. *Resources Policy* 46, 219-233

Isotope Geochemistry

Isotope Geochemistry is at the cross-roads of Chemistry, Physics and Geology. Radiogenic and stable isotopes are used widely in the Earth sciences to determine the ages of rocks and extra-terrestrial materials, and as tracers to understand geological and environmental processes. Isotope methods determine the age of the Earth, help reconstruct the climate of the past, and explain the formation of the chemical elements in the Universe. It contributes to the Earth Past theme in TIGeR.

Application of Radiogenic Isotopes in Geosciences – Overview and Perspectives.

Tessalina et al. (2015) summarised the recent advances in the application of radiogenic isotopes for Geosciences. Radiogenic isotope geochemistry forms an integrated part of Geosciences in a range of applications, starting from formation of planetary systems, genesis and evolution of Earth's lithosphere and associated mineral and oil deposits, as well as environmental tracers. There are two primary types of information available from radiogenic isotopes studies: age determination and isotopic source tracing. Tessalina et al., (2015) review the range of isotope systematics currently used in Geosciences and their applications, together with progress in analytical technologies.

Tessalina S., Jourdan F., Nunes L., Kennedy A., Denyszyn S., Puchtel I., Touboul M., Creaser R., Boyet M., Belousova E., Trinquier A. (2015) Application of Radiogenic Isotopes in Geosciences – Overview and Perspectives In: *Principles and Practice of Analytical Techniques in Geosciences* (Ed. Kliti Grice), RSC Detection Science Series, Royal Society of Chemistry, 49-93. ISBN 1849736499, 9781849736497

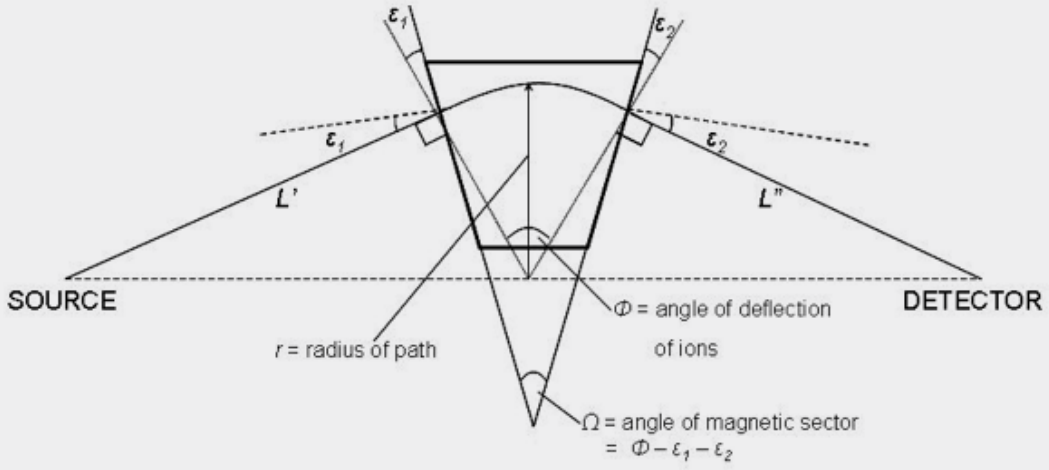

General schematic of a mass spectrometer magnetic sector arrangement.

Silver isotopes as new tracers of metal sources and ore formation processes.

Silver has two naturally occurring stable isotopes: ^{107}Ag and ^{109}Ag. Tessalina et al. (2015) examined samples of native silver metal extracted from porphyry Cu-Mo, volcanic-hosted massive sulphide (VHMS), sedimentary-exhalative (SEDEX) Pb-Zn, epithermal and placer Au deposits, which show a range of $\varepsilon^{107}Ag$ from -4.6 to +3.3. The most negative values were obtained for native silver from the Sorskoye porphyry Cu-Mo and Imiter epithermal Ag deposits, and correlate with a predominantly mantle source of ore metals. The most positive values were encountered for the clastic metasediment-hosted Nochnoye Ag-Pb-Zn deposit and the Broken Hill SEDEX polymetallic deposit, the latter with a crustal source of ore metals confirmed using other isotopic systematics. The $\varepsilon^{107}Ag$ values of the Teutonic Bore VHMS deposit ($\varepsilon^{107}Ag$ = -1.1) occupy an intermediate position, close to the Bulk Silicate Earth (BSE) value of -2.2±0.7. These variations in Ag isotopic composition in mineral systems maybe related with: (1) physico-chemical processes of ore formation at relatively low temperatures (100-150ºC); (2) inherited Ag isotopic variability from the protoliths or metal sources; and/or (3) nuclear volume decrease due to s-electron removal during the oxidation of Ag^0 to Ag^+. These factors may be interconnected in nature.

If Ag stable isotopes studies are found to assist in the identification of silver source(s) these data can be applied to the study of gold deposits. Gold itself is monoisotopic, and cannot provide an isotopic fingerprint of its source region to provide constraints on ore deposit processes. Gold won from Au deposits is rarely pure gold, and often contains >10% silver. As such, this study provides a real and perhaps unique opportunity to identify the source of noble metals in a range of gold deposits.

Tessalina S.G., Rankenburg K., Naumov E., Goryachev N.A., Savva N.E. (2015) The Ag Isotope Systematics in Native Silver from Some Hydrothermal Deposits: Toward a New Tool for Mineral Deposits Studies. In: *Mineral resources in a sustainable world*, 13th SGA Biennial meeting Proceedings, Nancy, France (Eds André-Mayer A.-S., Cathelineau M., Muchez P., Pirard E. and Sindern S., Vol 2, pp 647-650.

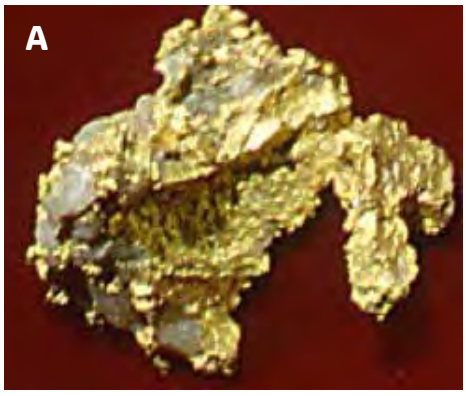

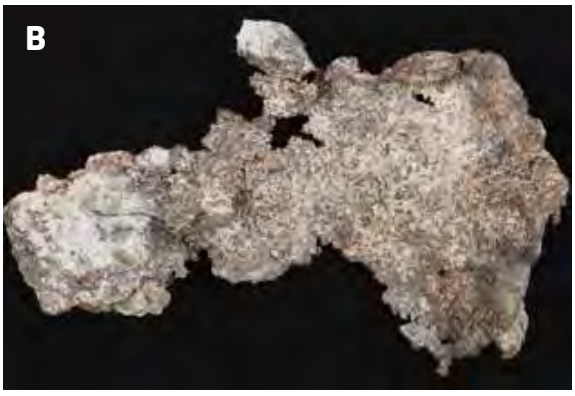

A. Native gold sample from Dickie Lee mine in Meekatharra, Western Australia (donated by WA Museum).
B. Native silver specimen from Elizabeth Hills, Pilbara (donated by WA Museum).

Dating basement units in the Buenos Aires region.

Chernicoff et al. (2015) present U–Pb Sensitive High Mass Resolution Ion MicroProbe (SHRIMP) data of unexposed igneous-metamorphic basement rocks from two areas of the southeastern Río de la Plata Craton and discuss the tectonic evolution of that portion of the craton based on both the new data and previous work. The newly-obtained geochronological data of drill cores indicate that: (a) arc magmatism occurred at 2164–2186 Ma corresponding to early 'Trans-Amazon' (early Rhyacian) arc magmatism; (b) the age of collision between the terranes is inferred to have commenced at ca. 2110 Ma; (c) peak metamorphism occurred at ca. 2069 Ma; and (d) the presence of rocks related to the craton is confirmed under Cenozoic sediments.

Chernicoff C.J., Zappettini E.O., Santos J.O.S., Pesce A., McNaughton N.J. (2015). Zircon and titanite U-Pb SHRIMP dating of unexposed basement units of the Buenos Aires region, southeastern Rio de la Plata Craton, Argentina. *International Geology Review* 58, 643-652.

The Kalgoorlie Gold field revisited.

The Neoarchaean Kalgoorlie Gold Field contains the giant Golden Mile and world-class Mt Charlotte deposits, which have been the subject of much research for over 100 years. Direct timing constraints on gold mineralization indicate that Fimiston- and Mt Charlotte-style mineralization formed within a relative short period of time around 2.64 Ga, and, as such, support a model of progressive deformation of a rheologically heterogeneous rock package late in the structural history. Fluid characteristics, combined with the structural, metamorphic and absolute timing, support description of gold mineralization at the Golden Mile as orogenic and mesozonal, and this allows direct correlation with orogenic gold deposits worldwide, which classically formed during accretion along convergent margins throughout Earth history.

Vielreicher N.M, Groves D.I., McNaughton N.J. (2015). The giant Kalgoorlie Gold Field revisited. *Geoscience Frontiers*. doi:10.1016/j.gsf.2015.07.006

Constraining the sediment provenance in the Sergipano orogeny, Brazil.

Oliveira et al. (2015) combined SHRIMP U–Pb detrital zircon geochronology and depleted-mantle Nd-model ages of clastic rocks to understand the sediment provenance in the Neoproterozoic Sergipano Belt. The Sergipano Belt is the main orogenic belt between the Borborema province and the São Francisco Craton, eastern South America; it is divisible into several lithostratigraphic domains from North to South: Canindé, Poço Redondo-Marancó, Macururé, Vaza Barris, and Estância. The preliminary results support a model in which sediments of the Marancó and Macururé domains were deposited on a continental margin of the ancient Borborema plate before its collision with the São Francisco Craton; the Canindé domain is likely to be an aborted Neoproterozoic rift assemblage within the southern part of the Borborema plate (Pernambuco-Alagoas massif). The basal units of the Vaza Barris and Estância domains have clast sources from the São Francisco Craton and are best interpreted as passive margin sediments. However, the uppermost units of the Estância and Vaza Barris domains come from foreland basins formed during collision of Borborema plate with the São Francisco Craton.

Oliveira E.P., McNaughton N.J., Windley B.F., Carvalho M.J., Nascimento R.S. (2015). Detrital zircon U-Pb geochronology and whole-rock Nd-isotope constraints on sediment provenance in the Neoproterozoic Sergipano orogen, Brazil: from early passive margins to late syn-orogenic basins. *Tectonophysics* 662, 183-194.

Using zircon ages to delimit the provenance of a sand extradite in Brazil.

Ion microprobe age determinations of 102 detrital zircon crystals from a sand extrudite, Cretaceous Paraná volcanic province, set limits on the origin of the numerous sand layers present in this major flood basalt province. The zircon U-Pb ages reflect four main orogenic cycles: Mesoproterozoic (1155-962 Ma), latest Proterozoic-early Cambrian (808-500 Ma) and two Palaeozoic (Ordovician- 480 to 450 Ma, and Permian to Lower Triassic- 296 to 250 Ma). Two additional small concentrations are present in the Neoarchean (2.8 to 2.6 Ga) and Paleoproterozoic (2.0 to 1.7 Ga). Zircon age peaks closely match the several pulses of igneous activity in the Precambrian Brazilian Shield and active orogeny in Argentina.

Pinto V.M., Hartmann L.A., Santos J.O.S., McNaughton N.J. (2015). Zircon ages delimit the provenance of a sand extradite from the Botucatu Formation in the Parana volcanic province, Irai, Brazil. *Anais de Academia Brasileira de Ciencias* 87, 1611-1622.

The timing of gold mineralisation in the eastern Yilgarn craton.

The highly mineralized Eastern Goldfields of the eastern Yilgarn craton is an amalgamation of dominantly Neoarchaean granitoid-greenstone terranes and domains that record a history of early rifting, followed by westward directed collision with initial arc formation, collision and clastic basin formation, and final accretion to the western Yilgarn proto-craton between 2.66 and 2.60 billion years ago. The gold deposits that define this region as a world-class gold province are the product of orogenic processes that operated during accretion late in the tectonic history, after initial compressional deformation and the majority of granitoid magmatism. Vielreicher et al. (2015) present robust SHRIMP U–Pb geochronology of gold-related hydrothermal xenotime and monazite showing that gold mineralization occurred during late transpressional events shortly before cratonization.

Vielreicher N.M., Groves D.I., McNaughton N.J., Fletcher I.R. (2015a). The timing of gold mineralization across the eastern Yilgarn craton using U–Pb geochronology of hydrothermal phosphate minerals. *Mineralium Deposita* 50, 391–428.

Vielreicher N.M., Groves D.I., McNaughton N.J. (2015b). Reply to Discussion: The timing of gold mineralization across the eastern Yilgarn craton using U–Pb geochronology of hydrothermal phosphate minerals. *Mineralium Deposita* 50, 889-894.

Geochronological constraints in tectonic evolution of the North China Craton

The Taihua Complex is an important metamorphic rock suite at the southern margin of the Trans-North China Orogen and hosts important mineral deposits. Its protolith and metamorphic ages are still controversial. Li et al. (2015) report new U/Pb age data on zircons and titanite that supports a tripartitite division into the Beizi Group (3.0–2.55 Ga), the Dangzehe Group (2.55–2.3 Ga) and the Shuidigou Group (2.3–2.1 Ga). Compiling zircon U–Pb ages indicate that in the Trans-North China Orogen, the 1.95 Ga and 1.85 Ga metamorphic events are widespread and prominent.

Li N., Chen Y.J., McNaughton N.J., Ling X.X., Deng X.H.,Yao J.M., Wu Y.S. (2015). Formation and tectonic evolution of the khondalite series at the southern margin of the North China Craton: geochronological constraints from a 1.85 Ga Mo deposit in the Xiong'ershan area. *Precambrian Research* 269, 1-17.

Clarifying the age of a metasedimentarty sequence from Minas Gerais, Brazil.

The itabirite-bearing metasedimentary sequence from Morro Escuro Ridge comprises the basal units of the Espinhaço Supergroup and makes up a small tectonic inlier developed during one of the Brasiliano orogenic events (800-500 Ma), exposed within the Archean TTG gneisses, including sheared granites of the anorogenic Borrachudos Suite (~1700 Ma). The maximum Statherian deposition age (1668 Ma) was established using SHRIMP U–Pb isotopic constraints on zircon grains from conglomerate and quartzite units overlying the itabirite. The itabirite is predominantly hematitic and its geochemical characteristics are typical of a Lake Superior-type BIF deposited in a platformal, suboxic to anoxic environment distant from Fe-bearing hydrothermal vents.

Braga F.C.S., Rosiere C.A., Queiroga G.N., Rolim V.K., Santos J.O.S., McNaughton, N.J. (2015). The Statherian itabirite-bearing sequence from the Morro Escuro Ridge, Santa Maria de Itabira, Minas Gerais, Brazil. *Journal of South American Earth Sciences* 58, 33-53.

Age, composition and source of granites of the Serginpano Belt, Brazil.

The Sergipano belt is the outcome of collision between the Pernambuco-Alagoas Domain (Massif) and the São Francisco Craton during Neoproterozoic assembly of West Gondwana. Although the understanding of the Sergipano belt evolution has improved significantly, the timing of emplacement, geochemistry and tectonic setting of granitic bodies in the belt is poorly known. Oliveira et al. (2015) recognized two granite age groups: 630–618 Ma granites in the Canindé, Poço Redondo and Macururé domains, and 590–570 Ma granites in the Macururé metasedimentary domain. These granitoids are dominantly high-K calc-alkaline, magnesian, metaluminous, mafic enclave-rich (Queimada Grande and Lajedinho), or with abundant inherited zircon grains (Poço Redondo and Sitios Novos).

Oliveira E.P., Bueno J.F., McNaughton N.J., Silva Filho A.F., Nascimento R.S., Donatti-Filho J.P. (2015). Age, composition, and source of continental arc- and syn-collision granites of the Neoproterozoic Sergipano Belt, Southern Borborema Province, Brazil. *Journal of South American Earth Sciences* 58, 257-280.

Subducted slabs in the Bohemian Massif.

Four detrital zircon concentrates from the metasediments and metavolcanics of the Central Sudetes, Bohemian Massif, have been dated using SHRIMP II. The dated samples come from two adjacent suspect terranes – the Orlica–Śnieżnik dome and the Kłodzkomassif in the Central Sudetes that are characterised by contrasting timing of metamorphism and exhumation. Despite this difference, the results obtained show, in conjunction with earlier data, a similar provenance of the studied units and their common affinity to the Saxo-Thuringian terrane.

Mazur S., Turniak K., Szczepański J., McNaughton N.J. (2015). Vestiges of Saxothuringian crust in the Central Sudetes, Bohemian Massif: Zircon evidence of a recycled subducted slab provenance. *Gondwana Research* 27, 825-839.

Geochronological constraints on the Tropicana Gold Deposit.

Gold mineralization at the Tropicana mine occurs within the Plumridge terrane along the eastern margin of the Archean Yilgarn craton in the Albany-Fraser orogen, Western Australia. Mineralization is hosted in a favorable syenitic lithofacies of the Tropicana Gneiss with a minimum igneous age of 2638 ± 4 Ma (2σ) and which was metamorphosed to mid-amphibolite to lower granulite facies in the period ca. 2638 to 2520 Ma. The Tropicana Gneiss was exhumed to crustal levels equivalent to greenschist-facies conditions by the time of economic gold mineralization at ca. 2.52 Ga. The major gold-bearing pyrite-biotite-sericite mineralization formed in association with shear zones during northeast-southwest compression that postdated W- to NW-verging thrusting. The late fluid-induced event produced a mineral assemblage indicative of greenschist-facies conditions.

Doyle M.G., Fletcher I.R., Foster J., Large R.R., Mathur R., McNaughton N.J., Meffre S., Muhling J.R., Phillips D., Rasmussen B. (2015). Geochronological constraints on the Tropicana Gold Deposit and Albany Fraser Orogen, Western Australia. *Economic Geology* 110, 355-386.

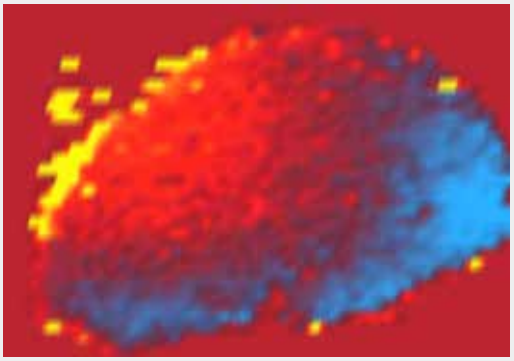

Map of W-content in a 100 micron rutile grain.

Low temperature thermochronology and reactivation of the Beishan Orogenic Belt.

The Beishan Orogenic Collage (BOC) is located in the southeast of the Central Asian Orogenic Belt (CAOB) and formed during final consumption of the Palaeoasian Ocean in the late Palaeozoic. Gillespie et al., (2015) applied low temperature thermochronology to constrain the Meso-Cenozoic history of the BOC. The cooling events described in the paper are thought to be related to the progressive closure of the (Palaeo-)Tethys ocean to the south. Associated collision and accretion of micro-continental blocks and island–arcs at the southern Eurasian margin are interpreted to have induced more widespread reactivation and exhumation in Central Asia than previously anticipated, extending to the northern margin of the Tarim Craton. This observation hence refines the existing tectonic history models for Central Asia.

Gillespie J., Glorie S., Xiao W., Zhang Z., Collins A.S., Evans, N.J., McInnes B.I.A., De Grave J. (2015). Mesozoic reactivation of the Beishan, southern Central Asian Orogenic Belt: Insights from low-temperature thermochronology. *Gondwana Research*. 10.1016/j.gr.2015.10.004

Thermal history of the Qulong porphyry Cu–Mo deposit, Tibet.

Zhao et al., (2015) present a complete thermal history for this deposit. Zircon U–Pb geochronology indicates that the mineralization at Qulong resulted from brecciation-veining events associated with the emplacement of a series of intermediate-felsic intrusions. Combined with previously published ages, their results reveal a whole intrusive history of the Qulong composite pluton. Their AHe thermochronology results suggest that neither the Gangdese thrust system, nor the Yadong–Gulu graben affected or accelerated exhumation at the Qulong deposit.

Zhao J., Qin K., Xiao B., McInnes B., Li G., Evans N.J., Cao M., Li J. (2015). Thermal history of the Qulong giant Cu-Mo deposit, Gangdese metallogenic belt, Tibet: Constraints on magmatic-hyrdothermal evolution and exhumation. *Gondwana Research* doi:10.1016/j.gr.2015.07.005

Petrogenesis of granitoids from Tibet.

Li et al., (2015) describe Triassic granitoids, around the Longmu–Shuanghu suture and in the Qiangtang terrane, central Tibet. The majority can be classified as high-K calc-alkaline in nature and yield negative Ba and Sr anomalies on primitive mantle-normalized diagrams. In addition, they are: enriched in light rare earth elements (LREE) ((La/Yb)N = 1.61–21.79); strongly enriched in large ion lithophile elements (LILE: e.g., Cs, Rb, and K), and depleted in high field strength elements (HFSE: e.g., Nb and Ti). The granitoids may have formed during melting of southern Qiangtang crust, heated by upwelling asthenosphere mantle, a result of break-off and delamination of the Paleo-Tethys slab in a collisional setting.

Li G.M., Li X.J., Zhao J.X., Qin,K.Z., Cao M., Evans N.J. (2015). Petrogenesis and tectonic setting of Triassic granitoids in the Qiangtang terrane, central Tibet: Evidence from U–Pb ages, petrochemistry and Sr–Nd–Hf. *Journal of Asian Earth Sciences*, 105. DOI: 10.1016/j.jseaes.2015.02.017

Thermochronometry to constrain the emplacement and exhumation.

De Grave et al., (2015) have used multi-method thermochronometry to constrain the emplacement and exhumation of Kunashir island in the Kuril island arc system. Differentiated, tonalitic–granodioritic rocks were collected from these small intrusive bodies. An early Oligocene zircon LA-ICP-MS U/Pb age of 31 Ma for the Prasolov Complex was obtained, showing that the basement of Kunashir Island is older than previously thought. Thermochronometry (apatite fission-track and U-Th-Sm/He and zircon U-Th/He analyses) further showed that the magmatic basement of the island was rapidly exhumed in the Pleistocene to present levels in a differential pattern, with He-ages ranging from 1.9 to 0.8 Ma. It is shown that the northern section of the island was therefore exhumed more intensely.

De Grave J., Zhimulev F.I., Glorie S., Kuznetsov G.V., Evans N., Vanhaecke F., McInnes B. (2015). Late Palaeogene emplacement and late Neogene–Quaternary exhumation of the Kuril island-arc root (Kunashir island) constrained by multi-method thermochronometry. *Geoscience Frontiers*, doi: 10.1016/j.gsf.2015.05.002.

A new technique for in situ double dating.

Evans et al (2015) report on a new laser-based technique for rapid, quantitative and automated in situ double dating (U–Pb and (U–Th–Sm)/He) of minerals, for applications in geochronology, thermochronology and geochemistry. In situ laser microanalysis offers several advantages over conventional bulk crystal methods in terms of spatial resolution, productivity, and safety. This new approach/methodology utilizes an interoperable and integrated suite of analytical instruments including a 193 nm ArF excimer laser system, quadrupole ICP-MS, quadrupole helium mass spectrometry system and swappable flow-through and ultra-high vacuum analytical chambers.

The in situ double dating method described is applied to the Ellendale lamproite pipe and country rocks, Western Australia and successfully replicates conventional U–Pb and (U–Th–Sm)/He age variations determined previously by conventional techniques.

Evans N.J., McInnes B.I.A., McDonald B., Danisik M., Becker T., Vermeesch P., Shelley M., Marillo-Sialer E., Patterson D.B. (2015). An in situ technique for (U-Th-Sm)/He and U-Pb double dating. *Journal of Analytical Atomic Spectroscopy*, 30, 1636-1645

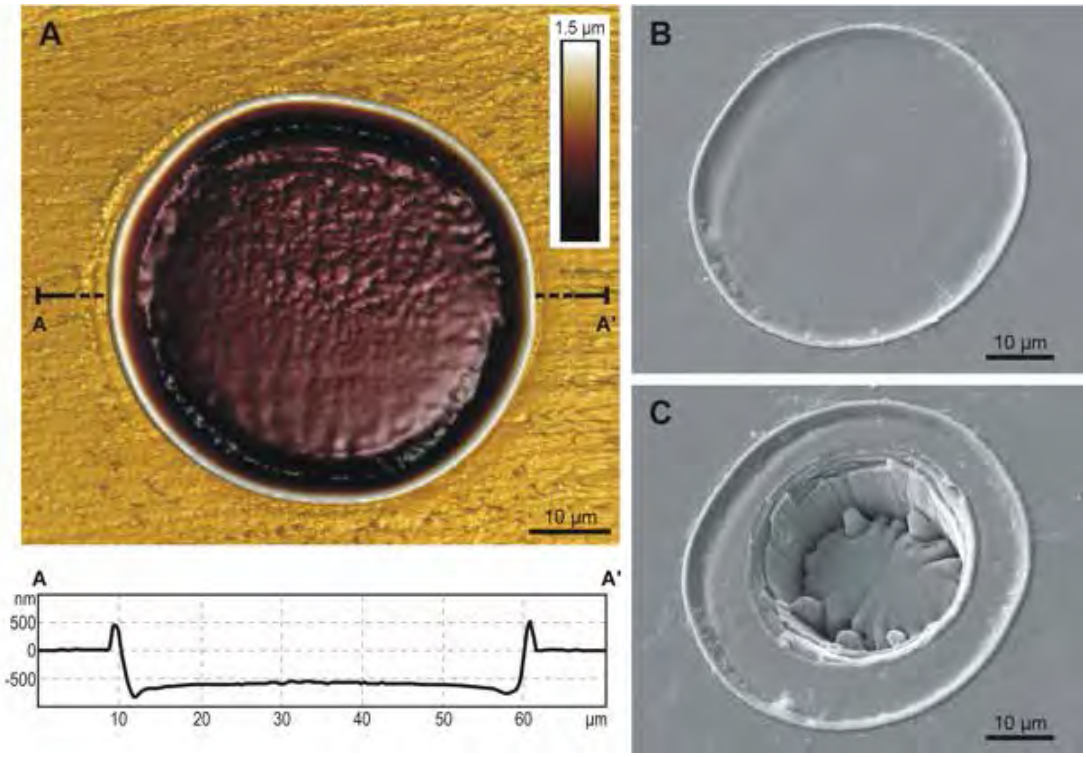

(A) Topographic AFM image of a shallow 4He ablation pit in zircon. The volume of the raised rim surrounding the laser pit was excluded for volume analysis, with the volume calculated from the 3D topography of the pit below the surface level of the sample. Note the simple 'top-hat' cross-sectional profile with a well-defined, flat bottom. (B) SEM image of first, shallow ablation pit for helium measurement and (C) after second ablation pit for U, Th, Sm, Pb and trace element analysis.

Geochronological and thermal modeling of Cenozoic events in the Pannonian Basin.

Danišík et al., 2015 applied Independent geochronological and thermal modelling approaches to a biostratigraphically exceptionally well-controlled borehole, Alcsútdoboz-3 (Ad-3), in order to constrain the age of Cenozoic geodynamic events in the western Pannonian Basin and to test the efficacy of the methods for dating volcanic rocks. Their results demonstrate that, contrary to common perception, the apatite (U–Th)/He method is likely to record 'apparent' or 'mixed' ages resulting from subsequent thermal events rather than 'cooling' or 'eruption' ages directly related to distinct geological events. It follows that a direct conversion of 'apparent' or 'mixed' (U-Th)/He ages into cooling, exhumation or erosion rates is incorrect.

Danišík M., László Fodor, L., Dunkl I., Gerdes A., Csizme, J., Hámor-Vidó M., Evans N.J. (2015). A multi-system geochronology in Ad-3 borehole, Pannonian Basin (Hungary) with implications for dating volcanic rocks by low-temperature thermochronology. *Terra Nova*, doi: 10.1111/ter.12155.

Zircon Th/U ratios in WA magmatic rocks.

Kirkland et al., (2015) examine a comprehensive database of zircon composition in West Australian magmatic rocks that reveals negative correlations between both U and Th zircon/whole rock ratio and the zircon saturation temperature, with the observed change with temperature less for $U_{(zircon/whole\ rock)}$ than for $Th_{(zircon/whole\ rock)}$. This observation implies a systematic increase in the zircon/rock ratio with falling crystallisation temperature, a result that replicates findings from experimental partition coefficient studies.

Kirkland C.L., Smithies H., Taylor R., Evans N.J., McDonald B. (2015). Zircon Th/U ratios in magmatic environs. *Lithos* 212-215, 397-414.

Exhumation history of mineralizing systems in Tibet.

Zhao et al (2015) have used multiple mineral chronometers to determine the thermal history of ore-forming porphyritic intrusions in the large, newly discovered Sharang porphyry Mo deposit and nearby Yaguila skarn Pb–Zn–Ag (–Mo) deposit in the central Lhasa terrane, northern Gangdese metallogenic belt, Tibet. Multiple mineral chronometers (zircon U–Pb, sericite ^{40}Ar–^{39}Ar, and zircon and apatite (U–Th)/He) reveal that ore-forming porphyritic intrusions experienced rapid cooling (> 100ºC/Ma) during a monotonic magmatic–hydrothermal evolution. The magmatic–hydrothermal ore-forming event at Sharang lasted ~ 6.0 Myr (~ 1.8 Myr for cooling from > 900 to 350ºC and ~ 4.0 Myr for cooling from 350 to 200ºC) whereas cooling was more prolonged during ore formation at Yaguila (~ 1.8 Myr from > 900 to 500ºC and a maximum of ~ 16 Myr from > 900 to 350ºC). All porphyritic intrusions in the ore district experienced exhumation at a rate of 0.07–0.09 mm/yr (apatite He ages between ~ 37 and 30 Ma). Combined with previous studies, this work implies that uplift of the eastern section of the Lhasa terrane expanded from central Lhasa (37–30 Ma) to southern Lhasa (15–12 Ma) at an increasing exhumation rate.

Zhao J., Qin K., Li G., Cao M., Evans N.J., McInnes B.I.A., Li J., Xiao B., Chen L. (2015). The exhumation history of collision-related mineralizing systems in Tibet: Insights from the thermal history of the Sharang and Yaguila deposits, central Lhasa. *Ore Geology Reviews*, 65 (4), 1043-1061.

Trace element and isotopic composition of titanite.

Titanite (sphene, $CaTiSiO_5$) is sensitive to changes in temperature, oxygen and water fugacity, and fluid composition. In order to understand formation processes and the nature of hydrothermal fluids, Cao et al., (2015) chose various types of titanite from Cu ores at the Baogutu reduced porphyry Cu deposit for detailed study. Magmatic titanite is associated with biotite, plagioclase and K-feldspar, whereas hydrothermal titanite occurs with K-feldspar, chlorite, actinolite and calcite. Both magmatic and hydrothermal titanite are believed to have been predominantly derived from a mantle source.

Cao M., Qin K., Li G., Evans N.J., Jin L. (2015). In situ LA-MC-ICP-MS trace element and Nd isotopic composition and genesis of polygenetic titanite from the Baogutu reduced porphyry Cu deposit, Western Junggar, NW China. *Ore Geology Reviews*, 65, 940-954.

Ore forming fluids at Baogutu reduced porphyry Cu deposit, Western Junggar.

Cao et al. (2015) have used isotopic data of sulfide He–Ar–S and calcite C to identify a fluid source for this unusual reduced deposit. Data from fluid inclusions suggests a predominantly crustal source for the fluids with minor mantle input (less than 5%). The $\delta^{13}C$ values of carbonate yielded a value of −7.8‰ (n = 3), implying that CO_2 was probably sourced from mantle or juvenile lower crust. According to the restricted sulfide $\delta^{34}S$ values, the total S isotopic composition of the hydrothermal system was estimated to be 0.0–0.5‰, suggesting that the sulfur was derived from mantle or lower crust magmatic source. They propose that small proportion of mantle-derived fluids (less than 5%), probably rises up and then mixes with the fluids of juvenile lower crust under an extensional tectonic setting, forming the mantle-derived Sr–Nd–Pb–S–C but crustal He–Ar isotopic compositions.

Cao M., Qin K., Li G., Evans N.J., He H., Jin L. (2015). A mixture of mantle and crustal derived He-Ar-C-S-H-O ore-forming fluids at the Baogutu reduced porphyry Cu deposit, Western Junggar. *Journal of Asian Earth Sciences*, 98, 188-197.

The Western Australian $^{40}Ar/^{39}Ar$ Isotope Facility (WAAIF).

The $^{40}Ar/^{39}Ar$ dating method is used to measure the age and timing of a large variety of geological processes, from meteorite samples as old as the Earth (4.5 billion years) to the age of historical events such as the Vesuvius eruption (79 AD). The Ar technique can be applied to any rocks and minerals that contain K (e.g. hornblende, sanidine, plagioclase and basalts) is also used to date a myriad of other geological events such as volcanism, tectonic plate movements, mountain building rates, sediment formation, weathering and erosion, hydrothermal fluid movements, and alteration and diagenesis of minerals. The Western Australian Argon Isotope Facility includes two noble gas mass spectrometer (MAP 215-50 and the ultra-precise ARGUS VI) and is equipped with two laser systems and a furnace and is operated by A/ Prof Fred Jourdan.

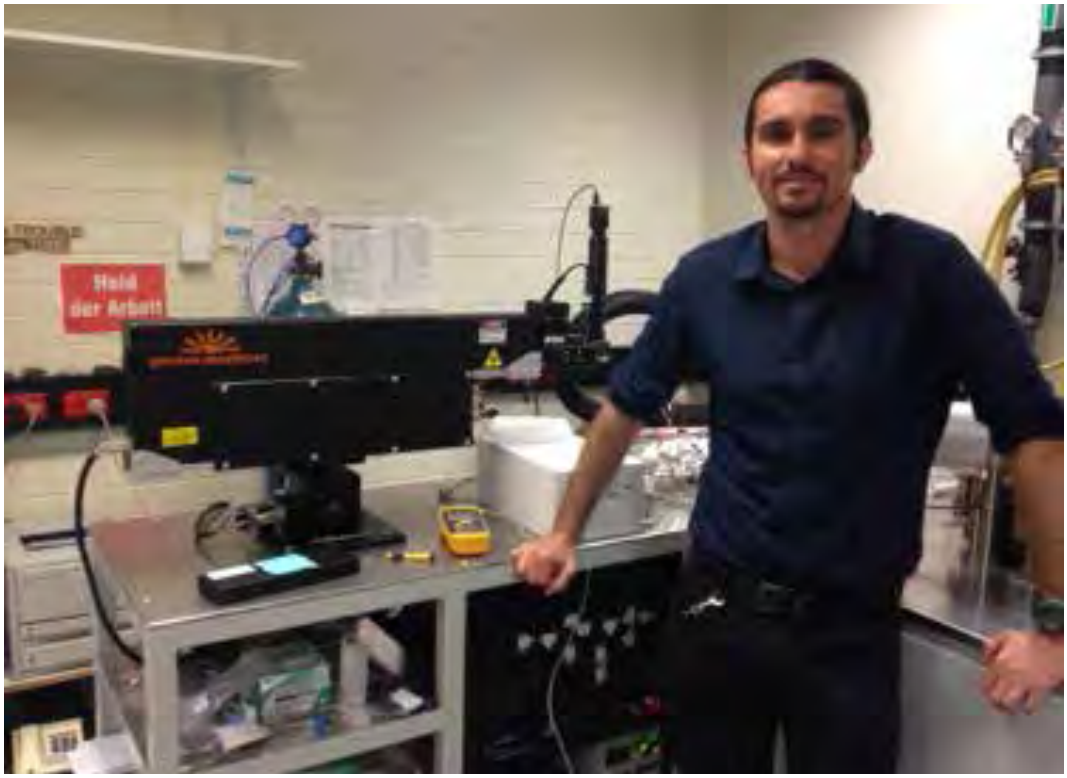

A/ Prof Fred Jourdan with the the ARGUS VI noble gas mass spectrometer.

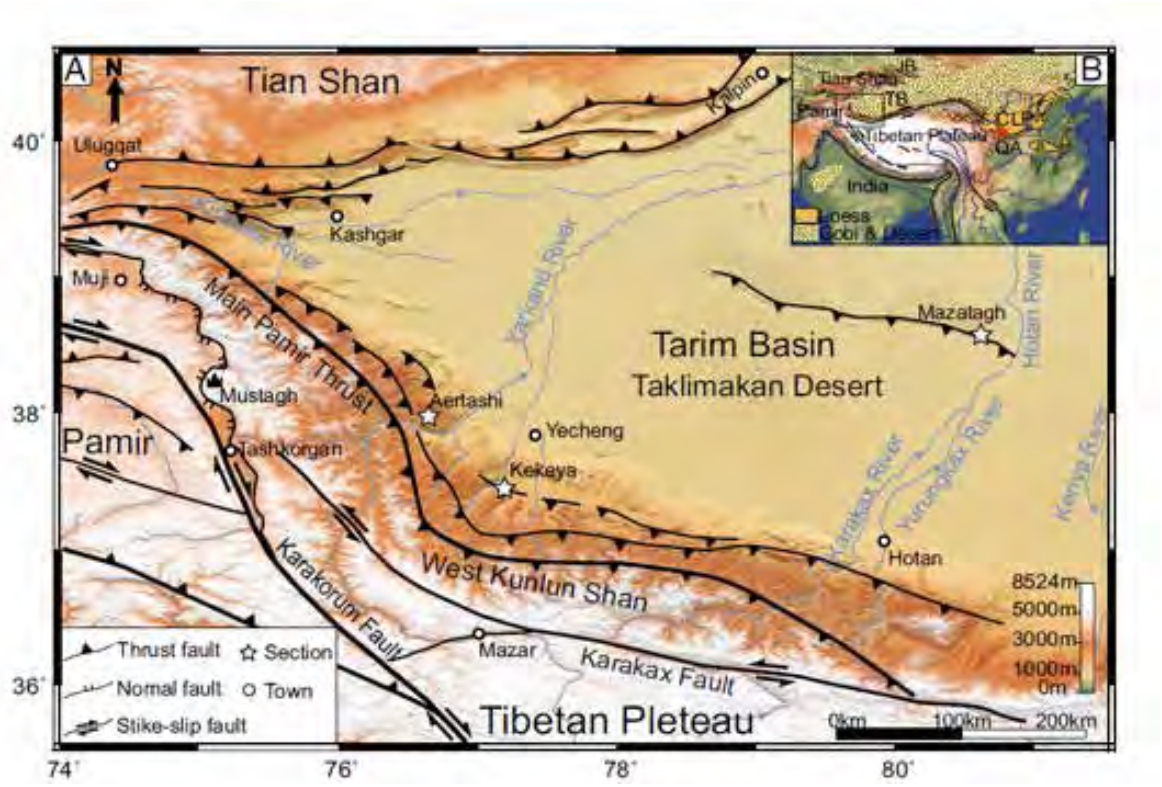

Location map. Topographic map showing the western portion of the Taklimakan Desert (Tarim Basin) and the surrounding mountain ranges with major active faults.

Desert research settles sands of time debate.

Zheng et al. (2015) used 40Ar/39Ar age dating of volcanic tuffs to show that the Taklimakan Desert the world's second largest sand sea and one of the most important dust sources to the global aerosol system, initiated between ~26.7 Ma and 22.6 Ma. Sand dust affect the global climate by scattering and absorbing solar radiation and thus, the presence of the Taklimakan desert needs to be considered as an important source of dust for climate modelling. Prior to this study, the age of the Taklimakan desert remained controversial, with the dominant view being that the desertification initiated from ~3.4 Ma to ~7 Ma based on magnetostratigraphy of sedimentary sequences within and along the margins of the desert. Determining when and how the desert formed holds the key to better understanding the tectonic–climatic linkage in this critical region. They suggested that the desert was formed as a response to a combination of widespread regional aridification and increased erosion in the surrounding mountain fronts, both of which are closely linked to the tectonic uplift of the Tibetan–Pamir Plateau and Tian Shan, which had reached a climatically sensitive threshold at this time.

Zheng H., Wei X., Tada R., Clift P., Jourdan F., Wang P., He M. (2015) Late Oligocene-early Miocene birth of the Taklimakan Desert. Proceedings of the National Academy of Sciences 112, 7662-7667.

Age of the Wallaby plateau volcanism, offshore Western Australia.

Olierook et al. (2015) presented the first accurate geochronological constraints from a suite of volcanic and volcaniclastic rocks dredged from the 70,000 km2 submerged Wallaby Plateau situated on the Western Australian passive margin. They carried out plagioclase $^{40}Ar/^{39}Ar$ and zircon U-Pb sensitive high-resolution ion microprobe dating that showed that a portion of the plateau formed at ca. 124 Ma. These ages are at least 6 m.y. younger than the oldest oceanic crust in adjacent abyssal plains (minimum = 130 Ma). Geochemical data indicate that the Wallaby Plateau volcanic samples are enriched tholeiitic basalt, similar to continental flood basalts. These authors suggested that magma could not erupt prior to 124 Ma because of the lack of space adjacent to the plateau and that eruption was made possible at 124 Ma via the opening of the Indian Ocean during the breakup of Greater India and Australia along the Wallaby-Zenith Fracture Zone. The scale of volcanism and the temporal proximity to breakup challenges the prevailing theory that the Western Australian margin formed as a volcanic passive margin suggest that there is a continuum between the two end members, magma-poor and volcanic passive margins.

Olierook H.K.H., Merle R.E., Jourdan F., Sircombe K., Fraser G., Timms N.E., Nelson G., Dadd K.A., Kellerson L., Borissova I. (2015) Age and geochemistry of magmatism on the oceanic Wallaby Plateau and implications for the opening of the Indian Ocean. *Geology* 43, 971-974.

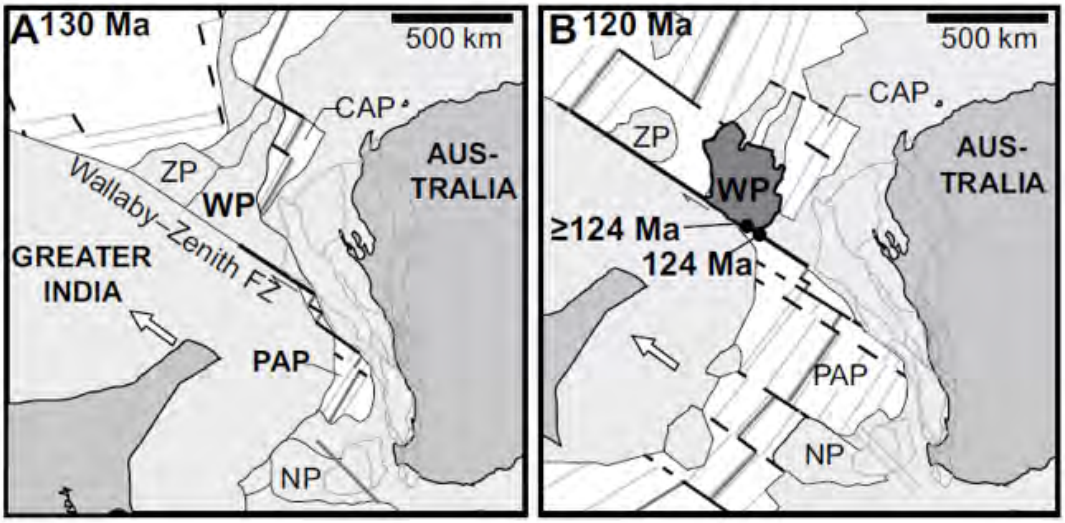

Plate reconstructions during breakup of Greater India from Austral- Antarctic portion of Gondwana.

A hydrated mantle underneath the late Archean Yilgarn Craton.

Ivanic et al. (2015) looked at two adjacent Igneous Complexes in Western Australia: The ca. 2813 Ma Windimurra and ca. 2800 Ma Narndee intrusions. A key difference in the chemistry of the two plutons is the presence of crystal-bound water in the Narndee Igneous Complex, represented primarily by abundant hornblende. $^{40}Ar/^{39}Ar$ ages showed that the hornblende is a primary mineral, yielding a plateau age of ca. 2805 Ma, in agreement with zircon age of ca. 2800 Ma from the same pluton. These findings illustrate a fast temporal transition, in proximal bodies, from anhydrous to hydrous mantle sources with very minor crustal contamination. These authors concluded that the source of the magmatic water at Narndee is the mantle, which, in conjunction with its absence in the adjacent Windimurra Igneous Complex, argues for a heterogeneous hydration ofmantle source regions under the Yilgarn Craton in the Mesoarchean.

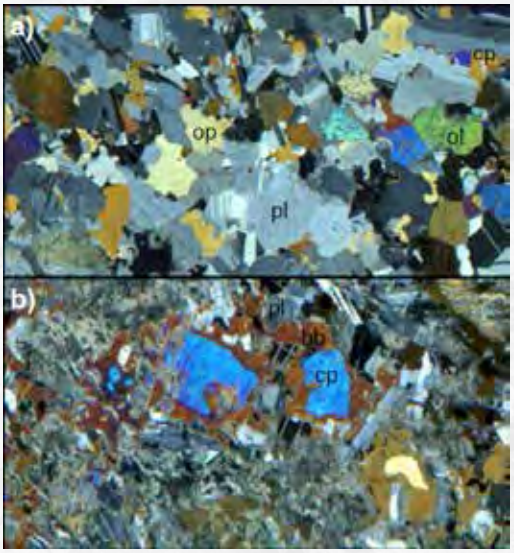

Thin-section photomicrographs: (a) Crossed-polars image of a "dry" gabbronorite sample from the Windimurra Igneous Complex and of a hydrated hornblende gabbro sample from the Narndee Igneous Complex.

Ivanic T.J., Nebel O., Jourdan F., Faure K., Kirkland C.L., Belousova E.A. (2015) A heterogeneously hydrated mantle underneath the late Archean Yilgarn Craton. *Lithos* 238, 76-85.

Research reports

ORGANIC AND ISOTOPE GEOCHEMISTRY

(Paleo)climate, oceans, continents, life and our resources

The molecular, genetic and stable isotopic composition of organic matter is determined by its source. The elements – hydrogen, carbon, sulfur and nitrogen are basic constituents of organic matter and play key roles in biochemistry, ecology, climate change, hydrologic and atmospheric processes. Therefore stable isotopic compositions preserved in organic matter can provide powerful insights into these processes.

Compound specific isotope analysis – CSIA is important for determining the stable isotopic compositions of individual organic components in complex mixtures (e.g., petroleum, natural gases, sediments, soils, groundwater, potable waters and extracts from plants and other media). The WA Organic & Isotope Geochemistry (WA-OIG) led by Professor Kliti Grice are applying the CSIA technique (carbon, hydrogen and nitrogen) and molecular geochemical and (paleo)genomic techniques to infer relationships between components so that their origins and formation pathways can be established.

Research Themes

The research themes investigated within WA-OIG using compound specific isotopes, lipid biomarker geochemistry and (paleo) genomics are:

1. Natural Resources (Petroleum & Minerals)
2. Microbial Communities
3. Biochemical Pathways
4. Integrated Ocean Drilling Projects (IODP) and Petroleum
5. Mass Extinctions
6. Climate and Paleoclimate
7. Environment
8. Medical Geochemistry

New analytical techniques.

Grice (2015) has edited a new book on analytical techniques in Geosciences published by the Royal Society of Chemistry. Within the book Blyth and Smith (2015) have reviewed how the relatively new technique of liquid chromatography – isotope ratio mass spectrometry has been applied in the geosciences, and discussed some of the advantages and limitations of the approach.

Principles and Practice of Analytical Techniques in Geosciences Grice, K. (invited editor) 2015. Royal Society of Chemistry, Cambridge.

Blyth, A. J., and C. I. Smith. 2015, Applications of Liquid Chromatography-Isotope Ratio Mass Spectrometry in Geochemistry and Archaeological Science." In Principles and Practice of Analytical Techniques in Geosciences, ed. Kliti Grice, 313-323. UK: The Royal Society of Chemistry.

Eiserbeck et al. (2015) and Greenwood et al., (2015) have also contributed chapters to a Royal Society of Chemistry book in production on Advances in two-dimensional gas chromatography. The technique reviewed by Greenwood et al. is on continuous flow compound specific sulfur isotope analysis (CSSIA) which is now possible by interfacing a gas chromatograph (GC) with a multicollector inductively coupled mass spectrometer (MC-ICPMS). This paper reviewed the Initial CSSIA applications of the three GC-MC-ICPMS facilities which now exist (including one at UWA) and which have included microbial sulphur cycling, biomarker taphonomy and exploration for petroleum and mineral resources. In the case of petroleum exploration, the large value range of the $\delta^{34}S$ values of OSCs in oils is very useful for oil–oil and oil-rock correlations. The major controls on the $\delta^{34}S$ of petroleum include the $\delta^{34}S$ of seawater sulphate and fractionation associated with microbial or thermochemical SO_4 reduction.

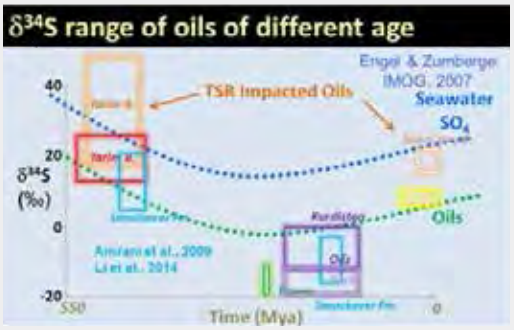

Eiserbeck C., Nelson R.K., Reddy R.K., Reddy C.M., Grice K. Advances in comprehensive two-dimensional gas chromatography. In: *Royal Society of Chemistry*.(Grice, K. editor), UK. 4, 324-365.

Greenwood, P.F., Grice, K., Amrani, A., Sessions, A.L, Raven, M.R., Holman, A., Dror, G., McCulloch, M.T., Adkins, J.F. 2015, Development and initial biogeochemical applications of compound specific sulfur isotope analysis In: Royal Society of Chemistry- Book in production. Edited by K. Grice. http://www.rsc.org/images/principles-and-practice_tcm18-235415.pdf Principles and Practice of Analytical Techniques in Geosciences. 285-312.

Organic inclusions in stalagmites.

Blyth et al. (2015) applied laser micropyrolysis to the study of speleothems for the first time, and established that distinct chemical signals can be recovered from different types of organic inclusions, indicating that the approach may be useful to palaeoenvironmental sciences with further proof of concept work.

Blyth A.J., Fuentes D., George S.C. Volk, H. (2015). Characterisation of organic inclusions in stalagmites using laser-ablation-micropyrolysis gas chromatography-mass spectrometry *Journal of Analytical and Applied Pyrolysis*, 113, 454-463.

Microbial communities in thawing Alaskan permafrost soils.

Coolen and Orsi (2015) used ultrahigh throughput sequencing to compare gene expression in pristine frozen vs. thawed permafrost soils. Bacterial gene expression under frozen conditions showed a predominance of processes involved in coping with stress and survival while thawing of permafrost soils stimulated microbial decomposition and respiration of sequestered carbon, resulting in a positive feedback to climate warming.

Coolen M.J.L., Orsi, W.D. (2015). The transcriptional response of microbial communities in thawing Alaskan permafrost soils. *Frontiers in Microbiology* 6.

The biology and ecology of calcarean sponges.

To better understand this group Fromont et al. (2015) sampled Calcarean sponge Leucetta prolifera from south-WA. Pulse amplitude modulated fluorometry analyses and extraction of photopigments established that the sponge was photosynthetic. Molecular analysis of the bacterial symbionts from the 16S rDNA gene suggested that 5 -22% of all sequences fitted to the phylum Cyanobacteria. Fatty acid analyses showed that the sponge obtained food via photosynthates from its symbionts.

Fromont J., Huggett M.J., Lengger S.L., Grice K., Schönber C.H.L. (2015). Characterisation of Leucetta prolifera, a calcarean cyanosponge from south-western Australia, and its symbionts. *Journal of the Marine Biological Association of the United Kingdom*, 1-12

Carbon isotopes as indicators of lipid pathways.

C_3-vs-C_4 variances in $\Delta^{13}C$ of wax lipids (relative to whole leaf tissue) is lipid-pathway dependent. These lipid dependent pathways can be clarified by C_3-vs-C_4 difference in carbon allocation. The importance of carbon allocation to lipid pathways are revealed in lipid $^{13}C/^{12}C$ ratios. Changes in the physiological functions of lipids between C_3 and C_4 plants are also revealed in lipid $^{13}C/^{12}C$ ratios.

Zhou, Y.P., Stuart-Williams, H., Grice, K., Kayler, Z.E., Zavadlav, S., Gessler, A., Farquhar, G.D., 2015. Allocate carbon for a reason: priorities are reflected in the 13C/12C ratios of plant lipids synthesized via three independent biosynthetic pathways. *Phytochemistry* 111, 14-20.

Higher plant biomarkers.

Grice et al. (2015) have investigated the molecular and stable carbon isotopic composition of higher plant biomarkers in Jurassic strata from the Isle of Skye, northwest Scotland. Aromatic hydrocarbons diagnostic of higher plants were identified in the samples from the Early Callovian to Early Kimmeridgian interval, a succession rich in fossil fauna including ammonites were used to determine age. Local tectonics, resulting in alterations to the relief and landscape of the hinterland probably influenced the palaeoflora. The stable isotopic connection between terrigenous and marine-derived biomarkers is consistent with a strong coupling of the atmosphere and ocean.

Grice K., Foster C.B., Riding J.B., Naehar S., Greenwood P.F. (2015). Vascular plant biomarker distributions and stable carbon isotopes from the Middle and Upper Jurassic (Callovian-Kimmeridgian) strata of Staffin Bay, Isle of Skye, northwest Scotland. *Palaeogeography, Palaeoclimatology, Palaeoecology*, 440, 307-315.

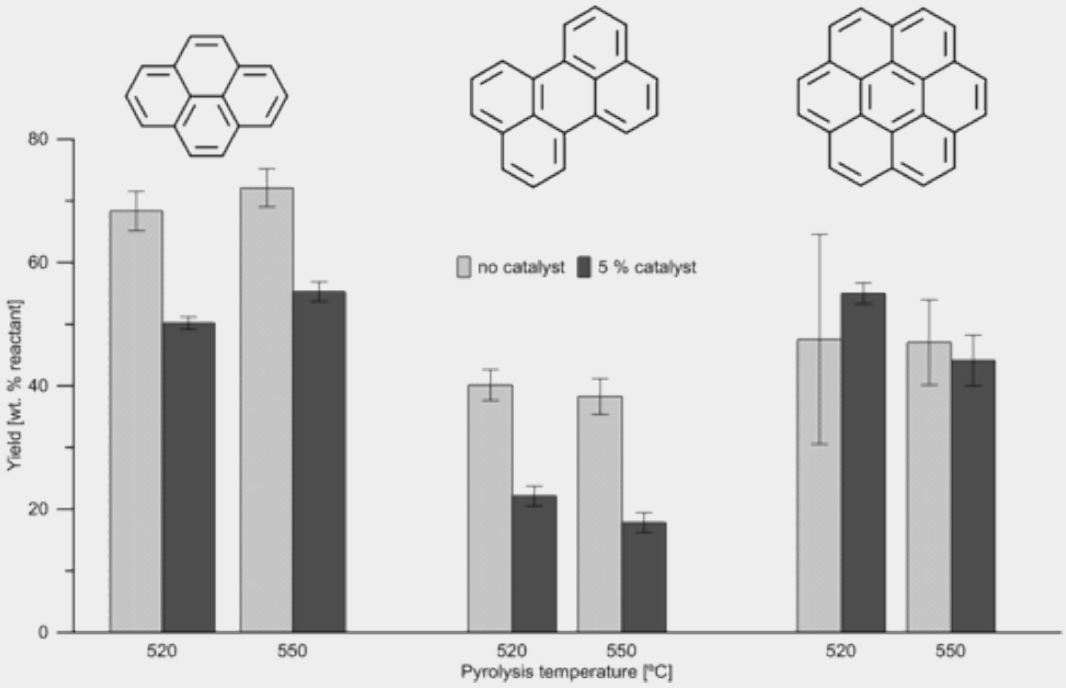

Polycyclic aromatic hydrocarbons.

Grotheer et al (2015) describe the chemical behavior of PAHs during hydro pyrolysis, to understand the effects and artifacts of this new analytical technique, with respect to the molecular composition of organic matter in orogenic gold deposits.

Grotheer H., Robert A., Greenwood P.F., Grice K. (2015). Stability and hydrogenation of polycyclic aromatic hydrocarbons during hydropyrolysis (HyPy) – Implications of highly matured organic matter. *Organic Geochemistry*, 86, 45-54.

Radiolytic molecular markers.

Bulk kerogen compositions show land plant sources for organic matter in the Mulga rock uranium deposit. Radiolysis led to cleavage of macromolecules forming medium chain length n-alkyl moieties. Secondary and tertiary reactions with OH− radicals progressed the formation of alkanones. These were termed “Radiolytic molecular markers” implying new molecular markers resulting from radiolytic cracking. A mechanism was proposed for the formation of n-alkanes and n-alkanones.

Jaraula C.M.B., Schwark L., Moreau X., Pickel W., Bagas L., Grice, K. (2015). Radiolytic alteration of biopolymers in the Mulga Rock uranium deposit. *Applied Geochemistry*, 52, 97-108.

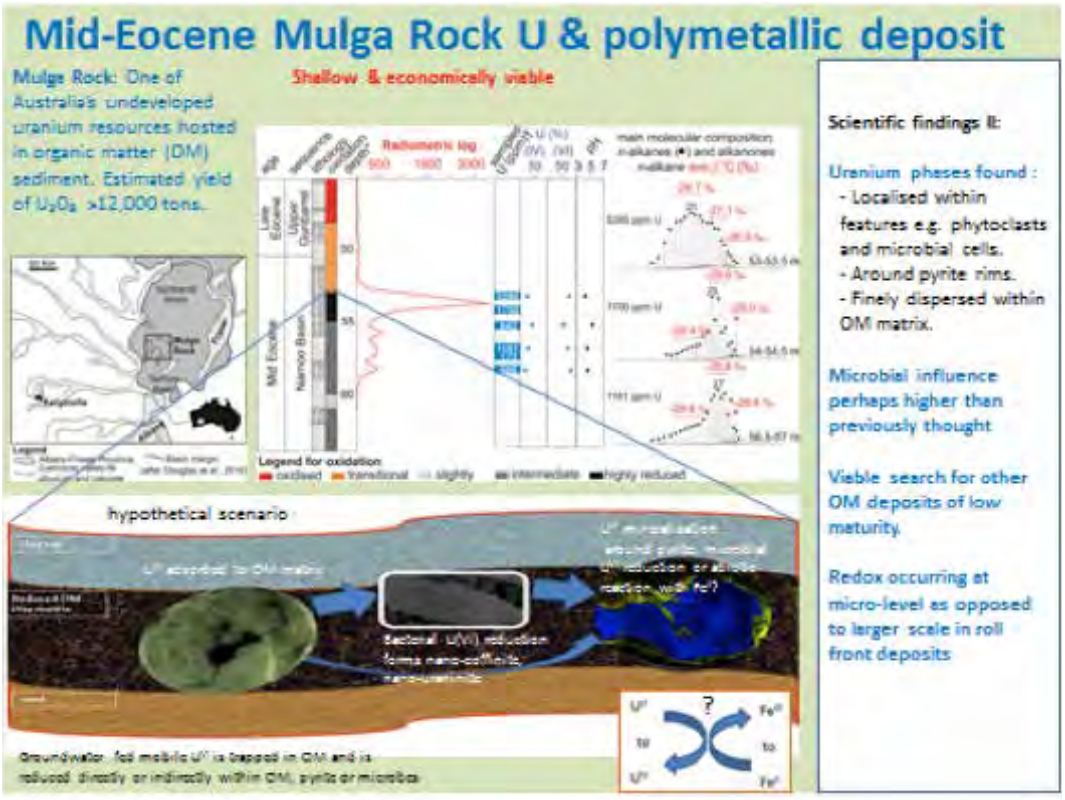

Carbonaceous material in orogenic gold deposits.

Four different types of carbonaceous materials were identified in a gold deposit and its host rocks from Macraes New Zealand using Raman spectroscopy and petrographic analyses. The carbonaceous materials are to contribute to the source and deposition of gold.

Hu S.Y., Evans K., Craw D., Rempel K., Bourdet J., Dick J., Grice K. (2015). Raman characterisation of carbonaceous material in the Macraes orogenic gold deposit and metasedimentary host rocks New Zealand. *Ore Geology Reviews* 70, 80-95.

Fe-P cycling under contrasting redox conditions.

Kraal et al. (2015) made detailed spectroscopic analyses of Fe and P species and P sorption in oxic to highly reducing sediments. The reducing sediments showed slight P sorption, nonetheless Fe-associated P is an essential P burial phase under all redox conditions. Oxic micro-environments can only be identified by µm-scale X-ray analyses and have shown important in Fe–P sequestration.

Kraal P., Burton E.D., Rose A.L, Kocar B.D., Lockhart R.S., Grice K., Bush R.T. (2015). Sedimentary Iron-phosphorus cycling under contrasting redox conditions in a eutrophic estuary. *Chemical Geology* 392, 19-31.

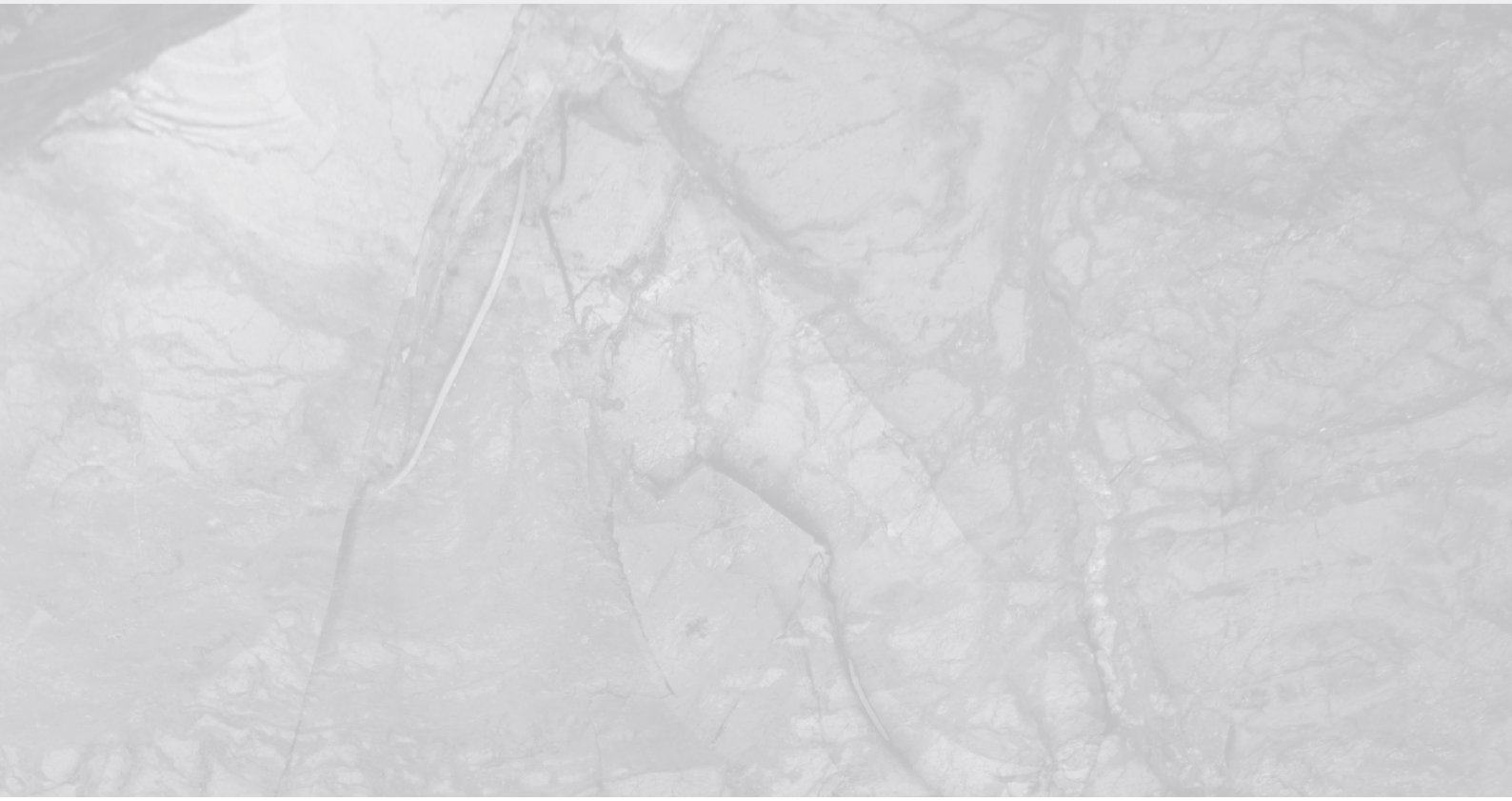

Adamantane acids as fingerprints for polluted water from oil sands.

Adamantanes are the smallest hydrocarbons possessing a diamondoid cage-like structure and are highly resistant to microbial biodegradation. However, the presumed breakdown products, adamantine acids have now been found in biodegraded oils and are especially rich in the process-affected waters derived from the oils sands industry in Alberta, Canada. Lengger et al. (2015) used the distribution profiles of the adamantine acids to create "fingerprints" for water samples taken from different storage ponds. These methods have now been used by Environment Canada to help identify sources of leaks from storage ponds.

Lengger SK, Scarlett AG, West CE, Frank RA, Hewitt LM, Milestone CB, Rowland SJ (2015) Use of the distributions of adamantane acids to profile short-term temporal and pond-scale spatial variations in the composition of oil sands process-affected waters. *Environmental Science: Processes & Impacts* doi:10.1039/C5EM00287G

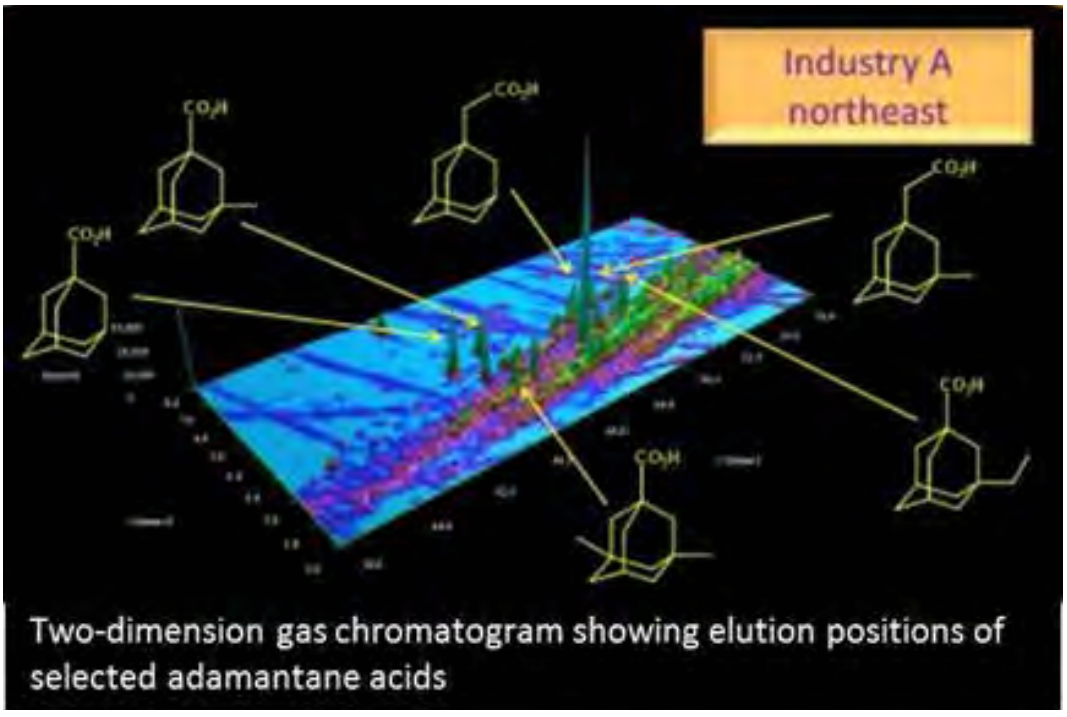

Two-dimension gas chromatogram showing elution positions of selected adamantane acids

Iron and sulphur cycling bacteria in coastal acid soils.

Coastal acid sulfate soils (CASS) represent a global environmental and economic concern. Whilst benign when undisturbed, severe acidification of soil and expelled waters occur when these iron sulfide-rich sediments are oxidised by exposure to air. This typically occurs as a result of anthropogenic actions (e.g. drainage for residential development or agricultural use) but sometimes also as a consequence of natural droughts. One of the most promising and affordable approaches to restore such acidic sites is the re-introduction of controlled tidal inundation, which triggers microbial sulfate and iron reduction that efficiently neutralise acidity. However, in-situ studies of re-inundated sites to provide an in-depth understanding of the associated biogeochemical processes and to observe long-term effects are scarce. Ling et al. (2015) investigated microbial community structures and functional guild distributions across naturally occurring redox gradients along a tidal transect in a re-inundated CASS site. The results indicate close associations and a spatial overlap of iron and sulfate reducing bacteria in an organic matter-rich environment. Microbial communities were controlled by parameters such as pH values, redox conditions, degrees of mineralisation and water saturation as well as type and abundance of organic matter.

Ling Y.C., Grice K., Tulipani S., Berwick L., Bush R., Moreau J.W. (2015). Distribution of iron- and sulfur-cycling bacteria across a coastal acid sulfate soil environment: implications for natural bioremediation. *Frontiers in Microbiology*, 6, 624.

Maleimide proxies for euxinia.

Naeher and Grice (2015) have developed a new, robust maleimide proxy for reconstructions of the degree of photic zone euxinia that is widely applicable in ancient and modern systems. They determined which environmental changes are associated with mass extinctions and can use the maleimides to understand oxygen depletion in past environments.

Naeher S., Grice K., 2015. Novel 1H-Pyrrole-2,5-dione (maleimide) proxies for the assessment of persistent photic zone euxinia. *Chemical Geology* 404, 100-109.

Modern microbial mats from Shark Bay.

Modern microbial mats from Shark Bay present some structural similarities with ancient stromatolites; thus, the functionality of microbial communities and processes of diagenetic preservation of modern mats can provide an insight into ancient microbial assemblages and preservation. Pagès et al (2015) investigated the vertical distribution of microbial communities in a well-laminated smooth mat from Shark Bay. Biolipid and compound-specific isotopic analyses were performed to investigate the distribution of microbial communities and preservation of biosignatures in four distinct layers of the mat.

Pagès A., Grice K., Welsh D.T., Teasdale P.T., Van Kranendonk M.J., Greenwood P.F. (2015). Lipid biomarker and isotopic study of community distribution and biomarker preservation in a laminated microbial mat from Shark Bay, Western Australia. *Microbial Ecology*, 40, 1-14.

Molecular proxies as indicators of salinity stratification.

Tulipani et al. (2015) identify methyltrimethyltridecylchromans (MTTCs) as potential sedimentary markers for riverine freshwater incursions into marine environments, a condition which often leads to salinity-related density stratification of the water-column. Such water-column stratification and the associated persistent anoxia and euxinia have been a significant feature throughout Earth's history, with a particular relevance for mass extinction events and petroleum source rock deposition. Here we investigated relative abundances of MTTC isomers (chroman ratio) in Late Devonian sediments deposited in a marine setting under photic zone euxinic conditions and water-column stratification.

The strong correlation of the chroman ratio to other molecular, isotopic and elemental indicators of redox conditions, water-column stratification and terrigenous input throughout the investigated core strongly suggested a dependency to terrigenous freshwater incursions. This broadens the utilization of MTTCs as paleoproxies by adding freshwater stratification to their general application of salinity reconstructions.

Tulipani S., Grice K., Greenwood P.F., Schwark L. Summons R.E., Böttcher M.E., Foster, C.B. (2015). Molecular proxies as indicators of freshwater incursion-driven salinity stratification. *Chemical Geology* 409, 61-68.

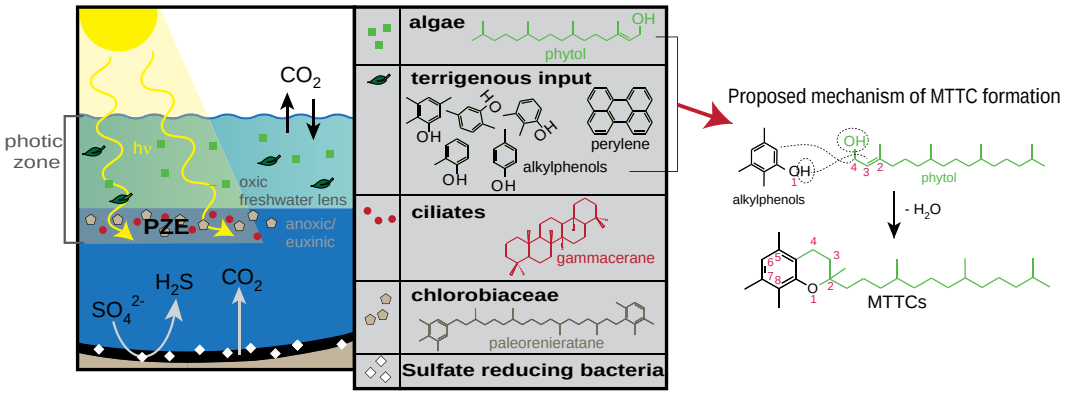

Schematic model of Late Devonian water column, Canning Basin, Western Australia.

An integrated elemental, biomarker and stable isotope approach to study a sedimentary record.

Tulipani et al. (2015) have investigated palaeoenvironmental changes in the time period leading up to the Late Devonian mass extinction using an integrated elemental, biomarker and stable isotope approach to study a sedimentary record associated with ancient reef systems from the Western Australian Canning Basin. Evidence was found for a distinct time interval with elevated biotic stress near the Givetian-Frasnian boundary, which was related to an increased nutrient input from terrestrial vegetation. The resulting enhancement of phytoplanctonic productivity in combination with a stratified water-column (freshwater overlying more saline bottom waters) led to the development of oxygen-depletion and high concentrations of toxic hydrogen sulphide, which extended into the upper, light-penetrated water layer. Such conditions represent ideal conditions for petroleum source rock deposition, and therefore highlight the potential of the Mid to Late Devonian Gogo Formation as a source rock of the high-quality oils in the Canning Basin. The findings also highlight the potential significance of the rising terrestrial vegetation throughout that era, for the Late Devonian extinctions.

Tulipani S., Grice K., Greenwood P., Schwark L., Haines P.W., Sauer P.E., Schimmelmann A., Summons R.E., Foster C.B., Böttcher M.E., Payton T.D., Schwark L. (2015). Changes of palaeoenvironmental conditions recorded in Late Devonian reef systems from the Canning Basin, Western Australia: A biomarker and stable isotope approach. *Gondwana Research* 409, 61-68.

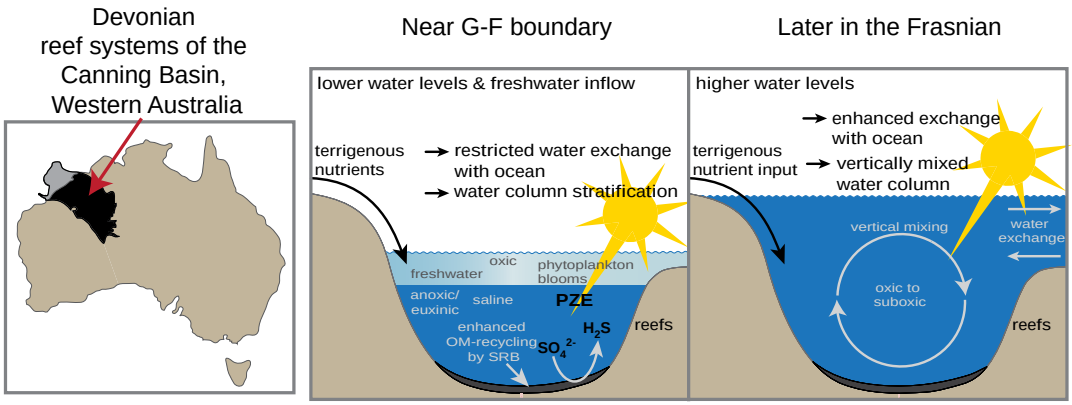

Research reports

TECTONICS AND GEODYNAMICS

Tectonics and geodynamics

Tectonics and geodynamics involve the understanding of processes related to the motion of tectonic plates through time such as mountain building, basin formation and cyclic evolution of supercontinents, and the interaction of tectonic plates with the Earth's deep interior. Such knowledge is essential for understanding life evolution, environmental changes, and the exploration of mineral and energy resources. Such research therefore contributes to both the Earth-past and Earth-present themes in TIGeR.

Tectonic plate velocities, collisional frequency and supercontinent cycle.

To address the question of secular changes in the speed of the supercontinent cycle, Condie et al. (2015) used the timing and locations of collisional and accretionary orogens, and average plate velocities as deduced from paleomagnetic and paleogeographic data. Peaks in craton collision occur at 1850 and 600 Ma with smaller peaks at 1100 and 350 Ma. Distinct minima occur at 1700–1200, 900–700, and 300–200 Ma. Assembly of Nuna at 1700–1500 Ma correlates with low collision rates, whereas assemblies of Rodinia and Gondwana at 1000–850 and 650–350 Ma, respectively correspond to moderate to high rates. Low collision rates occur at times of supercontinent breakup at 2200–2100, 1300–1100, 800–650, and 150–0 Ma. A peak in plate velocity at 450–350 Ma correlates with early stages of growth of Pangea and another at 1100 Ma following breakup of Nuna. Orogens and passive margins show the same two cycles of ocean basin closing: an early cycle from Neoarchean to 1900 Ma and a later cycle, which corresponds to the supercontinent cycle, from 1900 Ma to the present. The cause of these cycles is not understood, but may be related to increasing plate speeds during supercontinent assembly and whether or not long-lived accretionary orogens accompany supercontinent assembly. LIP (large igneous province) age peaks at 2200, 2100, 1380, 800, 300, 200 and 100 Ma correlate with supercontinent breakup and minima at 2600, 1700–1500, 1100–900, and 600–400 Ma with supercontinent assembly. Breakup durations are short, generally 100–200 Myr. The history of angular plate velocities, craton collision frequency, passive margin histories, and periodicity of the supercontinent cycle all suggest a gradual speed up of plate tectonics with time.

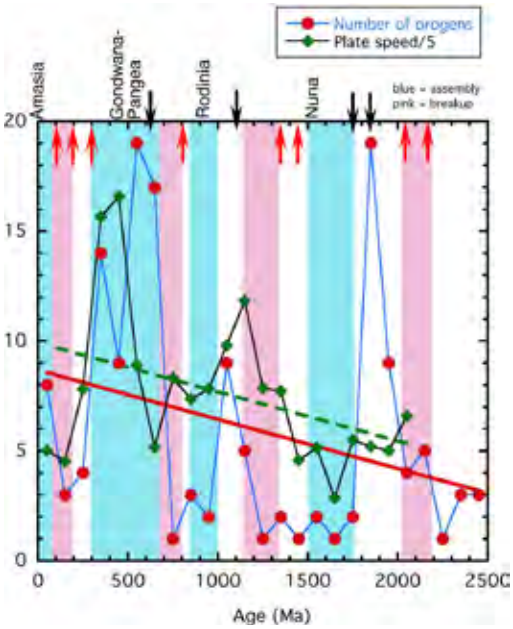

Secular changes in craton collision frequency and average area-weighted plate speed (deg/100 Myr). Collision frequency between cratons is expressed as number of orogen segments per 100-Myr bin moving in 100 Myr increments. Also shown are supercontinent assembly (blue stripes) and breakup (pink stripes) times. Major LIP (large igneous provinces) events: red arrows corre-spond to LIPs associated with supercontinent breakup black arrows correspond to other LIPs.

Condie K., Pisarevsky S.A., Korenaga J., Gardoll S. (2015). Is the rate of supercontinent assembly changing with time? *Precambrian Research*, 259, 278-289.

Paleomagnetism of 2.4 Ga mafic dykes in southern Yilgarn helps to reconstruct Paleoproterozoic supercontinent.

Pisarevsky et al. (2015) carried a paleomagnetic study of the previously undated Erayinia dykes intruding the south-eastern Yilgarn Craton. The U–Pb TIMs baddeleyite age of these dykes is now 2401 ± 1 Ma, which is about 10 m.y. younger than the 2418–2410 Ma Widgiemooltha dyke swarm. The paleomagnetic study isolated a stable primary remanence with steep downward direction, and the paleomagnetic pole (22.7ºS,150.5ºE, A95= 11.4º) is similar, but not identical to that of the previously studied Widgiemooltha dykes. This implies a movement of the Yilgarn Craton toward the pole at~1◦/m.y. angular speed, which is comparable with tectonic plates' velocities during the Phanerozoic. Paleomagnetic polarities of Widgiemooltha and Erayinia dykes suggest that at least one geomagnetic reversal occurred between these two magmatic events. The estimated amplitude of geomagnetic secular variations at c. 2400 Ma is slightly higher than predicted by the existing models for the last 5 m.y. at the c. 64º latitude.

Paleomagnetic data and patterns of c. 2.6–2.1 Ga mafic dyke swarms permit the above reconstruction of a Paleoproterozoic (2.4 Ga) supercontinent.

Pisarevsky S.A., Bogdanova S.V., Lubnina N.V., Murphy J.B. (2015). Supercontinental cycles and geodynamics. *Precambrian Research*, 259, 1-4.

South China in Gondwana.

Yao et al. (2015a, 2015b) documented a detailed clastic provenance analysis of lower Palaeozoic samples from South China, which revealed that massive clastic deposition on the Cathaysia side of South China during the late Precambrian and the Cambrian time was mainly sourced from northern India and adjacent orogens when South China collided with northern India to join Gondwana. In addition, provenance analysis of Cambrian clastic rocks along the Yangtze side of the Nanhua Basin revealed an affinity with Cathaysian sediments, arguing that the Nanhua Basin was not a broad ocean as speculated by some researchers; instead, it was a failed Neoproterozoic continental rift that was inverted during the Lower Palaeozoic Wuyi-Yunkai Orogeny.

Yao W.-H., Li Z.-X., Li, W.-X. (2015a) Was there a Cambrian ocean in South China? – Insight from detrital provenance analyses: *Geological Magazine*, 152, 184-191.

Yao W.-H., Li Z.-X., Li W.-X., Su L., Yang J.-H. (2015b) Detrital provenance evolution of the Ediacaran–Silurian Nanhua foreland basin, South China: *Gondwana Research*, 28, 1449-1465.

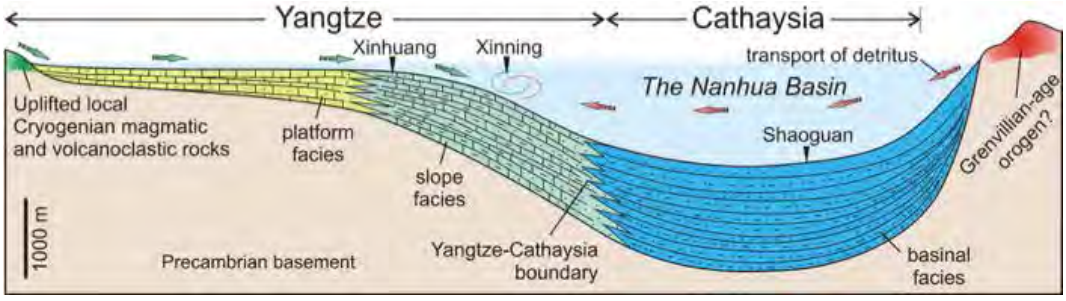

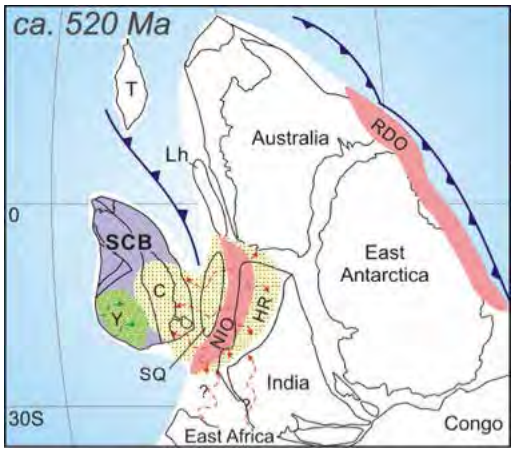

Collision of the South China Block (SCB) with Gondwana during the Cambrian (left), and provenance analysis suggesting sediments shed off northern Gondwana deposited not only on the Cathaysia side of the Nanhua Basin, but also on the Yangtze side (above), therefore arguing against the exist of a broad ocean.

Flat-subduction model for South China helps to explain ponded basin in North America.

Early Mesozoic flat subduction of an oceanic plateau from the Palaeo-Pacific has been used to explain not only the formation of an enormously broad (up to 1300 km) Mesozoic mountain belt and magmatic province in South China, but also a broad sag basin that sits immediately above that mountain belt. Zhu et al. (2015) reported a variety of magmatic melts formed during this complex process. In addition, Li (2015) extended the South China model to explain the so-called Eocene "ponded basin" system in western North America. He argued that, like what happened in Mesozoic South China, the flat-subducted oceanic plateau beneath the Laramide Orogen was gradually changed from having positive buoyancy to having negative buoyancy when enough of the plateau basalts had been transformed into denser eclogite through dewatering. This transformation process took ~15 m.y. in the South China case, and ~27 m.y. in the Laramide case. The gravitational pull of the eclogitizing oceanic plateau, which is coupled with the overriding continental lithosphere, caused the formation of a broad sag basin atop the young and broad orogen. The sag basin ceased to develop further once the flat slab was delaminated, and its lateral extent reflects the dimension of the flat-subducted oceanic plateau.

Flat-laying Eocene Green River Formation in the Great Basin System (also known as the Eocene "ponded basin").

Li Z.-X. (2015) Paleogeographic record of Eocene Farallon slab rollback beneath western North America: COMMENT: *Geology*, 43, 362.

Zhu K.-Y., Li Z.-X., Xu X.-S., Wilde S. A., Chen, H.-L. (2016) Early Mesozoic ferroan (A-type) and magnesian granitoids in eastern South China: Tracing the influence of flat-slab subduction at the western Pacific margin: *Lithos*, 240–243, 371-381.

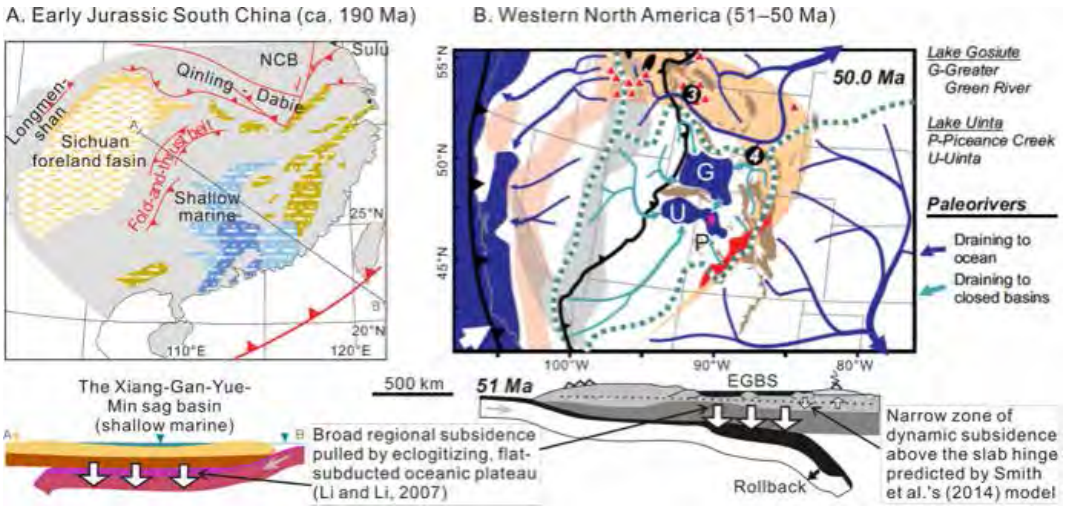

Cartoon diagrams illustrating the formation of a broad continental sag basin in both Mesozoic south China (A, after Li and Li, 2007) and in Eocene western North America (B, after Smith et al., 2014) due to the gravitational pull of eclogitizing flat-subducted oceanic plateau (Li and Li, 2007). EGBS = Eocene Great Basin System.

Closure of the Paleo-Asian Ocean and Amalgamation of the Central Asian Orogenic Belt.

The Central Asian Orogenic Belt (CAOB) is one of the largest accretionary orogens in the world, yet the timing of final amalgamation remains controversial. It appears that closure commenced in the west and progressively evolved eastward in a scissor-like motion, with the final segment – the Mongol-Okhotsk Belt in NE Russia – closing in the mid-Jurassic. Although the Inner Mongolia segment in northern China had closed by the late Permian (~250 Ma), as evidenced by I-type granites and adakites along the Solonker-Xar Moron suture, the actual location of the suture requires re-investigated, since the Xar-Moron shear zone lies approximately 50 km south of the Solonker shear zone. Furthermore, the Xar Moron segment is a zone of intense deformation, whereas the Solonker shear zone contains considerably less-deformed rocks.

Wilde S.A., Zhou J.B., Wu F.Y. (2015). Development of the North-Eastern segment of the Central Asian Orogenic belt. In: The Central Asian Orogenic Belt (Ed. Kroner, A.) "Contributions to the Regional Geology of the Earth", E. Schweitzerbart Science Publishers, Stuttgart, Germany, pages 184-210.

Wilde S.A. (2015). Final amalgamation of the Central Asian Orogenic Belt in NE China: Paleo-Asian Ocean closure versus Paleo-Pacific plate subduction – A review of the evidence. Tectonophysics 602, 345-362

Zhou J-B, Wang B., Wilde S.A., Zhao G-C., Cao J-L., Zheng C-Q., Zeng W.S. (2015). Geochemistry and U-Pb zircon dating of the Toudaoqiao blueschists in the Great Xing'an Range, northeast China, and tectonic implications. Journal of Asian Earth Sciences 97, 197-210.

Strongly sheared gneisses along the Xar Moron suture zone, 1 km south of the Xar Moron River, Inner Mongolia.

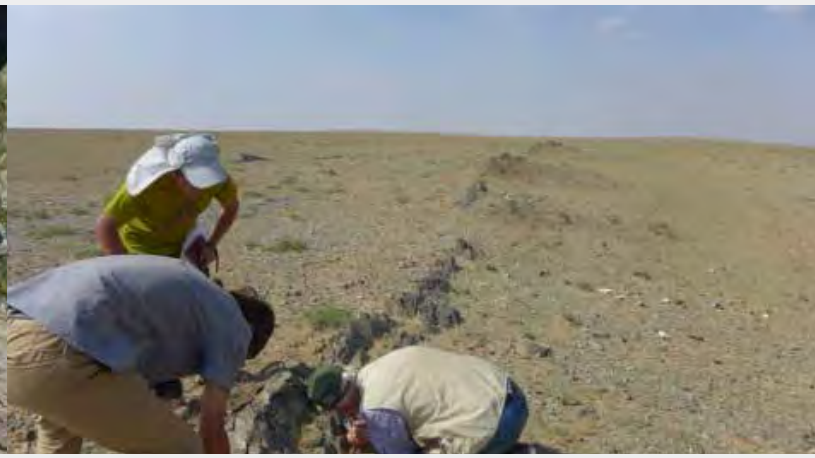

Measuring weakly-deformed metasedimentary rock in the Solonker suture zone, 10 km east of Solonker.

Pb mobility at the nano- and atomic-scale in zircon.

Studies of Eoarchean zircons from the Napier Complex of East Antarctica reveal a level of complexity not previously recognised. Ion imaging using the Cameca 1280 initially identified regions within individual zircon grains that recorded different 207Pb/206Pb ratios, resulting in age variations commonly in excess of 500 Ma. Further work using Raman spectroscopy, TEM and nano-SIMS has identified the presence of lead nanospheres within metamict domains. This remobilisation of elements within zircon is attributed to the fact the rocks have undergone two high-grade metamorphic events, one under UHT conditions. This redistribution of Pb is more extreme than that revealed by the Atom Probe study of ancient Jack Hills zircons, where Pb mobility is more local and attributed to alpha-recoil.

Kusiak M., Dunkley D. J., Wirth R., Whitehouse M., Wilde S. A., Marquardt K. (2015). Metallic lead nanospheres discovered in ancient zircons. *Proceedings of the National Academy of Sciences of the United States of America* 112, 4958-4963.

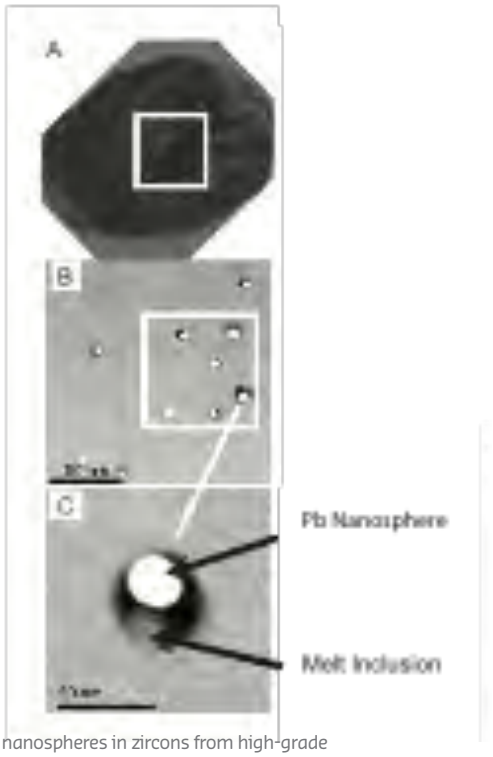

Lead nanospheres in zircons from high-grade metamorphic rocks of the Napier Complex, Antarctica. (a) Cathodoluminescence (CL) image of zircon with rectangle marking site of image B. (b) Distribution of Pb nanospheres in metamict zircon. (c) Close-up of a single nanosphere indicating the presence of metallic Pb within a melt inclusion.

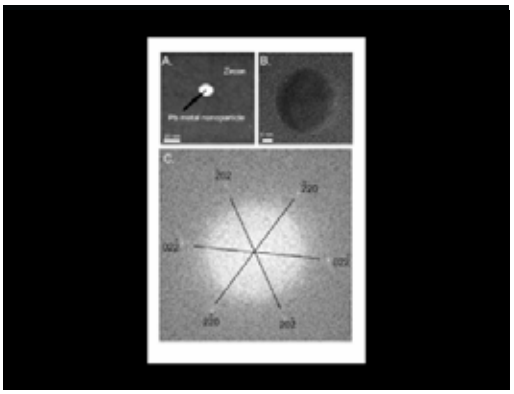

(a). Another Pb nanosphere in zircon. (b) HRTEM image of this Pb nanosphere. (c) Diffraction pattern indexing the material as cubic Pb.

Tertiary Volcanism in Tibet.

The Suyingdi rhyolites in the northern Qiangtang Terrane of Tibet record zircon U–Pb ages of 38.2 ± 0.8 Ma. They have low initial (87Sr/86Sr)i ratios (0.707860 to 0.708342) and enriched Nd isotopic compositions, with εNd(t) values ranging from −8.4 to −5.0, indistinguishable from Cenozoic potassic and ultrapotassic lavas exposed farther north in Tibet. They were most likely produced by partial melting of thickened lower crust in the garnet stability field and indicate that the lower crust in northern Tibet is heterogeneous in nature. A field trip was undertaken in late 2014 and samples collected are currently being investigateded.

Long X.P., Wilde S.A., Wang Q., Yuan C., Wang X-C., Li J., Jiang, Z., Dan W. (2015). Partial melting of thickened continental crust in central Tibet: Evidence from geochemistry and geochronology of Eocene adakitic rhyolites in the northern Qiangtang Terrane. *Earth and Planetary Science Letters* 414, 30-44.

Sparse outcrops of volcanic rocks at over 5,000 m in the Lhasa Terrane, ca. 200 km east of Lhasa, Tibet.

TIGeR member Xuan-Ce Wang and Curtin visitor Xiaoping Long collecting an alkali granitoid from the giant Gangdese Batholith, ca. 60 km east of Lhasa.

Geology of the Tarim Craton, North China.

The Tarim Craton lies to the west of the North China Craton and shares characteristics with both the North and South China cratons. The northern part of the Tarim Craton contains many rocks that have similar characteristics and ages to rocks reported from the North China Craton and indicate a possible linkage of the two areas in the Archean and Paleoproterozoic.

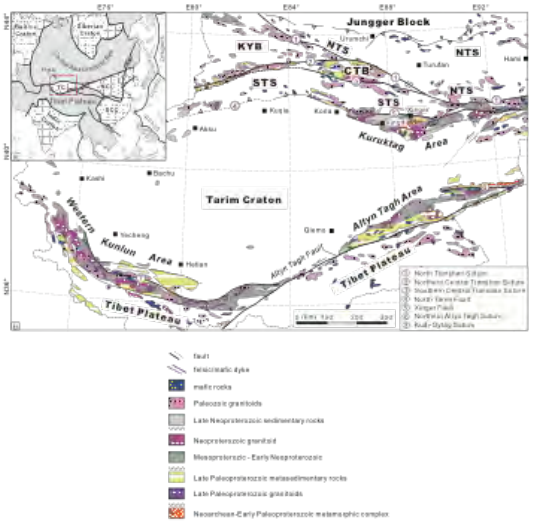

(a) Location of the Tarim Craton within Asia. (b) Simplified geological map of the Tarim Craton (from Ge et al., Bull Geol Soc of America 2014).

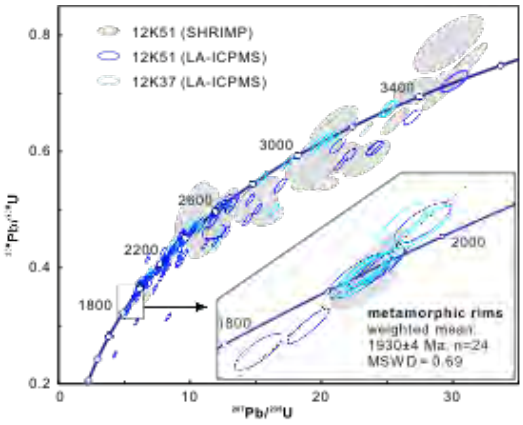

U-Pb concordia diagram of two paragneiss samples from the northern Tarim Craton showing detrital zircon ages up to 3.5 Ga and the development of metamorphic rims at 1.93 Ga (modified from Ge et al., Precambrian Research 2014).

Long X.P., Wilde S.A., Yuan C., Hu A.Q., Sun M. (2015). Provenance and depositional age of Paleoproterozoic metasedimentary rocks in the Kuluketage Block, northern Tarim Craton: Implications for tectonic setting and crustal growth. *Precambrian Research* 260, 76-90.

Ge R.F., Zhu W.B., Wilde S.A. (2015). Synchronous crustal growth and reworking recorded in late Paleoproterozoic granitoids in the northern Tarim craton: In situ zircon U-Pb-Hf-O isotopic and geochemical constraints and tectonic implications. *Geological Society of America Bulletin* 127, 781-803.

Geology of the Nadanhada and Sikote-Alin terranes of NE China and Far East Russia.

The coastal terranes in NE China and the Russian Far East reflect the onset of Paleo-Pacific subduction following closure of the Paleo-Asian Ocean and amalgamation of the Central Asian Orogenic Belt (CAOB). Closure of the Paleo-Asian Ocean in China at ~250 Ma resulted in a cessation of the northward drift of continental masses from a peri-Gondwana position. The onset of a tectonic regime dominated by westward-directed Paleo-Pacific subduction was initiated in the Late Triassic to Early Jurassic and has dominated since that time. Importantly, the timing of accretion on either side of the Jiamusi-Khanka-Bureya Massif at the eastern margin of the CAOB was coeval in the Middle Jurassic, with a rift basin closing between the massif and the CAOB in the west and subduction of the Paleo-Pacific Plate commencing in the east. Further work in 2016 will involve cotutelle PhD student Kai Liu of Peking University who is undertaking studies in the Russian segment of the terrane.

The 54 Ma Fujin Granodiorite intruding sandstone at Wuerhuli Hill at the eastern margin of the Jiamusi Block, close to the contact with the Nadanhada Terrane, NE China.

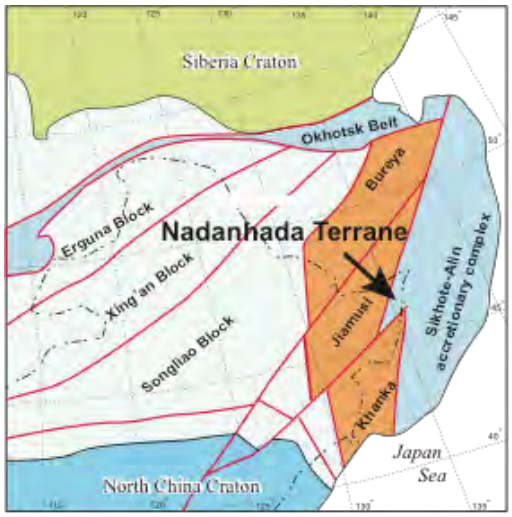

Location of the Nadanhada Terrane in NE China.

Sun M.D., Xu Y-G., Wilde S.A., Chen H-L., Yang S-F. (2015). The Permian Dongfanghong island-arc gabbro of the Wandashan Orogen, NE China: Implications for Paleo-Pacific subduction. *Tectonophysics* 659, 122-136.

Sun M-D., Xu Y-G., Wilde S.A., Provenance of Cretaceous trench slope sediments from the Mesozoic Wandashan Orogen, NE China: Implications for determining ancient drainage systems and tectonics of the Paleo-Pacific. *Tectonics* 34, 1269-1289.

Geological Traverse along the Namibia-Angolan border.

One of the most inaccessible parts of Africa is in NW Namibia, with no road between the Epupa Falls and Marrienfluss. A 120 km foot-traverse was made in 2008 to collect the dominant Paleoproterozoic gneisses. The rocks form part of a large magmatic province at the southwestern margin of the Congo Craton and ranged in age from 1861 to 1801 Ma. However, Mesoproterozoic granitoids with ages of 1530 to 1520 Ma were also identified.

The end of the traverse near Marienfluss; packing-up camp and heading for a cold beer (or two) at the lodge.

Epupa Falls on the Kunene River, Namibia-Angola border. This was the starting point of a 120 km-long traverse along the river to examine and collect Proterozoic gneisses. There is no road and the whole journey was across country with six donkeys and a variable number of Himba tribesmen.

Continental flood basalts derived from the hydrous mantle transition zone.

It has previously been postulated that the Earth's hydrous mantle transition zone may play a key role in intra-plate magmatism, but no confirmatory evidence has been reported. Here, Wang et al., (2015) demonstrate that high temperature hydrothermally-altered subducted oceanic crust was involved in generating the Late Cenozoic Chifeng continental flood basalts of East Asia.

The most striking observation in this study is that oxygen isotopes, $^{39}Ar/^{40}Ar$ ages, and other geochemical features of the Chifeng CFBs (SiO_2, Nb, Sm/Nd, and Ce/Pb) are correlated with distance to the western edge of the stagnant Pacific slab. In a westward direction, the lavas decrease in age, are depleted in silica and have lower Sm/Nd ratios, whereas they show progressive enrichment in Nb and have higher Ce/Pb ratios. Importantly, the olivine $d^{18}O$ values of the basalts increase westward away from the stagnant slab. Thus the lavas immediately above the western edge of the stagnant Pacific slab are characterised as being over-saturated in silica, having the oldest eruptive ages, the lowest olivine $d^{18}O$ values and possibly the highest fluid contents. The low-$d^{18}O$ lavas are characterized by enrichment of silica, Sr with high positive Sr anomalies, Al2O3, and depletion of incompatible trace element compositions and subduction slab-like Ce/Pb ratios.

The detailed geochemical analysis leads Wang et al. to propose an alternative thermochemical model, whereby slab-triggered wet upwelling produces large volumes of melt that may rise from the hydrous mantle transition zone. This model explains the lack of pre-magmatic lithospheric extension or a hot-spot track and also the arc-like signatures observed in some large-scale intra-continental magmas. Deep-Earth water cycling, linked to cold subduction, slab stagnation, wet mantle upwelling, and assembly-breakup of supercontinents, can account for the chemical diversity of many continental flood basalts.

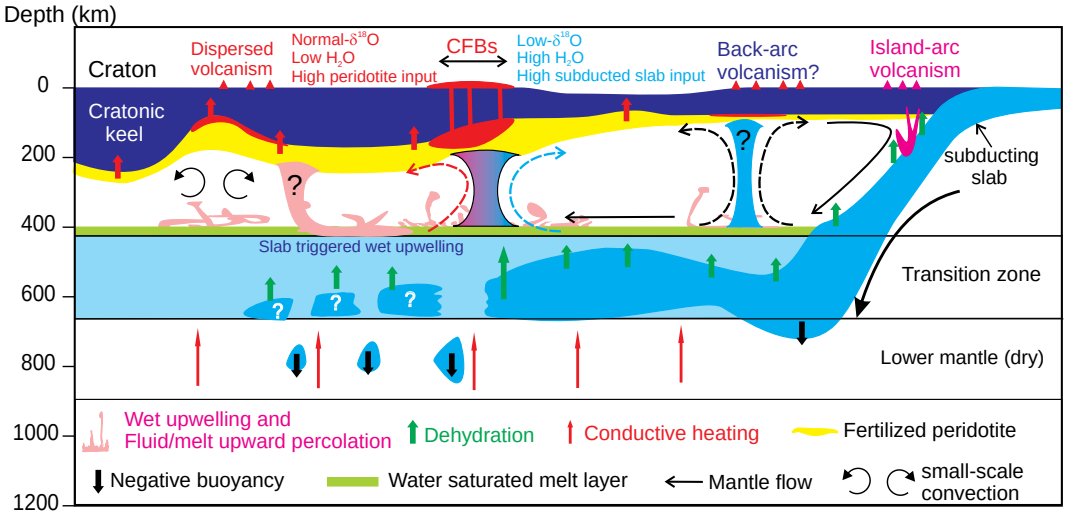

Effect of slab stagnation and water cycling (wet upwelling, upward percolation, and re-fertilization) on the upper mantle thermochemical state. This model is mainly based on the strong spatial correlation of geochemical features with distance of eruptive lavas relative to the edge of the stagnant slab. This is based on water partitioning in the Earth's mantle, behaviour of slab-triggered wet upwelling and upward percolation, hydrous mantle melting, the mantle wedge model, and upwelling from the hydrated mantle transition zone.

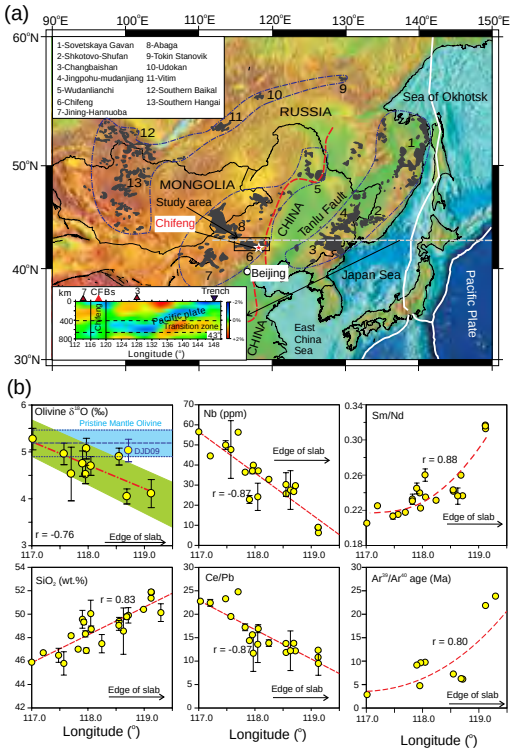

(a) Schematic map of the Late Cenozoic intraplate volcanic province in Central East Asia. (b) Covariations of olivine d^{18}O, major-trace elements, and 39Ar/40Ar ages as a function of eruptive longitude. Data points represent average of analysed whole-rock or olivine samples from individual Chifeng CFBs; error bars represent one standard deviation for each group of lava or olivine. r: correlation coefficient.

Wang X., Wilde S.A., Li Q., Yang Y. (2015). Continental flood basalts derived from the hydrous mantle transition zone. *Nature Communications* 6, DOI 10/1038/ncomms8700.

Disequilibrium-induced initial Os isotopic heterogeneity in basaltic rock powders: implications for dating and source tracing.

The Re–Os isotopic system has been widely used to date a variety of materials ranging from mafic–ultramafic rocks and sulfides, to black shale, and even oil. Given their chalcophile and siderophile geochemical behavior, both Re and Os have a strong affinity to trace phases (e.g., sulfides and alloys) and, thus, their budgets in these rocks are controlled mainly by these trace phases. The contribution of unequal distribution of these discrete trace phases on poor reproducibility of both Re and Os concentrations in applications of the isotopic system has been well documented in the past two decades, known as the nugget effect. However, its effect on the scale of initial Os isotopic heterogeneity is unclear. In light of the nugget effect for both Re and Os concentrations, it is possible that the Os isotopic compositions of individual hand-specimen samples were not totally homogenized when the rocks formed. Consequently, the apparent isochron of replicate analyses of individual samples does not faithfully record the radiogenic ingrowth of ^{187}Re to ^{187}Os, and, therefore, the apparent isochron ages and the calculated initial Os isotopic compositions may bias the timing of formation events and the tracing of mantle sources, respectively. To clarify these uncertainties, it is necessary to investigate whether homogenization of the Os isotopic composition was achieved in these rock systems during their formation.

Li et al., (2015) report that replicate analyses of gram aliquots of single basaltic powders (one of reference material BHVO-2 and three of the Hatu basalts from the western Junggar region, China) show large variations in both Os concentrations and isotopic ratios. Duplicate analyses of a single powered whole-rock sample including both Hatu basalts and international reference rock (BHVO-2) defined good apparent Re-Os isotope isochron lines and linear trends between $1/^{192}Os$ and $^{187}Os/^{188}Os$ diagrams. They demonstrated that these relationships signify the disequilibrium-induced small-scale Re-Os heterogeneity. Therefore, for basaltic rock systems or other rocks with relatively low Os concentrations, caution should be used when Re-Os isotope isochron dating technique and individual initial Os isotopes to investigate their mantle source, especially for the rock units with large range of measured $^{187}Re/^{188}Os$ and $^{187}Os/^{188}Os$ ratios. When using the Re–Os isotopic system to date and to trace the source of basaltic rocks or other rocks with relatively low Os concentrations, it is necessary to consider whether the initial Os isotopic composition was heterogeneous or whether it had reached complete isotopic equilibrium. The results obtained in this study is crucial for dating of low-temperature system using Re-Os isotopes, such as black shale, crude oil and bitumen.

Li J., Wang X.-C., Xu J.-F., Xu Y.-G., Tang G.-J., Wang Q. (2015). Disequilibrium-induced initial Os isotopic heterogeneity in gram aliquots of single basaltic rock powders: Implications for dating and source tracing. *Chemical Geology* 406, 10-17.

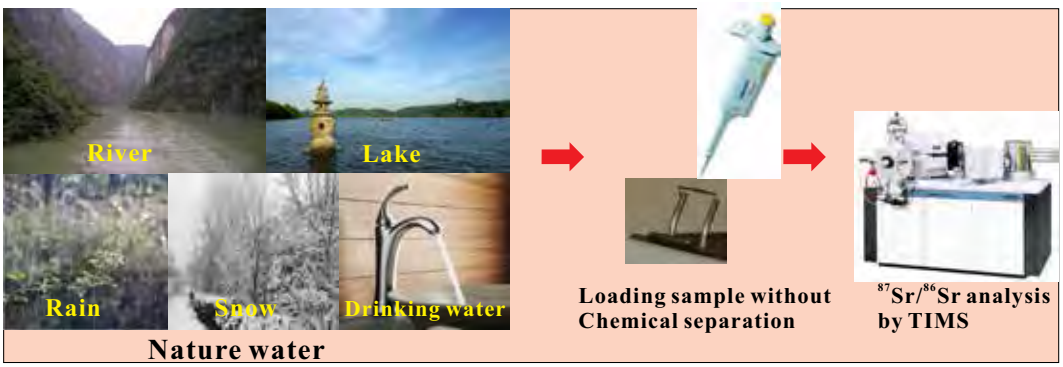

Illustrating the new protocol to directly determine Sr isotopes of nature water.

Direct high-precision measurements of the $^{87}Sr/^{86}Sr$ isotope ratio in natural water.

Thermal ionization mass spectrometry (TIMS) allows excellent precision for determining Sr isotope ratios in natural water samples. Traditionally, a chemical separation procedure using cation exchange resin has been employed to obtain a high purity Sr fraction from natural water, which makes sample preparation time-consuming. In this study, Li et al., (2015) present a rapid and precise method for the direct determination of the Sr isotope ratio of natural water using TIMS equipped with amplifiers with two 10^{12} Ω resistors.

To validate the applicability of our method, twenty-two natural water samples, including different water types (rain, snow, river, lake and drinking water), that show a large range in Sr content variations (2.54–922.8 ppb), were collected and analyzed from North and South China. Analytical results show good precision (0.003–0.005%, 2 RSE) and the method was further validated by comparative analysis of the same water with and without chemical separation.

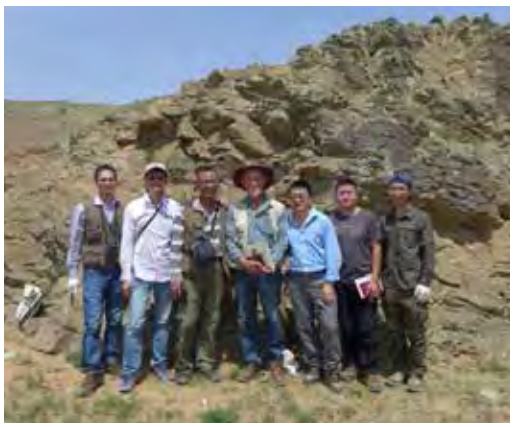

In Mongolia.

Li C.-F., Guo J.-H., Chu Z.-Y., Feng L.-J., Wang X.-C. (2015). Direct High-Precision Measurements of the $^{87}Sr/^{86}Sr$ Isotope Ratio in Natural Water without Chemical Separation Using Thermal Ionization Mass Spectrometry Equipped with 10^{12} Ω Resistors. *Analytical Chemistry* 87, 7426-7432.

Research reports

PLANETARY SCIENCE

Planetary science

Planetary science is a historical area of strength at Curtin: John de Laeter was a world-renowned cosmochemist and planetary scientist. That strength continues through to the present day. TIGeR is home to the largest planetary science group in Australia, with 14 members of staff publishing in the field, 7 as their principal area of interest. 6 PhD students are full time on planetary projects, with 4 more starting in 2016. In addition to a large number of papers in specialist journals across the field, in 2013 and 2014 DAG published 4 papers in Nature, Nature Geoscience, and Nature Communications on planetary science research. We also direct the Australia node for the NASA Solar System Exploration Research Virtual Institute, representing Australia's planetary research community to NASA.

Desert Fireball Network.

The DFN is a distributed network of fully autonomous observatories spread across outback Australia. It is able to observe a sample of solar system objects that we cannot see in any other way. We can determine where they come from in the solar system by triangulating trajectories of bright fireballs made by large debris, to derive a precise pre-entry orbit. From fireball brightness, deceleration and fragmentation, we can calculate mass and physical properties. If it survives to the surface, we can pinpoint the fall site, recover it, and analyse it in the lab. Not only are these objects too small to image with a telescope, no telescope can deliver this suite of data. Most recently we have developed a completely automated software pipeline for data reduction. We successfully recovered a meteorite from Lake Eyre on 31st December 2015 (pictured), using that pipeline – an event that made news worldwide.
By end-2015 we had built a supercomputer database for storage, allowing us to process our entire archive. By February 2016 we had reduced our complete fireball dataset, deriving precise orbits for 280 bright fireballs: the largest single dataset of its kind ever collected. This provides a unique window on cosmic debris in the inner solar system. Its also turned up an additional 11 meteorite falls that we can search for.

Bland P.A., Benedix G.K. and the DFN Team (2015) Catching a falling star (or meteorite) – fireball camera networks in the 21st century. *Elements* 11, 160-161.

Sansom E.K., Bland P.A., Paxman J., Towner M.C. (2015) A novel approach to fireball modeling: The observable and the calculated. *Meteoritics and Planetary Science* 50, 1423-1435.

Bunburra Rockhole in the field (fell 2007).

Bunburra Rockhole – first meteorite recovered by DFN.

This meteorite looks like a rock from the largest group of basaltic meteorites in the world's collections – a basaltic eucrite. In a combined mineralogic, petrologic, isotopic study of the meteorite, Spivak-Birndorf et al., (2015) showed this is the case for a number features including ages. However, it's orbit and oxygen isotopic composition do not fit that scenario. Current thinking is that Bunburra Rockhole samples a new differentiated asteroid.

Meteorite recovered from Lake Eyre, 31 Dec. 2015.

Spivak-Birndorf L.J., Bouvier A., Benedix G.K., Hammond S., Brennecka G.A., Howard K.T., Rogers N.W., Wadwha M., Bland P.A., Spurny P., Towner M.C. (2015) Geochemistry and chronology of the Bunburra Rockhole ungrouped achondrite. *Meteoritics and Planetary Science* 50, 958-975.

Discovery of a new primitive iron-silicate meteorite end member.

Van Roosbroek et al. (2015) studied fragment of the Mont Dieu iron meteorite. The meteorite contains abundant inclusions of silicate minerals. Geochemistry and 40Ar/39Ar analyses of silicate minerals showed that this meteorite represent an old group of iron meteorite (~4.5 Ga) which has not been perturbed by a subsequent event. These authors showed that this meteorite represent in fact an intermediate stage in a continuum between chondrites and differentiated bodies. When combined with petrographic observations showing fast cooled silicate and slow cooled iron, these data lead the authors to suggest that this type of iron-silicate meteorite (and perhaps all iron-silicate meteorites) has been created by an impact of a small (magmatic) iron asteroid on a larger a H-chondritic asteroid, very early in the history of the solar system. The impact allows mixing the silicate mineral in hot molten pool of iron magma.

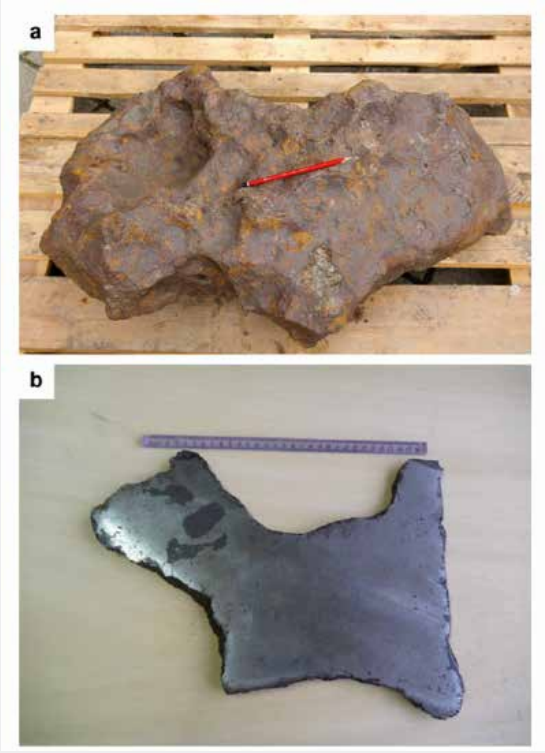

Pictures of the Mont Dieu iron silicate meteorite.

Van Roosbroek N., Debaille V., Pittarello L., Goderis S., Humayun M., Hecht L., Jourdan F., Spicuzza M.J, Claeys Ph. (2015) A new Primitive IIE member: the chondrule-bearing Mont Dieu II meteorite. *Meteoritics & Planetary Science* 50, 1173–1196.

Mars meteorite spectra.

The geology of the surface of Mars comes to us by means of remote sensing – mineralogical data is derived from thermal infrared and visible spectroscopy. For both types of spectra, terrestrial minerals are generally used as calibration points. This is in part because meteorites are too valuable to powder (the usual way the calibration standards are prepared). Benedix et al. (2015), used EBSD to examine mineral orientations in thin section and showed that as long as random orientation is present, an average of all mineral spectra will provide a good match to particulate spectra.

Benedix G.K., Hamilton V.E., Reddy S.M. (2015) Assessing mineral orientation in Martian meteorites using IR microspectroscopy and EBSD techniques. *Meteoritics and Planetary Science*, 50, abstr. #5202. (78th Ann. Meeting Meteorit. Soc.)

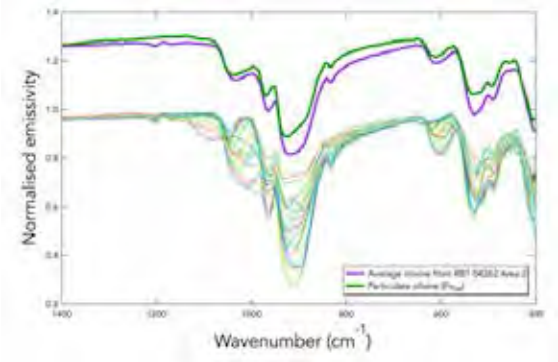

Spectral characteristics of randomly oriented olivine in area shown in previous figure. Also plotted (offset for clarity) is the average spectrum of thin section olivines compared to the spectrum of a particulate olivine of composition Fo68.

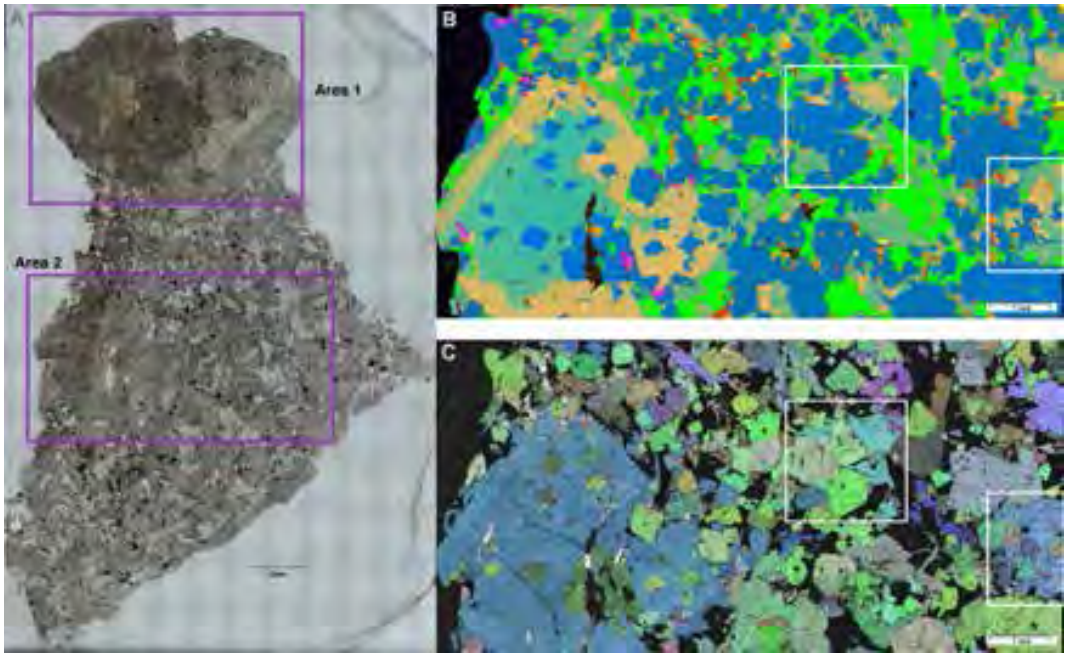

Transmitted light photomicrograph of meteorite Roberts Massif 04262, a Martian basaltic (Lherzolitic) meteorite. The highlighted region labelled Area 2 is extracted in (B) a combined x-ray element map where blue is olivine, teal is low-Ca pyroxene, orange is high-Ca pyroxene and bright green is shocked plagioclase (maskelynite) and (C) an all Euler angle figure of the same area depicted in (B). The smaller boxes highlight regions of olivine and pyroxene.

Automated Crater Counting.

The effort to understand Mars is one of the highest profile areas of planetary science globally. Our contribution to this work involves automating the crater counting technique and locating the youngest craters on the surface of Mars. These craters are the most likely to be associated with meteorites that have travelled to Earth, in which we can analyze, with great precision, both crystallization and ejection ages. Although still preliminary, the results of an iVEC internship in 2014 form the backbone of a DP grant submission.

Galloway M.J., Paxman J., Benedix G.K., Tan T., Towner M.C., Bland P.A. (2015). Auomated Crater Detection and Counting Using the Hough Transform and Canny Edge Detection. Workshop on Issues in Crater Studies and the Dating of Planetary Surfaces 1841, 9024

Na-rich chondrules in meteorites.

Chondrules are spherical particles that are among th oldest materials in the solar system. It is likely that planets were built up from small particles like this. The composition of chondrules is generally Mg and Ca-rich. Plagioclase is dominated by anorthite. Benedix et al., (2015) found a number of Na-rich chondrules in a unique lithology that may lead to a new way to think about chondrule formation and understanding the early conditions of the solar system.

Benedix G.K., Russell S.S., Forman L.V., Bevan A.W.R., Bland P.A. (2015) A new unequilibrated chondrite lithology discovered in the Murchison CM2 meteorites. 46th Lunar and Planetary Science Conference Abstract # 1143.

The shape evolution of Iapetus.

Kuchta et al., (2015) investigated the shape evolution of Saturn's moon Iapetus triggered by a giant impact, as a combination of despinning due to internal dissipation and an abrupt change in rotation due to a giant impact. They showed that stresses arising from shape change affect the viscosity structure by enhancing dislocation creep and can lead to the formation of a large-scale ridge at the equator as a result of rapid rotation change for initial rotation periods of 6 h.

Kuchta M., Tobie G., Miljković K., Běhounková M., Souček O., Choblet G., Čadek O. (2015) Despinning and shape evolution of Saturn's moon Iapetus triggered by a giant impact, Icarus, 252, 454–465, doi: 10.1016/j.icarus.2015.02.010.

Lead isotopes in Martian meteorites.

Across a compositionally diverse range of available Martian samples (meteorites), Bellucci et al. (2015,2016) have developed a robust lead isotopic model for the early evolution of the Martian silicate mantle, differentiating at ~4.52 Ga and indicating a role for precipitation of sulphides. They have identified a significantly younger differentiation event(s) at ~3.6 – 4 Ga in the source for the Nakhla and Chassigny meteorites. Their work was also instrumental in the recent recognition of presence of Martian crust as a real global reservoir that is enriched in the incompatible elements, similar to lunar KREEP and continental crust on the Earth. Currently ongoing in situ analysis of stable isotopes of oxygen, sulphur, iron and chlorine are revealing interactions of Martian crust with surface fluids, including brines, helping to constrain temporal changes in Martian environment (soils, hydrosphere and atmosphere) and assess the question of habitability.

Bellucci J.J., Nemchin A.A., Whitehouse M.J., Snape J.F., Kielman R.B., Bland P.A., Benedix G.K. (2016) A Pb isotopic resolution to the Martian meteorite age paradox. *Earth and Planetary Science Letters*, 433, 241-248.

Bellucci J.J., Nemchin A.A., Whitehouse M.J., Snape J.F., Bland P., Benedix G.K. (2015) The Pb isotopic evolution of the Martian mantle constrained by initial Pb in Martian meteorites (2015) *Journal of Geophysical Research E: Planets*, 120, 2224-2240.

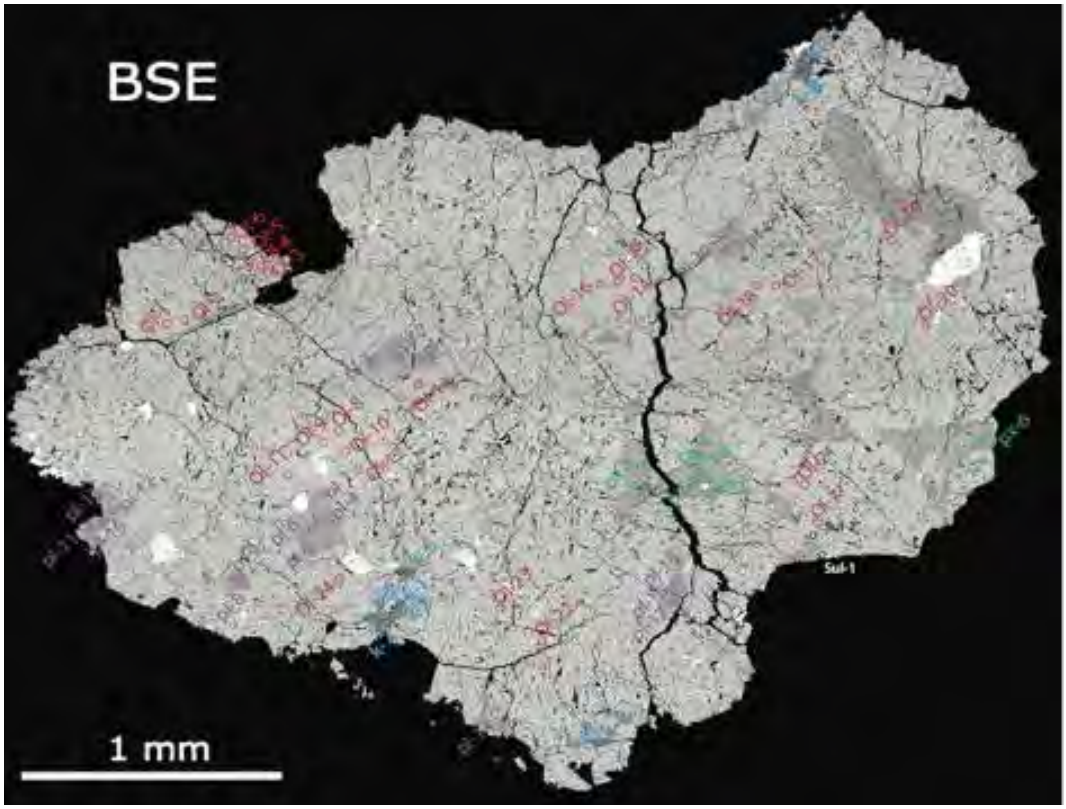

Polished section of Chassigny, one of Martian meteorites analysed in the studies of Pb isotopes in Martian rocks (analytical spots in different minerals are shown as circles of different colour).

Thermal history of ordinary chondrites.

Unraveling the temperature and pressure history of a meteorite provides constraints on parent body size. Although it is well known that most meteorites come from asteroids, it is less well understood how heat is distributed in these bodies. Using a newly re-calibrated thermal model, Johnson et al. (2016), showed that minor element chemistry in some meteorites can be used to determine temperatures. These can be compared to other thermometers (most notably two-pyroxene and olivine-chromite) to independently test the results. The new model offers insight into the pressures experienced by the meteorites.

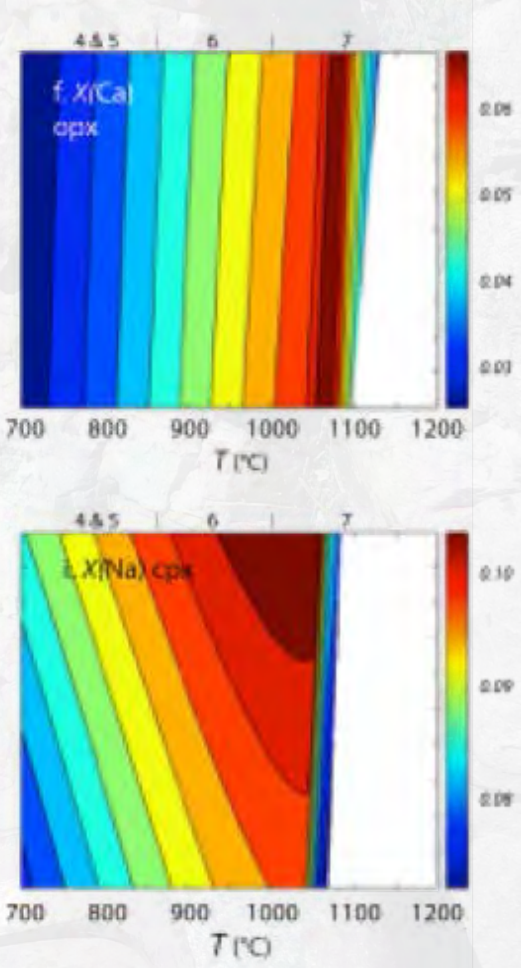

Johnson T.E., Benedix G.K., Bland P.A. (2016). Metamorphism and partial melting of ordinary chondrites: Calculated phase equilibria. *Earth and Planetary Science Letters* 433, 21–30. doi:10.1016/j.epsl.2015.10.035

Pyrite in the Martian meteorite NWA 7533.

Martian meteorite NWA7533 (paired with 7 other stones) is a polymict breccia formed on the southern, more ancient hemisphere of Mars and contains fine grained clasts chemically similar to those identified in soil from the Gusev crater by the Spirit rover. NWA 7533 is made up of pieces of plutonic rocks, impact melt rock, basalt and melt spherules welded together by a fine-grained matrix. It is also characterised by abundance of pyrite (up to 1% by weight) throughout its different lithologies, both clast or matrix. Pyrite shows a variety of shapes, from cube or truncated cube to octahedral, and sizes, from a few micrometers to clusters of up to 200 µm. Its presence throughout the breccia components and the planar features that affect most grains suggesting weak shock metamorphism indicate that pyrite formed on Mars once the breccia was assembled. Our study of chemistry as well as Pb and S isotopes suggests that pyrite precipitated from hot (~400-500ºC) hydrothermal sulphurous fluids at fO2 > FMQ+2 (Fayalite-Magnetite-Quartz buffer) percolating through the regolith breccia. This thermal event is likely to take place at ~1.4 Ga.

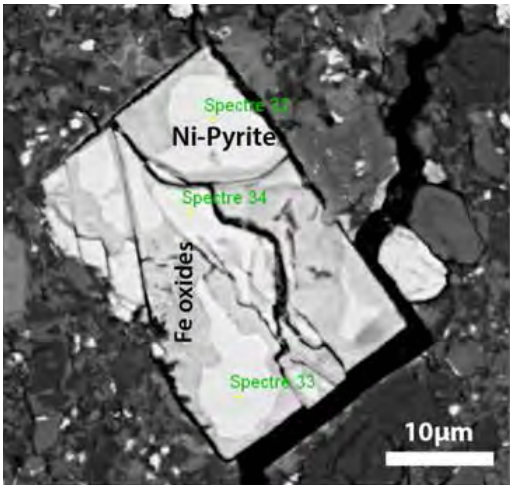

Near perfect Ni-Pyrite cube showing alteration to Fe-oxides.

Lorand J.-P., Hewins R.H., Remusat L., Zanda B., Pont S., Leroux H., Marinova M., Jacob D., Humayun M., Nemchin, A., Grange M., Kennedy A., Göpel C. (2015) Nickeliferous pyrite tracks pervasive hydrothermal alteration in Martian regolith breccia: A study in NWA 7533 (2015) Meteoritics and Planetary Science. Article in Press.

Zircon radiation damage age of Apollo 14 breccia 14311.

Zircon naturally integrates Uranium (U) and Thorium (Th) when crystallising and over time radioactive decay of these isotopes damage the zircon structure. Most damage is created by the alpha (α) particles emitted by the decaying isotopes and is proportional to the time since the grain formed and the amount of Th and U in the zircon: the older the grain and the higher the U and Th concentration, the higher the damage. This damage can be quantitatively measured by Raman spectroscopy, as this technique is sensitive to the degree of crystallinity of the studied material. In addition, ε-decay damages can be repaired (annealed), i.e. the zircon can become crystalline again, if it is exposed to temperatures above ~230ºC. Combination of these properties of the zircon can be used to investigate late low temperature events that affected lunar breccias and add to the understanding of their history and provenance. Pidgeon et al. (2016) tested this approach using lunar zircons from the Apollo 14 impact melt breccia 14311 and indicated that these grains were annealed at about 3410 ± 80 Ma. The annealing event is interpreted to represent a prolonged period of mare volcanism in the vicinity of the sample location.

Pidgeon R.T., Merle R., Grange M., Nemchin A.A., Whitehouse M.J. (2016). Annealing of radiation damage in zircons from Apollo 14 impact breccia 14311: implications for the thermal history of the breccia. *Meteoritics and Planetary Science* 51(1), 155-166.

Ages of phosphates from Apollo 14 breccia samples.

The results of precise U-Pb dating of phosphate grains from several Apollo 14 breccia samples indicate that they have been likely formed by tow closely spaced in time, but separate impact events. One at 3926±2 Ma, interpreted to represent the formation of Imbrium basin and one at 3944±4 Ma, that could represent either Humorum or Serenitatis basin-forming event. These new results show that two basin-forming impact events can be resolved within ~15 myrs and have important implications for the rate of lunar bombardment.

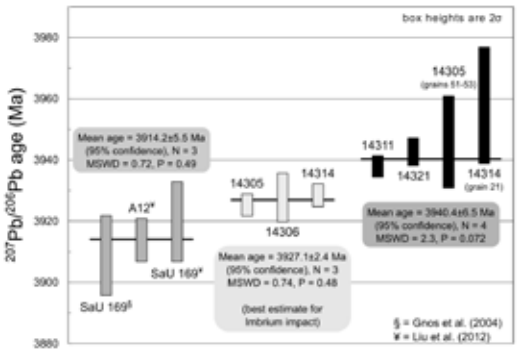

Precise Apollo 14 breccia ages allowing to investigate the possibility of closely timed impacts in the history of the Moon.

Pb isotope systematics of lunar basalts.

We have been able circumvent some of the problems that have previously hindered measurements of Pb isotope compositions of lunar samples by using in situ Secondary Ion Mass Spectrometry (SIMS) analyses of the Pb isotopic compositions in individual minerals. Utilysing this newly developed approach we have been able to obtain precise crystallisation ages (2σ errors typically within ±10 Ma) for several lunar basalts. Also assuming that the least radiogenic compositions measured in several of these samples represent initial Pb isotope compositions, we have begun to construct a multiple stage Pb isotope evolution model to describe the development of major lunar silicate reservoirs. This model places important constraints on the timing of lunar formation and differentiation, indicating that the Moon formed no later than ~4495 Ma, and experienced a major magmatic event at 4376±18 Ma.

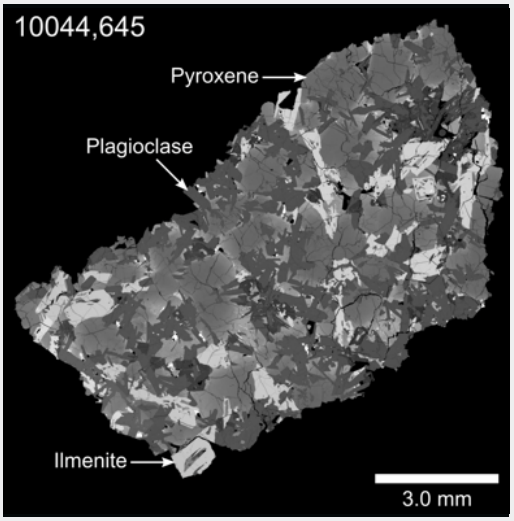

Lunar Mare basalt investigated as a part of the study of Pb isotope evolution of global lunar mantle reservoirs

Snape J.F., Nemchin A.A., Grange M.L., Bellucci J.J., Thiessen F., Whitehouse M.J. (2016) Phosphate ages in Apollo 14 breccias: Resolving multiple impact events with high precision U-Pb SIMS analyses. *Geochimica et Cosmochimica Acta*, 174, 13-29.

Excavating mantle material by impact events on the Moon.

Global maps of crustal thickness on the Moon, derived from gravity measurements obtained by NASA's Gravity Recovery and Interior Laboratory (GRAIL) mission, have shown that the lunar crust is thinner than previously thought. Hyperspectral data obtained by the Kaguya mission have also documented areas rich in olivine that have been interpreted as material excavated from the mantle by some of the largest lunar impact events. Miljkovic et al. (2015) performed numerical simulations (using iSALE-2D hydrocode) to investigate the conditions under which mantle material may have been excavated during large impact events and where such material should be found. The results show that excavation of the mantle could have occurred during formation of the several largest impact basins on the nearside hemisphere as well as the Moscoviense basin on the farside hemisphere. Even though large areas in the central portions of these basins were later covered by mare basaltic lava flows, surficial lunar mantle deposits are predicted in areas external to these maria. The results support the interpretation that the high olivine abundances detected by the Kaguya spacecraft could indeed be derived from the lunar mantle.

Miljković K., Wieczorek M.A., Collins G.S., Solomon S.C., Smith D.E., Zuber M.T. (2015) Excavation of the mantle in basin-forming impact events on the Moon. *Earth Planet. Sci. Lett.*, 409, 243–251.

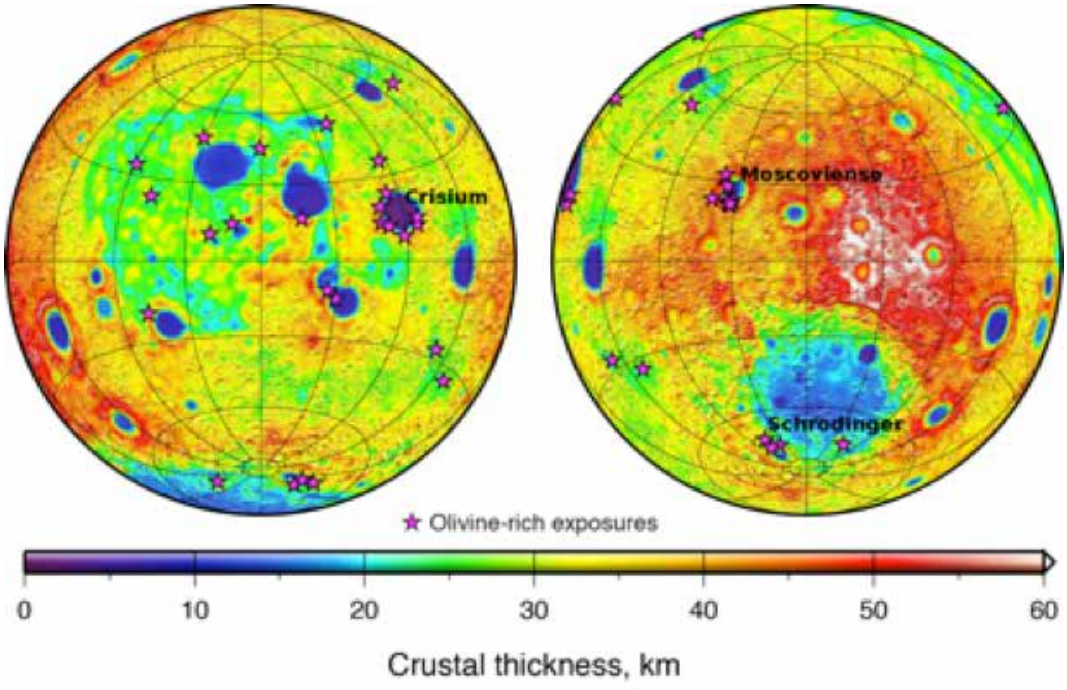

Crustal thickness of the Moon derived from GRAIL gravity data (Wieczorek et al., 2013), updated with the gravity model of Konopliv et al. (2013), and locations of olivine-rich exposures (stars) as documented by Kaguya (Yamamoto et al., 2010). The largest expanses of olivine are observed around the Crisium and Moscoviense basins, which have crustal thickness values close to zero. The maps are Lambert azimuthal equal-area projections centered over (left) the Procellarum KREEP Terrane (200 N, 3350 E) and (right) the opposite hemisphere; grid lines are spaced every 300.

Lunar Impact Basins.

Observations from the Gravity Recovery and Interior Laboratory (GRAIL) mission indicate a marked change in the gravitational signature of lunar impact structures at the morphological transition, with increasing diameter, from complex craters to peak-ring basins. Our GRAIL inventory of lunar basins also improves upon earlier lists that differed in their totals by more than a factor of 2. The size-frequency distributions of basins on the nearside and farside hemispheres of the Moon differ substantially; the nearside hosts more basins larger than 350 km in diameter, whereas the farside has more smaller basins. Hemispherical differences in target properties, including temperature and porosity, are likely to have contributed to these different distributions.

Neumann G.A., Zuber M.T., Wieczorek M.A., Head J.W., Baker D.M.H., Solomon S.C., Smith D.E., Lemoine F.G., Mazarico E., Sabaka T.J., Goossens S., Melosh H.J., Phillips R.J., Asmar S.W., Konopliv A.S., Williams J.G., Sori M.M., Soderblom J.M., Miljković K., Andrews-Hanna J.C., Nimmo F., Kiefer W.S. (2015) Lunar Impact Basins Revealed by Gravity Recovery and Interior Laboratory Measurements, *Sci. Adv.*, 1, e1500852, doi:10.1126/sciadv.1500852.

Porosity in the lunar highlands from impact cratering.

This study by Soderblom et al., (2015) showed that Impact-generated porosity of the bulk fractured lunar crust is likely to be in a state of equilibrium for craters smaller than ~30 km in diameter, but consistent with an ~8 km thick lunar megaregolith, whereas the gravity signature of larger craters is still preserved and provides new insight into the cratering record of even the oldest lunar surfaces.

Soderblom J.M., Evans A.J, Johnson B.C., Melosh H.J., Miljković K., Phillips R.J, Andrews-Hanna J.C., Head III J.W., Milbury C., Neumann G.A., Nimmo F., Smith D.E., Solomon S.C., Sori M.M., Thomason C.J., Wieczorek M.A., Zuber M.T. (2015) Production and saturation of porosity in the lunar highlands from impact cratering, *Geophys. Res. Lett.*, 42, 6939-6944.

Scaling laws inverted from Apollo seismic data.

Gudkova et al., (2015) demonstrated that the seismic cutoff frequencies for 40 selected lunar impact sites correlate with an impact-related proxy for local porosity. Our finding shows that lunar seismic records of meteoroid impacts represent unique geophysical data documenting medium to high-energy (0.1–1 kt TNT yield) impact processes, including the interaction of shock waves with porous media.

Gudkova T., Lognonné P., Miljković K., Gagnepain-Beyneix J. (2015) Impact cutoff frequency - momentum scaling law inverted from Apollo seismic data. *Earth Planet. Sci. Lett.*, 427, 57–65.

Research reports

PALAEONTOLOGY AND BIOSTRATIGRAPHY

Dating and interpreting the Kinta Limestone Formation using conodont stratigraphy.

Haylay et al., (2015a,b) have completed work on the palaeobiography of this problematic formation using detailed conodont stratigraphy from three new exploration wells, drilled using PETRONAS funding (Y-UTP). This has enabled the group to understand the palaeobiography of how mainland South East Asia was assembled in the Late Palaeozoic and to understand the probability of petroleum resources in this region.

Age and timing of the formation of the Late Palaeozoic (Devonian-Carboniferous) Sibumusu Terrain of mainland Southeast Asia.

(Hunter et al., 2015) report on research resulting from the continued association with the Shell-funded Southeast Asia Carbonate Laboratory (SEACaRL) at the PETRONAS University of Technology, Malaysia, under the research theme "High resolution Biostratigraphy carbonate systems of Southeast Asia for Petroleum Exploration". Within this theme the project "Age and timing of the formation of the Late Palaeozoic (Devonian-Carboniferous) Sibumusu Terrain of mainland Southeast Asia", is part of the IGCP 596 Climate Change and Biodiversity Patterns in Mid-Palaeozoic. This included publishing work on our Devonian-Carboniferous section in Langgun Island, Langkawi, Malaysia in the UNESCO supported book.

Fieldwork in Malaysia: Langgun Island section, Langkawi (left); selecting the drilling site for the Kinta Limestone (middle): recovered drill core (right).

Haylay, H. T. G., Sum, C. W., Hunter, A. W., (2015a). Preservation of Marine Chemical Signatures in Upper Devonian Carbonates of Kinta Valley, Peninsular Malaysia: Implications for Chemostratigraphy. pp. 291-302, *ICIPEG 2014*. Springer.

Haylay, H. T. G., Sum, C., Gatovsky, Y., Hunter, A. W., Talib, J. A., (In review). Discovery of Upper Devonian - Lower Carboniferous conodonts in the Kinta Limestone, Western Belt of Peninsular Malaysia: Implication for continuous sedimentation in the paleo-Tethys. *Geological and Stratigraphic Correlation*.

Hunter, A.W., Bashardin, A., Meor, H.A.H. (2015). The Pulau Langgun section in the north-western Terrain (Upper Devonian). pp. 154-155. In: T.J. Suttner, E. Kido, P. Königshof, J.A. Waters, L. Davis and F. Messner (Eds.) *Planet Earth-In Deep Time-Palaeozoic Series: Devonian & Carboniferous*. Schweizerbart Science Publishers, Stuttgart, Germany.

Origins of early animal life.

Lefebvre et al. (in press) have studied the diversification of echinoderms in the Lower Ordivician. This paper is part of a broad research theme on "Origins of early animal life" looking at the origins of complex life in the late Mesoproterozoic through to the community dynamics during the Palaeozoic. Within this theme "The Origins of the asterozoans" is a collaborative project with University of Lyon 1 (France), funded by the National Geographic and the CNRS, investigating the evolutionary origins of modern post-Palaeozoic starfish and brittle stars by studying exceptional specimens from the Ordovician of Great Britain, southern France, and Anti-Atlas, Morocco. Many of these deposits represent the first appearance of these animals in the fossil record. The main aim of the project is to look at how these animals emerged suddenly at the base of the Cambrian in a recognisable but primitive form and have increased in complexity through the Palaeozoic, while observing how each has responded to changing palaeobiogeography in the early to late Ordovician. They are a difficult group to study being morphologically complex and this project aims to solve a long-standing debate about the relationship between the asteroids (starfish), ophiuroids (brittle stars) and their presumed common ancestor the somasteroids.

Lefebvre et al. is part of a special volume looking at the Fezouata Shale (Morocco), which is described as the last refuge of the ancient Cambrian fauna which is typified by the Burgess Shale in Canada. The volume documents all of the preserved animals within this exceptionally preserved assemblage, including the shift and extinction of the Cambrian echinoderm communities as they were being replaced by new Ordovician animals at the start

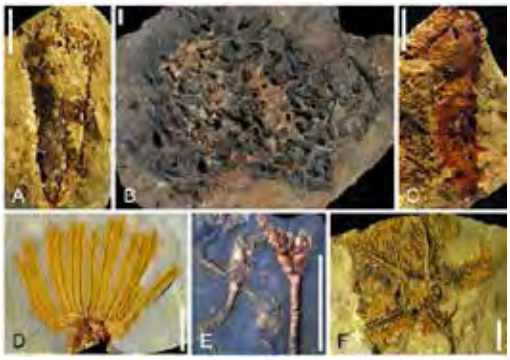

Exceptionally preserved animals fossils from the Fezouata Shale of Anti Atlas Morocco.

of the Great Ordovician Biodiversification Event (GOBE). The special volume includes a specially commissioned artistic reconstruction of the sea floor. This paper will be followed in 2016 by describing one of the earliest starfish animals that features within it. Other aspects of this research theme include looking at changes in echinoderm meadows in the Devonian of the Falklands and South Africa in collaboration with the Natural History Museum, London, British Geological Survey and University of Cape Town, and the Permo/Triassic of Western Australia and Timor, to investigate the effects of climatic changes on continental shelf echinoderm meadows such as those in Antarctica today in collaboration with the University of Western Australia, University of Cambridge and British Antarctic Survey. This resulted in two manuscripts submitted in 2015 with additional manuscripts planned for 2016.

Lefebvre B., N. Allaire N., T.E. Guensburg T. E., Hunter A. W., K. Kouraïss K., Nardin E., Noailles F., Pittet B., Zamora S., Sumrall C. D., (accepted for a Special Volume) Palaeoecological aspects of the diversification of echinoderms in the Lower Ordovician of central Anti-Atlas, Morocco, *Palaeogeography, Palaeoclimatology, Palaeoecology.*

A new stalked crinoid from cold methane seeps in the Upper Cretaceous.

Hunter et al. (in press) describe an exceptionally preserved methane seep assemblage, containing a previously undocumented crinoid that turned out to be an entirely new suborder. Although you would expect that most of the major groups of crinoids had already been documented over the last 200 years, this turned out to be a big surprise and a significant addition to the 'Treatise' of invertebrate fossils. The main reason this fossil remained undiscovered was that it was almost never found intact and in order to reconstruct this animal they had to prospect and process many hundreds of ossicles over 7 year period to reassemble an animal that could be published. The unusual morphology of this crinoid reflects a unique adaptation to the benthic island cold methane seep it inhabited and it is the first crinoid to be found living it such as ecosystem in the fossils record.

Hunter, A. W., Larson, N. L., Landman, N. H. and Oji, T., (In-press) *Lakotacrinus brezinai* n. gen.and sp., A New Stalked Crinoid From Cold Methane Seeps In The Upper Cretaceous (Campanian) Pierre Shale, South Dakota, United States. *Journal of Paleontology*

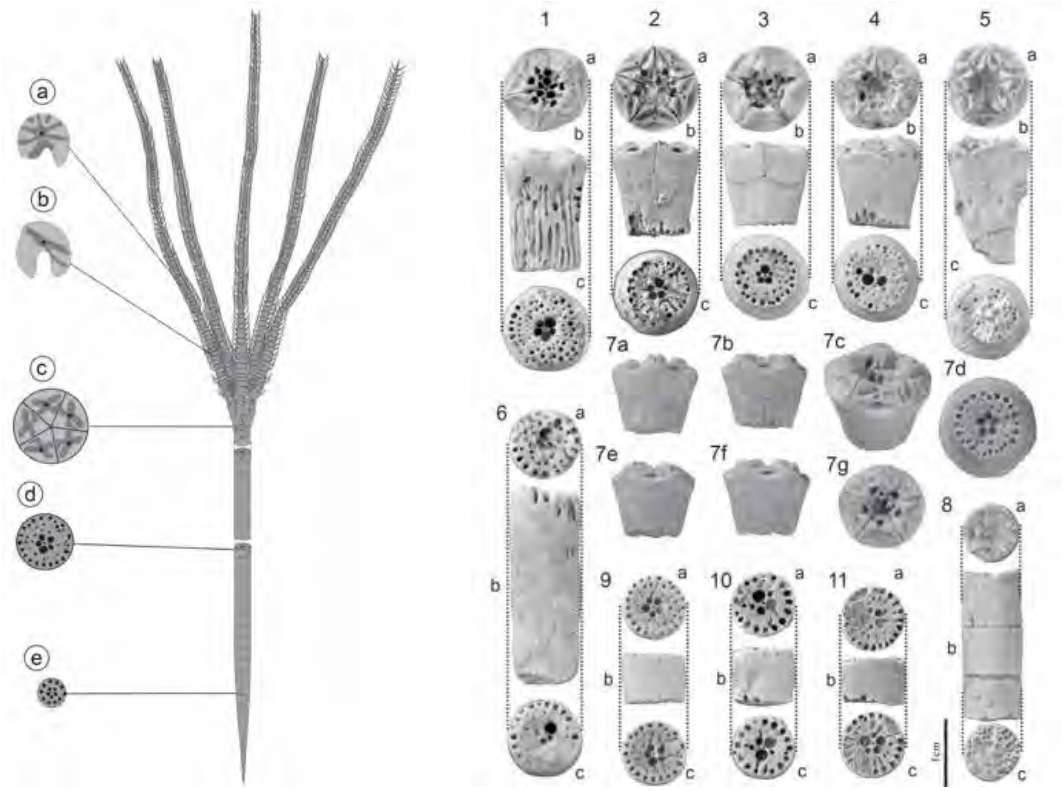

Bizarre new crinoid from South Dakota, USA: Reconstruction (left) and piecing together the fossil remains (right).

Sexual dimorphism in primitive vertebrates.

Evidence for sexual dimorphism and internal fertilization was reported in the most primitive of the jawed vertebrates. Further work showed that the reproductive structures were separated from the pelvic fins. This had major implication for the origin of how limbs formed. Pelvic fins are essentially copies of pectoral fins and it had previously been though that paired appendages could not form posterior to the pelvic girdle. We showed that placoderm claspers were a third set of posteriopaired appendages.

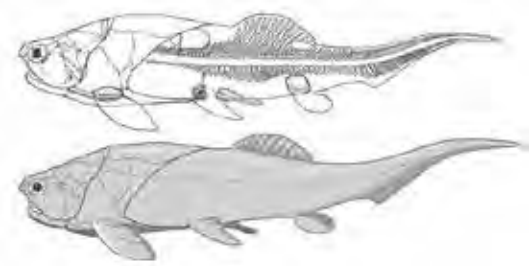

Long J., Mark-Kurik E., Johanson Z., Lee M., Young G., Min Z., . . . Trinajstic K. (2015). Copulation in antiarch placoderms and the origin of gnathostome internal fertilization. *Nature*. 517, 196-199.

Trinajstic K., Boisvert C., Long J., Maksimenko A., Johanson, Z. (2015). Pelvic and reproductive structures in placoderms (stem gnathostomes). *Biological Reviews*, 90, 467-501.

The first fossil shark from the Gogo Formation.

Long et al. (2015) described the first fossil shark from the Gogo Formation. This specimen represents the transition between sharks with a more boney skeleton to sharks with a skeleton made up of cartilage, which is the advanced condition. This shows that sharks today are not an evolutionary throwback, but highly derived.

Long J., Burrow C., Ginter M., Maisey J., Trinajstic K., Coates M., . . . Senden T. (2015). First shark from the late devonian (frasnian) Gogo formation, Western Australia sheds new light on the development of tessellated calcified cartilage. PloS One. 10, 1-24.

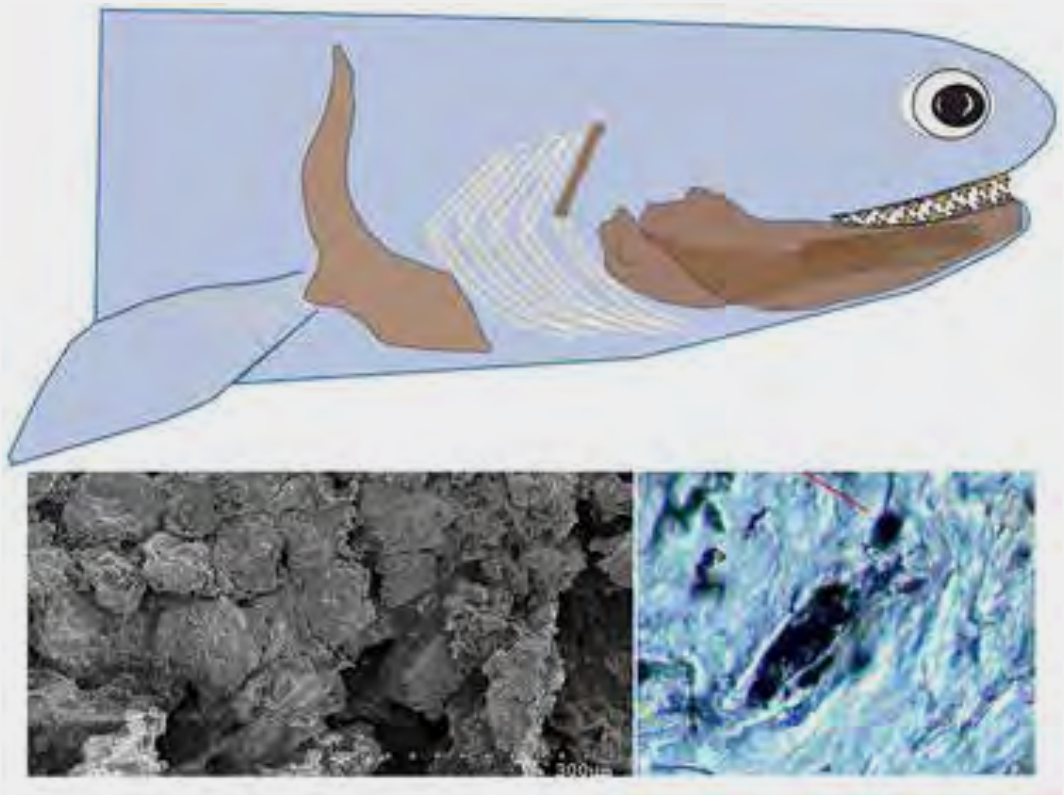

Figure supplied Dr John Long Flinders University.

Conodonts and the recognition of the Viséan-Serpukhovian (Carboniferous) boundary in Ireland.

Barham et al (2015) discuss the evolution of a biostratigraphically important conodont genus, Lochriea, to assist selection of a species to define the base of the Serpukhovian Stage. The work raises significant questions for conodont biostratigraphy in general with respect to taphonomy, pathology and species definition.

Barham, M., Murray, J., Sevastopulo, G.D., Williams, D.M. (2015). Conodonts of the genus *Lochriea* in Ireland and the recognition of the Viséan-Serpukhovian (Carboniferous) boundary. *Lethaia* 48, 151-171.

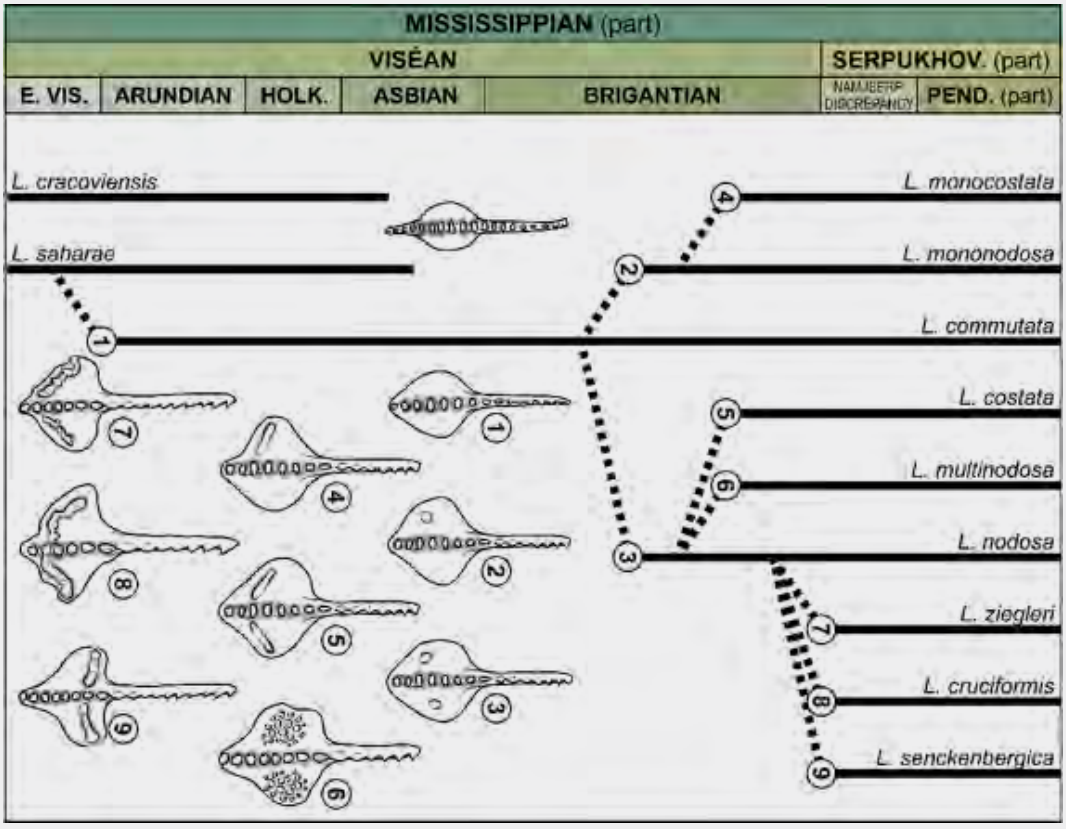

Illustration of probable relationships for the species of Lochriea discussed in this work. Note that there is no current GSSP defined for the Viséan-Serpukhovian boundary but that the proliferation of species and origination of L. ziegleri is currently the best candidate to define the revised base of the Serpukhovian.

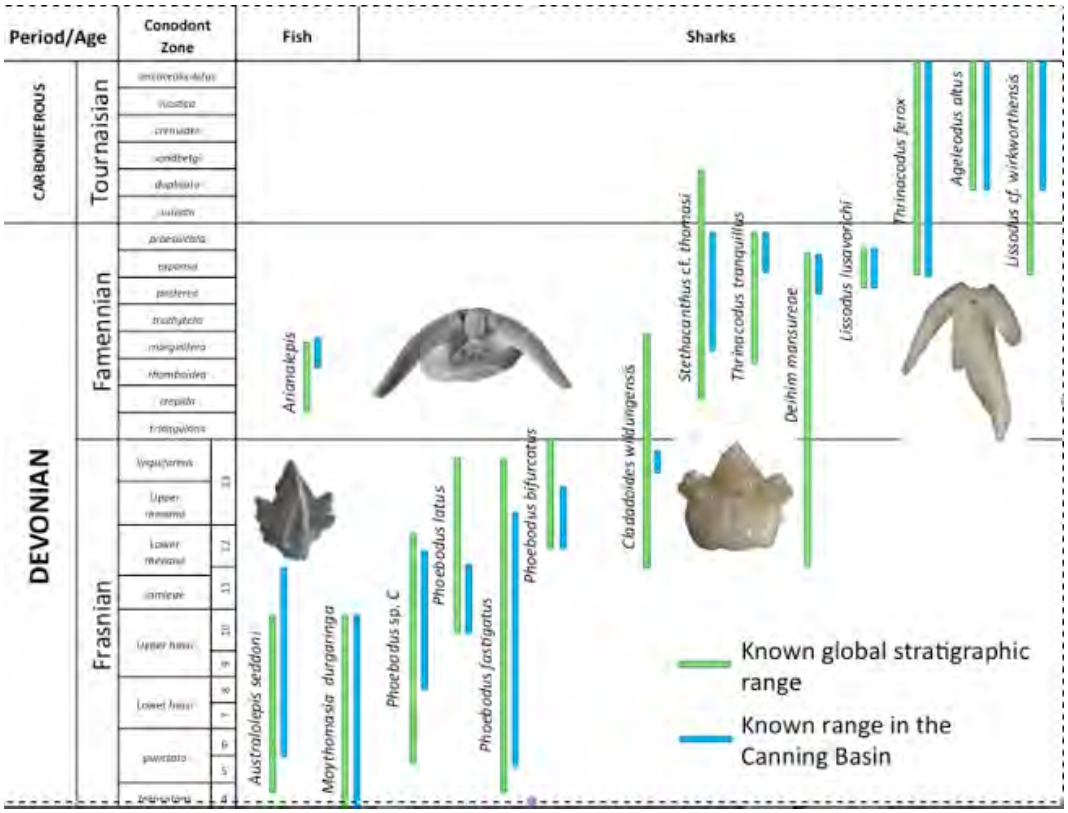

Microvertebrates and their significance.

The utility of mircrovertebrates for dating and correlation of restricted marine environments was determined. The diversity and known age range of sharks in the Canning Basin was extended indicting sharks are biostratigraphically important for the Late Devonian and Early Carboniferous. This work formed part of an Australian Research Council grant LP0883812 Chronostratigraphic Framework for the Devonian Canning Basin – A Multidisciplinary Record of Environmental Change

Hansma J., Tohver E., Yan M., Trinajstic K., Roelofs B., Peek S., . . . Hocking R. (2015). Late Devonian carbonate magnetostratigraphy from the Oscar and Horse Spring Ranges, Lennard Shelf, Canning Basin, Western Australia. *Earth and Planetary Science Letters*, 409, 232-242

Roelofs B., Playton T., Barham M., Trinajstic K. (2015). Upper Devonian microvertebrates from the Canning Basin, Western Australia. *Acta Geologica Polonica* 65, 69-100.

Hillbun K., Playton T. E., Tohver E., Ratcliffe K., Trinajstic K., Roelofs B., . . . Ward P. (2015). Upper Kellwasser carbon isotope excursion predates the F-F boundary in the Upper Devonian Lennard Shelf carbonate system, Canning Basin, Western Australia. *Palaeogeography, Palaeoclimatology, Palaeoecology*, 438, 180-190.

Research reports

SEDIMENTARY ENVIRONMENTS, BASINS AND ENERGY RESOURCES

Sedimentary environments, basins and energy resources

Research into sedimentary environments, basins and energy resources at Curtin University received a big boost with the establishment of the Chevron University Partnership Programme in 2013. A petroleum geoscience research group is now firmly established, focusing mainly on the evolution of sedimentary basins on the various continental margins of Australia, complimenting ongoing research in the department into sedimentary environments, palaeontology and basin evolution.

Evolution of the North West Shelf and Perth Basin

The North West Shelf of Australia is an unusual passive margin. It has been located close to a continental margin throughout much of its history, and has been subject to numerous rift events. Research on the Northwest Shelf and in the Perth Basin is aimed at understanding basin evolution on a regional scale, with particular emphasis on:

- the tectonic setting, timing and distribution of Carboniferous and Permian extension in onshore and offshore basins, and the extent to which it forms the fundamental architecture for subsequent rift events
- the significance or otherwise of the "Fitzroy Movement" beyond the well documented transpressional structures that occur in the Canning Basin
- variations in the distribution, timing and orientation of Jurassic extension in the Perth, Northern Carnarvon, Browse and Bonaparte Basins, and its relation to rifting of micro-continental fragments from the North West Shelf margin
- variations in the distribution, timing and orientation of Lower Cretaceous extension in the Perth, Northern Carnarvon, Browse and Bonaparte Basins, and its relation to the separation of Greater India from Australia
- the distribution of uplift, erosion during each of these rift events, and the implications of this for syn-rift sediment distribution and pathways
- the distribution, timing and tectonic significance of post break-up compression on the NW Shelf and in the Perth Basin
- the response of salt to these different tectonic events in the Petrel Basin

These projects form part of our contribution to the ARC Research Hub for Basin Geodynamics and Evolution of Sedimentary Systems (Basin Genesis Hub), a showcase of connecting "Big Data" analysis and high-performance computing in an open innovation framework. The aim of the hub is to fuse multidimensional data into 5D basin models (space and time, with uncertainty estimates) by coupling the evolution of mantle flow, crustal deformation, erosion and sedimentary processes using open-source modelling tools.

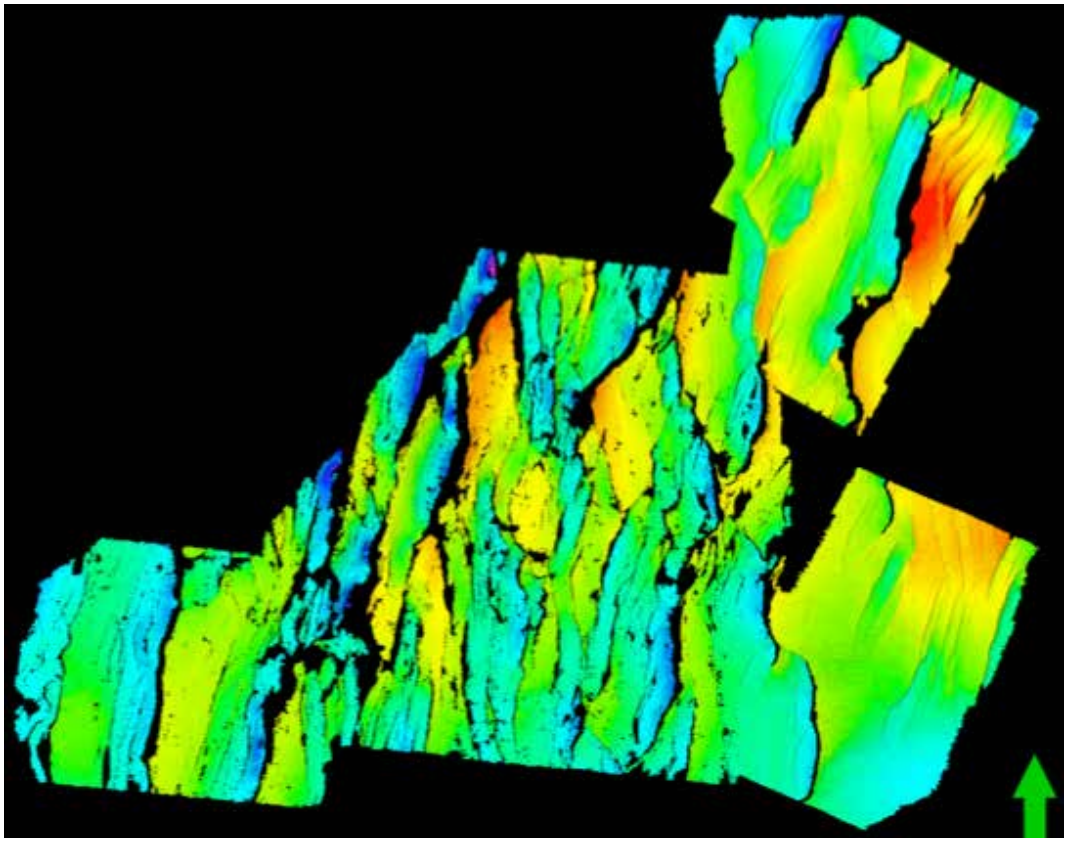

Regional scale map of the top of the Triassic Mungaroo Formation in the outer part of the Exmouth Plateau showing extensional fault blocks formed as a result of Jurassic rifting.

The results of this research have been presented at the following conferences in 2015:

- **ASEG-PESA, Perth, February 2015**
  - Oblique reactivation of inherited fabrics, Northern Carnarvon Basin (Chris Elders)

- **AAPG International Conference & Exhibition, Melbourne, September 2015**
  - The Pre-Permian History of the North Perth and South Carnarvon Basins, Western Australia (Chris Elders)
  - Structural Evolution of the SE Margin of the Browse Basin (Chris Elders)

- **Specialist Group in Tectonics and Structural Geology, Caloundra, November 2015**
  - What moved in the Fitzroy Movement? (Chris Elders)

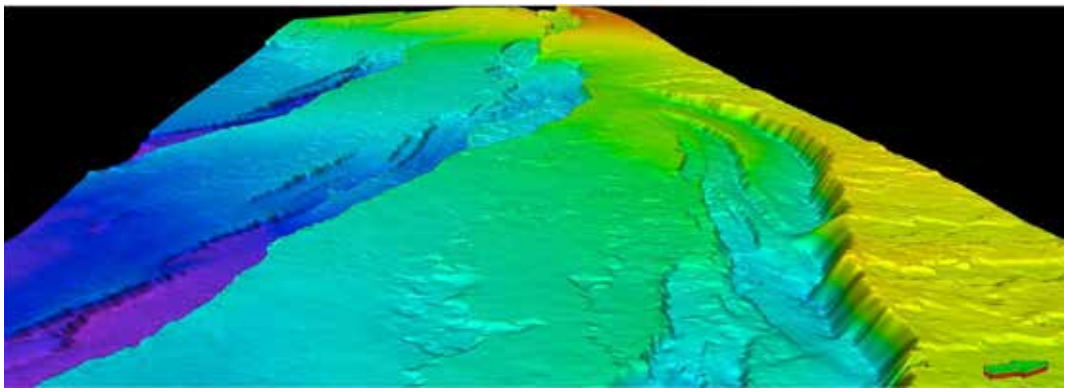

Gravitationally induced listric extensional faults developed in Cretaceous sequences in the Ceduna Delta.

Evolution of the Southern Margin of Australia

In comparison to the North West Shelf, the southern margin of Australia is a more "typical" passive margin. Despite this, there are many complex aspects of its evolution which are yet to be understood and which have implications for understanding petroleum systems in this frontier hydrocarbon province. Our current research is focussed on:

- understanding the role played by deep basement structures on the rift architecture of the margin
- the potential of syn-rift petroleum systems in the Eyre sub-basin
- the evolution of gravitationally induced fault systems in the Ceduna Delta and their interaction with sedimentary systems
- the occurrence and distribution of igneous activity and the significance of Eocene uplift in the Ceduna Delta

The results of this research have been presented at the following conferences in 2015:

- **AAPG International Conference & Exhibition, Melbourne, September 2015**
  - Cretaceous Fault Growth and Linkage in the Ceduna Shelf, Bight Basin, Southern Australia (Jane Cunneen)
  - Stratigraphy, Age and Provenance of Madura Shelf Sediments, WA: Implications for the Evolution of the Bight Basin and Australia's Southern Margin (Milo Barham)
- **Specialist Group in Tectonics and Structural Geology, Caloundra, November 2015**
  - Basement influences on structural styles in the Bight Basin, southern Australia (Jane Cunneen)

Research reports

GEODESY AND SPATIAL SCIENCES

Geodesy

Geodesy involves the study of the Earth's shape and gravity field. It forms the scientific basis for precise positioning over large areas, navigation, mapping and charting, and studies of the physics and dynamics of the Earth. It therefore contributes to the Earth-present theme in TIGeR.

Subsidence in the Perth Basin.

Featherstone et al. (2015) used a combination of independent evidence (continuous GPS, repeat levelling, groundwater, satellite altimetry, and tide gauge records) to show that the long-recording Fremantle tide gauge has been subsiding in a nonlinear way since the mid-1970s due to time-variable groundwater abstraction. The vertical land motion rates vary from approximately -2 to -4 mm/yr (i.e., subsidence), thus producing a small apparent acceleration in mean sea level computed from the Fremantle tide gauge records. In the Perth Basin, they show that groundwater extraction records can be used as a diagnostic tool for identifying nonlinear subsidence that is not evident in GPS time series alone. This work attracted some substantial attention from the media (television, online and print).

Featherstone W.E., Penna N.T., Filmer M.S., Williams S.D.P. (2015) Nonlinear subsidence at Fremantle, a long-recording tide gauge in the Southern Hemisphere. *Journal of Geophysical Research: Oceans*, 120, 7004-7014.

The Fremantle tide gauge has been subsiding in a nonlinear way since the mid 1970s.

Lithospheric structure of Venus.

Jiménez-Díaz et al. (2015) show that there are many fundamental and unanswered questions on the structure and evolution of the Venusian lithosphere, which are key issues for understanding Venus in the context of the origin and evolution of the terrestrial planets. They investigated the lithospheric structure of Venus by calculating its crustal and effective elastic thicknesses (Tc and Te, respectively) from an analysis of gravity and topography. They found that the Venusian crust is usually 20–25 km thick with thicker (up to 94 km) crust under the highlands. The crustal plateaus are near-isostatically compensated, consistent with a thin elastic lithosphere, showing a thickened crust beneath them, whereas the lowlands exhibit higher Te values, maybe indicating a cooler lithosphere than that when the Venusian highlands were emplaced. The large volcanic rises show a complex signature, with a broad range of Te and internal load fraction values. Their results also reveal a significant contribution of the upper mantle to the strength of the lithosphere in many regions.

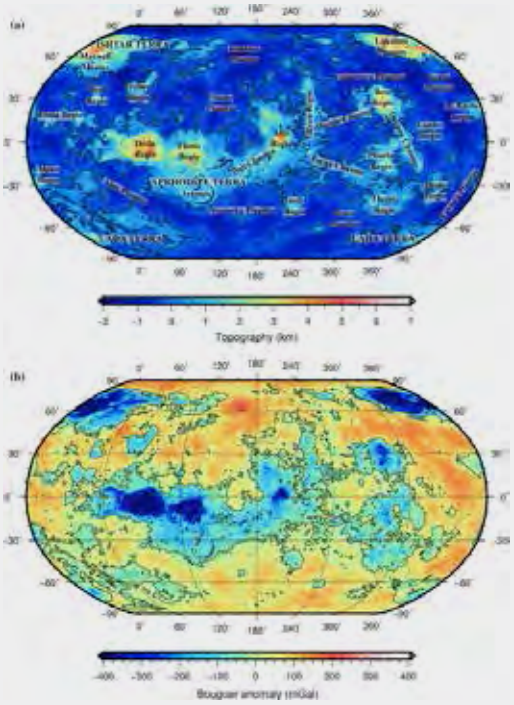

Topography (km) and Bouguer gravity anomalies (milliGal) on Venus.

Jiménez-Díaz A., Ruiz J., Kirby J.F., Romeo I., Tejero R., Capote R. (2015) Lithospheric structure of Venus from gravity and topography. *Icarus*, 260, 215-231.

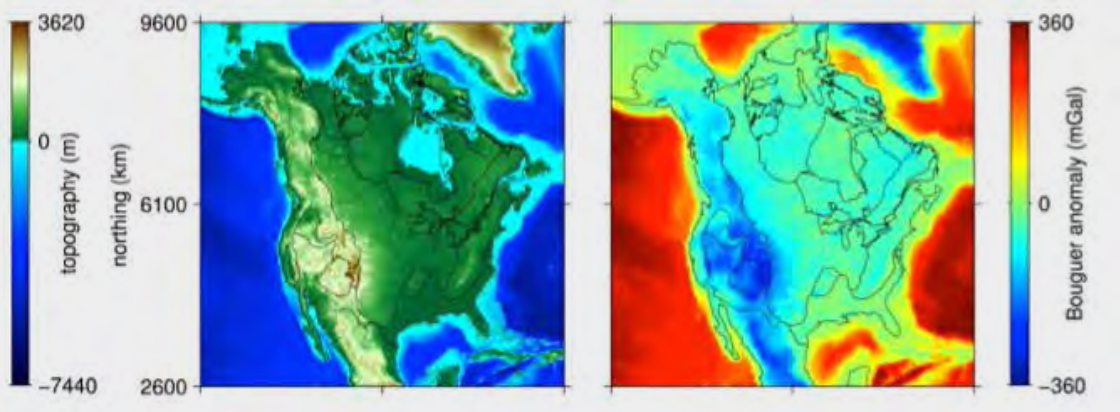

Topography (m) and Bouguer gravity anomalies (milliGal) over North America.

Mechanical anisotropy in the continental lithosphere.

Kalnins et al. (2015) argue that anisotropy in the coherence between topography and gravity anomalies is often observed, but whether it corresponds to an elastic thickness that is anisotropic remains an open question. If coherence is used to estimate flexural strength of the lithosphere, the null-hypothesis of elastic isotropy can only be rejected when there is significant anisotropy in both the coherence and the elastic strengths derived from it, and if interference from anisotropy in the data themselves can be plausibly excluded.

They considered coherence estimates made using multitaper and wavelet methods, from which estimates of effective elastic thickness are derived. The primary case study of the North American continent does not exhibit meaningful anisotropy in its mechanical strength. Similarly, a global reanalysis of continental gravity and topography using multitaper methods produces only scant evidence for lithospheric flexural anisotropy.

Kalnins L.M., Simons F.J., Kirby J.F., Wang D.V., Olhede S.C. (2015) On the robustness of estimates of mechanical anisotropy in the continental lithosphere: A North American case study and global reanalysis. *Earth and Planetary Science Letters*, 419, 43-51.

Spectral expression of gravity anomalies.

Claessens and Hirt (2015) contend that a surface spherical harmonic expansion of gravity anomalies with respect to a geodetic reference ellipsoid, rather than a mean Earth sphere, can be used to model the global gravity field and reveal its spectral properties. They derived a direct and rigorous transformation between solid spherical harmonic coefficients of the Earth's disturbing potential and surface spherical harmonic coefficients of gravity anomalies in ellipsoidal approximation with respect to a reference ellipsoid.

The method was used to create a surface spherical harmonic model of gravity anomalies with respect to the GRS80 ellipsoid from the EGM2008 global gravity model. Internal validation shows a global RMS precision of <1 nanoGal, significantly more precise than previous solutions.

Claessens S.J., Hirt C. (2015) A surface spherical harmonic expansion of gravity anomalies on the ellipsoid. *Journal of Geodesy*, 89, 1035-1048.

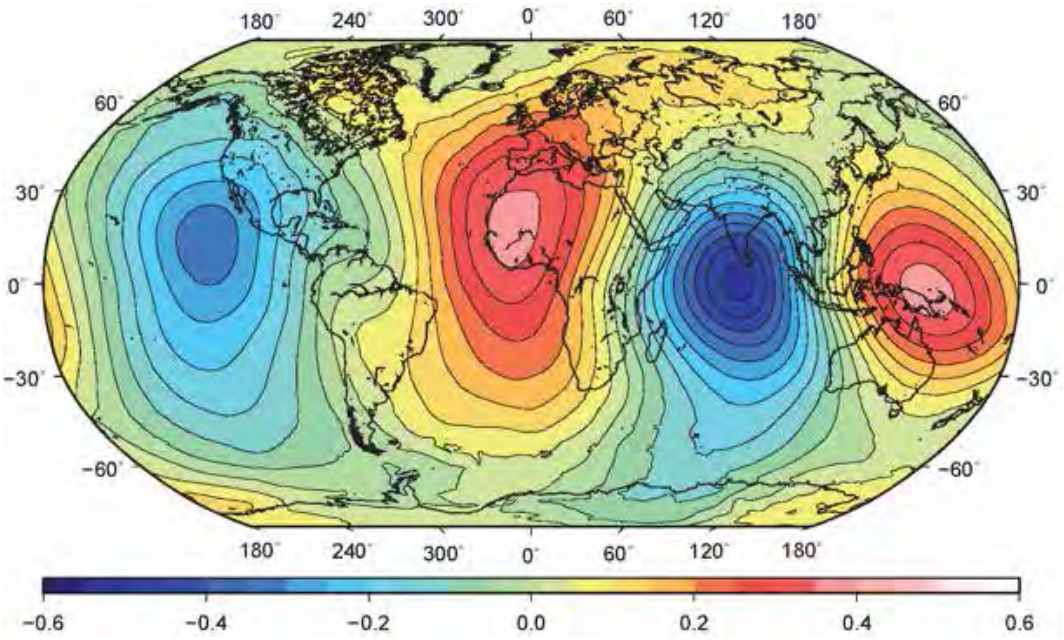

Ellipsoidal corrections (m) to a global gravimetric geoid from EGM2008.

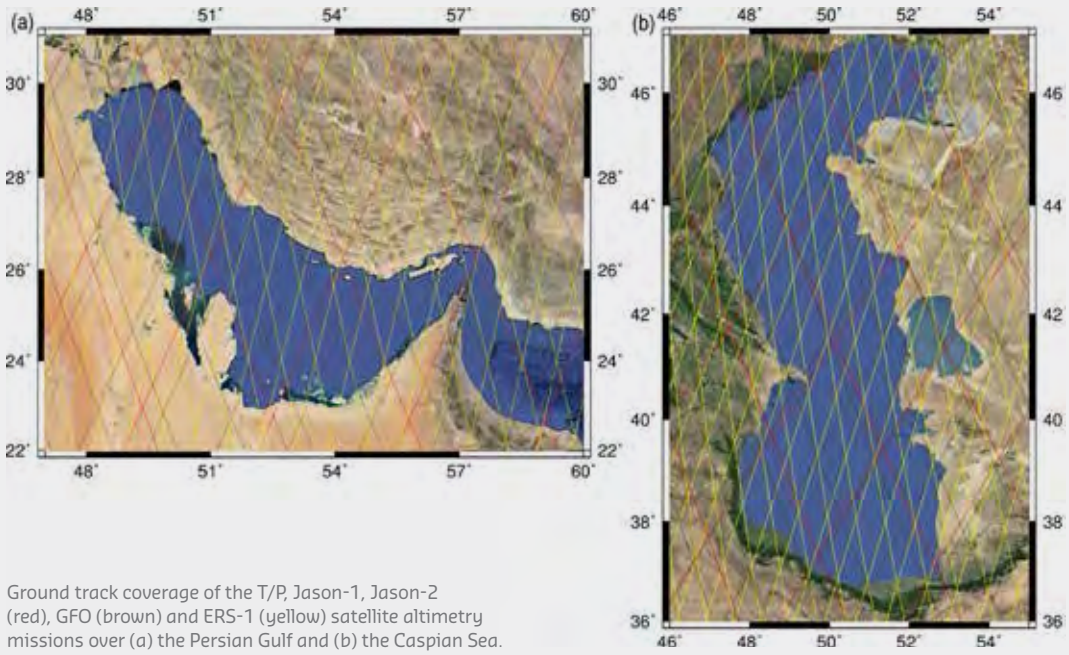

Ground track coverage of the T/P, Jason-1, Jason-2 (red), GFO (brown) and ERS-1 (yellow) satellite altimetry missions over (a) the Persian Gulf and (b) the Caspian Sea.

Gravity anomalies over the Persian Gulf and Caspian Sea.

This study By Kahki et al. (2015) uses retracked satellite radar altimeter observations to derived improved gravity anomaly fields over the Persian Gulf and Caspian Sea, areas with limited coverage of in-situ and ship-borne gravity observations. Retracking is required to remove observation biases due to land contaminations in the satellite altimeter footprints close to the coast. The newly developed retracking algorithm 'Extrema Retracking' (ExtR) has been employed to improve sea surface height (SSH) observations made by the five satellite radar altimeter missions TOPEX/ POSEIDON, JASON-1, JASON-2, GFO and ERS-1 providing repeat observations for over two decades. Upon the improved satellite radar altimeter observations deflections of the vertical and gravity anomalies have been derived through an iterative estimation process including a remove-restore algorithm based on the fast Fourier transform to convert deflections of the vertical into gravity anomalies.

Results for the estimated altimetry-derived gravity anomalies (with and without implementing the ExtR algorithm) have been compared to ship-borne free air gravity anomaly observations, and free air gravity anomalies from the Earth Gravitational Model 2008 (EGM2008). The comparison has been made for selected satellite altimeter ground tracks over the study areas and is illustrated for the Persian Gulf. The significant improvement is also confirmed by comparing root-mean-square-error (RMSE) values of the residuals before and after application of ExtR showing an average improvement from a level of about ±10 mGal down to a level around ±2 mGal.

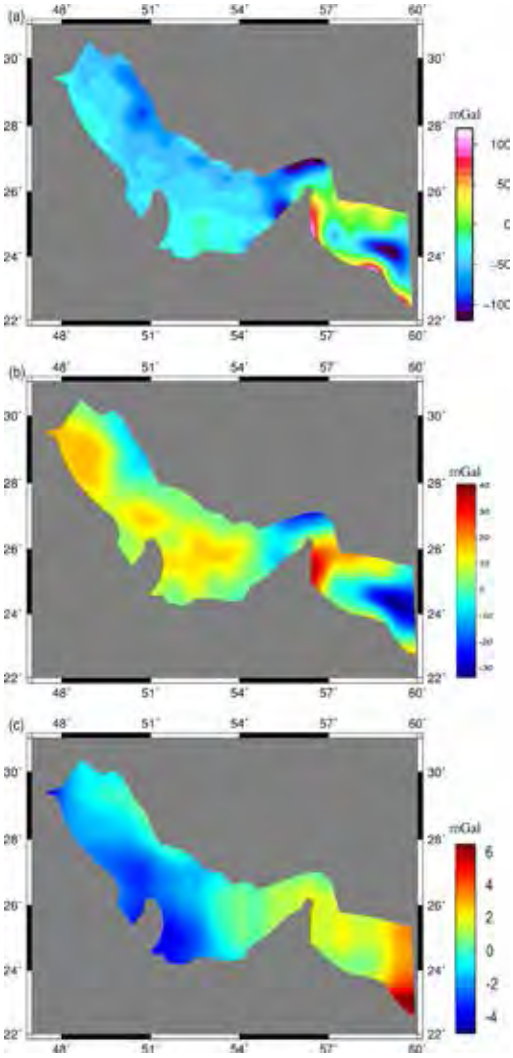

Marine gravity anomaly over the Persian Gulf (a). Differences between ship-borne gravity anomalies and altimetry-derived gravity anomalies before application of ExtR (b) and after application of ExtR (c).

Khaki M., Forootan E., Sharifi M.A., Awange J., Kuhn M. (2015) Improved gravity anomaly fields from retracked multimission satellite radar altimetry observations over the Persian Gulf and the Caspian Sea. *Geophysical Journal International*, 202, 1522-1534.

The geoid-to-quasigeoid correction.

In geodesy, the geoid and the quasigeoid are reference surfaces for heights and depths. Over the continents, the geoid-to-quasigeoid correction reaches several metres especially in the mountainous, polar and geologically complex regions. Tenzer et al. (2015) provide a summary of existing theoretical and numerical studies on the geoid-to-quasigeoid correction. They then compare these methods with a newly developed procedure in the spectral domain based on spherical harmonic analysis and synthesis of global gravity, terrain and crustal structure models. Tenzer et al. (2015) argue that the newly developed procedure is numerically more stable than existing inverse models that utilise downward continuation. In addition, the new method takes not only the terrain geometry but also the mass density heterogeneities within the whole Earth into consideration.

Tenzer R., Hirt C., Claessens S., Novák P. (2015) Spatial and spectral representations of the geoid-to-quasigeoid correction. *Surveys in Geophysics*, 36, 627-658.

Mathematical correction of the gravimetric geoid.

Paláncz et al.(2015) solve the problem of geoid correction based on GPS ellipsoidal height measurements via symbolic regression (SR). In this case, when the quality of the approximation is overriding, SR employing Keijzer expansion to generate initial trial function population can supersede traditional techniques, such as parametric models and soft computing models (e.g., artificial neural network approach with different activation functions). To demonstrate these features, numerical computations for correction of the Hungarian geoid was carried out using the DataModeler package of Mathematica. Although the proposed SR method could reduce the average error to a level of 1–2 cm, it has two handicaps. The first one is the required high computation power, which can be eased by the employment of parallel computation via multicore processor. The second one is the proper selection of the initial population of the trial functions. This problem may be solved via intelligent generation technique of this population (e.g., Keijzer-expansion).

Paláncz B., Awange J. L., Völgyesi L (2015) Correction of Gravimetric Geoid Using Symbolic Regression. *Mathematical Geosciences* 47, 867–883

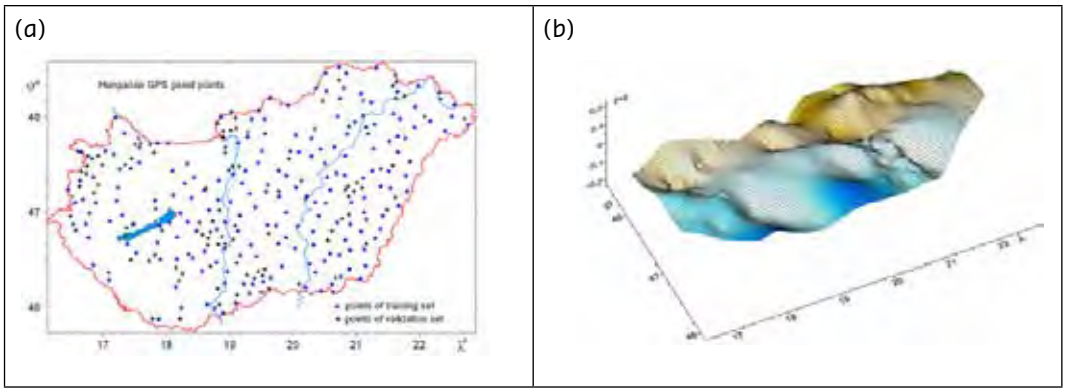

(a) Hungarian GPS geoidal height data: 194 training sets (marked by circles) and the 108 validation sets (marked by crosses) were used, and (b) the corrector surface computed using the SR model employing Keijzer expansions.

Environmental geodesy

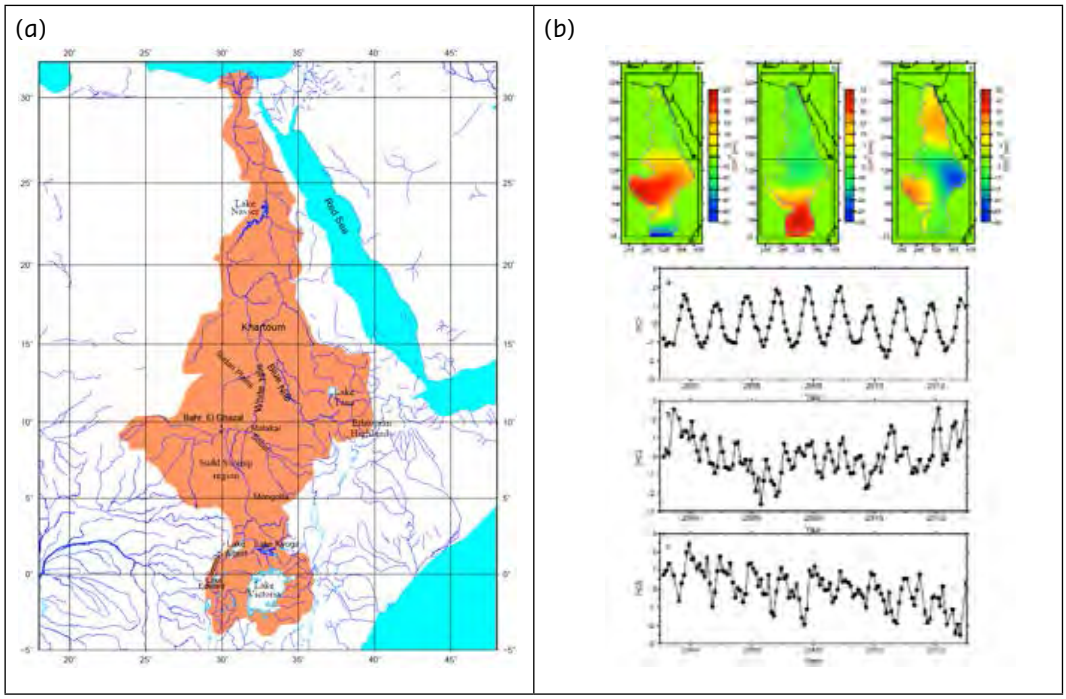

(a) The Nile basin (brown shaded region) with the major features, and (b) An overview of the PCA decomposition of TWS changes from the GRACE products over the Nile basin. Empirical orthogonal functions (EOFs) represent anomaly maps of the TWS variations. Principal components (PC)s are their unit-less normalized temporal evolution. PC1 and EOF1 presents 79% of the TWS variance, PC2 and EOF2 presents 9% of the variance, and 5% of the variance is the contribution of PC3 and EOF3.

Water resources in the Nile Basin.

Water resources within the Nile basin are under intense pressure from both human use and the changing climate. Remote sensing methodologies allow the water storage (WS) changes to be assessed, thereby providing essential information for water resource management. Awange et al. (2015) have analysed WS changes over the Nile basin derived from monthly Gravity Recovery And Climate Experiment (GRACE), Tropical Rainfall Measuring Mission (TRMM), and NDVI (Normalized Digital Vegetation Index) products, covering the period of 2003 to 2013. TRMM analysis showed no significant trend in the rainfall over the Nile basin. Principal Component Analysis (PCA) results indicated a general decrease in GRACE derived water storage in the northern part of the basin at a rate of 3 mm/yr. In contrast, Ethiopian highlands in the east exhibited a mass gain, with an average linear rate of 2.8 mm/yr. A lag of one to two months was derived between TRMM-rainfall and GRACE-WS time series. This might represent the large-scale relationship between accumulated rainfall patterns and storage changes over the basin. NDVI results showed a downward trend in vegetation cover during low rainfall.

Awange J., Forootan E., Fleming K., Odhiambo G.O. (2015) Dominant Patterns of Water Storage Changes in the Nile Basin During 2003–2013. In *Remote Sensing of the Terrestrial Water Cycle*, ed. Venkataraman Lakshmi, 367-382. New Jersey: John Wiley.

Evaporation and transpiration in the Volta Basin, West Africa.

The estimation of large-scale evapotranspiration (ET) is complex, and typically relies on the outputs of land surface models (LSMs) or remote sensing observations. However, over some regions of Africa, inconsistencies exist between different estimations of ET fluxes, which should be investigated. Andam-Akorful et al (2015) evaluate and combine different ET estimates from moderate-resolution imaging spectroradiometer (MODIS), Global Land Data Assimilation System (GLDAS) and terrestrial water budget (TWB) approaches over the Volta Basin, West Africa. ET estimates from water balance equation are obtained as residuals from monthly terrestrial water-storage (TWS) changes derived from Gravity Recovery and Climate Experiment (GRACE), Tropical Rainfall Measurement Mission (TRMM)'s rainfall data, and in situ discharge from Akosombo Dam (Ghana). Overall, out of the seven investigated ET estimates (two from the water balance approach of which one considers water storage using GRACE-derived TWS and the other ignoring it, four from GLDAS and one from MODIS), only MODIS (28.12mm month^{-1}), GLDAS–NOAH (32.74mm month^{-1}) and TWB (32.84mm month–1) were found to represent the range of variability close to the computed averaged reference ET (30.25mm month^{-1}). ET estimations inferred from MODIS were also found to represent relatively lower magnitude of uncertainties, that is, 3.99mmmonth^{-1} over the Volta Basin (cf. 7.06 and 18.85mm month–1 for GLDAS-NOAH and TWB-based ET estimations, respectively).

Andam-Akorful S.A., Ferreira V.G., Awange J.L., Forootan E. , He, X.F. (2015) Multi-model and multi-sensor estimations of evapotranspiration over the Volta Basin, West Africa. *International Journal of Climatology* 35: 3132–3145, doi: 10.1002/joc.4198.

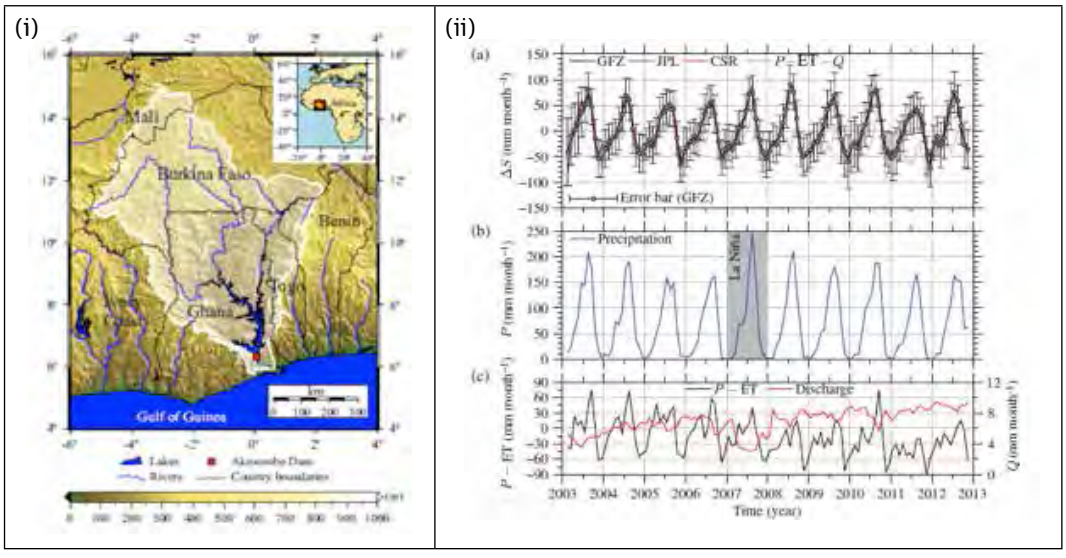

Figure 2: (i) The Volta River Basin (shadowed portion with an area of approximately 417,382 km2) and its riparian countries in West Africa. The scale is related to the parallel 10o N, and (ii) (a) GRACE-derived water-storage changes (ΔS) from the three different processing centers [Center for Space Research (CSR), Jet Propulsion Laboratory (JPL), GeoForschungsZentrum (GFZ)] and as a residual from P–ET –Q using ERA-Interim reanalysis and river discharge data, (b) Tropical Rainfall Measurement Mission (TRMM) precipitation; the grey-coloured rectangle shows the La Niña event in 2007, and (c) P–ET using ERA-interim, and in situ discharge data.

Global navigation satellite systems (GNSS)

Improving GPS systems over Australia.

El-Mowafy and Yang (2015) have been experimentally investigating the current availability of advanced Receiver Autonomous Integrity Monitoring (ARAIM) for the Localizer Performance with Vertical guidance down to 200 feet (LPV-200), using real GPS measurements collected at 60 stations across Australia. User Range Accuracy (URA), User Range Error (URE), and nominal biases for integrity and accuracy, which are used for the computation of the positioning protection level have been investigated. They have shown that incorporation of other GNSS constellation with GPS in ARAIM is needed to achieve LPV-200 Australia wide. The inclusion of BeiDou with GPS at two tests sites in Western and Eastern Australia demonstrates the promising potential of achieving this goal.

El-Mowafy A., Yang C. (2015). Limited Sensitivity Analysis of ARAIM Availability for LPV-200 over Australia using real data. *Advances in Space Research*, 57, 2659-670.

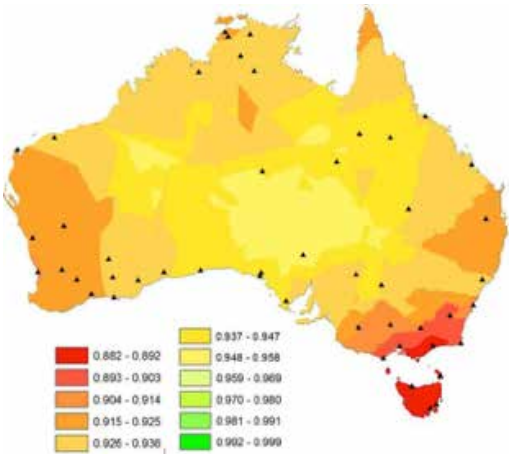

ARAIM Availability using current broadcast URA.

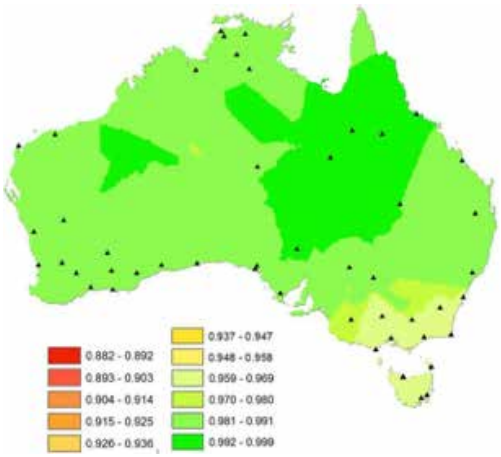

ARAIM Availability using URA=1m.

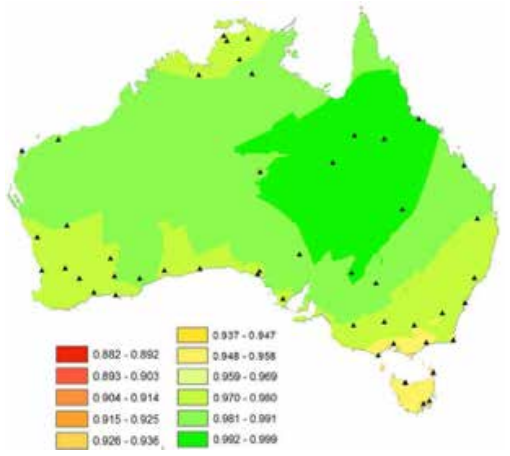

ARAIM Availability with 5° mask angle.

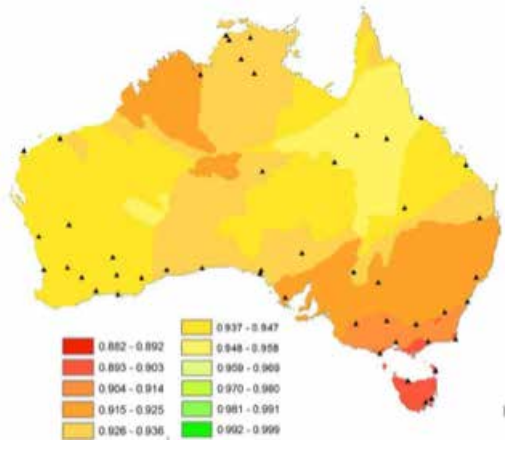

ARAIM Availability with 10° mask angle.

A new method for estimating stochastic properties of multi-constellation GNSS observations.

El-Mowafy et al (2015) have used parameters of the single-receiver single-satellite validation method to screen data from each satellite independently to detect and identify faulty observations. Agreement of the characteristics of the validation statistics with theory was used as the criterion to select the best precision of the observations, spectral density and correlation time of the unknowns. The method is applicable to any GNSS with any arbitrary number of frequencies. Demonstration of the method results and performance is given using multiple-frequency data from GPS, GLONASS and Galileo in static and kinematic modes.

El-Mowafy, A. (2015) Estimation of Multi-Constellation GNSS Observation Stochastic Properties Using a Single-Receiver Single-Satellite Data Validation Method, *Survey Review*, 47, 341, 99-108.

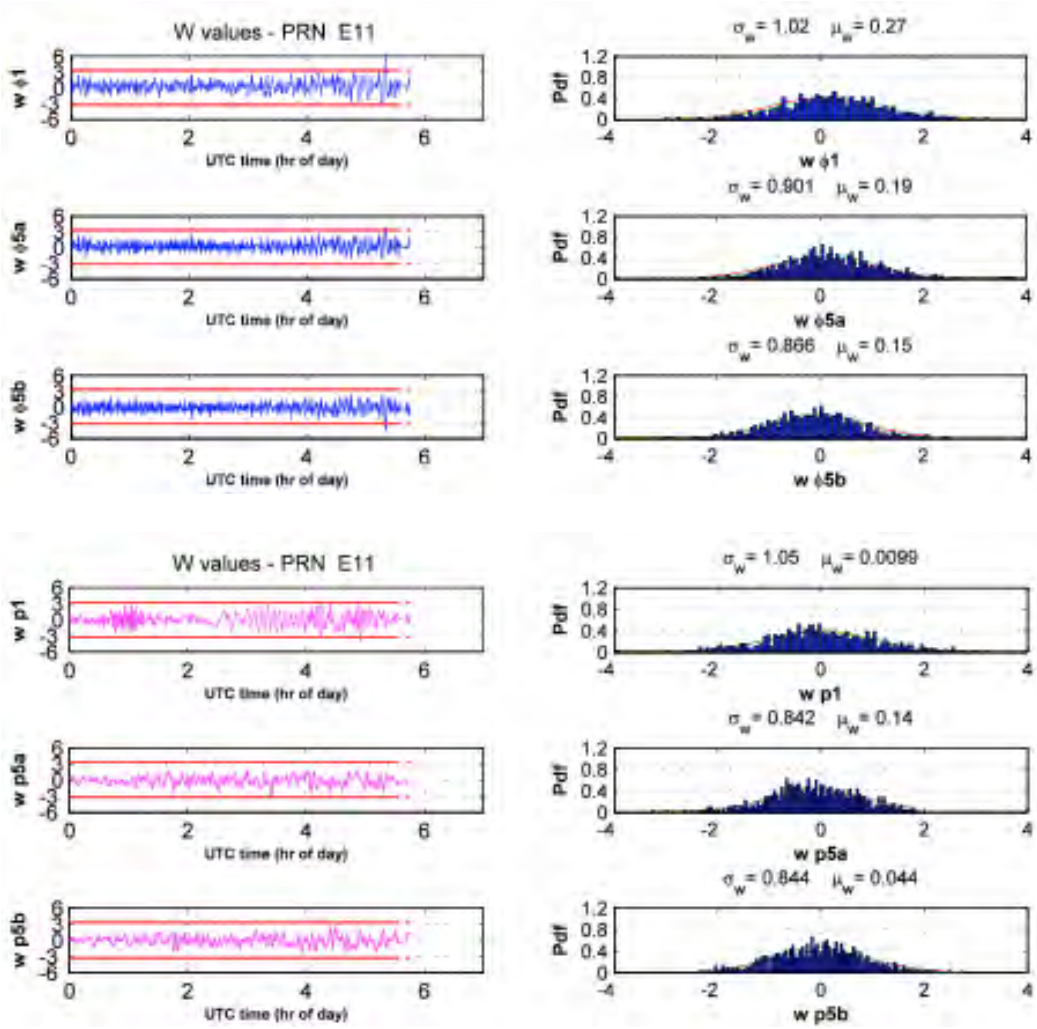

Time-series and histograms of w-statistic for Galileo measurements.

Validating GNSS data.

El-Mowafy (2015) used single-receiver single-satellite data validation parameters for numerical and graphical diagnostics of the multi-frequency observations. This method validates GNSS measurements of a single receiver where data from each satellite are independently processed using geometry-free observation model with a reparameterised form of the unknowns.

El-Mowafy, A. (2015). Diagnostic Tools Using a Multi-Constellation Single-Receiver Single-Satellite Data Validation Method. *Journal of Navigation*, 68, 196-214.

Improving Precise Point Positioning from GNSS data.

Deo and El-Mowafy (2015) propose algorithms for detecting and repairing cycle slips and clock jumps in Precise Point Positioning (PPP) using multi-constellation and multi-frequency (MCMF) GNSS data. They show that the availability of a third frequency enables reliable validation of detected cycle slips. A clock jump detection and repair procedure is also proposed for a receiver with both carrier phase and code measurements showing jumps. The algorithm can effectively determine clock jumps for single frequency data from a single constellation as well as MCMF GNSS data. However, MCMF GNSS data adds redundancy, hence improves the reliability of the clock jump detection algorithm.

Deo, M., El-Mowafy, A. (2015). Cycle Slip and Clock Jump Repair with Multi-Frequency GNSS data for improved Precise Point Positioning. *Proc. of IGNSS Symposium 2015*, Gold Coast, 14-16 July, 2015.

Research reports

EXPLORATION GEOPHYSICS

Theoretical rock physics

Seismic signatures of patchy saturation.

A major effort of the group is focused on the study of the effects of patchy saturation on seismic signatures (Müller, Qi, Lebedev, Gurevich et al, 2015). This effort was partially funded by the ARC Discovery Project Seismic response of partially saturated petroleum reservoir zones: towards quantitative recovery monitoring. The main objective is to quantify the effect of random spatial distribution of fluid patches in hydrocarbon reservoirs. The approach is based on the general theory of heterogeneous poro-elasticity developed by Curtin Reservoir Geophysics Consortium (CRGC) over the last decade. The aim of the current effort is to build a general model for elastic properties of partially saturated rock with a given statistical distribution of fractures and with arbitrary contrast between the properties of the two fluids (e.g., gas and liquid). We are also performing a series of fluid injection experiments with X-ray Computer Tomography and ultrasonic control to validate the theoretical findings. The effect of capillary forces on the elastic properties of partially saturated rocks is also being explored. On field scale, the results of theoretical research have been applied to time-lapse logs acquired at the Nagaoka CO2 storage site.

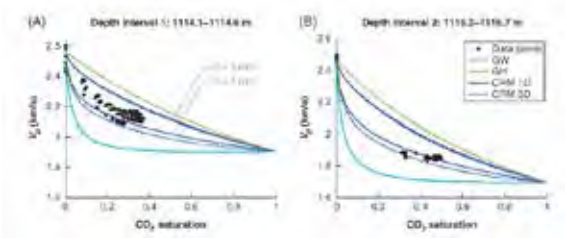

Comparison between velocity-saturation relations (VSR) models and time-lapse log data for the (A) shallower and (B) deeper depth interval at sonic frequencies. The continuous random media (CRM) models correspond to patch sizes d of 1 and 5 mm. GW, GH, and CRM are the Gassmann–Wood, Gassmann–Hill, and continuous random media models, respectively.

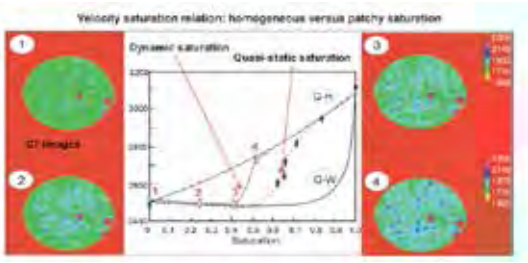

P-wave velocity versus water saturation for a forced imbibition experiment into a sandstone sample. Depending on the injection rate ("Quasi-static" = low or "Dynamic" = high), the VSR is different. However, both VSRs are bounded by the GW and GH relations. For the dynamic saturation experiment, CT images indicate the accumulation and clustering of water patches with increasing saturation.

Müller T.M., Caspari E., Qi Q., Rubino J.G., Velis D., Lopes S., Lebedev M., Gurevich B. (2015) Seismic Exploration of Hydrocarbons in Heterogeneous Reservoirs. ttp://dx.doi.org/10.1016/B978-0-12-420151-4.00003-9, Chapter 3 Acoustics of Partially Saturated Rocks: Theory and Experiments.

Researchers:
Prof. Boris Gurevich
B.Gurevich@curtin.edu.au
Dr. Stanislav Glubokovskikh
stanislav.glubokovskikh@curtin.edu.au
Dr. Maxim Lebedev
M.Lebedev@curtin.edu.au

Modelling of attenuation and dispersion due to squirt flow in rocks saturated with viscous and viscoelastic fluid.

We have developed a new squirt flow model in which all parameters can be independently measured or estimated from measurements. The pore space of the rock is assumed to consist of stiff porosity and compliant (or soft) pores present at grain contacts. The effect of isotropically distributed soft pores is modelled by considering pressure relaxation in a disk-shaped gap between adjacent grains. This derivation gives the complex and frequency-dependent effective bulk and shear moduli of a rock, in which the soft pores are liquid-saturated and stiff pores are dry. The resulting squirt model is consistent with Gassmann's and Mavko-Jizba equations at low and high frequencies, respectively. As expected, the dispersion and attenuation are the strongest at low effective stress and much smaller at higher effective stress (Glubokovskikh, Gurevich et al, 2015). The department will be testing and refining this model using ultrasonic and low-frequency measurements on clastic and carbonate rocks saturated with different fluids. The model is also being extended to partial saturation, anisotropy and viscoelastic fluids.

Glubokovskikh S., Gurevich B., Saxena N. (2015) A dual porosity scheme for fluid/solid substitution, *Geophysical Prospecting*.

Researchers:
Dr. Stanislav Glubokovskikh
stanislav.glubokovskikh@curtin.edu.au
Prof. Boris Gurevich
B.Gurevich@curtin.edu.au

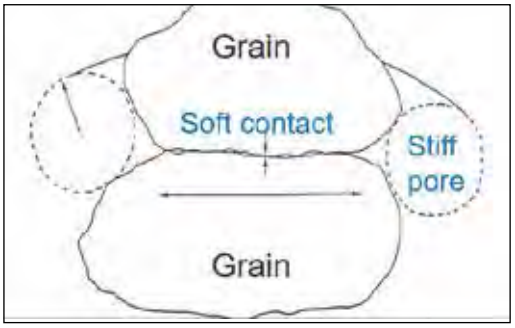

In a dry rock at low confining stress the grain contacts are soft. In a liquid-saturated rock at low frequencies the fluid pressure can equilibrate; the contacts are still soft (Gassmann). At high frequencies, the pressure has no time to equilibrate thus contacts are stiff, which leads to dispersion. Confining pressure closes the soft pores (reduces dispersion) producing Squirt flow.

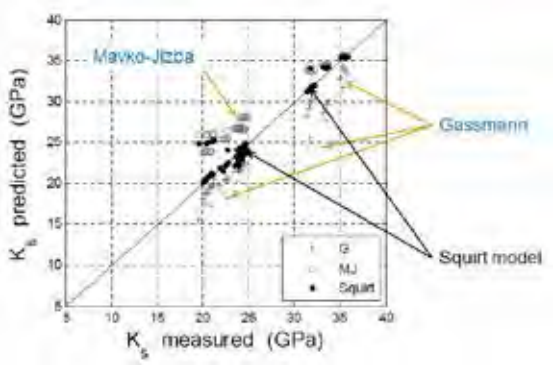

Predicted versus measured saturated bulk moduli for the pressure range from 5 to 50 MPa: for clean sandstones as measured by Han et al., (1986). Gassmann (crosses) predictions underestimate and Mavko -Jizba model (open circles) overestimates the experimental data. The prediction of the newly developed squirt-flow dispersion model (solid circles) with the intermediate porosity gives in a better agreement with the data, for the clean sandstones.

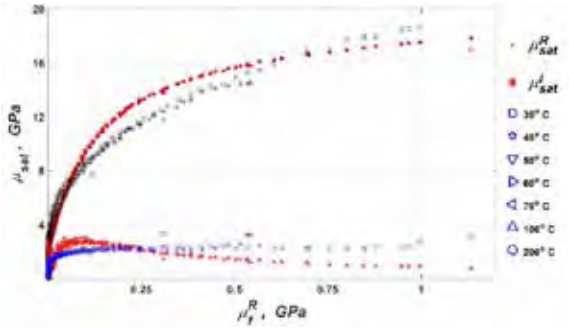

Best-fit theoretical estimates complex shear moduli of the Uvalde heavy oil rock computed according to the developed squirt model (red symbols) along with the measured values (blue symbols).

Modelling elastic properties of fractured reservoirs.

A major effort of the department's rock physics group is directed towards modelling attenuation, dispersion and frequency dependent anisotropy of porous reservoirs permeated by aligned fractures. Over the last decade, this group has developed a methodology of fluid substitution in fractured reservoirs, which is based on the combination of anisotropic Gassmann equations and Schoenberg's linear slip parameterisation of the effect of fractures on rock properties. The group has developed a model for attenuation and dispersion of P-waves propagating perpendicular to a periodic system of parallel planar fractures and validated this model with numerical simulations using a poroelastic extension of the reflectivity method. These simulations helped to extend the attenuation/dispersion model to randomly spaced fractures and to oblique incidence. The group also developed a model for seismic attenuation and dispersion caused by the presence of sparsely distributed finite fractures in the porous reservoirs. The model is based on the combination of Biot's theory of poroelasticity with the ideas of a multiple scattering theory. The current effort (Gurevich et al, 2015) in this area is focused on the deeper understanding of the implications of this theory and its extensions to:

- Oblique incidence;
- Shear waves;
- Higher fracture densities;
- Arbitrary aspect ratios.

While all of the above models are designed for a single set of aligned fractures, real reservoirs often contain multiple fracture sets. Moreover, similar phenomena (fluid flow between pores and fractures) lead to frequency dependent attenuation and dispersion in isotropic rocks with micro-cracks, compliant grain contacts, etc. These effects are being studied by extending the aligned fracture models to arbitrary angular distributions of fractures.

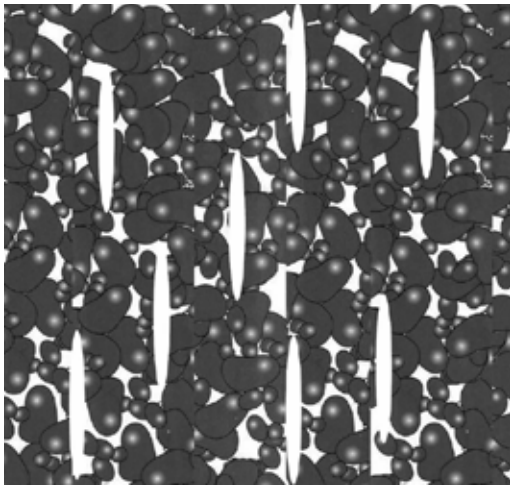

A porous medium containing a sparse distribution of circular cracks.

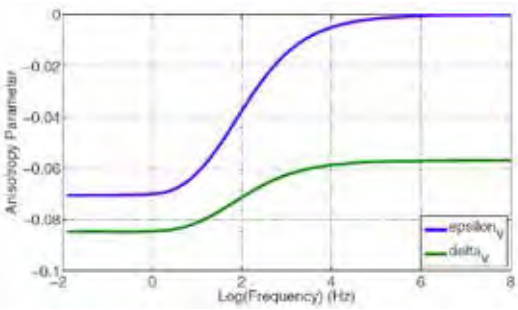

Frequency dependence of Thomsen's anisotropy parameters, epsilon (the long offset effect) and delta (the short offset effect), for vertical symmetry axis in a porous medium permeated by aligned circular cracks.

Galvin R.J., Gurevich B. (2015) Frequency-dependent anisotropy of porous rocks with aligned fractures, *Geophysical Prospecting* 63, 141-150.

Researchers:
Dr. Stanislav Glubokovskikh
stanislav.glubokovskikh@curtin.edu.au
Prof. Boris Gurevich
B.Gurevich@curtin.edu.au
Dr. Mahyar Madadi
M.Madadi@curtin.edu.au
Dr. Robert Galvin
Robert.Galvin@curtin.edu.au

Modelling stress-dependent properties of rocks.

Stress is one of the major causes of anisotropy in the earth. Understanding it is important for imaging, reservoir characterisation and monitoring. There is a need to be able to distinguish stress-induced from fracture-induced anisotropy. Recently, we developed theoretical models of stress-induced anisotropy of rocks (Glubokovskikh, Gurevich et al, 2015). We first considered an isotropic linearly elastic medium (porous or nonporous) permeated by a distribution of discontinuities with random (isotropic) orientation (such as randomly oriented compliant grain contacts or cracks). When this isotropic rock is subjected to a small compressive stress (isotropic or anisotropic), the number of cracks along a particular plane is reduced in proportion to the normal stress traction acting on that plane. This effect is modelled using the Sayers-Kachanov non-interactive approximation. The model predicts that such an anisotropic crack closure yields elliptical anisotropy, regardless of the value of the ratio of the normal to shear compliance. It also predicts the ratio of Thomsen's anisotropy parameters as a function of the compliance ratio and Poisson's ratio of the unstressed rock. The model is tested using laboratory data. In addition, it has been extended to large stresses, and also to a general triaxial stress state (leading to orthotropic symmetry). The results can potentially be used for differentiating between stress and fracture induced anisotropy, and also for predicting P-wave anisotropy from S-wave anisotropy; the latter may be estimated from shear-wave splitting as measured by modern sonic logs or VSP. We are also exploring micro-mechanical mechanisms of stress dependency of elastic properties of rocks based on the analysis of deformation of individual asperities.

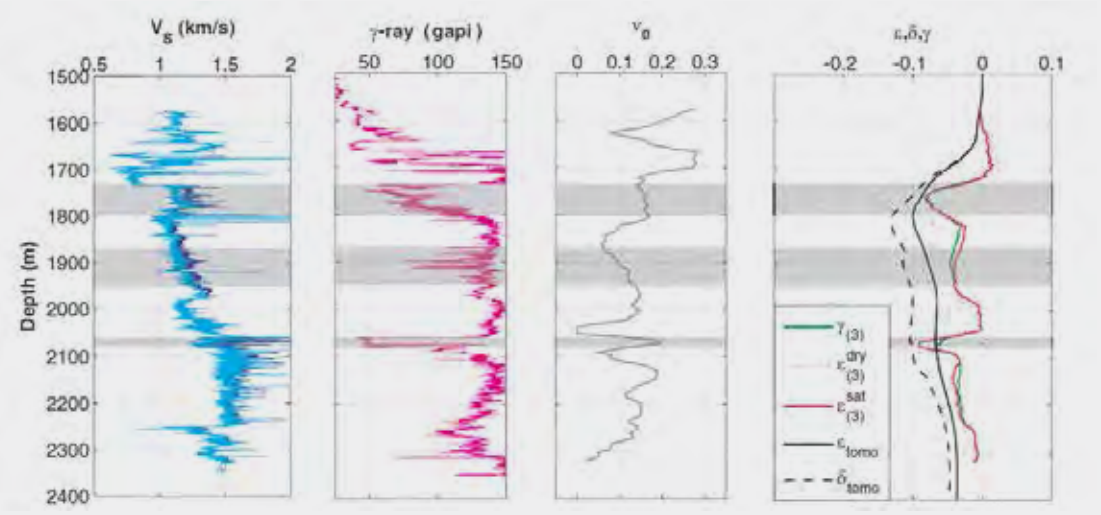

Stybarrow 2 well: (a) S-wave velocity log showing the fast (dark blue) and slow (light blue) wave velocities; (b) γ -ray log; (c) inverted Poisson's ratio of the dry unstressed rock; (d) azimuthal anisotropy parameters obtained using the methodology developed in the present work (green and red curves) compared with those estimated by orthorhombic tomography (black curves).

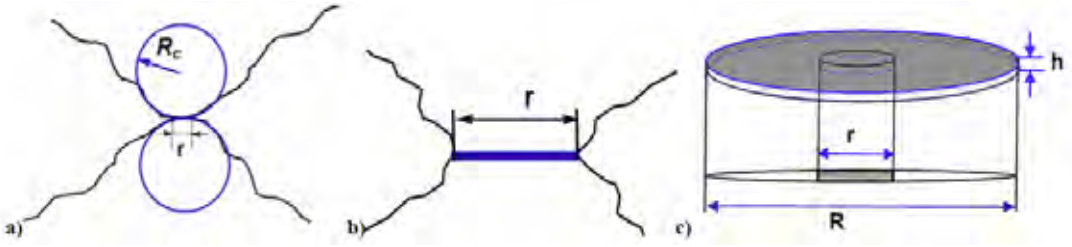

Geometries corresponding to a) Hertz contact; b) welded-area contact and c) annular crack.

Collet O., Gurevich B., Duncan G. (2015) Estimating azimuthal stress-induced P-wave anisotropy from S-wave anisotropy using sonic log or vertical seismic profile data, *Geophysical Prospecting*, 2015, doi: 10.1111/1365-2478.12307

Glubokovskikh, S., Gurevich, B., Lebedev, M., Mikhaltsevitch, V., Tan, S. (2016) Effect of asperities on stress dependency of elastic properties of cracked rocks, *International Journal of Engineering Science* 98, 116-125.

Researchers:
Dr. Stanislav Glubokovskikh
stanislav.glubokovskikh@curtin.edu.au
Prof. Boris Gurevich
B.Gurevich@curtin.edu.au

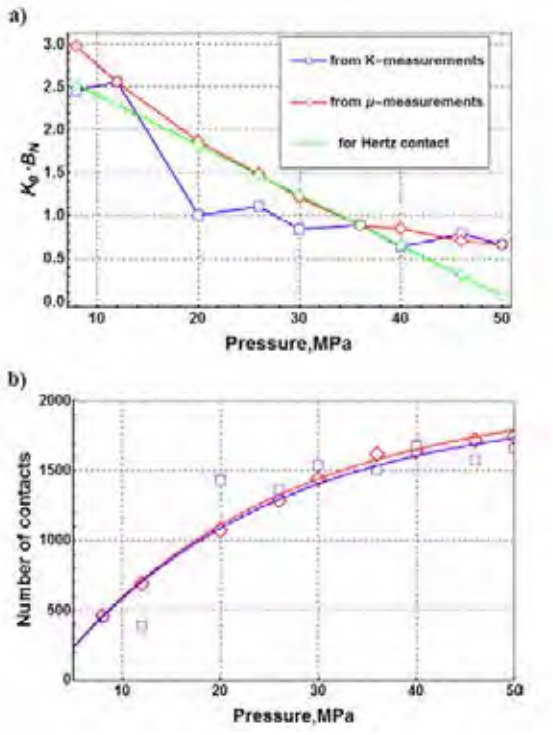

Results of the experiment analysis a) scaled overall compliance caused by cracks versus pressure; b) number of contacts for each pressure level along with the best-fit exponential functions (solid curves).

Experimental rock physics

Broadband acoustic measurements: from seismic to ultrasonic frequencies.

Theoretical rock physics models need to be tested and calibrated using laboratory measurements. To this end, the department is performing comprehensive experimental testing of these theories using broadband measurements of dynamic elastic properties (elastic moduli) and attenuation of rock samples (Mikhaltsevitch, Lebedev and Gurevich, 2015). Experiments are conducted at reservoir conditions using a combination of patent protected forced-oscillation ultra-sensitive strain gauge measurements (0.01 Hz – 200 Hz) and ultrasonic testing (1 MHz). The results are being compared with theoretical predictions computed using numerical simulations.

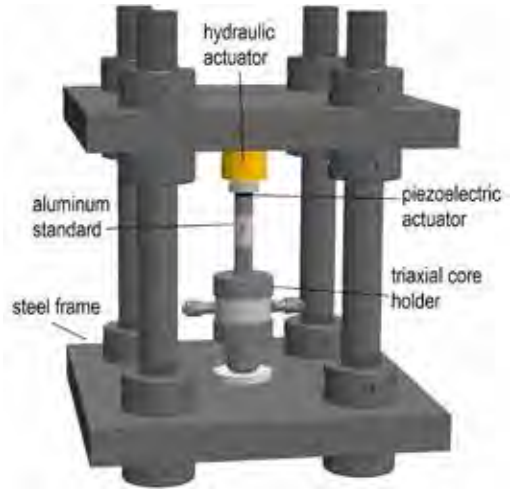

Seismic frequency apparatus at the Rock Physics Lab.

Mikhaltsevitch V., Lebedev M., Gurevich B. (2015) A laboratory study of attenuation and dispersion effects in glycerol-saturated Berea sandstone at seismic frequencies, *SEG Technical Program Expanded Abstracts* 2015, 3085-3089

Mikhaltsevitch, V., Lebedev, M., Gurevich, B.,2015, A laboratory study of the barrel shape effect Mikhaltsevitch V., Lebedev M., Gurevich B. (2015) A laboratory study of the barrel shape effect in a viscoelastic cylindrical sample at seismic frequencies, *ASEG Extended Abstracts* 2015 (1), 1-2.

Mikhaltsevitch V., Lebedev M., Gurevich B. (2015) A Laboratory Study of the Elastic and Anelastic Properties of the Eagle Ford Shale. 77th EAGE Conference and Exhibition 2015.

Mikhaltsevitch, V., Lebedev, M., Gurevich, B., 2015, Laboratory measurements of the effect of fluid saturation on elastic properties of carbonates at seismic frequencies, Accepted for publication in *Geophysical Prospecting*.

Researchers:
Dr. Vassili Mikhaltsevitch
V.Mikhaltsevitch@curtin.edu.au
Dr. Maxim Lebedev
M.Lebedev@curtin.edu.au

Rock Physics Lab at Curtin.

Quantitative microstructure characterisation from micro-CT and nano-indentation.

Rocks exhibit a complex microstructure, which is the result of both transport and deposition of various minerals and diagenetic alterations. This complexity in microstructure will translate in complex relationships between geophysical observables and rock parameters (e.g. elastic moduli vs. porosity, permeability vs. porosity) and thus makes reservoir quality prediction difficult. The Rock Physics laboratory is equipped with a 3D X-ray Microscope Versa XRM 500 (Zeiss - XRadia), which allows imaging of rocks and sediments with a resolution down to 0.6um. In-house built flow cells enable the department to reproduce reservoir conditions of temperature and pressure and to circulate various fluids though the rock (single or multiphase conditions). Various rock parameters such as porosity, connectivity, saturations, etc., can then be obtained with the use of visualization and computation software accessible through the Pawsey Supercomputing Center. Within the department and through collaborative projects, we are developing methods to compute rock properties, such as elastic wave velocity or electrical conductivity, from the 3D X-ray images (Vialle and Lebedev, 2015).

The department also owns a nano-indentation system (IBIS Fisher-Crips Laboratories Pty.Ltd.). This technique provides static and dynamic Young's moduli at the micro-meter scale as well as various mechanical parameters such as hardness, fracture toughness or creep behavior.
We have used nano-indentation tests to map and quantify mechanical weakening due to exposure of the rock to CO2-rich fluids as well as to map heterogeneities in Young's moduli of carbonates and relate it to microstructure heterogeneities acquired by SEM. Through a statistical analysis of

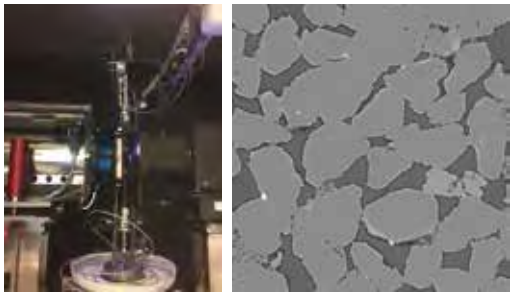

High pressure cell inside microCT; Right: microCT images of Bentheimer sandstone performed at a confining pressure 20 MPa (right hand side). The physical size of the shown slices is 0.95mm * 0.95mm.

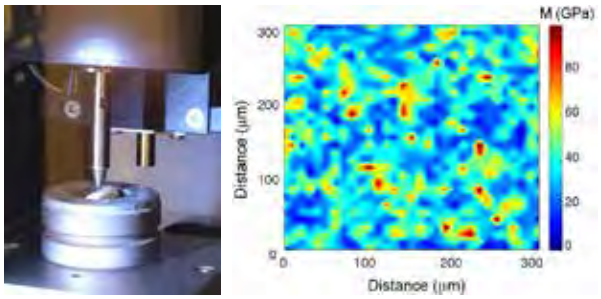

Nano-indentation measurement on a carbonate sample; Right: Map of indentation moduli.

the data, and with the use of rock physics models and micro-CT images, we are currently developing techniques to upscale these data at the core- and reservoir-scale.

Vialle S., Lebedev M. (2015) Heterogeneities in the elastic properties of microporous carbonate rocks at the microscale from nanoindentation tests, *SEG Technical Program Expanded Abstracts* 2015, 3279-3284, 2015

Vialle S., (2015) Acoustic response and CT imaging of rocks flooded with reactive fluids,3rd International Workshop on Rock Physics, Perth, 13th–17th, April 2015

Researchers:
Dr. Maxim Lebedev
M.Lebedev@curtin.edu.au
Dr. Stephanie Vialle
stephanie.vialle@curtin.edu.au

Laboratory measurements of intrinsic and stress-induced anisotropy.

Laboratory measurements of elastic properties of rocks are important for calibration of seismic data and for corroboration of theoretical models of rocks. The most common way of determining the elastic properties of rock samples in laboratory settings is to measure the velocities of the ultrasonic waves propagating in different directions. We are using an innovative approach to implement the Laser Doppler interferometer (LDI) for measuring the displacement on the sample surface upon arrival of waves into it (Bóna et al, 2015). LDI can measure the particle velocity of a small (0.01 mm2) element of the sample's surface along the direction of the laser beam. By measuring the particle velocity of the same surface element in three independent directions and transforming them to Cartesian coordinates, we can obtain three components of the particle velocity vector. Therefore LDI can be used as a localised three-component (3C) receiver of acoustic waves, and, together with a piezoelectric transducer or a pulsed laser as a source, can simulate a 3C seismic experiment in the laboratory. Performing such 3C measurements at various locations on the sample's surface produces a 3C seismogram, which can be used to separate P and two S waves, and to find polarisations and traveltimes of these waves. A 'walk away' laboratory experiment demonstrates high accuracy of the method. The measured data are consistent with the results from analytical modelling. From our results, we can conclude that it is possible to characterize elastic properties of materials from the described measurements. In particular, we are able to determine: 1) the angle between the particle movement and the direction of the wave propagation, i.e. the polarisation; 2) the type of waves; and 3) the arrival times of the wave at the point and thus the wave velocities.

True triaxial cell for investigation of stress-induced anisotropy using a laser Doppler interferometer.

Bóna, A., Gurevich, B., Pevzner, R., Lebedev, M., Madadi, M. (2015) Joint inversion of P-, and S-wave travel times for characterisation of anisotropic materials using laser Doppler interferometry measurements, ASEG Extended Abstracts 2015 (1), 1-4, 2015

Researchers:
Dr. Maxim Lebedev
M.Lebedev@curtin.edu.au
Dr. Mahyar Madadi
M.Madadi@curtin.edu.au
Prof. Boris Gurevich
B.Gurevich@curtin.edu.au
Dr. Andrej Bona
a.bona@curtin.edu.au

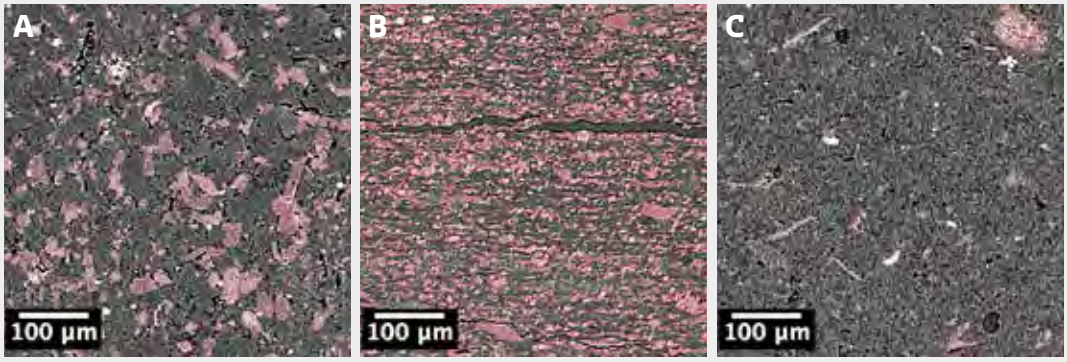

Micro-CT images of natural shales. A) Mancos shale B) Kimmeridge shale C) Pierre shale.

Compaction behaviour of clay sediments.

Mechanical compaction–one of the main rock-forming processes–occurs in the upper parts of the sedimentary basins, where the weight of overlying deposits compacts sediments below. During this process, initially unconsolidated sediments lose water and porosity, experience significant changes in microstructure and becomes stiff rock with different physical properties.

In this experimental work, we study how changes in microstructures affect elastic properties of quartz-kaolinite mixtures during mechanical compaction. A uniaxial stress is applied to the samples progressively to achieve distinct levels of porosity, at which transit times of ultrasonic P- and S-waves in the samples are measured. Velocities and anisotropy parameters are then calculated. The microstructure of the samples is characterized by micro-CT data and SEM image analysis, as well as neutron diffraction experiment and compared with microstructures of real shales.

Pervikhina, M., Gurevich, B., Dewhurst, D.N., Golodoniuc, P., Lebedev, M. (2015) Rock Physics Analysis of Shale Reservoirs, Fundamentals of Gas Shale Reservoirs, 19n1-205, 2015

Pervukhina, M., Uvarova, Y., Yurikov, A., Patrusheva, N., Dautriat, J., Dewhurst, D.N., Lebedev, M. (2015) Changes in microstructure and mineralogy of organic-rich shales caused by heating, *ASEG Extended Abstracts* 2015 (1), 1-4, 2015

Beloborodov, R.M., Pervukhina, M., Esteban, L., Lebedev, M. (2015) Compaction of Quartz-kaolinite Powders with Aggregated Initial Microstructure-Elastic Properties and Anisotropy,77th EAGE Conference and Exhibition 2015, 2015

Researchers:
Dr. Maxim Lebedev
M.Lebedev@curtin.edu.au
Dr. Vassili Mikhaltsevitch
V.Mikhaltsevitch@curtin.edu.au

Seismic processing and imaging

Passive seismic and Seismic Interferometry.

Seismic imaging and subsurface characterisation without the use of active sources has gained importance due to the need for both monitoring microseismic events and simplified acquisition of data. The department's focus in the area of passive seismic and interferometry (Sun, Bóna et al, 2015) includes: using drilling activities as a seismic source; passive imaging of diffractors and their characterisation and separation from microseismic events; and, generating shear-wave sources at the locations of 3C geophones in vertical seismic profile (VSP) type experiments for imaging and anisotropy estimation.

Sun B., Bóna A., King A., Zhou B. (2015) A comparison of coherency measurement using semblance and multiple signal classification, from a seismic-while-drilling perspective. *Geophysics* 80 (3), KS27-KS39.

Sun B., Bóna A., Zhou B., Van de Werken M. (2015) A comparison of radiated energy from diamond-impregnated coring and reverse-circulation percussion drilling methods in hard-rock environments. *Geophysics* 80 (4), K13-K23.

Khoshnavaz M.J., Bóna A., Urosevic M. (2015) Passive seismic imaging without velocity model prior to imaging. *ASEG Extended Abstracts 2015* (1), 1-4.

Khoshnavaz M.J., Chambers K., Bóna A., Urosevic M. (2015) Passive seismic localization without velocity model: application and uncertainty analysis. *SEG Technical Program Expanded Abstracts 2015*, 2467-2472.

Khoshnavaz M.J., Chambers K., Bóna A., Urosevic M. (2015) Passive seismic localization without velocity model: application and uncertainty analysis. *SEG Technical Program Expanded Abstracts 2015*, 2467-2472.

Researchers:
Dr. Andrej Bóna
A.Bona@curtin.edu.au
Dr. Roman Pevzner
R.Pevzner@curtin.edu.au

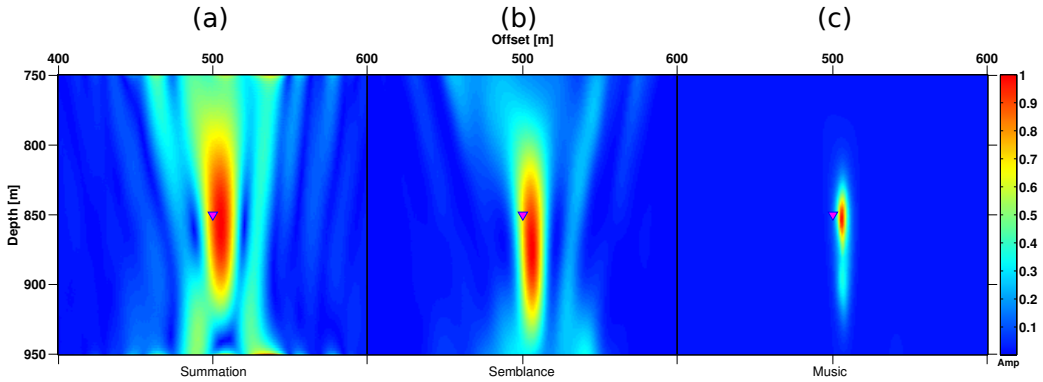

Coherent interferometry migration with large aperture based on summation (a); semblance (b); MUSIC (Multiple Signal Classification) (c)

Imaging methods that do not require separate velocity analysis.

Seismic migration methods rely on a background velocity model of the subsurface. Methods that can provide velocity models automatically along with the migrated seismic data can form an important part of the imaging and characterisation workflows. The department is developing various pre-stack imaging methods that result in subsurface velocity models. Currently, the focus is on time migration algorithms. The methods generally rely on estimation of extra attributes, such as local slopes or curvatures, or use of stationary phase in a summation over the velocities.

Khoshnavaz M.J., Bóna A., Urosevic, M. (2015) Pre-stack time migration in common source domain without velocity model, 77th EAGE Conference and Exhibition 2015, 2015

Researchers:
Dr. Andrej Bóna
A.Bona@curtin.edu.au
Konstantin Tertyshnikov
Konstantin.Tertyshnikov@curtin.edu.au

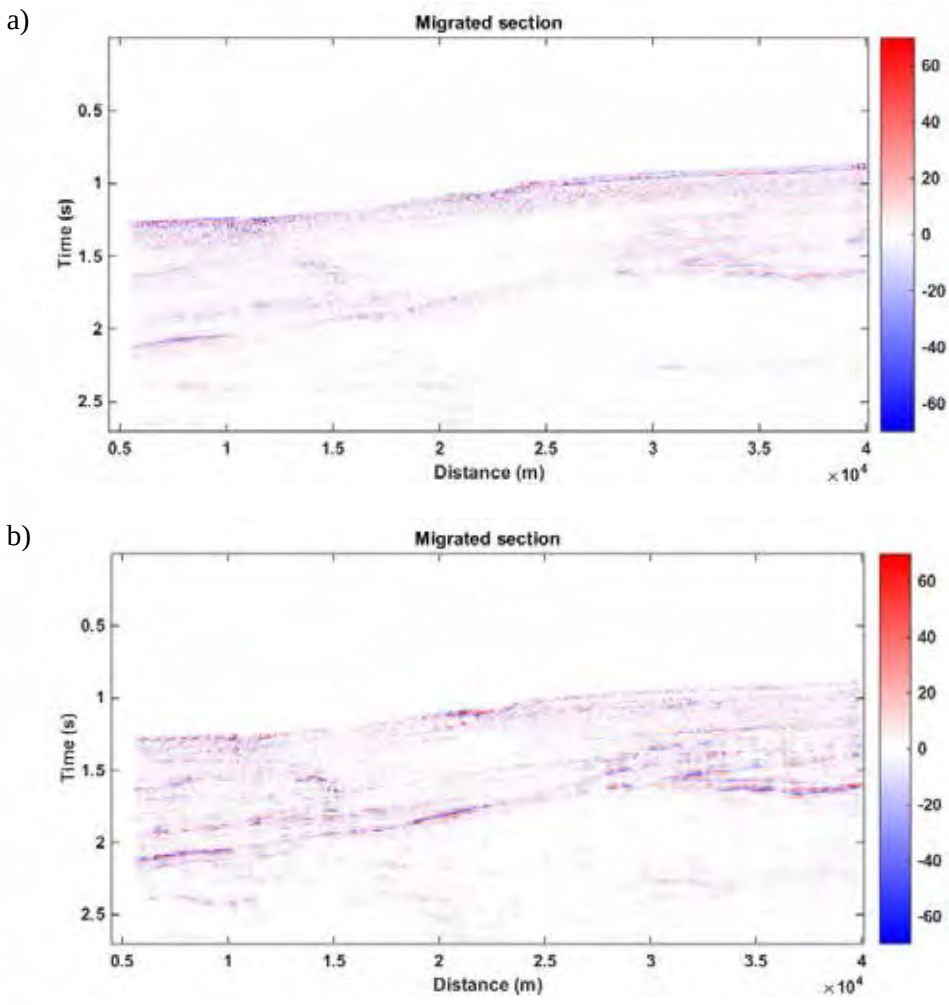

Final migrated sections by the application of previous technique (Bóna, 2011). Slopes were estimated by a) numerical gradient and b) plane wave destructor.

Using diffractions for imaging and migration steering.

Seismic diffractors correspond to many important subsurface features that are usually not well imaged using methods developed for reflection seismology. Specialised methods that focus on imaging of diffractors thus enhance the resolution of the subsurface images. One of the research topics of the department is imaging of the diffractors along with their seismic characterisation using their amplitude response (Bóna and Pevzner, 2015). This approach is closely linked to improving reflection imaging in low signal to noise environments since only small parts of the diffraction hyperbolae used for summation in standard migration algorithms contain the energy from the reflection. Therefore, the inclusion of all the traces from such diffraction hyperbola may not contribute constructively to the final image. One way of identifying the traces that do not contribute constructively to the final image is by using the amplitude/energy distribution information used in the abovementioned diffraction imaging/characterisation. The department uses a modified 3D Kirchhoff post-stack migration algorithm that utilises coherency attributes obtained by diffraction imaging algorithm in 3D to weight or steer the main Kirchhoff summation.

Bóna A., Pevzner, R. (2015) Using Fresnel Zone to Characterise and Image Different Types of Diffractors in Low S/N Situations,77th EAGE Conference and Exhibition 2015

Khoshnava MJ., Bóna A., Urosevic M., Ziramo, S., Ahmadi P. (2015) Pre-stack Diffraction Imaging and Its Application in Hard Rock Environment,77th EAGE Conference and Exhibition 2015

Tertyshnikov K., Pevzner R., Bóna A., Alonaizi F., Gurevich B. (2015) Steered migration in hard rock environments. *Geophysical Prospecting* 63 (3), 525-533.

Khoshnavaz, M.J., Chambers, K., Bóna, A., Urosevic, M. (2015) Passive seismic localization without velocity model: application and uncertainty analysis, *SEG Technical Program Expanded Abstracts 2015*, 2467-2472.

Researchers:
Dr. Andrej Bóna
A.Bona@curtin.edu.au
Dr. Roman Pevzner
R.Pevzner@curtin.edu.au
Konstantin Tertyshnikov
Konstantin.Tertyshnikov@curtin.edu.au

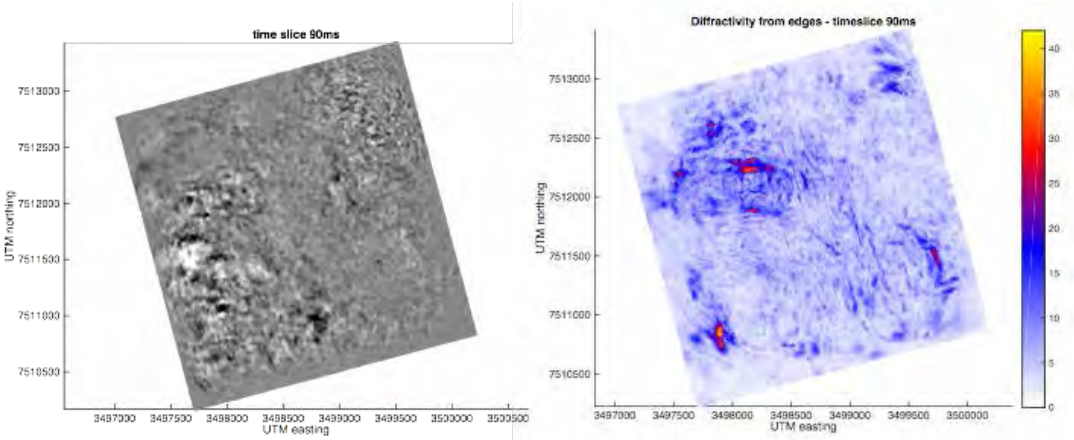

Standard pre-stack time migration (left) and diffractivity (right) time slices from 3D field data.

Modelling and processing of ghost waves.

Reflections from the sea surface play an important role in seismic data analysis. Temporal and spatial changes in the seismic wavelet caused by presence of the ghost waves have to be accounted for during processing. Similar issues can also arise in development and application of surface related multiple elimination techniques. An assumption of a flat sea surface with the reflection coefficient close to -1 has been known to be inadequate for many real life situations. A lot of attention has been paid to the topic of rough-sea problems in recent times, largely because of the development of the deghosting algorithms, where the abovementioned assumption can be violated. Egorov et al. (2015) presented a comparison of rough sea surface reflection modelling results with ultra-high resolution field seismic data acquired with deep-towed sources and receivers. The Kirchhoff approximation was used to model the sea surface response. Such a comparison is essential in establishing the validity of the modelling approaches used in data processing, such as deghosting. Deep towed sources and receivers permit the separation of sea surface reflections from primary events.

Egorov A., Glubokovskikh S., Bóna A., Pevzner R., Gurevich B., Tokarev M. (2015) Influence of rough sea surface on sea surface reflections: deep towed high-resolution marine seismic case study. *SEG Technical Program Expanded Abstracts 2015*, 3661-3665.

Researchers:
Dr. Andrej Bóna
A.Bona@curtin.edu.au
Dr. Stanislav Glubokovskikh
stanislav.glubokovskikh@curtin.edu.au

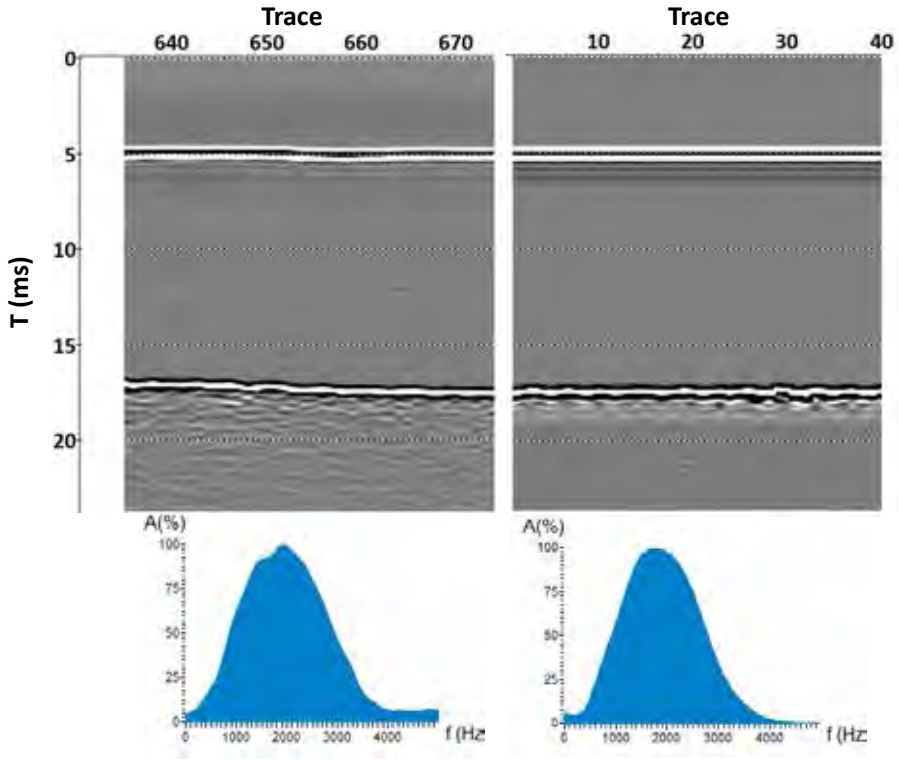

Comparison of field (left) and modelled (right) data and the amplitude spectra of reflected (ghost) wave.

Reservoir characterisation and monitoring

Sea-bed electromagnetic modelling: 3D visualisation and survey design.

The Deep Ocean Electromagnetic (EM) method, which typically include both Controlled Source EM and Magnetotelluric data, requires application of modelling, inversion and visualization in combination with high performance computing (see Pethick and Harris, 2015). Modern surveying equipment provides the possibility of multi-offset, multi-frequency and more recently multi-azimuth data sets. The arrangement and orientation of electromagnetic sources and receivers on the ocean floor relative to target and host rocks is a key part in determining the success of a deep ocean electromagnetic survey (Pethick and Harris 2014). The Curtin University Exploration Geophysics' Marine Controlled Source Electromagnetic (MCSEM) methods research team is focused on: (i) integrated visualisation and survey planning; (ii) interactive 2D/3D inversion of sea-bed electromagnetic data; (iii) design of novel instrumentation; and, (iv) understanding the impacts of electrical anisotropy on the sea-bed EM response (see figures below).

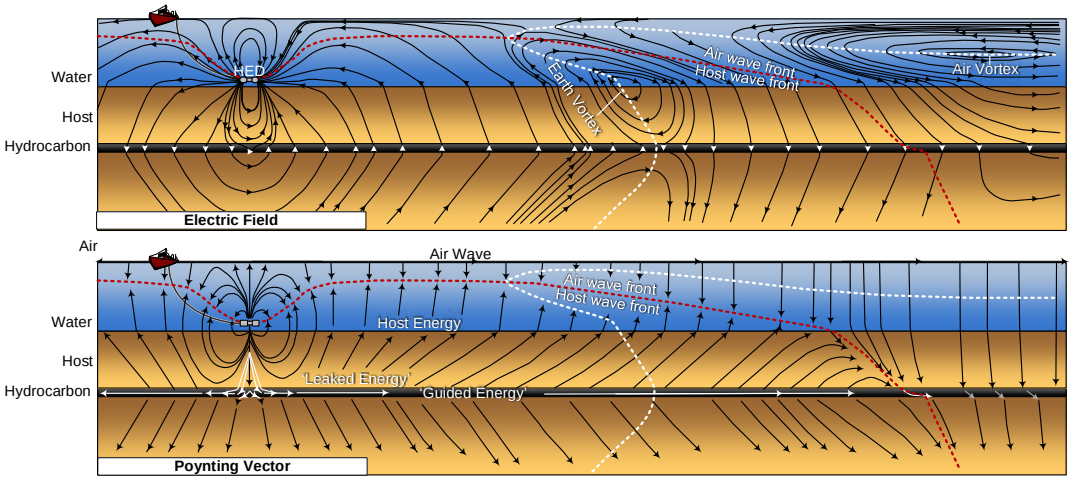

An interpretation guide of (top) electric and (bottom) Poynting vector streamlines. The airwave, as shown by the electric field streamlines, is the interaction between two vortices, (i) the earth vortex and (ii) air vortex. The centre of the earth vortex has zero amplitude and corresponds with the Ex phase inflection point seen in Figure 1. The airwave front is indicated by the dashed red line and represents the region where the contribution of 'earth' and 'air' energy flow is equal. As shown by the Poynting vector streamlines, there are no apparent direct, reflected or refracted energy flows; however, it appears to have 'guided' energy flow (Weidelt, 2007) within the hydrocarbon hosted layer and along the air–ocean boundary. (Reproduced from Pethick and Harris, 2013).

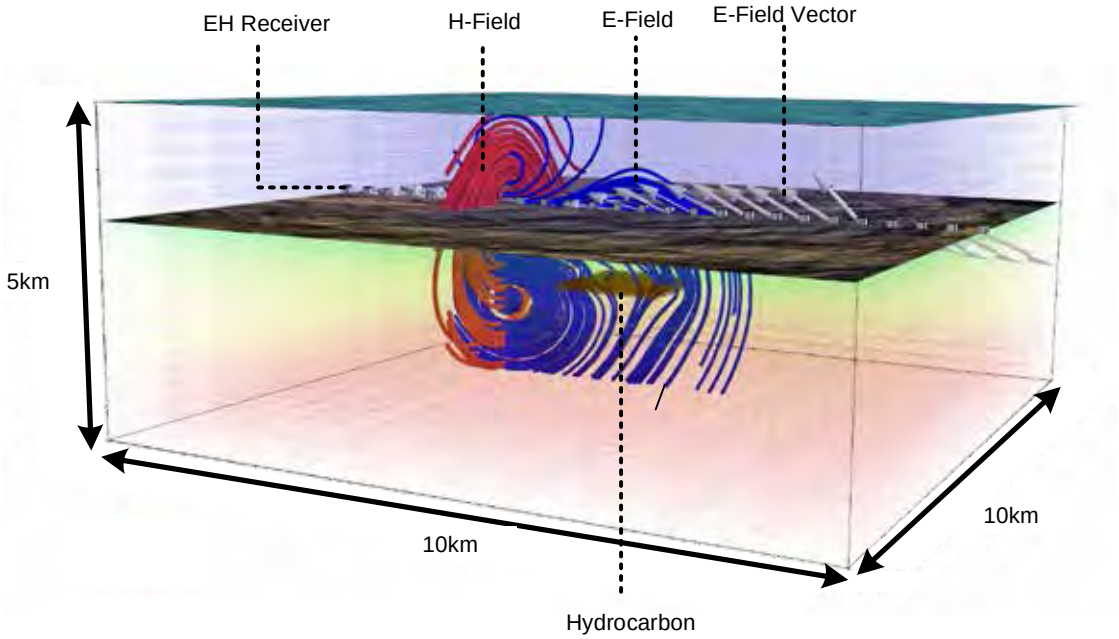

Schematic of electric and magnetic fields generated by a time harmonic 0.25 Hz electric dipole source displayed at t = 0.5 s. The earth model consists of multiple 1D layered earth and 3D resistive prism (i.e., the hydrocarbon). The computations of the EM field required to generate the image above is computed one thread. This image visualises the 3D electric and field lines that are derived from a single forward model. It provides a perspective on the scale of the electromagnetic fields generated during MCSEM (marine controlled source electromagnetic) surveys and shows level of complexity with which the electric and magnetic fields interact with the surrounding geo-electrical environment. The fields like those shown can be computed in parallel (i.e., simultaneously) for all transmission frequencies and transmitter positions for any MCSEM survey configuration. Using a macro-parallelisation implementation of Marco this type of inversion of a 50,000 cell region would require over 3 years to complete. This leads us to suggest that approximate IE solutions, or heavy optimisation are required for large scale inversions. (Reproduced from Pethick and Harris, 2016)

Pethick A., Harris B.D. (2016) Macro-parallelisation for controlled source electromagnetic applications, *Journal of Applied Geophysics* 124 (2016) 91–105

Pethick A., Harris B.D. (2014) Bathymetry, electromagnetic streamlines and the marine controlled source electromagnetic method, *Exploration Geophysics*, 2014, 45, 208–215

Pethick A., Harris B.D. (2013) Poynting Vector Streamlines and the Marine Controlled Source Electromagnetic Airwave, 75th EAGE Conference & Exhibition incorporating SPE EUROPEC 2013, Jun 10, 2013, London, UK: EAGE.

Researchers:
Dr Brett Harris
B.Harris@curtin.edu.au
Dr. Andrew Pethick
Andrew.Pethick@curtin.edu.au
Dr Anton Kepic
A.Kepic@curtin.edu.au

Research reports

EXTRACTIVE METALLURGY

Extractive metallurgy

Extractive Metallurgy is a specialisation field within the broader field of Resources Engineering and involves the study, evaluation, development and design of processes used in the extraction and beneficiation of economically important metals and minerals from their concentrates and ores. Extractive metallurgy utilises scientific research from, and interacts with, the fields of geology and mineralogy, chemistry, microbiology, chemical (process) engineering, electronic engineering and mechanical engineering. As it relates to the chemical environments in which minerals and rocks interacts and reacts with aqueous solutions (in the case of hydrometallurgy and mineral processing) or high temperature melts such as molten slags, mattes and alloys (in the case of pyrometallurgy), it strongly intersects the earth sciences and are often similar, albeit at accelerated reaction rates, to the ore genesis, metamorphosis and weathering processes occurring during the formation of mineral deposits. Conversely, these ore genesis, metamorphosis and weathering processes often inspire and serve as reference cases for the development of industrial metal and mineral extraction processes. Extractive metallurgy research under the research leadership of Prof Eksteen is reported here. The research work has been sponsored either directly, or indirectly (through AMIRA or MRIWA) by Anglogold Ashanti, Barrick Gold, Newmont Mining, Newcrest Mining, St Barbara, Zijin Mining, Harmony Gold, Randgold Resources, Orica, Kemix, Gekko Systems, Magotteaux, CSBP-AGR, Bateman Engineering, Mineral Research Institute of Western Australia, Panoramic Resources, Lhoist, Lynas Corporation and International Base Metals Limited.

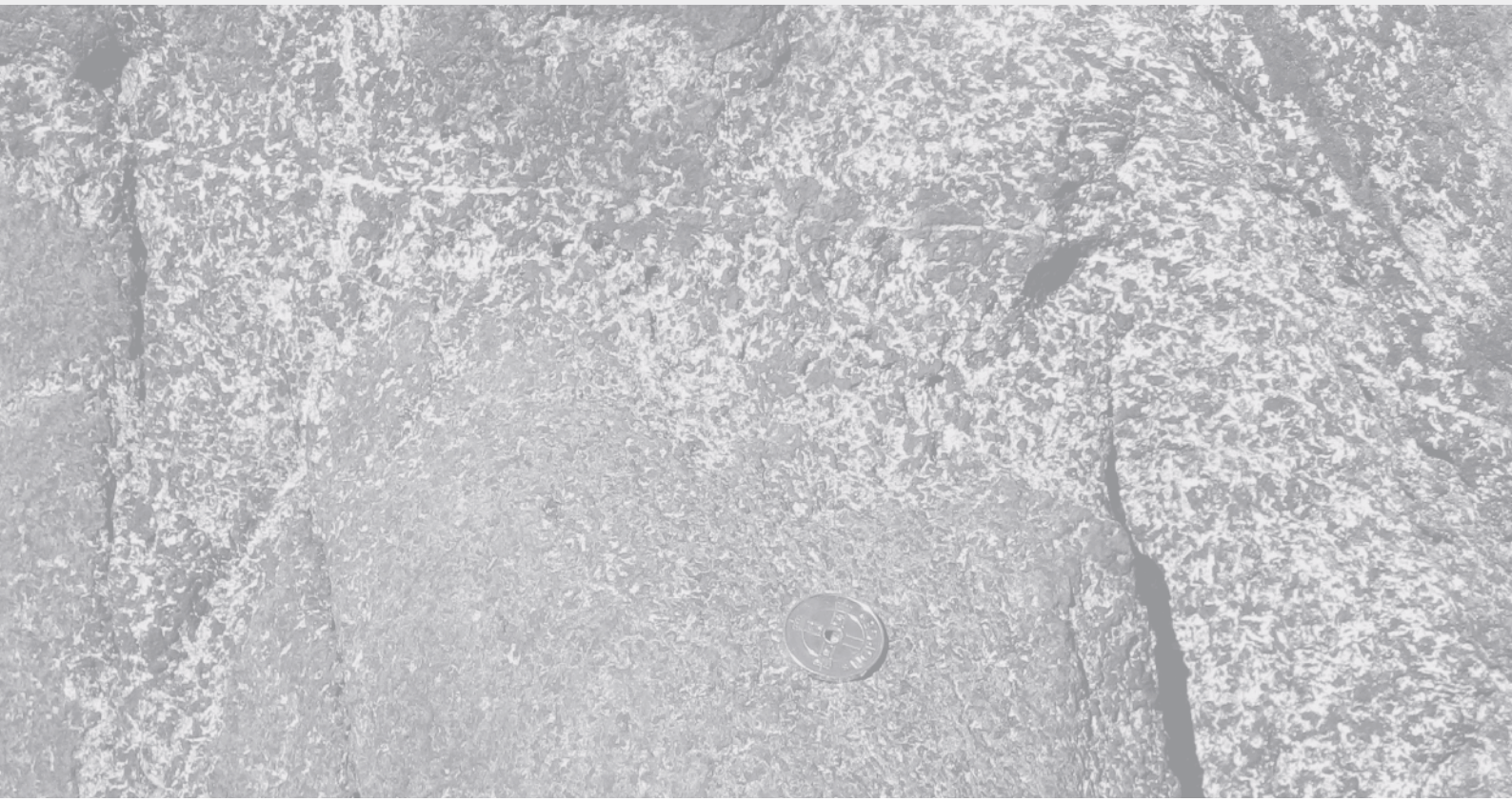

Interaction of amino acids in an alkaline environment with gold, silver and copper minerals.

Prof Jacques Eksteen and Dr Elsayed Oraby have patented (patents pending) a process to leach gold and silver from their ores and copper from a range of mineralogies using a solution of amino acids in an alkaline environment, with the bulk of the research focussing on the simplest amino acid namely glycine. They have developed processes to recover the metals from solution through adsorption onto activated carbon (in the case of precious metals) and precipitation and solvent extraction with electrowinning (in the case of copper). Copper has been shown to be extractable from a range of oxide and sulfide minerals as well as native copper. Minerals such as malachite, azurite, cuprite, tenorite, atacamite, antlerite, native copper, chalcocite, covelite, bornite, chalcopyrite, tetrahedrite-tennantite and enargite were all shown to dissolve in alkaline glycine at atmospheric pressure and at temperatures between ambient temperature and mildly elevated temperatures, for example at 60ºC. As important, from a metallurgical perspective, is non-interaction with gangue minerals such as pyrite, dolomite, calcite and phyllosilicate minerals which all tend to be acid (reagent) consuming minerals in conventional hydrometallurgical processing routes. In addition conventional (acidic) processing often lead to the formation of elemental sulfur (which is problematic if the ore also contain precious metals that are to be cyanide leached), jarosites (which lock up silver in the crystal lattice) and silica gels that leads to significant operational problems when copper sulfide minerals are acid leached. The use of glycine averts the pH swing normally associated with extracting base metals (e.g. copper) when followed by alkaline leaching (with sodium cyanide solution). The glycine therefore also provides an alternative to cyanide leaching, with all its associated problems of toxicity, reusability and costs associated with cyanide destruction. In the hydrometallurgical context the use of glycine has been shown to be particularly beneficial as it can be nearly completely recovered and recycled back to the leach, significantly lowering the reagent costs. Electrochemical studies (cyclic voltammetry and linear sweep voltammetry) indicated that glycine significantly enhances the rate of gold dissolution in the presence of copper ions and cyanide over the use of cyanide only.

Glycine and copper ore.

The following publications were recently published associated with glycine and amino acid leaching:

Oraby E.A., Eksteen J.J., (2014). The selective leaching of copper from a gold–copper concentrate in glycine solutions. *Hydrometallurgy*, 50, 14-19.

Oraby E.A., Eksteen J.J. (2015). The leaching and carbon based adsorption behaviour of gold and silver and their alloys in alkaline glycine-peroxide solutions. *Hydrometallurgy*. 152, 199–203

Eksteen J.J., Oraby E.A. (2015). The leaching and adsorption of gold using low concentration amino acids and hydrogen peroxide: Effect of catalytic ions, sulphide minerals and amino acid type. *Minerals Engineering*, 70, 36-42.

Oraby E.A., Eksteen J.J. (2015). Gold leaching in cyanide-starved copper solutions in the presence of glycine. *Hydrometallurgy*, 156, 81-88.

Developments in the processing of Platinum Group Elements.

Platinum Group Metals (PGE's) are a group of metals of significant economic and strategic interest due to their use in automobile catalytic converters, medical and advanced electronic technologies and low temperature fuel cell technologies in the field of clean energy. Whilst most of the PGM's are to be found in South Africa and Zimbabwe, both of which are known for their socio-political challenges, economically important deposits can also be found in more benign mining jurisdictions such as Australia, Canada, and the USA. However, in contrast to South Africa, where smelting of flotation concentrates constitutes the primary processing route for PGE processing, deposits elsewhere are often not of sufficient size and mine life to justify investment into smelting facilities. Moreover, they are often remote and have complex polymetallic mineralogies, often leading to these deposits remaining as "stranded" deposits, unless direct leach processing routes are developed. Mpinga et al. (2015) reviewed a number of processing routes for PGE-bearing ores, and has shown the challenges in developing direct leach processing solutions for PGE's, particularly due to the complexity of mineralisation of the PGE's and its way of association with gangue minerals and nickel and copper sulfides. Research is currently ongoing on various Australian deposits using novel leach approaches. In addition, Prof Eksteen is extending research he was involved in during his prior involvement with Lonmin Plc, looking into various aspects of pyrometallurgical processing, including the modelling and optimisation of sulfide matte converting processes. Moreover research on the liquors derived from the heap leaching of PGE deposits were studied in 2011-2014, and recent research focused on the elution of the PGE's from activated carbon. A few recent publications (2015) demonstrate some of the areas of research:

———

Mpinga C.N., Eksteen J.J., Aldrich C., Dyer L. (2015). Direct leach approaches to Platinum Group Metal (PGM) ores and concentrates: A review. *Minerals Engineering*,78, 93-113

———

Snyders C.A., Bradshaw S.M., Akdogan G., Eksteen J.J. (2015). Factors affecting the elution of Pt, Pd, and Au from activated carbon. *Minerals Engineering*, 80, 14-24.

———

Snyders C.A., Bradshaw S.M., Akdogan G., Eksteen J.J. (2015). Determination of the equilibrium and film diffusion constants of the platinum cyanide anions during the elution from activated carbon. *Minerals Engineering*, 80, 57-68.

———

Chibwe D.K., Akdogan G, Bezuidenhout G.A., Kapusta J.P.T., Bradshaw S., Eksteen J.J. (2015). Sonic injection into a PGM Peirce-Smith converter: CFD modelling and industrial trials. *Journal of the Southern African Institute for Mining and Metallurgy*, 115, 349-354.

———

Chibwe D.K., Akdogan G., Taskinen P., Eksteen J.J. (2015). Modelling of fluid flow phenomena in Peirce-Smith copper converters and analysis of combined blowing concept. *Journal of the Southern African Institute for Mining and Metallurgy*. 115, 363-374.

Developments in the extraction of Rare Earth Elements (REEs) and critical metals.

Hazel Lim is studying novel extraction routes for the leaching and recovery of Rare Earth Elements (REEs), zirconium and niobium and tantalum from REE-bearing eudialyte deposits, focussing on the eudialytes found in the Dubbo region of New South Wales and the southern areas of Greenland. In particular the emphasis of the research has been on the identification and evaluation of more benign lixiviants and reagents for the leaching of the targeted metals and their recovery from solution.

In addition, Prof Eksteen has been working with Prof Elizabeth Watkin, Dr Melissa Corbett and Mr Homayoun Fathollahzadeh in the development of a process whereby REE bearing phosphate minerals, such as monazite and xenotime, and their ores are leached using phosphate solubilising micro-organisms. Recent research has identified mirco-organisms with significant potential to release REEs and further research is being performed to obtain a better understanding of the mechanisms of REE leaching, focussing on monazite minerals. Publications are currently under preparation.

Development in gold processing and recovery.

Teresa McGrath and co-researchers investigated the behaviour of gravity recoverably gold in flash flotation circuits and looked into the role of particle morphology and flotation conditions on the recovery of liberated gold particles from ores (McGrath et al. 2015a and 2015b).

Dr Elsayed Oraby and Prof Eksteen developed a novel method of suppressing the dissolution of nuisance copper from it minerals that are co-recovered during the gravity recovery of gold from copper-gold ores. They have shown that the use of sodium hydroxide during intensive cyanidation of gravity gold concentrates suppresses the dissolution of copper and accelerates the leaching of gold and allows the use of significantly reduced levels of cyanide. It was sown that it is particularly the use of sodium hydroxide over calcium hydroxide that gave the best copper dissolution suppression and gold leaching, even at the same solution pH.

Recent publications on the processing of gold ores (other than those mentioned above under amino acid processing) are listed below:

Oraby E.A., Eksteen J.J. (2016). Gold dissolution and copper suppression during leaching of copper-gold gravity concentrates in caustic soda-low free cyanide solutions. Minerals Engineering, 87, 10-17

McGrath T.D.H., Eksteen J.J., Heath J. (2015). The behaviour of free gold particles in a simulated flash flotation environment. Journal of the Southern African Institute for Mining and Metallurgy, 115, 103-112

McGrath T.D.H., Eksteen J.J., O' Connor L. (2015). A Comparison of 2D and 3D Characterisations of Free Gold Particles in Gravity and Flash Flotation Concentrates. Minerals Engineering. 82, 45-53.

MAJOR EQUIPMENT ACQUISITIONS

Advanced Resource Characterisation Facility (ARCF)

The Geoscience Atom Probe facility, a component of the National Resource Sciences Precinct's ARCF, was commissioned in July 2015 and comprises a Cameca LEAP 4000X HR and a Tescan LYRA FIB-SEM. The atom probe is the first system focussed on the development and application of the technique to geoscience research.

Atom probe microscopy is a technique that allows the 3D compositional and spatial imaging of atoms at the sub-nanometre scale. The technique involves time-controlled field emission of atoms by applying a high electric field to a needle-shaped sample whose tip is then heated by a pulsing UV laser. On evaporation, the atom is immediately ionized and accelerates along field lines to hit a position-sensitive detector. The x-y coordinates of the detector, combined with the order in which the ions hit the detector, enable reconstruction of the original 3D positions of the atoms in the sample. The time of flight between the start of the laser pulse and collision of the ion with the detector is a function of the mass/charge ratio of the ion and is used to identify the atom species emitted from the tip. Typical data sets comprise tens to hundreds of millions of atoms.

The Geoscience Atom Probe will be used to investigate nanoscale elemental and isotopic distributions in minerals and the processes responsible for producing these distributions (e.g. Fig. 1). Current research involves the fundamental development of atom probe microscopy to a range of rock-forming and accessory minerals as well as focused studies targeting the compositional modification of minerals by deformation, the processes of precious metal segregation in ore bodies, processes of fluid-rock interaction and material transfer in metamorphic rocks and the use of atom probe in geochronological studies.

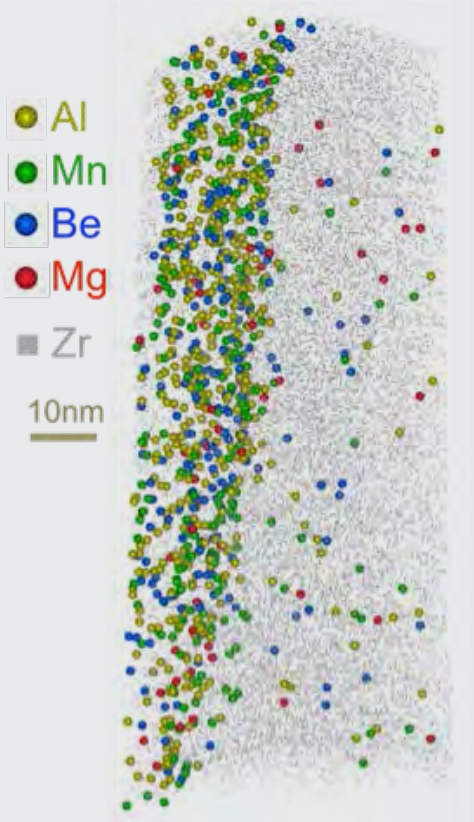

Figure 1: Atom probe data from reidite-bearing zircon from the Stac Fada impactite, UK. Data shows migration of interstitial trace elements into reidite during the impact.

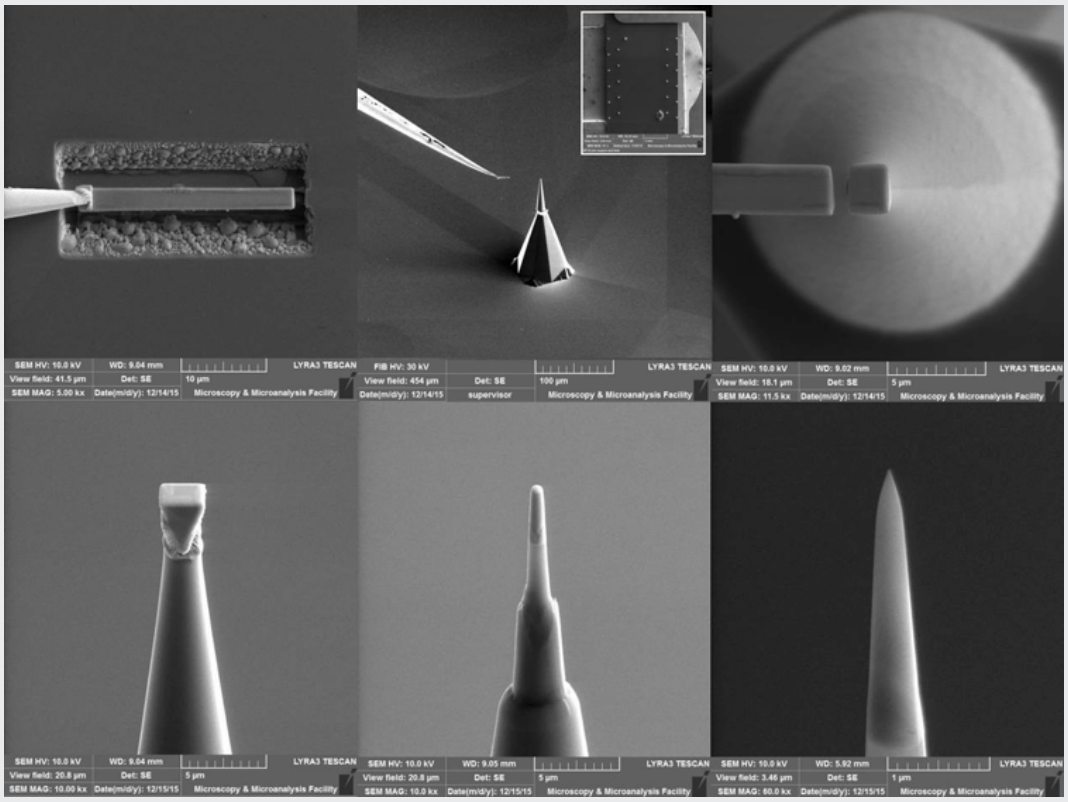

Figure 2. Sequence of stages in the preparation of atom probe specimens using the ARCF's new Tescan Lyra FIB-SEM.

A critical aspect of atom probe analysis is specimen preparation and this requires a focussed ion beam scanning electron microscope (FIB-SEM). A Tescan LYRA FIB-SEM, funded by the NRSP consortia, was installed at Curtin University in mid-2015 primarily to support atom probe research (Fig. 2). HOWEVER, the FIB-SEM at Curtin is a high performance instrument that is fitted with an orthogonal Time of Flight Secondary Ion Mass Spectrometer (ToF-SIMS) as well as Oxford EDS and EBSD detectors. FIB-ToF-SIMS is being used for surface and depth resolved elemental and isotopic mapping to provide context for atom probe samples.

Significant benefits in light element and trace element mapping can be achieved when compared to X-ray based techniques. The small information volume (about the same size as the FIB probe, <25nm) allows for high spatial resolution elemental maps. When low beam currents are used, only a few tens of nanometers of material is removed from the sample surface allowing the mapped region to be prepared for subsequent atom probe analysis.

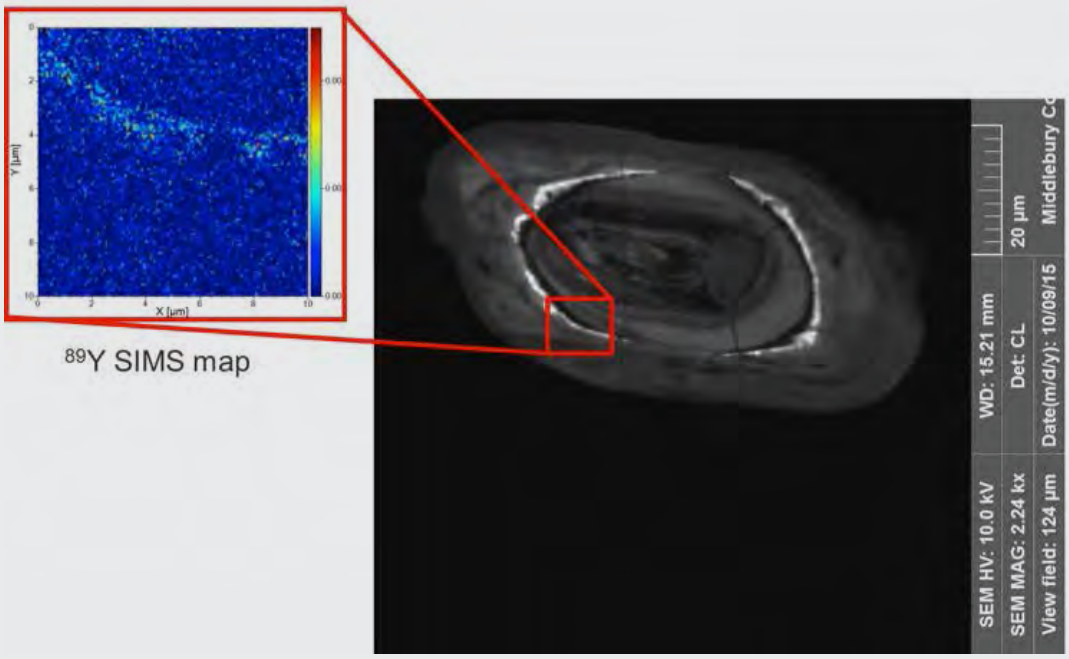

The detector array on the Tescan Lyra FIB-SEM enables it to be used for high precision site-selective atom probe sample preparation (Fig. 2) and for advanced microanalysis in 2D and 3D. Results from surface analyses (electron and ion imaging, EDS, EBSD), sub-surface analyses (3D imaging, 3D EDS, 3D EBSD), and unique in-situ ToF-SIMS analyses (Fig. 3) are correlated with site specific atom probe tomography results, which enables a microstructural and microchemical characterisation of highly complex materials on a wide range of length scales, from centimetre down to the nanoscale.

FUNDED PROJECTS

A fully automated, fully shielded palaeomagnetic system.

Palaeomagnetism is a key research field that has applications to a broad range of pure and applied geoscience disciplines. Australia has been a world leader in this field, including the application of palaeomagnetism to both global and regional tectonic studies. Palaeomagnetic studies demand a labourintensive process of treating and measuring a large number of samples. This proposal aims to establish the first fully automated and magnetically fully shielded superconducting palaeomagnetic data acquisition system in Australia. The system will significantly enhance the efficiency and accuracy of palaeomagnetic analysis, and thus enhance Australia's research capacity in this and related research fields.

Prof. Z.X. Li, Curtin University, Dr. E. Tohver, The University of Western Australia, Prof. A.P. Roberts, Australian National University, Associate Prof. G. Rosenbaum, University of Queensland, Associate Prof. C. O'Neill, Macquarie University, Dr. S. Pisarevsky, Associate Prof. C. Clark, Prof. C., Elders, Prof. P. Bland, Prof. S. Wilde, Curtin University

---

ARC LIEF grant LE150100065: $560,000 from the SARC, $300,000 + a further $250,000 from Curtin University, $80,000 from The University of Western Australia, $30,000 from the Australian National University, and $20,000 each from the University of Queensland, Associate and Macquarie University.

Assembling of the magnetic shielded room.

Dr Gary Scott selecting non-magnetic items brought from the U.S., along with items from the Curtin team, to be placed in the Time Capsule sealed inside the magnetic shield (photo above).

Careful degaussing of the magnetic shield.

RESEARCH GRANTS

How the Earth works – toward building a new tectonic paradigm

Prof. Z.X. Li, Curtin University

ARC Australian Laureate Fellowship grant FL150100133, 2015-2020: $2.9 million.

Half a century after the inception of plate tectonics theory, we are still unsure how the Earth 'engine' works, particularly the forces that drive plate tectonics. This project will build on the latest technological and conceptual advances to establish the first-order patterns of Earth evolution as far back as 2,000 million years ago, and use this information to examine a ground-breaking geodynamic hypothesis which links cyclic plate aggregation and dispersion to deep Earth processes. The project, a team effort involving extensive national and international collaboration, will potentially create a paradigm shift in our understanding of global tectonics, and will help to understand the formation and distribution of Earth resources.

IGCP project 648: Supercontinent cycles and global geodynamics

Professors Z.X. Li, Curtin University, D.A.D. Evans, Yale University, S. Zhong, University of Colorado, B. Eglington, University of Saskatchewan, plus over 150 members from many countries.

UNESCO-IUGS International Geoscience Program (IGCP) project 648, 2015–2019: up to USD50,000.

Rapid recent progress in supercontinent research indicates that Earth's history has been dominated by cycles of supercontinent assembly and breakup. New developments in geophysical imaging power and computer simulation have provided increasingly clearer views of the Earth's interior, and how the moving plates on the Earth's surface interact with the deep planetary interior. In this project, we will bring together a diverse range of geoscience expertise to harness these breakthroughs in order to explore the occurrence and evolution history of supercontinents through time, and the underlying geodynamic processes. As part of this project, we will establish/improve global databases of geotectonics, palaeomagnetism, mineral deposits, and the occurrences of past mantle plume events, and examine how the supercontinent cycles interacted with the deep mantle to produce episodic and unevenly distributed Earth resources. The project builds on the success of a series of previous IGCP projects. It will not only lead to major scientific breakthroughs, but also develop user-friendly GIS-based databases that can be used by anyone who wants to reconstruct palaeogeography, test geodynamic models, model major climatic events such as Snowball Earth events, and predict exploration targets for Earth resources.

ARC Discovery grant DP130100130

Unravelling the geodynamics of eastern Australia during the Permian: the link between plate boundary bending and basin formation.

Rosenbaum, G. (University of Queenslnd), Pisarevsky, S.A. (Curtin University), Fielding, C. (University of Nebraska), Speranza, F. (Istituto Nazionale di Geofisica e Vulcanologia, Rome, Italy).

Awarded $384,709

The main aim of this project is to unravel the history of the oroclinal bending of the Carboniferous – Permian New England Orogen in eastern Australia. To achieve this goal paleomagnetic, geochronological and structural studies are carried out.

Collaborative project with the University of Oslo

Updating of the Global Paleomagnetic Database

Pisarevsky, S.A. (Curtin University)

Regular updating of the Global Paleomagnetic Database.

Awarded : A$30,000

ARC Discovery Project. DP 160103449

Just add water – a recipe for the deformation of continental interiors.

CIs: A. Putnis (Curtin) T. Raimondo (Univ. South Australia) N. Daczko (Macquarie).

The plate tectonics paradigm argues that continental interiors are usually stable, rigid and undeformable, yet mountain belts have formed in these locations throughout Earth's history. Their existence suggests that strong crust can be significantly weakened to allow the accommodation of deforming forces, but the underlying causes for this change in behaviour are not clear. This project aims to investigate the largely unexplored impact of fluid flow on the characteristics of intraplate deformation. This outcome will improve our understanding of what modulates the strength of continental crust, including its susceptibility to seismic activity, and the ways in which fluids interact with the deep crust, including their mineralisation potential.

Awarded: A$319,500

ARC LIEF Project LE160100103

Australian Virtual Experimental Laboratory: a multimode geoscience facility.

CIs: S. Foley (Macquarie) K.Evans (Curtin) John Mavrogenes (ANU) Andrew Putnis (Curtin) Joel Brugger (Monash) Simon Clark (Macquarie)

Seven types of high-pressure equipment will augment existing facilities to form a multi-node experimental laboratory at four locations across Australia (Macquarie, ANU, Monash and Curtin). These nodes will work as a team to further the effectiveness of high-pressure experimental geoscience research, coordinating the acquisition and use of a range of equipment relevant to research at all pressures from crust to core. Equipment includes hydrothermal and piston-cylinder systems for applications with fluids and melts relevant to the movement and deposition of precious metals, and multi-anvil and portable Laser-heated diamond-anvil systems for mantle and core pressures, some of which can also be used in synchrotron applications.

Awarded: A$547,000.

ARC Discovery Project DP150102773

Migmatites, charnockites and crustal fluid flux during orogenesis.

CIs: I.C.W. Fitzsimons (Curtin), M.B. Holness (Cambridge), C. Clark (Curtin).

Migration of volatile fluid and molten rock controls many Earth processes including rock deformation and the formation of mineral and energy deposits. Deep crustal fluids are hard to study directly, and their characteristics are usually inferred from lower crustal rock brought to the surface by erosion. For over 30 years one such rock called charnockite has been used to argue that lower crust is dehydrated by influx of CO2-rich fluid, while other evidence supports dehydration by water extraction in silicate melt. This project will use the shape, distribution, and chemistry of mineral grains to trace the passage of volatiles and melt through charnockite, constrain the nature of lower crustal fluids, and resolve a long-standing controversy.

Awarded A$183,000.

Australian Antarctic Science Project 4355

Reconstructing East Antarctica in Gondwana: ground-truthing a new tectonic model.

CIs: J.A. Halpin (University of Tasmania), N.R. Daczko (Macquarie), I.C.W. Fitzsimons (Curtin), J.M. Whittaker (University of Tasmania).

The sub-glacial geology of East Antarctica remains one of the most mysterious frontiers on Earth, and the Queen Mary Land and Wilkes Land sectors are particularly poorly understood although available data suggest that they comprise multiple continental fragments that collided to form part of the East Gondwana continent ~500 million years ago. This project will analyse rock samples previously collected near the collision zone to derive new age and geochemical constraints and to ground-truth a number of domains delineated by recent geophysical surveys. Determining the geometry, chemical composition and geological history of terranes in this sector of East Antarctica will lead to a greater appreciation of the role of ancient tectonic boundaries and geothermal heat flow on the behaviour of the Antarctic ice sheet.

Awarded A$36,000.

ARC Discovery Project DP160102427

Developing and testing a new dating tool for Quaternary science

CIs: Dr Martin Danisik; A/Prof Noreen Evans; Professor Dr Axel Schmitt; Associate Professor Phil Shane; Professor Takehiko Suzuki; Professor Shanaka de Silva.

Awarded A$289,500.

ARC LIEF Project LE150100013:

Laser ablation multiple split streaming.

CIs: Kemp, McCulloch, Fiorentini, McCuaig, Rate and 12 others.

Awarded A$860,000.

ARC Discovery Project DP150101730

Building Central Asia: Linking the Growth of Asia to its Exhumation.

CIs: Glorie, Collins, Xiao and N.Evans.

Awarded A$216,300.

ARC LIEF Project LE150100145

The South Australian Thermochronometry Hub

CIs: Prof Collins, A/Prof Glorie, Prof Holford, A/Prof Evans, Prof McInnes, Prof Gleadow, Prof Reid.

Awarded A$170,000.

NSFC Project 41373051

The preservation and exhumation of the Indonesian porphyry Cu deposits in the Zhongdian Arc, Northwest Yunnan: constraints from low-temperature thermochronology.

CIs: Zhang, McInnes, Evans, Zhu, Zhao, Wang, Wang and Leng.

850,000 CNY ($146,200 AUD).

Curtin Senior Research Fellowship to A/Prof N.J. Evans (2015-2018): 4-year salary and operating support at A/Professor level to complete a research program in laser-based elemental and chronological research. Est. $800,000.

ASI-Curtin RESOchron R&D Support (2014-2017): 3 year salary and operating support for a Research Associate to develop protocols for (U-Th-Sm)/He in situ dating using the RESOchron facility. $780,000 with an option to extend to 5 years ($1,339,215).

Australian Technology Network (ATN) – FAPESP (Brazil) grant

4D evolution of mineralization in Archean Terranes of Brazil.

CIs McNaughton, Rasmussen, Wilde.

This research is to provide reliable age information on key mineral deposits in Archean terranes of Brazil, and extends the decade-long collaboration in SHRIMP research between Curtin University and University of Campinas. It will be underpinned by the facilities and experience of Curtin researchers in dating ore deposits and related events, and the complementary experience in tectonics and ore genesis of Brazilian colleagues.

External support: A$18K.

MRIWA Project M446

4D evolution of WA ore systems (WA4D): Re-Os sulphide geochronology.

CIs: McNaughton, Tessalina, McInnes, Jourdan.

This proposal seeks to utilize the Re-Os isochron method on sulphides to determine precise ages for two classes of metal deposits in WA: i.e. volcanic-hosted massive sulphide (VHMS) Zn-Pb-Cu deposits and orogenic gold deposits. Each deposit type typically contains ore-related pyrite+/-arsenopyrite, which apart from rare molybdenite, are the two most reliable common sulphides for Re-Os geochronology. Re-Os isochron ages will be complemented by precise U-Pb and Ar-Ar ages on the selected deposits and their environs, including host rock, stratigraphic ages, alteration and metamorphic ages, to build a precise 4D framework of ore formation.

External support: A$325K.

MRIWA Project M448

4D evolution of WA ore systems (WA4D): Rutile – pathfinders to ore.

CIs: McNaughton, Evans, McInnes, Jourdan.

This proposal is about the development of rutile protocols for metals exploration in WA, and directly supports "Searching the deep earth: the future of Australian resource discovery and utilization" proposed by the Australian Academy of Sciences: i.e. the initiative on "Resolving the 4D geodynamic and metallogenic evolution of Australia". The proposal focusses on (1) establishing new trace element fingerprints carried by rutile grains to identify their environment of formation (i.e. ore-associated vs barren), and (2) the age of rutile formation, given that published and unpublished age data for known hydrothermal ore formation in WA tends to be synchronous within a terrain. The proposal seeks to build a database of these two independent indicators of mineralization in WA (i.e. chemical fingerprint and age), to provide a foundation for metals exploration using rutile grains encountered in rocks/drillcore, or as detrital grains in heavy mineral concentrates from field sampling.

External support: A$490K.

MRIWA Project M467

Mineralogical and lithological controls on REE distribution in the Argyle diamond deposit.

CIs: O'Connor (WASM), McNaughton, Aldrich (WASM), Evans.

Mantle-derived alkaline and silica-undersaturated rocks such as kimberlites, lamproites and carbonatites naturally contain high REE-contents, compared to most other common rock types. However, with a few exceptions, very little is known about the REE-minerals in such rocks in WA. A PhD project has been established to characterise the REE minerals of the Argyle lamproite, AK1, which is currently mined for diamonds. The project is supported by the mine operators, Rio Tinto, and seeks to:

1) Identify REE-enriched zones within different areas of AK1, and determine REE concentration mechanisms, whether primary igneous or secondary alteration/weathering;

2) Identify REE-bearing minerals and the concentrations of the REEs in those minerals; and

3) Provide a case study for the potential development of REE resources in WA in similar rock types.

External support: A$60K.

Geochronology for the Greenland Ministry of Mineral Resources

CIs: C.L. Kirkland, N.J. Gardiner

The aims of this one-year research proposal are to develop the structure of, and populate a geochronology database holding U-Pb information on Greenland. Additionally, new U-Pb geochronology will be acquired for a set of new Greenlandic samples. Subject to funding, it is envisaged that this project will be ongoing.

Crustal Evolution Research for the Geological Survey of Western Australia

CIs: C.L. Kirkland, N.J. Gardiner

The aims of this three-year research proposal are to further develop GSWA's capacity in isotope geology and fully utilize isotopic datasets already collected and currently being collected by GSWA. To this end innovative analysis mechanisms will be applied to isotopic datasets and the results presented via client accessible spatially interpolated images and reports (including but not limited to, time evolving isotopic maps).

Mineral systems on the margin of cratons: Albany-Fraser Orogen / Eucla Basement case study

CIs: C.L. Kirkland, C. Clark, K. Evans, S. Reddy

Modern exploration requires a new integrated approach, utilizing a broad range of techniques, which can collectively enhance the geological knowledge of a region's mineral endowment. Craton margins host significant lithospheric discontinuities that focus fluids and heat and which, under favourable circumstances, may become mineralized corridors. Additionally, high-grade terrains are frequently viewed as less prospective for some mineralization (e.g. gold) than lower grade regions. However, recent discoveries in the Albany-Fraser Orogen highlight that many common models for mineral endowment are lacking and their resolution through cover limited. Significant ore systems with mantle tapping roots are the manifestation of physical and thermo-chemical processes associated with specific sites of fluid mobility, driven frequently by regional-scale tectonic activity. Hence, a means to enhance the discovery of new Australian resources, which may be buried, is to boost our detection of the distal signature carried within mineral phases. The aims of this project are to enhance petrochronology, crustal evolution and sulphur isotopic studies of the AFO and the covered Eucla basement.

Sediment in the Great Australian Bight: Basement information recovered through detrital minerals and implications for the evolution of Australia's southern margin.

CIs: C.L. Kirkland, M. Barham

The exposed mineralised Gawler and Yilgarn cratons are separated by nearly one thousand kilometres of basement that represents a large prospective mineral province, but this region is buried by sedimentary basins formed during the development of Australia's southern margin. In this project new geochronology will be performed on legacy drill core material from the offshore Eucla basin to understand its provenance.

ARC Future Fellowship project (FT140100826):

Xuan-Ce Wang

The main goal of this project is to test a provocative and potentially ground-breaking hypothesis that links fluid cycling, large-scale intra-continental magmatism, volcanic volatile flux, climate changes, mantle chemical geodynamics, plate tectonics, and slab stagnation in a self-consistent geodynamic system. This research will integrate geochemistry, petrology, geophysics, global tectonics, and thermodynamical modelling to reach a new level of understanding of the fluid cycling and Earth's dynamics through time. The outcomes will fill the knowledge gap of how fluids work in the Earth's system, and will help us to understand how deep-Earth's geodynamic processes influence paleoclimate changes. This work will also help us to identify ways to improve future mineral exploration success.

ARC LINKAGE Project (Woodside)

Chronostratigraphic, molecular and isotopic approaches to age petroleum

CIs: Grice, Coolen and Murray

The project aims to reduce the costs of drilling in deep-water offshore by better identifying potential drilling sites. The North-West shelf offshore Australia is the main supplier of liquefied natural gas. However, there is uncertainty about the age of petroleum (oil and gas) discovered in the region. It is not currently possible to constrain an age of fluids to a number of source rocks. The aims are to develop a high-level age discriminative tool for fluids. An interdisciplinary approach will be applied using state-of-the-art techniques including comprehensive two dimensional gas chromatography time-of-flight mass spectrometry, compound specific isotope analysis of hydrocarbons, clumped isotopes of methane and metagenomics.

Awarded A$810K.

ARC Discovery Project

The Pace and rhythm of climate: 600,000 years in a biological hot-spot

CIs: Stevenson, Coolen

This project aims to generate knowledge of long-term changes in vegetation and rainfall for the Indo-Pacific Warm Pool (IPWP). The IPWP exerts enormous influence on the Earth's climate through its interactions with the El Niño-Southern Oscillation, the Austral–Asian monsoons and the Inter-tropical Convergence Zone. Yet despite its importance, the response of the IPWP to global climate change remains uncertain. Through palynology, ancient sedimentary DNA and compound specific stable isotope analyses, this project aims to produce a terrestrial vegetation, fire and biodiversity record for the last 600 000 years in Sulawesi. The unrivalled length and resolution of this record for the region would make it a benchmark reconstruction of palaeoclimate that may transform our understanding of the IPWP.

Awarded A$413K

Chevron – WA:ERA

Asphaltite characterisation based on a biomarker stable isotopic study.

CI: Grice

Awarded A$360K

Petrobras- International partner

Geochemical assessment of oil and rock-extract samples of the Brazilian basins based on saturate and aromatic biomarkers and isotope analysis

CI: Grice

Awarded A$360K

ARC LIEFP

High resolution mass spectrometer for metabolics and proteinomics

CIs: Millar, Clode et al., Grice

Awarded: A$670K

ARC Discovery Project

Sulfur cycling in modern microbialites, toxic oozes and petroleum.

CIs: Grice, Visscher, Sessions, Schwark

Compound specific sulfur isotope analyses will be applied to sulfur-rich deposits from extreme environments: sulfidic black oozes (Peel-Harvey estuary); modern microbialites (for example, Shark Bay) and oils/source (established and frontier oil fields). Sulfur isotopic data, integrated with other stable isotopic and molecular data, will greatly assist our studies of sulfur biogeochemical cycles and mechanisms of organic sulfurisation at different diagenetic stages or geological ages. The research will address national concerns; a measure of the respective impact of anthropogenic and natural changes on environments; help understand the evolution of life on Earth; and contribute to efficient discovery of our natural petroleum systems.

Awarded: A$430K

ARC LIEFP

Isotope analyser for water samples.

CIs: Skrzypek, Grierson, Edwards, McCulloch, Grice

Awarded $160K

ARC Discovery – Discovery Outstanding Research Award-3 Fellowship Grice ($710K) extended until end of 2017 Grice, Summons.

Tackling the resurgences of life, advanced dating tools of oils by sophisticated molecular and isotopic analyses from major geological events

The long-term impacts (over millions of years) of present global warming are poorly understood. However, recovery mechanisms evident in past related mass extinctions are invaluable in helping to understand the pace of recovery of marine and terrestrial ecosystems. Grice's world-leading expertise in biomarkers and stable isotopes will be applied to paleoclimate change, evolution and energy. Cutting-edge petroleum exploration technologies especially dating oil without having to drill it's source is important in addressing the global energy crisis. Strongly interrelated themes also support Grice's enthusiasm for training young scientists meeting Australia's Earth science research and industry needs.

CSIRO/ Minerals Collaboration Cluster Fund ($3M)

Organic-Inorganic interactions

CIs: Grice, Evans, Rasmussen, Gale, McCulloch, Greenwood, McCuaig, Brocks, Moreau.

The Organic Geochemistry of Mineral Systems (OGMS) Cluster was a $6 million multi-institutional research initiative supported by the CSIRO National Flagships program which focused on understanding the role played by organic components and processes in the formation of major mineral deposits. The project was led by Curtin University, and involved the collaboration of researchers from the University of Western Australia, the University of Melbourne and the Australian National University. The academic group was collaboratively complemented by a large cohort of CSIRO researchers from the Minerals Downunder Flagship, and the unique expertise of several key international scientists.

ARC LINKAGE Project

Subterranean invertebrate communities of arid zone Western Australia: diversity, assessment and food-web structure

CIs: Austin, Cooper, Humphreys, William; Blyth; Mitchell; Munguia, Harvey, Byrne, Halse, Humphreys, Garth

This project uses a powerful combination of genetic data and isotopic analyses to elucidate the biodiversity and foodweb structure of unique subterranean fauna in WA, providing crucial information for the monitoring and management of groundwater in the area

Awarded $340K

AINSE/ANSTO fellowship

Molecular, stable isotopic and radiocarbon analyses of organic matter preserved in terrestrial records

CI: Blyth

TIGeR PUBLICATIONS 2015

Agangi A., Hofmann A., Kamenetsky V.S., Vroon P. (2015). Palaeoarchaean felsic magmatism: a melt inclusion study of 3.45 Ga old rhyolites from the Barberton Greenstone Belt, South Africa. *Chemical Geology* 414, 69-83.

Agangi A., Przybylowicz W., Hofmann A. (2015). Trace element mapping of pyrite from gold deposits – A comparison between PIXE and EPMA. *Nuclear Inst. and Methods in Physics Research*, B 348, 302-306.

Agangi A., Hofmann A., Rollion-Bard C., Marin-Carbonne J., Cavalazzi B., Large, R., Meffre, S. (2015). Gold accumulation in the Archaean Witwatersrand Basin, South Africa – evidence from concentrically laminated pyrite. *Earth Science Reviews* 140, 27-53.

Anczkiewicz A.A., Danišík M., Środoń J. (2015). Multiple low temperature thermochronology constraints on exhumation of the Tatra Mts. – new implication for the complex evolution of the Western Carpathians in the Cenozoic. *Tectonics* 34, 11, 2296-2317.

Andam-Akorful S.A., Ferreira V.G., Awange J.L., Forootan E., He, X.F. (2015). Multi-model and multi-sensor estimations of evapotranspiration over the Volta Basin, West Africa. *International Journal of Climatology* 35: 3132–3145.

Archibald D., Collins A.S., Foden J.D., Payne J.L, Taylor R., Holden P., Razakamanana T., Clark, C. (2014) Towards unravelling the Mozambique Ocean conundrum using a triumvirate of zircon isotopic proxies on the Ambatolampy Group, central Madagascar. *Tectonophysics*. 662, 167-182.

Arosi H.A., Wilson M.E.J. (2015). Diagenesis and fracturing of a large-scale, syntectonic carbonate platform. *Sedimentary Geology*, 326, 109-134.

Atahan P., Heijnis H., Dodson J., Grice K., Le Métayer P., Taffs K., Hembrow S., Woltering M., Zawadzki A. (2015). Pollen, biomarker and stable isotope evidence of late Quaternary environmental change at Lake McKenzie, southeast Queensland *Journal of Paleolimnology* 53, 139-156

Awange, J., E. Forootan, K. Fleming, and G. O. Odhiambo (2015) Dominant Patterns of Water Storage Changes in the Nile Basin During 2003–2013. In Remote Sensing of the Terrestrial Water Cycle, ed. Venkataraman Lakshmi, 367-382. New Jersey: John Wiley.

Barham M., Murray J., Sevastopulo G.D., Williams D.M. (2015). Conodonts of the genus Lochriea in Ireland and the recognition of the Viséan-Serpukhovian (Carboniferous) boundary. *Lethaia* 48, 151-171.

Barham M. (2015) Fossils explained 64: Comprehending conodonts. *Geology Today* 31 (2), 74-80.

Bellucci J.J., Nemchin A.A., Whitehouse M.J., Snape J.F., Bland P., Benedix G.K. (2015) The Pb isotopic evolution of the Martian mantle constrained by initial Pb in Martian meteorites (2015) *Journal of Geophysical Research E: Planets*, 120, 2224-2240.

Blades M. L., Collins A.S., Foden J., Payne J.L., Xu X., Alemu Woldetinsae G., Clark C., Taylor R.J.M. (2015). Age and hafnium isotopic evolution of the Didesa and Kemashi Domains, western Ethiopia. *Precambrian Research*, 270, 267-284.

Blyth A. J., Smith C.I. (2015). Applications of Liquid Chromatography-Isotope Ratio Mass Spectrometry in Geochemistry and Archaeological Science." In Principles and Practice of Analytical Techniques in Geosciences, ed. Kliti Grice, 313-323. UK: The Royal Society of Chemistry.

Blyth A.J., Fuentes D., George S.C. Volk, H. (2015). Characterisation of organic inclusions in stalagmites using laser-ablation-micropyrolysis gas chromatography-mass spectrometry *Journal of Analytical and Applied Pyrolysis*, 113, 454-463.

Bóna A., Gurevich B., Pevzner R., Lebedev M., Madadi M. (2015) Joint inversion of P-, and S-wave travel times for characterisation of anisotropic materials using laser Doppler interferometry measurements. *ASEG Extended Abstracts 2015* (1), 1-4.

Braga F.C.S., Rosiere C.A., Queiroga G.N., Rolim V.K., Santos J.O.S., McNaughton, N.J. (2015). The Statherian itabirite-bearing sequence from the Morro Escuro Ridge, Santa Maria de Itabira, Minas Gerais, Brazil. *Journal of South American Earth Sciences* 58, 33-53.

Bufarale, G., Collins, L.B. (2015). Stratigraphic architecture and evolution of a barrier seagrass bank in the mid-late Holocene, Shark Bay, Australia. *Marine Geology* 359, 1-21.

Cao M., Qin K., Li G., Evans N.J., Jin, L. (2015). In situ LA-MC-ICP-MS trace element and Nd isotopic composition and genesis of polygenetic titanite from the Baogutu reduced porphyry Cu deposit, Western Junggar, NW China. *Ore Geology Reviews*, 65, 940-954.

Cao M., Qin K., Li G., Evans N.J., He H., Jin L. (2015). A mixture of mantle and crustal derived He-Ar-C-S-H-O ore-forming fluids at the Baogutu reduced porphyry Cu deposit, Western Junggar. *Journal of Asian Earth Sciences*, 98, 188-197.

Cavosie A.J., Erickson T.M., Timms N.E. (2015). Nanoscale Records of Ancient Shock Deformation: Reidite ($ZrSiO_4$) in Sandstone at the Ordovician Rock Elm Impact Crater. *Geology*, 43, 315-318.

Cavosie A.J., Erickson T.M., Timms N.E., Reddy S.M., Talavera C., Montalvo S.M., Pincus M.R., Gibbon R., Moser D. (2015). A terrestrial perspective on using ex situ shocked zircons to date lunar impacts. *Geology*, 43, 999-1002.

Cawood P.A., Strachan R.A., Merle R.E., Millar I.L., Loewy S.L., Dalziel I.W.D., Kinny P.D., Jourdan F., Nemchin A.A., Connelly J.N. (2015) Neoproterozoic to early Paleozoic extensional and compressional history of East Laurentian margin sequences: The Moine Supergroup, Scottish Caledonides. *Geological Society of America Bulletin* 127, 349–371 (2015)

Centrella S., Austrheim H., Putnis A. (2015) Coupled mass transfer through a fluid phase and volume preservation during hydration of granulite: An example from the Bergen Arcs, Norway. *Lithos*, 236,237, 245-255 (2015)

Chernicoff C.J., Zappettini E.O., Santos J.O.S., Pesce A., McNaughton, N.J. (2015). Zircon and titanite U-Pb SHRIMP dating of unexposed basement units of the Buenos Aires region, southeastern Rio de la Plata Craton, Argentina. *International Geology Review* 58, 643-652.

Chibwe D.K., Akdogan G, Bezuidenhout G.A., Kapusta J.P.T., Bradshaw S., Eksteen J.J. (2015). Sonic injection into a PGM Peirce-Smith converter: CFD modelling and industrial trials. *Journal of the Southern African Institute for Mining and Metallurgy*, 115, 349-354.

Chibwe D.K., Akdogan G., Taskinen P., Eksteen J.J. (2015). Modelling of fluid flow phenomena in Peirce-Smith copper converters and analysis of combined blowing concept. *Journal of the Southern African Institute for Mining and Metallurgy*. 115, 363-374.

Claessens S.J., Hirt C. (2015) A surface spherical harmonic expansion of gravity anomalies on the ellipsoid. *Journal of Geodesy*, 89,1035-1048.

Clark C., Healy D., Johnson T.E., Collins A.S., Taylor R.J.M., Santosh M., Timms N.E. (2015) Hot orogens and supercontinent amalgamation: a Gondwanan example from southern India. *Gondwana Research*. 28, 1310-1328.

Collet O., Gurevich B., Duncan G. (2015) Estimating azimuthal stress-induced P-wave anisotropy from S-wave anisotropy using sonic log or vertical seismic profile data, *Geophysical Prospecting*, 2015, doi: 10.1111/1365-2478.12307

Collins A.S., Patranabis-Deb S., Alexander E., Bertram C.N., Falster G.M., Gore R.J., Mackintosh J., Dhang P.C., Saha D., Payne J.L., Jourdan F., Backé G., Halverson G.P., Wade B.P. (2015) Detrital Mineral Age, Radiogenic Isotopic Stratigraphy and Tectonic Significance of the Cuddapah Basin, India. *Gondwana Research* 28, 1294-1309.

Collins, L. B., O'Leary, M., Stevens, A., Bufarale, G., Kordi, M., & Solihuddin, T. (2015). Geomorphic patterns, internal architecture and reef growth in a macrotidal, high-turbidity setting of coral reefs from the Kimberley bioregion. *Australian Journal of Maritime & Ocean Affairs*, 7(1), 12-22.

Condie K., Pisarevsky S.A., Korenaga J., Gardoll S. (2015). Is the rate of supercontinent assembly changing with time? *Precambrian Research*, 259, 278-289.

Conway S.J., Balme M.R., Kreslavsky M.A., Murray J.B., Towner M.C. (2015). The comparison of topographic long profiles of gullies on Earth to gullies on Mars: A signal of water on Mars, *Icarus*, 253, 189-204.

Coolen M.J.L., Orsi W.D. (2015). The transcriptional response of microbial communities in thawing Alaskan permafrost soils. *Frontiers in Microbiology* 6. doi:10.3389/fmicb.2015.00197

Cui X., Jiang X., Wang J., Wang X-C., Zhuo J., Deng Q., Liao S., Wu H., Jiang Z., Wei Y. (2015). Mid-Neoproterozoic diabase dykes from Xide in the western Yangtze Block, South China: New evidence for continental rifting related to the breakup of Rodinia supercontinent. *Precambrian Research* 268, 339-356.

Cui X., Zhu W., Fitzsimons I.C.W., He J., Lu Y., Wang X., Ge R., Zheng B., Wu X. (2015). U–Pb age and Hf isotope composition of detrital zircons from Neoproterozoic sedimentary units in southern Anhui Province, South China: Implications for the provenance, tectonic evolution and glacial history of the eastern Jiangnan Orogen. *Precambrian Research* 271, 65–82.

Dan W., Wang Q., Wang X.-C., Liu Y., Wyman D.A., Liu Y.-S. (2015). Overlapping Sr–Nd–Hf–O isotopic compositions in Permian mafic enclaves and host granitoids in Alxa Block, NW China: Evidence for crust–mantle interaction and implications for the generation of silicic igneous provinces. *Lithos* 230, 133-145.

Danišík M., László Fodor, L., Dunkl, I., Gerdes A., Csizmeg, J., Hámor-Vidó, M., Evans, N.J. (2015). A multi-system geochronology in Ad-3 borehole, Pannonian Basin (Hungary) with implications for dating volcanic rocks by low-temperature thermochronology. *Terra Nova*, doi: 10.1111/ter.12155.

De Grave J., Zhimulev F.I., Glorie S., Kuznetsov G.V., Evans N., Vanhaecke F., McInnes B. (2015). Late Palaeogene emplacement and late Neogene–Quaternary exhumation of the Kuril island-arc root (Kunashir island) constrained by multi-method thermochronometry. *Geoscience Frontiers*, 7, 211-220.

Deo M., El-Mowafy A. (2015). Cycle Slip and Clock Jump Repair with Multi-Frequency GNSS data for improved Precise Point Positioning. *Proc. of IGNSS Symposium 2015*, Gold Coast, 14-16 July, 2015.

Doyle M.G., Fletcher I.R., Foster J., Large R.R., Mathur R., McNaughton N.J., Meffre S., Muhling J.R., Phillips D., Rasmussen B. (2015). Geochronological constraints on the Tropicana Gold Deposit and Albany Fraser Orogen, Western Australia. *Economic Geology* 110, 355-386.

Egorov A., Glubokovskikh S., Bóna A., Pevzner R., Gurevich B., Tokarev M. (2015) Influence of rough sea surface on sea surface reflections: deep towed high-resolution marine seismic case study. *SEG Technical Program Expanded Abstracts 2015*, 3661-3665.

Eiserbeck C., Nelson R.K., Reddy R.K., Reddy C.M., Grice K. Advances in comprehensive two-dimensional gas chromatography. In: *Royal Society of Chemistry*.(Grice, K. editor), UK. 4, 324-365.

Eksteen J.J. Oraby E.A. (2015). The leaching and adsorption of gold using low concentration amino acids and hydrogen peroxide: Effect of catalytic ions, sulphide minerals and amino acid type. *Minerals Engineering*, 70, 36-42.

Elburg M., Jacobs J., Anderson T., Clark C., Laufer A., Ruppel A., Luka N., Damaske D. (2015) The metatonalites of Sør Rondane (East Antarctica): petrogenesis and implications for Rodinia reconstruction. *Precambrian Research*. 259, 189-206.

El-Mowafy A. (2015) Estimation of Multi-Constellation GNSS Observation Stochastic Properties Using a Single-Receiver Single-Satellite Data Validation Method, *Survey Review*, Vol. 47, 341, 99-108.

El-Mowafy A. (2015). Diagnostic Tools Using a Multi-Constellation Single-Receiver Single-Satellite Data Validation Method. *Journal of Navigation*, 68, 196-214.

Erickson T.M., Pearce M.A., Taylor R.J., Timms N.E., Clark C., Reddy S.M., Buick I.S. (2015). Deformed monazite yields high temperature tectonic ages. *Geology*, 43, 383-386.

Erickson T.M., Pearce M.A., Taylor R.J., Timms N.E., Clark C., Reddy S.M., Buick I.S. (2016). Deformed monazite yields high temperature tectonic ages: Reply. *Geology*, 44, 378.

Esteban L., Pimienta L., Sarout J., Delle Piane C., Haffen S., Geraud Y., Timms N.E. (2015). Study cases of thermal conductivity prediction from P-wave velocity and porosity. *Geothermics*, 53, 255-269.

Evans K.A., Powell R. (2015). Metamorphic effects on the redox budget of subducted mantle lithosphere. *Journal of Metamorphic Geology*, 33, 649-670.

Evans N.J., McInnes B.I.A., McDonald B., Danisik M., Becker T. Vermeesch P., Shelley M., Marillo-Sialer E., Patterson D.B. (2015). An in situ technique for (U-Th-Sm)/He and U-Pb double dating. *Journal of Analytical Atomic Spectroscopy*, 30, 1636-1645

Fan W., Wang Y., Zhang Y., Zhang Y., Jourdan F., Zi J., Liu, H. (2015). Paleotethyan subduction process revealed from Triassic blueschists in the Lancang tectonic belt of Southwest China. *Tectonophysics* 662, 95-108.

Featherstone W.E., Penna N.T., Filmer M.S., Williams S.D.P. (2015). Nonlinear subsidence at Fremantle, a long-recording tide gauge in the Southern Hemisphere. *Journal of Geophysical Research: Oceans*, 120, 7004-7014.

Fromont J., Huggett M.J., Lengger S.L., Grice K., Schönber C.H.L. (2015). Characterisation of Leucetta prolifera, a calcarean cyanosponge from south-western Australia, and its symbionts. *Journal of the Marine Biological Association of the United Kingdom*, 1-12.

Galvin R.J., Gurevich B. (2015) Frequency-dependent anisotropy of porous rocks with aligned fractures. *Geophysical Prospecting* 63 (1), 141-150.

Gardiner N.J., Searle M.P., Morley C.K., Whitehouse M.J., Spencer C.J., Robb L.J. (2015). The Closure of Palaeo-Tethys in Eastern Myanmar and Northern Thailand: New Insights from Zircon U-Pb and Hf Isotope Data. *Gondwana Research* doi:10.1016/j.gr.2015.03.001

Gardiner N.J., Sykes J.P., Trench A., Robb L.J. (2015). Tin mining in Myanmar: Production and potential. *Resources Policy* 46, 219-233

Ge R.F., Zhu W.B., Wilde S.A. (2015). Synchronous crustal growth and reworking recorded in late Paleoproterozoic granitoids in the northern Tarim craton: In situ zircon U-Pb-Hf-O isotopic and geochemical constraints and tectonic implications. *Geological Society of America Bulletin* 127, 781-803.

Geisler T., Nagel T., Kilburn M.R., Janssen A., Icenhower J.P., Fonseca R.O.C., Grange M., Nemchin A.A. (2015) The mechanism of borosilicate glass corrosion revisited. *Geochimica et Cosmochimica Acta*, 158, 112-129.

Gillespie J., Glorie S., Xiao W., Zhang Z., Collins A.S., Evans N.J., McInnes B.I.A., De Grave, J. (2015). Mesozoic reactivation of the Beishan, southern Central Asian Orogenic Belt: Insights from low-temperature thermochronology. *Gondwana Research*. 10.1016/j.gr.2015.10.004

Glorie S., Zhimulev F.I., Buslov M.M., Andersen T., Plavsa D., Izmer A., Vanhaecke F., De Grave J. (2015) Formation of the Kokchetav subduction-collision zone (northern Kazakhstan): Insights from zircon U-Pb and Lu-Hf isotope systematics. *Gondwana Research*, 27, 424-438.

Glubokovskikh S., Gurevich B. (2015) Effect of micro-inhomogeneity on the effective stress coefficients and undrained bulk modulus of a poroelastic medium: a double spherical shell model. *Geophysical Prospecting*, 63, 656-668.

Grice, K. (2015) Principles and Practice of Analytical Techniques in the Geosciences. *Royal Society of Chemistry*, UK.

Grice K., Foster C.B., Riding J.B., Naehar S., Greenwood P.F. (2015). Vascular plant biomarker distributions and stable carbon isotopes from the Middle and Upper Jurassic (Callovian-Kimmeridgian) strata of Staffin Bay, Isle of Skye, northwest Scotland. *Palaeogeography, Palaeoclimatology, Palaeoecology*, 440, 307-315.

Greenwood P.F., Amrani A., Sessions A.L., Raven M.R., Holman A., Dror G., Grice K., McCulloch M.T., Adkins, J.F. (2015). Development and initial biogeochemical applications of compound specific sulfur isotope analysis. *Royal Society of Chemistry* (Grice, K. editor), UK. 285-312.

Grotheer H., Robert A., Greenwood P.F., Grice K. (2015). Stability and hydrogenation of polycyclic aromatic hydrocarbons during hydropyrolysis (HyPy) – Implications of highly matured organic matter. *Organic Geochemistry*, 86, 45-54.

Guangli W., Chang X., Wang, T-G., Simoneit B.R.T. (2015). Pregnanes as molecular indicators for depositional environments of sediments and petroleum source rocks. *Organic Geochemistry*, 78, 110-120.

Gudkova T., Lognonné P., Miljković K., Gagnepain-Beyneix J. (2015) Impact cutoff frequency – momentum scaling law inverted from Apollo seismic data, *Earth Planet. Sci. Lett*., 427, 57–65.

Gutierrez-Alonso G., Collins A.S., Gonzalez-Clavijo E., Fernandez-Suarez J., Pastor-Galan D., Jourdan F., Weil A.B., Johnston S.T. (2015) Kinematic constraints on lithospheric bending. 40Ar/39Ar ages of syn-orocline strike-slip shear-zones in northwestern Iberia. *Tectonophysics* 643, 44-54.

Hansma J., Tohver E., Yan M., Trinajstic K., Roelofs B., Peek S., . . . Hocking R. (2015). Late Devonian carbonate magnetostratigraphy from the Oscar and Horse Spring Ranges, Lennard Shelf, Canning Basin, Western Australia. *Earth and Planetary Science Letters*, 409, 232-242.

Haylay H.T.G., Sum C.W., Hunter A.W. (2015). Preservation of Marine Chemical Signatures in Upper Devonian Carbonates of Kinta Valley, Peninsular Malaysia: Implications for Chemostratigraphy. pp. 291-302, *ICIPEG 2014*. Springer.

Healy D., Blenkinsop T.G., Timms N.E., Meredith P.G., Mitchell T.M., Cooke M.L., (2015). Polymodal faulting: Time for a new angle on shear failure. *Journal of Structural Geology*, 80, 57-71.

Healy D., Neilson J. E., Haines T. J., Michie E.A.H., Timms N.E., Wilson M.E.J. (2015). An investigation of porosity-velocity relationships in faulted carbonates using outcrop analogues, In: Agar et al. (Eds): Fundamental Controls on Fluid Flow in Carbonates: Current Workflows to Emerging Technologies. *Geological Society, London, Special Publications*, 406, 261-280.

Hillbun K., Playton T. E., Tohver E., Ratcliffe K., Trinajstic K., Roelofs B., . . . Ward P. (2015). Upper Kellwasser carbon isotope excursion pre-dates the F-F boundary in the Upper Devonian Lennard Shelf carbonate system, Canning Basin, Western Australia. *Palaeogeography, Palaeoclimatology, Palaeoecology*, 438, 180-190.

Hirt C., Rexer M., Claessens S.J. (2015). Topographic evaluation of fifth-generation GOCE gravity field models – globally and regionally. *Newton's Bulletin*, 2015(5), 1-24.

Howard H.M., Smithies R.H., Kirkland C.L., Kelsey D.E., Aitken A., Wingate M.T.D., . . . Maier, W. D. (2015). The burning heart – the Proterozoic geology and geological evolution of the west Musgrave Region, central Australia. *Gondwana Research* 27, 64-94.

Hu S.Y., Evans K., Craw D., Rempel K., Bourdet J., Dick J., Grice K. (2015). Raman characterisation of carbonaceous material in the Macraes orogenic gold deposit and metasedimentary host rocks New Zealand. *Ore Geology Reviews* 70, 80-95.

Hunter A.W., Bashardin A., Meor, H.A.H. (2015). The Pulau Langgun section in the north-western Terrain (Upper Devonian). pp. 154-155. In: T.J. Suttner, E. Kido, P. Königshof, J.A. Waters, L. Davis and F. Messner (Eds.) *Planet Earth-In Deep Time-Palaeozoic Series: Devonian & Carboniferous*. Schweizerbart Science Publishers, Stuttgart, Germany.

Ivanic T.J., Nebel O., Jourdan F., Faure K., Kirkland C.L., Belousova E.A. (2015) A heterogeneously hydrated mantle underneath the late Archean Yilgarn Craton. *Lithos* 238, 76-85.

Jaraula C.M.B., Schwark L., Moreau X., Pickel W., Bagas L., Grice, K. (2015). Radiolytic alteration of biopolymers in the Mulga Rock uranium deposit. *Applied Geochemistry*, 52, 97-108.

Jiménez-Díaz A., Ruiz J., Kirby J.F., Romeo I., Tejero R., Capote R. (2015) Lithospheric structure of Venus from gravity and topography. *Icarus*, 260, 215-231.

Johanson Z., Boisvert C., Maksimenko A., Currie P., Trinajstic K. (2015). Development of the Synarcual in the Elephant Sharks (Holocephali; Chondrichthyes): Implications for Vertebral Formation and Fusion. *PLOS ONE*, 10(9), 19 pages.

Johnson T.E., Clark C., Taylor R.J.M, Santosh M., Collins A.S. (2015) Prograde and retrograde growth of monazite during the assembly of Gondwana: an example from the Nagercoil Block, southern India. *Geoscience Frontiers*. 6, 373-387.

Johnson T. E., Kirkland C. L., Reddy S. M., Fischer S. (2015). Grampian migmatites in the Buchan Block, NE Scotland. *Journal of Metamorphic Geology*, 33, 695–709.

Kakar M.I., Mahmood K., Khan M., Plavsa D. (2015) Petrology and geochemistry of amphibolites and greenschists from the metamorphic sole of the Muslim Bagh ophiolite (Pakistan): implications for protolith and ophiolite emplacement. *Arabian Journal of Geosciences*, 8, 6105-6120.

Kalnins L.M., Simons F.J., Kirby J.F., Wang D.V., Olhede S.C. (2015). On the robustness of estimates of mechanical anisotropy in the continental lithosphere: A North American case study and global reanalysis. *Earth and Planetary Science Letters*, 419, 43-51.

Kemp A.I.S., Hickman A.H., Kirkland C.L., Vervoort J D. (2015). Hf isotopes in detrital and inherited zircons of the Pilbara Craton provide no evidence for Hadean continents. *Precambrian Research* 261, 112-126.

Khaki M., Forootan E., Sharifi M.A., Awange J., Kuhn M. (2015) Improved gravity anomaly fields from retracked multimission satellite radar altimetry observations over the Persian Gulf and the Caspian Sea. *Geophysical Journal International*, 202, 1522-1534.

Khoshnavaz M.J., Bóna A., Urosevic M. (2015) Passive seismic imaging without velocity model prior to imaging. *ASEG Extended Abstracts 2015* (1), 1-4.

Khoshnavaz M.J., Chambers K., Bóna A., Urosevic M. (2015) Passive seismic localization without velocity model: application and uncertainty analysis. *SEG Technical Program Expanded Abstracts 2015*, 2467-2472.

Khoshnavaz M.J., Chambers K., Bóna A., Urosevic M. (2015) Passive seismic localization without velocity model: application and uncertainty analysis. *SEG Technical Program Expanded Abstracts 2015*, 2467-2472.

Kirkland C.L., Smithies R.H., Spaggiari C.V. (2015). Foreign contemporaries - Unravelling disparate isotopic signatures from Mesoproterozoic Central and Western Australia. *Precambrian Research* 265, 218-231.

Kirkland C.L., Smithies H., Taylor R., Evans N.J., McDonald B. (2015). Zircon Th/U ratios in magmatic environs. *Lithos* 212-215, 397-414.

Kirkland C. L., Spaggiari C., Smithies R., Wingate M., Belousova E., Gréau Y., Sweetapple M., Watkins R., Tessalina S.G., Creaser R. (2015). The affinity of Archean crust on the Yilgarn-Albany-Fraser Orogen boundary: Implications for gold mineralisation in the Tropicana Zone. *Precambrian Research* 266: 260-281.

Klein E.L., Lucas F.R.A, Queiroz Saney J.D.S., Freitas C.F., Renac C., Galarza M.A., Jourdan F., Armstrong R. (2015) Metallogenesis of the Paleoproterozoic Piaba orogenic gold deposit, Sao Luis cratonic fragment, Brazil. *Ore Geology Reviews* 65, 1-25.

Korhonen F., Brown M., Clark C., Foden J.D.,Taylor R.J.M. (2015). Are granites and granulites consanguineous? *Geology*, 43, 991-994.

Kraal P., Burton E.D., Rose A.L, Kocar B.D., Lockhart R.S., Grice K., Bush R.T. (2015). Sedimentary Iron-phosphorus cycling under contrasting redox conditions in a eutrophic estuary. *Chemical Geology* 392, 19-31.

Kroner A., Rojas-Agramonte Y., Wong J., Wilde S.A. (2015). Zircon reconnaissance dating of Proterozoic gneisses along the Kunene River of northwestern Namibia. *Tectonophysics* 602, 125-139.

Kuchta M., Tobie G., Miljković K., Běhounková M.,Souček O., Choblet G., Čadek O. (2015) Despinning and shape evolution of Saturn's moon Iapetus triggered by a giant impact, *Icarus*, 252, 454–465.

Kusebauch C., John T., Whitehouse M.J., Klemme S., Putnis A. (2015) Distribution of halogens between fluid and apatite during fluid-mediated replacement processes. *Geochimica et Cosmochimica Acta* 170, 225-246.

Kusiak M., Dunkley D.J., Wirth R., Whitehouse M., Wilde S.A., Marquardt K. (2015). Metallic lead nanospheres discovered in ancient zircons. *Proceedings of the National Academy of Sciences of the United States of America* 112, 4958-4963.

Lengger S.K., Scarlett A.G., West C.E., Frank R.A., Hewitt L.M., Milestone C.B., Rowland S.J. (2015) Use of the distributions of adamantane acids to profile short-term temporal and pond-scale spatial variations in the composition of oil sands process-affected waters. *Environmental Science: Processes & Impacts* doi:10.1039/C5EM00287G

Li C.-F., Wang X.-C., Li Y.-L., Chu Z.-Y., Guo J.-H., Li X.-H. (2015). Ce-Nd separation by solid-phase micro-extraction and its application to high-precision 142Nd/144Nd measurements using TIMS in geological materials. *Journal of Analytical Atomic Spectrometry* 30, 895-902.

Li C.-F., Guo J.-H., Chu Z.-Y., Feng L.-J., Wang X.-C. (2015). Direct High-Precision Measurements of the $^{87}Sr/^{86}Sr$ Isotope Ratio in Natural Water without Chemical Separation Using Thermal Ionization Mass Spectrometry Equipped with 1012 Ω Resistors. *Analytical Chemistry* 87, 7426-7432.

Li G.M., Li X.J., Zhao J.X., Qin K.Z., Cao M., Evans, N.J. (2015). Petrogenesis and tectonic setting of Triassic granitoids in the Qiangtang terrane, central Tibet: Evidence from U–Pb ages, petrochemistry and Sr–Nd–Hf. *Journal of Asian Earth Sciences*, 105, 443-445.

Li J., Wang X.-C., Xu J.-F., Xu Y.-G., Tang G.-J., Wang Q. (2015). Disequilibrium-induced initial Os isotopic heterogeneity in gram aliquots of single basaltic rock powders: Implications for dating and source tracing. *Chemical Geology* 406, 10-17.

Li N., Chen Y.J., McNaughton N.J., Ling X.X., Deng X.H.,Yao J.M., Wu, Y.S. (2015). Formation and tectonic evolution of the khondalite series at the southern margin of the North China Craton: geochronological constraints from the a 1.85 Ga Mo deposit in the Xiong'ershan area. *Precambrian Research* 269, 1-17.

Li X., Li J., Yu X., Wang C., Jourdan F. (2015) 40Ar/39Ar ages of seamount trachytes from the South China Sea and implications for the evolution of the northwestern sub-basin. *Geoscience Frontiers* 6, 571-577.

Li Z.X. (2015) Paleogeographic record of Eocene Farallon slab rollback beneath western North America: COMMENT. *Geology* e362, doi: 10.1130/G36733C.1, 2015.

Ling Y.C., Grice K., Tulipani S., Berwick L., Bush R., Moreau J.W. (2015). Distribution of iron- and sulfur-cycling bacteria across a coastal acid sulfate soil environment: implications for natural bioremediation. *Frontiers in Microbiology*, 6, 624.

Liu, E., Wang, X.-C., Zhao, J.-x., Wang, X., 2015. Geochemical and Sr–Nd isotopic variations in a deep-sea sediment core from Eastern Indian Ocean: Constraints on dust provenances, paleoclimate and volcanic eruption history in the last 300,000 years. *Marine Geology* 367, 38-49.

Long J., Burrow C., Ginter M., Maisey J., Trinajstic K., Coates M., . . . Senden T. (2015). First shark from the late devonian (frasnian) Gogo formation, Western Australia sheds new light on the development of tessellated calcified cartilage. *PloS One*. 10, 1-24.

Long J., Mark-Kurik E., Johanson Z., Lee M., Young G., Min Z., . . . Trinajstic K. (2015). Copulation in antiarch placoderms and the origin of gnathostome internal fertilization. *Nature*. 517, 196-199.

Long J., Burrow C. J., Ginter M., Maisey J. G., Trinajstic K. M., Coates M. I., . . . Senden, T. J. (2015). Correction: First Shark from the Late Devonian (Frasnian) Gogo Formation, Western Australia Sheds New Light on the Development of Tessellated Calcified Cartilage. *PLOS ONE, 10*(6), e0131502.

Long X.P., Wilde S.A., Wang Q., Yuan C., Wang X-C., Li J., Jiang, Z., Dan W. (2015). Partial melting of thickened continental crust in central Tibet: Evidence from geochemistry and geochronology of Eocene adakitic rhyolites in the northern Qiangtang Terrane. *Earth and Planetary Science Letters* 414, 30-44.

Long X.P., Wilde S.A., Yuan C., Hu A.Q., Sun M. (2015). Provenance and depositional age of Paleoproterozoic metasedimentary rocks in the Kuluketage Block, northern Tarim Craton: Implications for tectonic setting and crustal growth. *Precambrian Research* 260, 76-90.

Lorand J.-P., Hewins R., Remusat L., Zanda B., Pont S., Leroux H., Jacob D., Humayun M., Nemchin, A., Grange M., Kennedy A., Göpel C. (2015). Nickeliferous pyrite tracks pervasive hydrothermal alteration in Martian regolith breccias: a study in NWA 7533. *Meteoritics and Planetary Science* 50, 2099–2120.

Lu Y.-J., McCuaig T.C., Li Z.-X., Jourdan F., Hart C.J.R., Hou Z.-Q., Tang S.-H. (2015) Paleogene post-collisional lamprophyres in western Yunnan, western Yangtze Craton: Mantle source and tectonic implications. *Lithos*, 233, 139-161.

Lukács R., Harangi S., Bachmann O., Guillong M., Danišík M., Buret Y., von Quadt A., Dunkl I., Fodor L., Sliwinski J., Soós I., Szepesi J. (2015). Zircon geochronology and geochemistry to constrain the youngest eruption events and magma evolution of the Mid-Miocene ignimbrite flare-up in the Pannonian Basin, eastern central Europe. *Contributions to Mineralogy and Petrology* 170, 5-6, 1-26.

Luttinen A., Heinonen J., Kurhila M., Jourdan F., Mänttäri J.I., Vuori S., Huhma H. (2015) Depleted mantle-sourced CFB magmatism in the Jurassic Africa-Antarctica rift: U-Pb and $^{40}Ar/^{39}Ar$ chronology and petrology of the Vestfjella dyke swarm, Dronning Maud Land. *Journal of Petrology* 56, 919-952.

Malusà M.G., Faccenna C., Baldwin S.L., Fitzgerald P.G., Rossetti F., Balestrieri M.L., Danišík M., Ellero A., Ottria G., Piromallo C. (2015). Contrasting styles of (U)HP rock exhumation along the Cenozoic Adria-Europe plate boundary (Western Alps, Calabria, Corsica). *Geochemistry, Geophysics, Geosystems* 16, 6, 1786-1824.

Mack C. L., Milne L. A. (2015) Eocene palynology of the Mulga Rocks deposits, southern Gunbarrel Basin, Western Australia. *Alcheringa* 39 (4), 444-458.

McGee B., Collins A.S., Trindade R.I.F., Jourdan F. (2015) Investigating mid-Ediacaran glaciation and final Gondwana amalgamation using coupled sedimentology and 40Ar/39Ar detrital muscovite provenance from the Paraguay Belt, Brazil. *Sedimentology* 62, 130-154.

McGrath T.D.H., Eksteen J.J., Heath J. (2015). The behaviour of free gold particles in a simulated flash flotation environment. *Journal of the Southern African Institute for Mining and Metallurgy*, 115, 103-112.

McGrath T.D.H., Eksteen J.J., O' Connor L. (2015). A Comparison of 2D and 3D Characterisations of Free Gold Particles in Gravity and Flash Flotation Concentrates. *Minerals Engineering*. 82, 45-53.

Maier W.D., Rasmussen B., Fletcher I.R., Godel B., Barnes S.J., Fisher L.A., Yang S.H., Huhma H., Lahaye G.T.K. (2015). Petrogenesis of the ~2.77 Ga Monts de Cristal Complex, Gabon: evidence for direct precipitation of Pt-arsenides from basaltic magma. *Journal of Petrology*, 56, 1285-1308.

Mazur S., Turniak K., Szczepański J., McNaughton N.J. (2015). Vestiges of Saxothuringian crust in the Central Sudetes, Bohemian Massif: Zircon evidence of a recycled subducted slab provenance. *Gondwana Research* 27, 825-839.

Mikhaltsevitch V., Lebedev M., Gurevich B. (2015) A laboratory study of attenuation and dispersion effects in glycerol-saturated Berea sandstone at seismic frequencies, *SEG Technical Program Expanded Abstracts 2015*, 3085-3089.

Mikhaltsevitch V., Lebedev M., Gurevich B. (2015) A laboratory study of the barrel shape effect in a viscoelastic cylindrical sample at seismic frequencies, *ASEG Extended Abstracts 2015* (1), 1-2.

Mikhaltsevitch V., Lebedev M., Gurevich B. (2015) A Laboratory Study of the Elastic and Anelastic Properties of the Eagle Ford Shale. *77th EAGE Conference and Exhibition 2015*.

Miljković, K., Wieczorek M.A., Collins G.S., Solomon S.C., Smith D.E, Zuber M.T. (2015) Excavation of the mantle in basin-forming impact events on the Moon, *Earth Planet. Sci. Lett*, 409, 243–251, doi: 10.1016/j.epsl.2014.10.041.

Morris G.A., Kirkland C.L., Pease V. (2015). Orogenic paleofluid flow recorded by discordant detrital zircons in the Caledonian foreland basin of northern Greenland. *Lithosphere* 7(2), 138-143.

Mpinga C.N., Eksteen J.J., Aldrich C., Dyer L. (2015). Direct leach approaches to Platinum Group Metal (PGM) ores and concentrates: A review. *Minerals Engineering*,78, 93-113.

Müller T.M., Caspari E., Qi Q., Rubino J.G., Velis D., Lopes S., Lebedev M., Gurevich B. (2015). Seismic Exploration of Hydrocarbons in Heterogeneous Reservoirs. ttp://dx.doi.org/10.1016/B978-0-12-420151-4.00003-9, Chapter 3 Acoustics of Partially Saturated Rocks: Theory and Experiments.

Naeher S., Grice K. (2015). Novel 1*H*-Pyrrole-2,5-dione (maleimide) proxies for the assessment of photic zone euxinia. *Chemical Geology* 404, 100-109.

Naeher S., Huguet A., Roose-Amsaleg C.L., Laverman A.M., Fosse C., Lehmann M.F., Derenne S., Zopfi J. (2015). Molecular and geochemical constraints on anaerobic ammonium oxidation (anammox) in a riparian zone of the Seine Estuary (France). *Biogeochemistry* 123, 237-250.

Neumann, G.A., Zuber M.T., Wieczorek M.A., Head J.W., Baker D.M.H, Solomon S.C., Smith D.E., Lemoine F.G., Mazarico E., Sabaka T.J., Goossens S., Melosh H.J., Phillips R.J., Asmar S.W., Konopliv A.S., Williams J.G., Sori M.M., Soderblom J.M., Miljković K., Andrews-Hanna J.C., Nimmo F., Kiefer W.S. (2015) Lunar Impact Basins Revealed by Gravity Recovery and Interior Laboratory Measurements, *Sci. Adv*., 1, e1500852.

Olierook H.K.H., Merle R.E., Jourdan F., Sircombe K., Fraser G., Timms N.E., Nelson G., Dadd K.A., Kellerson L., Borissov, I. (2015). Age and geochemistry of magmatism on the oceanic Wallaby Plateau and implications for the opening of the Indian Ocean. *Geology*, 34, 971-974.

Olierook H.K.H., Timms N.E., Wellmann J.F., Corbel S., Wilkes P. (2015). 3D structural and stratigraphic model of the Perth Basin, Western Australia: Implications for sub-basin evolution. *Australian Journal of Earth Sciences*. 62, 447-467.

Olierook H.K.H., Timms N.E. (2015). Quantifying multiple Permian–Recent exhumation events during the breakup of eastern Gondwana: sonic transit time analysis of the central to southern Perth Basin. *Basin Research*, DOI: 10.1111/bre.12133.

Olierook H.K.H., Jourdan F., Merle R.E., Timms N.E., Kusznir N., Muhling J.R. (2016). Bunbury Basalt: Gondwana breakup products or earliest vestiges of the Kerguelen mantle plume? *Earth and Planetary Science Letters*, 440, 20-32.

Olierook H.K.H., Timms N.E., Merle R.E. Jourdan F., Wilkes P.G. (2015). Paleodrainage and fault development in the southern Perth Basin, Western Australia during and after the breakup of Gondwana from 3D modelling of the Bunbury Basalt. *Australian Journal of Earth Sciences*, 62, 289-305.

Oliveira E.P., McNaughton N.J., Windley B.F., Carvalho M.J., Nascimento R.S. (2015). Detrital zircon U-Pb geochronology and whole-rock Nd-isotope constraints on sediment provenance in the Neoproterozoic Sergipano orogen, Brazil: from early passive margins to late syn-orogenic basins. *Tectonophysics* 662, 183-194.

Oliveira E.P., Bueno J.F., McNaughton N.J., Silva Filho A.F., Nascimento R.S., Donatti-Filho J.P. (2015). Age, composition, and source of continental arc- and syn-collision granites of the Neoproterozoic Sergipano Belt, Southern Borborema Province, Brazil. *Journal of South American Earth Sciences* 58, 257-280.

Oraby E.A., Eksteen J.J. (2015). The leaching and carbon based adsorption behaviour of gold and silver and their alloys in alkaline glycine-peroxide solutions. *Hydrometallurgy*. 152, 199–203.

Oraby E.A., Eksteen J.J. (2015). Gold leaching in cyanide-starved copper solutions in the presence of glycine. *Hydrometallurgy*, 156, 81-88.

Pagès A., Grice K., Welsh D.T., Teasdale P.T., Van Kranendonk M.J., Greenwood P.F. (2015). Lipid biomarker and isotopic study of community distribution and biomarker preservation in a laminated microbial mat from Shark Bay, Western Australia. *Microbial Ecology*, 40, 1-14.

Palancz B., Awange J. L., Völgyesi L (2015) Correction of Gravimetric Geoid Using Symbolic Regression. *Mathematical Geosciences* 47, 867–883.

Pervikhina M., Gurevich B., Dewhurst D.N., Golodoniuc P., Lebedev M. (2015) Rock Physics Analysis of Shale Reservoirs. *Fundamentals of Gas Shale Reservoirs*, 191-205.

Pang C.-J., Wang X.-C., Xu Y.-G., Wen S.-N., Kuang Y.-S., Hong L.-B. (2015). Pyroxenite-derived Early Cretaceous lavas in the Liaodong Peninsula: Implication for metasomatism and thinning of the lithospheric mantle beneath North China Craton. *Lithos* 227, 77-93.

Parker A. L., Biggs J., Walters R. J., Ebmeier S. K., Wright T. J., Teanby N. A., Lu Z. (2015) Systematic assessment of atmospheric uncertainties for InSAR data at volcanic arcs using large-scale atmospheric models: Application to the Cascade volcanoes, United States. *Remote Sensing of Environment*, 170, 102-114.

Pinto V.M., Hartmann L.A., Santos J.O.S., McNaughton N.J. (2015). Zircon ages delimit the provenance of a sand extradite from the Botucatu Formation in the Parana volcanic province, Irai, Brazil. *Anais de Academia Brasileira de Ciencias* 87, 1611-1622.

Piotraschke R., Cashman S.M., Furlong K.P., Kamp P.J.J., Danišík M., Xu G. (2015). Unroofing the klamaths-blame it on siletzia? *Lithosphere* 7, 4, 427-440.

Pisarevsky S.A., Bogdanova S.V., Lubnina N.V., Murphy J.B. (2015). Supercontinental cycles and geodynamics. *Precambrian Research*, 259, 1-4.

Pisarevsky S.A., De Waele B., Jones S., Söderlund U., Ernst R.E. (2015). Paleomagnetism and U–Pb age of the 2.4 Ga Erayinia mafic dykes in the south-western Yilgarn, Western Australia: Paleogeographic and geodynamic implications. *Precambrian Research*, 259, 222-231.

Plavsa D., Collins A.S., Foden J., Clark, C. (2015) The evolution of a Gondwanan collisional orogen: a structural and geochronological appraisal from the Southern Granulite Terrane, South India. *Tectonics*. 34, 820-857.

Putnis A. (2015) Transient porosity resulting from fluid-mineral interaction and its consequences. *Reviews in Mineralogy and Geochemistry* 80, 1-23.

Putnis A. (2015) Sharpened Interface. *Nature Materials* 14, 261-262.

Rasmussen B., Krapez B. and Muhling J.R. (2015). Seafloor silicification and hardground development during deposition of 2.5 Ga banded iron formations. *Geology* 43, 235-238.

Rasmussen B., Krapez B., Muhling J.R., Suvorova A. (2015). Precipitation of iron silicate nanoparticles in early Precambrian oceans marks Earth's first iron age. *Geology* 43, 303-306.

Reddy S. M., Johnson T.E., Fischer S., Rickard W.D., Taylor R.J.M. (2015) Precambrian reidite discovered in shocked zircon from the Stac Fada impactite, Scotland. *Geology*. 43, 899-902.

Rexer M., Hirt C., Claessens S.J., Braitenberg C. (2015). Use of topography in the context of the GOCE satellite mission – some examples. In: Ouwehand, L. (ed.) *Proc. 5th International GOCE User Workshop*, Paris, France, 25-28 November 2014, ESA SP-728, ESA Communications.

Roberts, N.M.W., Spencer, C.J. (2015). The zircon archive of continent formation, destruction and preservation, in: Roberts, N. M. W., Van Kranendonk, M., Parman, S., Shirey, S. & Clift, P. D. (eds) Continent Formation Through Time. Geological Society, London, Special Publications 389, p. doi:10.1144/SP389.14.

Roelofs B., Playton T., Barham M., Trinajstic K. (2015). Upper Devonian microvertebrates from the Canning Basin, Western Australia. *Acta Geologica Polonica* 65, 69-100.

Rolshausen G., Phillip D.A.T., Beckles D.M., Akbari A., Ghoshal S., Hamilton P.B., Tyler C.R., Scarlett A.G., Ramnarine I., Bentzen P., Hendry A.P. (2015). Do stressful conditions make adaptation difficult? Guppies in the oil-polluted environments of southern Trinidad. *Evolutionary Applications* 8, 854-870

Rucklin M., Long J., Trinajstic, K. (2015). A new selenosteid arthrodire ('Placodermi') from the Late Devonian of Morocco. *Journal of Vertebrate Paleontology*, 35(2), 13 pages.

Ruiz-Agudo C., Ruiz-Agudo E., Putnis C.V., Putnis A. (2015) Mechanistic principles of barite formation: From nanoparticles to micron-sized crystals. *Crystal Growth and Design* 15, 3724-3733.

Ruiz-Agudo C., Putnis C.V., Ruiz-Agudo E. and Putnis A. (2015) The influence of pH on barite nucleation and growth. *Chemical Geology*. 391, 7-18.

Ruiz-Agudo E., Putnis C.V., Hövelmann J., Álvarez-Lloret P., Ibáñez-Velasco A., Putnis A. (2015) Experimental Study of the replacement of calcite by calcium sulphates. *Geochimica et Cosmochimica Acta*. 156, 75-93.

Shaanan U., Rosenbaum G., Pisarevsky S.A., Speranza F. (2015). Paleomagnetic data from the New England Orogen (eastern Australia) and implications for oroclinal bending. *Tectonophysics*, 664, 182-190.

Sansom E.K., Bland P.A., Paxman J., Towner, M. C. (2015) A novel approach to fireball modeling: The observable and the calculated. *Meteoritics and Planetary Science* 50, 1423-1435.

Scherr K.E., Backes D., Scarlett A.G., Lantschbauer W., Nahold M. (2015) Biogeochemical gradients above a coal tar DNAPL. *The Science of the total environment* doi:10.1016/j.scitotenv.2015.11.036

Schmieder M., Tohver E., Jourdan F., Denyszyn S.W., Haines P.W. (2015) Zircons from the Acraman impact melt rock (South Australia): Shock metamorphism, U-Pb and 40Ar/39Ar systematics, and implications for the isotopic dating of impact events. *Geochimica et Cosmochimica Acta* 161, 71-100.

Scibiorski E., Tohver E, Jourdan F. (2015) Rapid Mesoproterozoic cooling and exhumation in the western Albany-Fraser Orogen, Western Australia. *Precambrian Research* 265, 232-248.

Smithies R., Kirkland C.L., Cliff J., Howard H., Quentin de Gromard R. (2015). Syn-volcanic cannibalisation of juvenile felsic crust: Superimposed giant 18O-depleted rhyolite systems in the hot and thinned crust of Mesoproterozoic central Australia. *Earth and Planetary Science Letters* 424, 15-25.

Snape J.F., Nemchin A.A., Grange M.L., Bellucci J.J., Thiessen F., Whitehouse M.J. (2016) Phosphate ages in Apollo 14 breccias: Resolving multiple impact events with high precision U-Pb SIMS analyses. *Geochimica et Cosmochimica Acta*, 174, 13-29.

Snyders C.A., Bradshaw S.M., Akdogan G., Eksteen J.J. (2015). Factors affecting the elution of Pt, Pd, and Au from activated carbon. *Minerals Engineering*, 80, 14-24.

Snyders C.A., Bradshaw S.M., Akdogan G., Eksteen J.J. (2015). Determination of the equilibrium and film diffusion constants of the platinum cyanide anions during the elution from activated carbon. *Minerals Engineering*, 80, 57-68.

Solihuddin, T., Collins, L.B., Blakeway, D., O'Leary, M.J. (2015). Holocene Reef Growth and Sea Level in a Macrotidal, High Turbidity Setting: Cockatoo Island, Kimberley Bioregion, Northwest Australia. *Marine Geology*, 359, 50-60.

Sobczyk A., Danišík M., Aleksandrowski P., Anczkiewicz A. (2015). Post-Variscan cooling history of the central Western Sudetes (NE Bohemian Massif, Poland) constrained by apatite fission-track and zircon (U-Th)/He thermochronology. *Tectonophysics* 649, 47-57.

Soderblom J.M., Evans A.J, Johnson B.C., Melosh H.J., Miljković K., Phillips R.J, Andrews-Hanna J.C., Head III J.W., Milbury C., Neumann G.A., Nimmo F., Smith D.E., Solomon S.C., Sori M.M., Thomason C.J., Wieczorek M.A., Zuber M.T. (2015) Production and saturation of porosity in the lunar highlands from impact cratering, *Geophys. Res. Lett*., 42, 6939-6944.

Song Y.-S., Lee, H.-S., Park, K.-H., Fitzsimons I.C.W., Cawood P.A. (2015). Recognition of the Phanerozoic "Young granite gneiss" in the central Yeongnam massif. *Geosciences Journal* 19, 1–16.

Spaggiari C. V., Kirkland C. L., Smithies R. H., Wingate M.T.D., Belousova E. A. (2015). Transformation of an Archean craton margin during Proterozoic basin formation and magmatism: The Albany-Fraser Orogen, Western Australia. *Precambrian Research*, 266, 440-466.

Spencer, C.J., Thomas, R.J., Roberts, N.M.W., Cawood, P.A., Millar, I., Tapster, S., 2015. Oblique island arc accretion and continental collision, Natal Metamorphic Province, South Africa: new isotopic constraints. *Precambrian Research* 265, 203-217.

Spencer, C.J., Cawood, P.A. Hawkesworth, C.J., Prave, A.R., 2015. Generation and Preservation of Continental Crust in the Grenville Orogenic Cycle. *Geoscience Frontiers* 6, 357-372.

Spivak-Birndorf L.J., Bouvier A., Benedix G.K., Hammond S., Brennecka G.A., Howard K.T., Rogers N.W., Wadwha M., Bland P.A., Spurny P., Towner M.C. (2015) Geochemistry and chronology of the Bunburra Rockhole ungrouped achondrite. *Meteoritics and Planetary Science* 50, 958-975.

Sun B., Bóna A., King A., Zhou B. (2015) A comparison of coherency measurement using semblance and multiple signal classification, from a seismic-while-drilling perspective. *Geophysics* 80 (3), KS27-KS39.

Sun B., Bóna A., Zhou B., Van de Werken M. (2015) A comparison of radiated energy from diamond-impregnated coring and reverse-circulation percussion drilling methods in hard-rock environments. *Geophysics* 80 (4), K13-K23.

Sun M.D., Xu Y-G., Wilde S.A., Chen H-L., Yang S-F. (2015). The Permian Dongfanghong island-arc gabbro of the Wandashan Orogen, NE China: Implications for Paleo-Pacific subduction. *Tectonophysics* 659, 122-136.

Sun M-D., Xu Y-G., Wilde S.A., Provenance of Cretaceous trench slope sediments from the Mesozoic Wandashan Orogen, NE China: Implications for determining ancient drainage systems and tectonics of the Paleo-Pacific. *Tectonics* 34, 1269-1289.

Swigert J.P., Lee C., Wong D.C.L., White R., Scarlett A.G., West C.E. (2015) Aquatic hazard assessment of a commercial sample of naphthenic acids. *Chemosphere* 124, 1-9.

Taneja R., O'Neill C., Lackie M., Rushmer T., Schmidt P., Jourdan F. (2015). 40Ar/39Ar geochronology and the paleoposition of Christmas Island (Australia), Northeast Indian Ocean. *Gondwana Research* 28, 391-406.

Taylor R.J.M, Harley S.L., Hinton R., Elphick S., Clark C. (2015) Experimental determination of REE partition coefficients between zircon, garnet and melt: a key to understanding high-temperature crustal processes. *Journal of Metamorphic Geology*. 33, 231-248.

Taylor R.J.M., Clark C., Johnson T.E., Collins A.S., Santosh M. (2015) Unravelling the complexities in high-grade rocks using multiple techniques – the Achankovil Zone of southern India. *Contributions to Mineralogy and Petrology*. 169, 1-19.

Tecchiato, S., Collins, L.B., Parnum, I., Stevens, A. (2015). The influence of geomorphology and sedimentary processes on benthic habitat distribution and littoral sediment dynamics: Geraldton, Western Australia. *Marine Geology*, 359, 148-162.

Tenzer R., Hirt C., Claessens S., Novák P. (2015) Spatial and spectral representations of the geoid-to-quasigeoid correction. *Surveys in Geophysics*, 36, 627-658.

Tertyshnikov K., Pevzner R., Bóna A., Alonaizi F., Gurevich B. (2015) Steered migration in hard rock environments. *Geophysical Prospecting* 63, 525-533.

Tessalina S, Malitch K.N., Auge T., Puchkov V.N., McInnes B.I.A. (2015). Origin of the Nizhny Tagil clinopyroxenite-dunite massif (Uralian Platinum Belt, Russia): insights from PGE and Os isotope systematics. *Journal of Petrology* 56, 2297-2318.

Tessalina S., Jourdan F., Nunes L., Kennedy A., Denyszyn S., Puchtel I., Touboul M., Creaser R., Boyet M., Belousova E., Trinquier A. (2015) Application of Radiogenic Isotopes in Geosciences – Overview and Perspectives In: Principles and Practice of Analytical Techniques in Geosciences (Ed. Kliti Grice), RSC Detection Science Series, *Royal Society of Chemistry*, 49-93. ISBN 1849736499, 9781849736497

Thomas, R.J., Spencer, C.J., Bushi, A.M., Baglow, N., Boniface, N., de Kock, G., Horstwood, M.S.A., Hollick, L., Jacobs, J., Kajara, S., Kamihanda, G., Key, R.M., Maganga, Z., Mbawala., F., McCourt, W., Momburi, P., Moses, F., Mruma, A., Myambilwa, Y., Roberts, N.M.W., Saidi, H., Nyanda, P., Nyoka, K., Millar, I. (2015) Geochronology of the central Tanzania Craton and its southern and eastern orogenic margins, *Precambrian Research* 277, 47-67.

Timms N.E., Olierook H.K.H., Wilson M.E.J., Delle Piane C., Hamilton P.J., Cope P., Stütenbecker L. (2015). Sedimentary facies analysis, mineralogy and diagenesis of the Mesozoic aquifers of the central Perth Basin, *Marine and Petroleum Geology*, 60, 54-78.

Tomkins A.G., Evans K.A. (2015). Separate zones of sulfate and sulfide release from subducted mafic ocean crust. *Earth and Planetary Science Letters* 428, 73-83.

Trinajstic K., Boisvert C., Long J., Maksimenko A., Johanson, Z. (2015). Pelvic and reproductive structures in placoderms (stem gnathostomes). *Biological Reviews*, 90, 467-501.

Tulipani S., Grice K., Greenwood P.F., Schwark L. Summons R.E., Böttcher M.E., Foster, C.B. (2015). Molecular proxies as indicators of freshwater incursion-driven salinity stratification. *Chemical Geology* 409, 61-68.

Tulipani S., Grice K., Greenwood P., Schwark L., Haines P.W., Sauer P.E., Schimmelmann A., Summons R.E., Foster C.B., Böttcher M.E., Payton T.D., Schwark L. (2015). Changes of palaeoenvironmental conditions recorded in Late Devonian reef systems from the Canning Basin, Western Australia: A biomarker and stable isotope approach. *Gondwana Research* 409, 61-68.

Valley J.W., Reinhard D.A., Cavosie A.J., Ushikubo T., Lawrence D.F., Larson D.J., Kelly T.F., Snoeyenbos D., Strickland A. (2015) Nano- and Micro-geochronology in Hadean and Archean zircons by atom-probe tomography and SIMS: New tools for old minerals. *American Mineralogist* 100, 1355-1377.

Van Kranendonk M., Kirkland C.L., Cliff J. (2015). Oxygen isotopes in Pilbara Craton zircons support a global increase in crustal recycling at 3.2Ga. *Lithos* 228-229: 90-98.

Van Roosbroek N., Debaille V., Pittarello L., Goderis S., Humayun M., Hecht L., Jourdan F., Spicuzza M.J. and Claeys Ph. (2015) A new Primitive IIE member: the chondrule-bearing Mont Dieu II meteorite. *Meteoritics & Planetary Science* 50, 1173–1196.

Vargas-Meleza L., Healy D., Alsop I., Timms N. (2015). Exploring the relative contribution of mineralogy and CPO to the seismic velocity anisotropy of evaporites. *Journal of Structural Geology*, 70, 39-55.

Vialle S., Lebedev M. (2015) Heterogeneities in the elastic properties of microporous carbonate rocks at the microscale from nanoindentation tests. *SEG Technical Program Expanded Abstracts 2015*, 3279-3284.

Vielreicher N.M., Groves D.I., McNaughton N.J., Fletcher I.R. (2015). The timing of gold mineralization across the eastern Yilgarn craton using U–Pb geochronology of hydrothermal phosphate minerals. *Mineralium Deposita* 50, 391–428.

Vielreicher N.M., Groves D.I., McNaughton N.J. (2015). Reply to Discussion: The timing of gold mineralization across the eastern Yilgarn craton using U–Pb geochronology of hydrothermal phosphate minerals. *Mineralium Deposita* 50, 889-894.

Waddell P.J., Timms N.E., Kirkland C.L., Wingate M., Spaggiari C.V. (2015). Analysis of the Ragged Basin, Western Australia: insights into syn-orogenic basin evolution within the Albany-Fraser Orogen. *Precambrian Research*, 261, 166-187.

Walsh A.K., Kelsey D.E., Kirkland C.L., Hand M., Smithies R. H., Clark C., Howard, H.M. (2015) A large, long-lived, ultrahigh-temperature Grenvillian belt in Central Australia. *Gondwana Research*. 28, 531-564.

Wang F., Chen H., Batt G.E., Lin X., Gong J., Gong G., Meng L., Yang S., Jourdan F. (2015) Tectonothermal history of the NE Jiangshan–Shaoxing suture zone: Evidence from 40Ar/39Ar and fission-track thermochronology in the Chencai region. *Precambrian Research* 264, 192-203.

Wang L., Putnis C.V., Ruiz-Agudo E., Hövelmann J., Putnis A. (2015) In situ imaging of interfacial precipitation of phosphate on goethite. *Environmental Science and Technology* 49, 4184-4192.

Wang X., Wilde S.A., Li Q., Yang Y. (2015). Continental flood basalts derived from the hydrous mantle transition zone. *Nature Communications* 6, DOI 10/1038/ncomms8700.

Wilde M.J., West C.E., Scarlett A.G., Jones D., Frank R.A., Hewitt M., Rowland S.J. (2015). Bicyclic naphthenic acids in oil sands process water: Indentification by comprehensive multidimensional gas chromatography-mass spectrometry. *Journal of Chromatography* A 1378, 74-87.

Wilde, S.A., 2015. Jack Hills Zircons. In: Rink, W.J. and Thompson, J.W. (eds). Encyclopedia of Scientific Dating Methods, p. 359. Springer.

Wilde S.A., Zhou J.B., Wu F.Y. (2015). Development of the North-Eastern segment of the Central Asian Orogenic belt. In: The Central Asian Orogenic Belt (Ed. Kroner, A.) "Contributions to the Regional Geology of the Earth", E. Schweitzerbart Science Publishers, Stuttgart, Germany, pages 184-210.

Wilde S.A. (2015). Final amalgamation of the Central Asian Orogenic Belt in NE China: Paleo-Asian Ocean closure versus Paleo-Pacific plate subduction – A review of the evidence. *Tectonophysics* 602, 345-362.

Wilson M.E.J. (2015). Oligo-Miocene variability in carbonate producers and platforms of the Coral Triangle biodiversity hotspot: habitat mosaics and marine biodiversity. *PALAIOS* 30, 150-167.

Wölfler A., Dekant C., Frisch W., Danišík M., Frank W. (2015). Cretaceous to Miocene cooling of Austroalpine units southeast of the Tauern Window (Eastern Alps) constrained by multi-system thermochronometry. *Austrian Journal of Earth Sciences* 108, 1, 18-35.

Wölfler A., Frisch W., Fritz H., Danišík M., Wölfler A. (2015). Ductile to brittle fault zone evolution in Austroalpine units to the southeast of the Tauern Window (Eastern Alps). *Swiss Journal of Geosciences* 108/2-3, 239-251.

Yakymchuk C., Brown M., Clark C., Korhonen F.J., Piccoli P. M., Siddoway C.S., Taylor, R.J.M., Vervoort J. D. (2015). Decoding polyphase migmatites using geochronology and phase equilibria modelling. *Journal of Metamorphic Geology*, 33, 203-230.

Yang C., Li X.-H., Wang X.-C., Lan Z. (2015). Mid-Neoproterozoic angular unconformity in the Yangtze Block revisited: Insights from detrital zircon U–Pb age and Hf–O isotopes. *Precambrian Research* 266, 165-178

Yao W.H., Li Z.X., Li W.X. (2015). Was there a Cambrian ocean in South China? – Insight from detrital provenance analyses. *Geological Magazine* 152, 184–191.

Yao W.H., Li Z.X., Li W.X., Su L., Yang J.H. (2015). Detrital provenance evolution of the Ediacaran–Silurian Nanhua foreland basin, South China. *Gondwana Research* 28, 1449–1465.

Zhao J., Qin K., Xiao B., McInnes B., Li G., Evans N.J., Cao, M., Li J. (2015). Thermal history of the Qulong giant Cu-Mo deposit, Gangdese metallogenic belt, Tibet: Constraints on magmatic-hydrothermal evolution and exhumation. *Gondwana Research* doi:10.1016/j.gr.2015.07.005

Zhao J., Qin K., Li G., Cao M., Evans N.J., McInnes B.I.A., Li J., Xiao B., Chen L. (2015). The exhumation history of collision-related mineralizing systems in Tibet: Insights from the thermal history of the Sharang and Yaguila deposits, central Lhasa. *Ore Geology Reviews*, 65, 1043-1061.

Zheng H., Wei X., Tada R., Clift P., Jourdan F., Wang P., He M. (2015) Late Oligocene-early Miocene birth of the Taklimakan Desert. *Proceedings of the National Academy of Sciences 112*, 7662-7667.

Zhou J-B, Wang B., Wilde S.A., Zhao G-C., Cao J-L., Zheng C-Q., Zeng W.S. (2015). Geochemistry and U-Pb zircon dating of the Toudaoqiao blueschists in the Great Xing'an Range, northeast China, and tectonic implications. *Journal of Asian Earth Sciences* 97, 197-210.

Zhou Y.P., Stuart-Williams H., Grice K., Kayler Z.E., Zavadlav S., Gessler A., Farquhar G.D. (2015). Allocate carbon for a reason: priorities are reflected in the 13C/12C ratios of plant lipids synthesized via three independent biosynthetic pathways. *Phytochemistry* 111, 14-20.

Zhu K.Y., Li Z.X., Xu X.S., Wilde S.A., Chen H.L (2015) Early Mesozoic ferroan (A-type) and magnesian granitoids in eastern South China: Tracing the influence of flat-slab subduction at the western Pacific margin. *Lithos* 240–243, 371-381.

Zi J.-W., Rasmussen B., Muhling J.R., Fletcher I.R., Thorne A.M., Johnson S.P., Cutten H.N., Dunkley D.J. and Korhonen, F.J. (2015). In situ U–Pb geochronology of xenotime and monazite from the Abra polymetallic deposit in the Capricorn Orogen, Australia: Dating hydrothermal mineralization and fluid flow in a long-lived crustal structure. *Precambrian Research* 260, 91-112.

TIGeR MEMBERSHIP

Director
Andrew Putnis

TIGeR Business Manager
Yacoob Padia

The TIGeR Executive Committee
Andrew Putnis
Chris Clark
Will Featherstone
Kliti Grice
Boris Gurevich
Brent McInnes

Academic and Research Staff
Andrea Agangi
Joseph Awange
Milo Barham
Andreas Beinlich
Phil Bland
Gretchen Benedix-Bland
Alison Blyth
Andrej Bona
Aaron Cavosie
Dr Sten Claessens
Chris Clark
Marco Coolen
Grant Cox
Martin Danisik
Jacques Eksteen
Timmons Erickson
Katy Evans
Noreen Evans
Ahmed El-Mowafy
Will Featherstone
Mick Filmer
Ian Fitzsimons
Nicholas Gardiner
Marion Grange
Paul Greenwood
Kliti Grice
Boris Gurevich
Brett Harris
Alex Holman
Aaron Hunter
Caroline Jaruala
Tim Johnson
Fred Jourdan
Pete Kinny
Jon Kirby
Chris Kirkland
Brian Krapez
Michael Kuhn
Zhen Li
Zheng-Xiang Li
Brent McInnes
Neal McNaughton
Mahyar Madadi
Robert Madden
Renaud Merle
Katarina Miljkovic
Sebastian Naeher
Alexander Nemchin
Amy Parker
Bob Pidgeon
Sergei Pisarevskiy
Diana Plavsa
Birger Rasmussen
Steven Reddy
Kirsten Rempel
Alan Scarlett
Christopher Spencer
Richard Taylor
Svetlana Tessalina
Nick Timms
Martin Towner
Kate Trinajstic
Svenja Tulipani
Stephanie Vialle
Guangli Wang
Xuan-Ce Wang
Simon Wilde
Moyra Wilson
Weihua Yao
Nan Zhang
Jianwei Zi

TIGeR Research students
Khalid Alhamoud
Sonia Armandola
Hamed Arosi
Eleanore Blereau
Giada Buferale
Jaime Cesarcolmenares
Peng Chen
Rosalind Crossley
Luke Daly
Hadrien Devillepoix
Imogen Fielding
Lucy Forman
Hendrik Grotheer
Joao Pinto Bravo Correia Guerreiro
Sarah Hayes
Nannan He
Siyu Hu
Omar Imbarek
Inalee Jahn
Moataz Kordi
Sureyya Kose
Marco Loche
Shaojie Li
Yebo Liu
Sam McHarg
Charlotte Mack
Holly Meadows
Therese Morris
Korien Oostingh
Chloe Plet
Jennifer Porter
Alexander Prent
Brett Roelofs
Clinton Roga
Ellie Sansom
Tubagus Solihuddin
Gemma Spaak
Camilla Stark
Ni Tao
Qian Wang
Bryant Ware

Curtin University

Curtin University
THE INSTITUTE FOR
GEOSCIENCE RESEARCH (TIGeR)

CONTACT:

Andrew Putnis
Director
The Institute for Geoscience Research (TIGeR)

Curtin University
Kent Street Bentley WA 6102
GPO Box U1987 Perth WA 6845

Tel: +61 8 9266 7978
Email: andrew.putnis@curtin.edu.au

scieng.curtin.edu.au

ADV086992